Imperial College London

Robustness and Resilience Analysis of Urban Road Networks

By

Wenlong Shang

BSc MSc

A thesis submitted for the degree of Doctor of Philosophy of
Imperial College London

Centre for Transport Studies

Department of Civil and Environmental Engineering

Imperial College London, United Kingdom

August, 2016

Ways which can be spoken of are not the eternal way. Names which can be spoken are not eternal names (道可道非常道。名可名非常名。)

-----Laozi (老子)

Scientific knowledge, the crowning glory and the safeguard of the empire (SCIENTIA IMPERII DECUS ET TUTAMEN)

----- The motto of Imperial College London

Dedicated to my grandmother and grandfather

DECLARATION

I hereby certify that all materials in this thesis is my own work and I am the sole author of this thesis. The contribution of my supervisors was editorial and supervisory. Any quotation from, or description of the work of others is acknowledged by reference to the sources, whether published or unpublished.

WENLONG SHANG

ABSTRACT

This thesis investigates the robustness and resilience of urban road networks (URNs) in the presence of either local or global disruptions. The problem is approached from the two perspectives of complex network theory and traffic network modelling. The former mainly considers the topological characteristics of the networks, while the latter explores the flow characteristics, demand distribution, user behaviour, control mechanisms, and their combined effect on the network's performance under disruption.

Building on complex network theory, the thesis conducts a topological analysis of URNs using topological indices such as clustering coefficient (*CC*) and weighted betweenness centrality (*WBC*). The relationships among indegree, outdegree, *WBC* and *CC* are also examined. Following this, the small-world property and community detections for URNs are conducted. The topological indices are then examined in detail in conjunction with operational indices that take into account link capacity, travel demand and driver behaviour. The potential correlations between these various indices are investigated based on their importance for the nodes/links in the network. The thesis also proposes a new relative area index (RAI) quantitatively to analyse the robustness of URNs afflicted by global capacity disruptions, and this index may shed light on the planning and management of URNs.

In the second approach, the thesis employs day-to-day evolutionary dynamics to capture the transient state of URNs in the event of disruption. Both agent-based and continuum modelling approaches are considered for the network simulation, employing novel concepts such as percolation theory to quantify the network performance. Different network control measures, such as variable message signs (VMS) and adaptive signal control are incorporated into the day-to-day models in order to mitigate the congestion and delays caused by unexpected disruptions. Two key performance indicators (KPI), rapidity, and the new relative area index (RAI), are derived to represent and quantify the resilience and robustness respectively. Extensive simulation studies are conducted to assess the performance of networks equipped with various control mechanisms and under different levels of degradation.

ACKNOWLEDGEMENTS

Eventually, I have completely finished my PhD thesis. Looking back over these four years, there has been much laughter and many tears, and there are many people I should be thankful for.

Firstly, I would like to thank the patient and continuous supervision and guidance from my supervisors: Professor Washington Ochieng and Dr. Ke Han. In particular, I would like to thank Professor Ochieng for his assistance and encouragement in some very difficult times. What he taught me has not just been scientific methods but also leadership. In addition, I thank Professor Ochieng for funding me twice to attend the TRB conference, and I appreciate that he always put students' benefits as a priority. I also thank Dr. Han very much for his effective supervision, valuable suggestions, research direction, mathematical guidance and critical comments on my research throughout my PhD study. Dr. Han treats me not only like a student but also like a friend, and he spent lots of time on my journal papers and thesis correction. I am also very thankful for his valuable suggestions on the slides for Viva. Without the guidance and support of Dr. Han, I cannot finish my thesis smoothly. What he provides is more than supervision.

I am thankful to my friends who have provided me help all the time, they are Dr. Zhenggang Nie, Dr. Shuoren Du, Mr. Huibo Bi, Dr. Guotao Hu, Dr. Kuang-chang Pien, Dr Thalis Zis, Dr.Aravinth Thiyangarajah, Dr. Shane Canavan, Miss Sophie Damy, Dr. Shaojun Feng and so on. Particularly, I would like to thank my friend Huibo, we always have happy discussions ranging from academics to life, and he is patient to listen my boring complains when I get depressed. In addition, I am also thankful for the academic discussion with Miss Shiming Xu, Dr. Wei Pan and Dr. Kuang-chang Pien from Imperial College London, with Mr. Yiou Wang, Dr. Hongcheng Liu, Mr. Zhaohu Fan and Miss Wenjing Wang from Pennsylvania State University and with Yanjun Wang from Nanjing University of Aeronautics and Astronautics.

I would like to thank my family for their support and understanding. During the period of my PhD studies, I spent little time with them, indeed, I never even managed to go back for spring festival for those four years. I also appreciate the support of my girlfriend and apologize for not having been able to spend as much time with her as I would have liked.

I would like to acknowledge the support and assistance from all the members of the Graduate Student Union of Chinese Scholars and Students Association (GSUCSSA):we did many great things together. Heartfelt thanks are also offered to the personnel of the education section of the Chinese Embassy.

I would like to thank all CTS (Centre Transport Studies) members. I have had a wonderful time with all these talented scholars and PhD students in CTS. And I also would like to thank the people in the Civil and Environmental Engineering Department who kindly helped me, especially Madam Nicole Lau, Professor Chris Cheeseman and Professor Chris Onof.

Finally, thanks to all the people I met in the UK, thanks to Imperial College for providing all types of resources, and I am very grateful for to my great motherland China, and for the sponsorship from the China Scholarship Council (CSC).

Wenlong Shang

Centre for Transport Studies

Imperial College London

30/08/2016

TABLE OF CONTENTS

LIST OF FIGURES

LIST OF TABLES

NOMENCLATURE

An alphabetical list of commonly used acronyms and abbreviations used in this thesis:

ABDTD	: Agent-based day-to-day
ABS	: Agent-based simulation
AI	: Artificial Intelligence
APL	: Average path length
ATIS	: Advanced Traveller Information System
ATNC	: Air transport network of China
AWBC	: Average weighted betweenness centrality
BC	: Betweenness centrality
BNN	: Brown-von Neumann-Nash
BR	: Bounded rationality
BTN	: Bus-transport networks
CC	: Clustering coefficient
CFDTD	: Continuous flow day-to-day
CR	: Compliance rate
CRN	: China Railway Network
CTAC	: Combined Traffic Assignment and Control
DTD	: Day-to-day
ESTT	: Expected system travel time
ICT	: Information and Communication Technologies
IOA	: Iterative Optimization and Assignment
ITS	: Intelligence transport system
KPI	: Key Performance Indicator
NIRA	: Networked Infrastructure Resiliency Assessment

NL : Network loading

RAI-SO : RAIs based on System Optimum

RAI-UE : RAIs based on User Equilibrium

NRI : Network Robust Index

NTP : Network tatonnement process

OD : Origin-destination

OSLOM : Order Statistics Local Optimization Method

PAP : Proportional adjustment process

PDS : Projected dynamical system

POA : Price of Anarchy

PSAP : Proportional switch adjustment process

PTN : Public transport network

RAI : Relative Area Index

RPAP : Restricted proportional-switch adjustment process

SO : System optimum

SUE : Stochastic User Equilibrium

UE : User equilibrium

URN : Urban road network

VMS : Variable Message Sign

WAN : World air network

WBC : Weighted betweenness centrality

WCC : Weighted Closeness Centrality

WEff : Weighted efficiency measure

Chapter 1 INTRODUCTION

1.1 Background and motivation

On 1 August 2007, the abrupt collapse of the I-35W Bridge over the Mississippi River in Minneapolis led to the disturbance of 140,000 daily vehicle trips, with a consequent significant influence on the flow patterns of the road network. This disaster not only caused casualties and infrastructural costs, but also led to significant social and economic costs due to the heavy congestion, longer travel distances and possible opportunity losses induced, all of which have been estimated to amount to between $71000 and $220000 per day (Xie and Levinson, 2011). In fact, the Minnesota Department of Transportation (2007) arrived at an estimate of up to $400,000 per day, due to the assumption that only two detour routes were available (Zhu and Levinson, 2012). Similarly, in 1994, the Northbridge Earthquake in California caused the destruction of four freeways in the Los Angeles basin, 57 deaths and more than 8700 injures. This earthquake was one of the costliest natural disasters in the USA history and led to earthquake-caused property damage of between $13 billion and $40 billion with transport-related costs alone being up to $1.6 million per day (National Geophysical Data Center, n.d.).

In the USA as a whole, the costs lost in transportation systems due to poor maintenance, natural disasters and malicious attacks are up to approximately $94 billion per year (American Society of

Civil Engineers 2005). Furthermore, in the USA, Americans are stuck in traffic for approximately 3.5 billion hours per year due to breakdowns in transport networks, with a corresponding cost of up to $63.2 billion per year (American Society of Civil Engineers 2005). Given the significant costs associated with such disruption, the assessment and analysis of transport network robustness and resilience is economically and practically important.

Due to the diversity in network type, infrastructure, constraints, and objectives, there are no universal definitions of the robustness and resilience of networks. The detailed definitions for robustness used in this thesis are presented in **Section 3.1.1.1**. In general, however, robustness refers to an ability to maintain the original performance and functionality of the system. Resilience, meanwhile, has overlapping meanings with robustness: in the field of infrastructure, Bruneau and Reinhorn (2007) and O'Rourke (2007) define resilience from four perspectives: robustness, redundancy, resourcefulness and rapidity. Other definitions of resilience and a detailed discussion, are provided in **Section 3.1.1.2**.

In a real-world environment, road traffic networks and infrastructure are frequently at risk from internal disturbances and external disruptions (Nagurney, 2011a), and this poses fundamental scientific questions regarding the robustness and resilience of our transportation systems and other relevant infrastructure. The fact that the frequency of disasters at various levels of severity has increased drastically (see Error! Reference source not found.) further highlights the urgency of devising a systematic approach to understanding and engineering transportation systems' capabilities in order to withstand disruptions and thus maintain functionality at a satisfactory level.

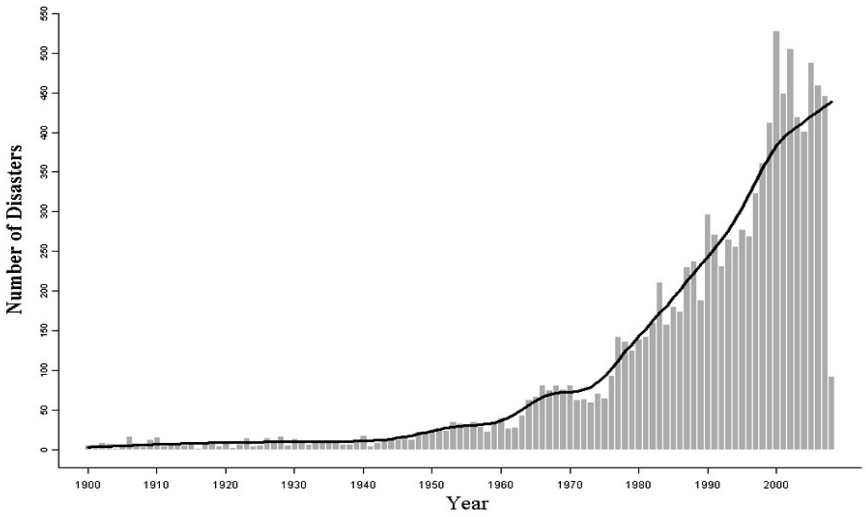

Fig.1.1 **Disaster frequency (Nagurney, 2011a)**

Error! Reference source not found. shows the increasing frequency of disasters, which are defined as an event satisfying one of the four criteria: *1) 10 or more people killed; 2) 100 or more people affected; 3) Declaration of a state of emergency; 4) Call for international assistance* (Nagurney, 2011a). These disasters are taken here to include events like the Indonesian tsunami, Hurricane Katrina, the Sichuan Wenchuan earthquake, the Haiti earthquake, floods in north-eastern Australia and Brazil and so on. These are all caused by nature. In the meantime, some disasters are caused by unexpected political situations, for example the Malaysia Airlines Flight 17 crash in Ukraine. In addition, terrorist attack are also increasingly rampant, for example the 9/11 attacks in 2001, the London bombings in 2005, the Paris attacks in 2015, and the Brussels bombings in 2016, and so on. Regardless of the type of these disasters, however, they all have the potential to result in the destruction of infrastructure and/or significant disruption. It is worth noting that such disasters do not only directly lead to loss of life and economic loss because of the degradation of the transport network, but they also indirectly cause further loss of life and economic loss since they may contribute to disruption in evacuation activities and the delivery of critical needs such as vaccines, medicine, food and water (Amdal and Swigart, 2010, Nagurney, 2011b).

The infrastructure mentioned here refers to physical infrastructure such as roads, bridges, energy services, water supplies and telecommunications, as well as social infrastructure such as education, emergency services, financial services and the health care system (Hughes and Healy, 2014), all of which are regarded worldwide as vital components of a healthy society and stable economy.

Croope (2010) states that, "critical infrastructure not only responds to the needs of society for the smooth daily continuation of activities, but also provides the basis on which society exists and relies".

Two reasons for the importance of the robustness and resilience of infrastructure are listed as follows by Godschalk (2002):

1. *Because the vulnerability of technological, natural, and social systems cannot be predicted completely, the ability to accommodate change gracefully and without catastrophic failure, is critical in times of disaster (Foster, 1997)*.
2. *People and property fare better in resilient cities struck by disasters, than in less flexible and adaptive places faced with uncommon stress. Fewer buildings collapse, fewer power outages occur, fewer businesses are put at risk, and fewer deaths and injuries occur.*

The first reason emphasizes the difficulty of predicting the exact effects of disasters and therefore the importance of broadly resilient systems, while the second reason points out the negative impacts caused by less resilient systems.

Transportation networks are the fundamental infrastructure for city living (Nagurney, 2011a). As a matter of fact, transportation networks have been playing an important role in underpinning our society and economy: providing for the movement of goods and people that is essential for the development of the economy. **Fig.1.2** shows how the growth of passenger travel and freight travel can be related to the growth in gross domestic product (GDP) in China from 1978 to 2012.

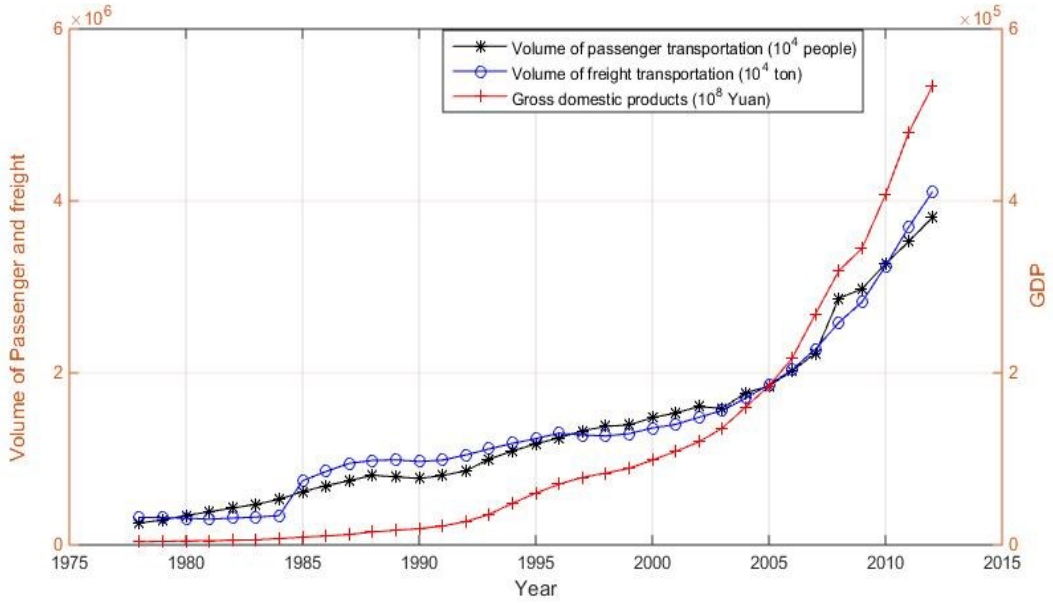

Fig.1.2 Growth of passenger travel, freight travel and gross domestic product (National Bureau of Statistics of China)

As can be seen from **Fig.1.2**, there is a positive relationship between national wealth and the amount of travel. More movements of people and goods lead to a higher volume of economic activities, which may generate more wealth. More money allows people to participate in a wider range of activities via travelling or, and encourages people to consume more frequently. In addition, more investment in transport infrastructure also stimulates the growth of the economy. This partially explains how transportation contributes to the expansion of economy.

In addition to these things, the importance of transport networks is also confirmed by the complex interdependencies between these transport networks and other infrastructure networks. For example, transport networks are able to be used for fuel transportation, which is shipped to supply electric networks and oil networks, and these energy networks in turn can provide power or other products to transportation networks. Hence performance fluctuations in transport networks may greatly influence other urban lifeline systems. Some of these interdependencies are presented in **Fig.1.3.**

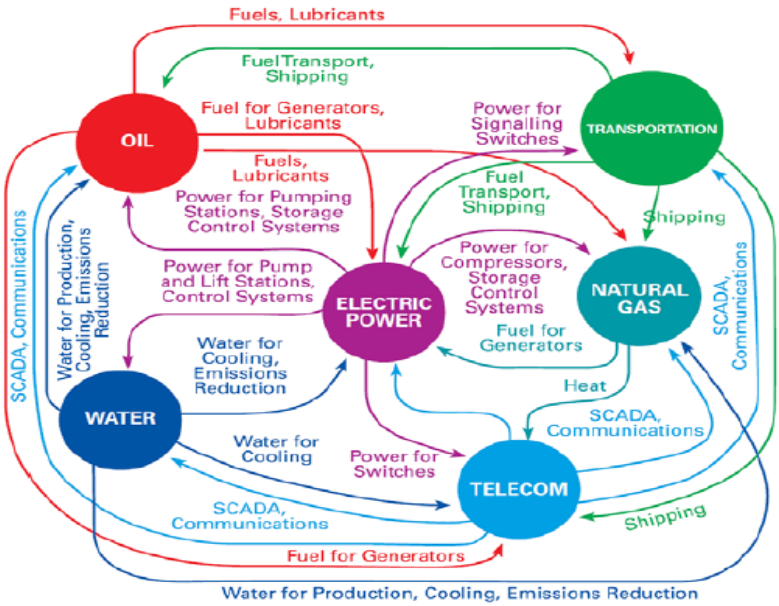

Fig.1.3 Complex interdependencies between transport networks and other infrastructure (O'Rourke, 2007)

Given the long-established reliance of societies and economies on transportation networks, appropriate assessments and analyses of the robustness and resilience of transport networks have been a central focus of network planning and management. Although many methods have been utilized to explore this robustness and resilience, these can generally be classified into two types. The first is topological indices based on complex network theory, which only takes into account the topology of networks. The other can be referred to as operational indices, which are based on traffic assignment taking into more complex factors such as travel demand, driver behaviour and link capacity. The following discussion explores these two broad approaches to transport network robustness and resilience more fully.

Complex network theory is a good tool to conduct such research from a topological perspective, and represent an active field of research stemming from network science, and starting from a famous problem – the Seven Bridges of Konigsberg. In 18th century, the city of Konigsberg (now its name is Kaliningrad) was divided by the Pregel river, and connected by the seven bridges (shown in **Fig.1.4**). The people in Konigsberg created a game that is to walk cross every bridge once and only once (Joli et al., 2010).

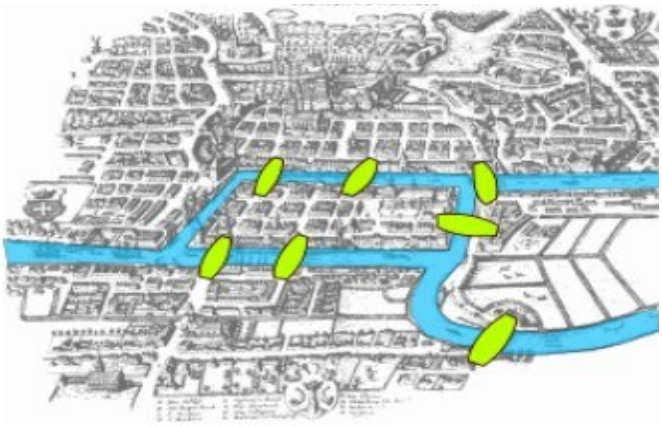

Fig.1.4 The Seven Bridges of Konigsberg (MacTutor History of Mathematics Archive, n.d.)

In the course of two centuries, and especially since the seminal work of Erdős and Rényi (1960), the scientific study of complex networks has advanced by leaps and bounds with a surge in the literature in relevant subjects. In Erdős and Rényi's (*ER*) model, the connections between nodes of graphs are random. When many people did not understand the mechanisms by which large-scale complex networks formed, this model was accepted due to its simplification. The *ER* model has dominated for nearly 40 years in network science field, until Watts and Strogats (1998) proposed a small-world network model. Following this, Barabasi and Albert published a paper in *Science* in which they proposed scale-free networks, whose degree distribution follows a power law (Barabasi and Albert, 1999). Both these findings greatly facilitated the development of complex network theory.

In the real world, many networks can be regarded as complex networks. Networks are regarded as the backbone of complex systems that consist of many components with many underlying properties are embedded in their topology. An understanding of the structure and relevant characteristics of this complicated world and how the components of such systems interact with each other is important. The range of complex networks research is broad ranging from the World Wide Web (WWW), biological networks to knowledge networks. **Fig.1.5** shows some examples.

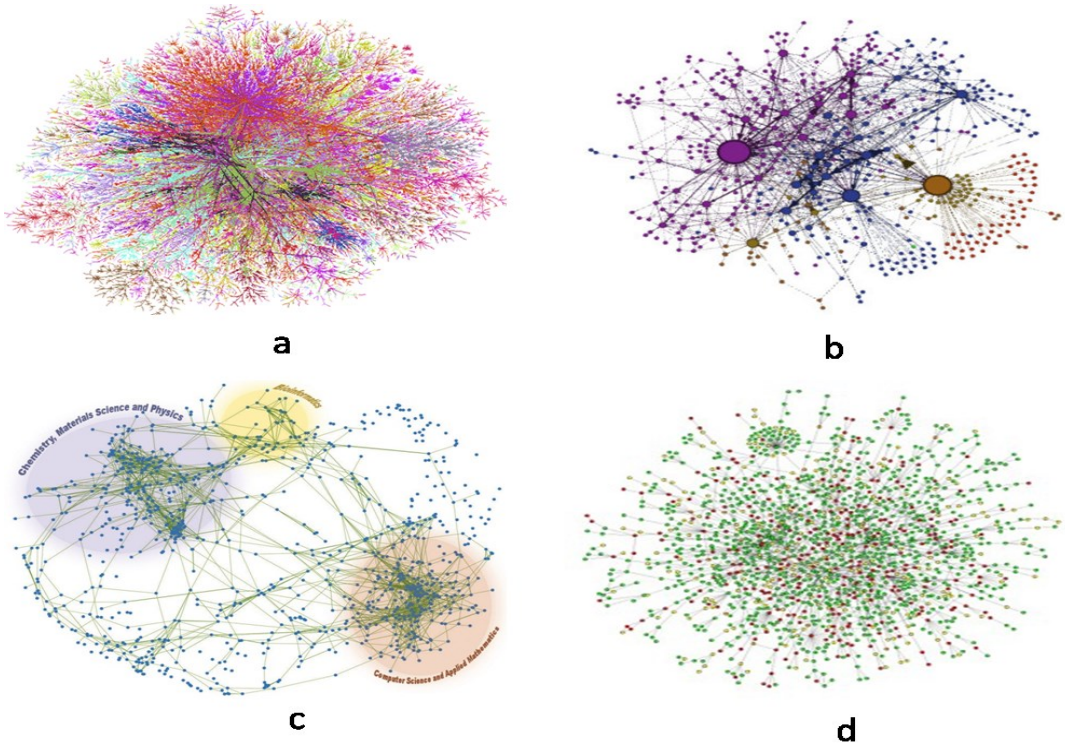

Fig.1.5 Examples of complex networks
(a) Internet network (Complex Networks-New Media Lab); (b) Social network(Physics.org); (c) Knowledge network(Complex Networks & Systems); (d) Biological network (Complex Networks-New Media Lab).

Whereas the structure and topology of simple networks can be directly observed visually , for large-scale networks, as shown in **Fig.1.5**, it is difficult to directly observe and understand such networked systems in depth. Transport networks can be regarded as complex systems in that, on the one hand, they tend to have many nodes and links, whereas on the other hand there are many phenomena such as small-worldness, scale-freeness (see definitions in **Section 2.1.3**) and communities embedded in such networks. Complex network theory provides many methods and indices of statistical mechanics to explore these complicated phenomena, including the characteristics of robustness and resilience that are the central focus in this thesis.

Many topological indices have been used for the exploration of robustness and resilience in complex network theory. For example, degree centrality, clustering coefficient, betweenness centrality, and so on, can be referred to as measures of robustness and resilience due to the fact that these indices are able to reflect the efficiency and functionality of networked systems (Holme et al., 2002, Crucitti

et al., 2003, Crucitti et al., 2004c, Albert et al., 2000a). These indices provide a relatively effective way to assess and analyse robustness and resilience due to their low computation time, but they are less likely to take into account more complex factors such as driver behaviour, travel demand and link capacity. In order to overcome such weaknesses, traffic assignment theory is also utilized to study the dynamics of network systems experiencing disruptions. Traffic assignment is one step within traffic planning models, and the four steps can be shown as follows (SHIFTAN, 2000, Meyer and Miller, 2000, Heydecker, n.d., Chow, 2007a):

1. *Trip generation* provides an estimation of trip frequency from each origin zone to each destination zone, which is dependent on land uses, social-economic factors and household demographics.
2. *Trip distribution* provides an estimation of trip frequency between each Origin-Destination (O-D) pair, which can be obtained by a gravity model or an entropy maximizing model (Levinson and Kumar, 1995).
3. *Mode choice* computes the proportion of trip frequency between O-D pairs that use a certain type of transportation mode.
4. *Traffic assignment* allocates trips in a particular mode between an O-D pair to routes of this O-D.

Traffic assignment problems seek to distribute traffic to certain routes by following traffic assignment principles, most notably Wardrop's user equilibrium (UE) and system optimal (SO) principles (Wardrop, 1952), and taking into account the behaviour of users. The UE principle assumes that each individual driver seeks to minimize his/her disutility selfishly with rational behaviour under perfect knowledge of the network. On the other hand, the SO principle assumes that drivers behave in a collaborative way or that there exists a centralized control such that the network-wide benefits (or disutility) are maximized (or minimized). These two principles therefore explore the traffic flow distribution from user-optimal and system-optimal perspectives. If

disruptions occur, the route flow and total costs vary accordingly. Based on this, the robustness and resilience of networks can be analysed and assessed.

Under the principles of UE and SO, drivers, or a central authority, are assumed to have perfect knowledge of route costs and route flows, and their decisions are completely rational. Traffic assignment is largely influenced by information provision, however, and complete information and absolutely rational decisions are ideal abstractions of reality. In the real world, perfect information is rarely attainable in the event of disruptions due to sudden changes in the network structure or traffic conditions, and therefore drivers' perceptions regarding certain routes may change depending on their travel experience. In this context, *Day-to-day* (DTD) traffic assignment models are appropriate for analyzing how traffic flows evolve under disequilibrium conditions due to their flexibility in terms of accommodating various behavioural rules and different levels of aggregation (Friesz et al., 1994, Watling and Hazelton, 2003, Bie and Lo, 2010, Cantarella, 2013). In this thesis, DTD evolutionary dynamics are utilized to describe and predict the daily variation of traffic flows and drivers' route adjustment processes.

In order to explore and improve the ability of urban road networks to withstand disturbances and maintain satisfactory performance, a considerable number of control measures are employed to mitigate the immediate negative impacts of local or global disruptions, and provide means to guide traffic towards long-term and stable network states. Among these control mechanisms, Variable Message Signs (VMS) and adaptive traffic signal control have been widely adopted

Variable Message Signs (VMS) are usually installed along roadsides to disseminate information to drivers (Huo and Levision, 2003, Han et al., 2015a). In general, such facilities can present information about congestion, incidents, roadwork zones and speed limits, and they may also be used to suggest alternative routes to enable drivers to avoid the locations of incidents. A complete message on a VMS board includes a problem statement (e.g. roadwork, special event and incident), a location statement such as where the special event happens, an effect statement (e.g. the degree of capacity

degradation, delay and closure), and may also include an action statement on what to do (New York, Deparment of Tansportation. 2001).

As an instrument for temporal and spatial management of congestion (Durand-Raucher et al., 1993, Bierlaire et al., 2006), Variable Message Sign (VMS) boards have been used more frequently to provide traffic information (Transport Bureau, 1998).

In addition to VMS, nowadays, a large number of road intersections are controlled by traffic signals, especially within urban areas (Meneguzzer, 2012). Adaptive signal control is an effective way to improve the performance of urban road networks (URNs) and thus to mitigate congestion and delays by adjusting the red/green time split based on information on route costs (Liu et al., 2015). **Fig.1.6** presents how adaptive signal control mutually react with route choices.

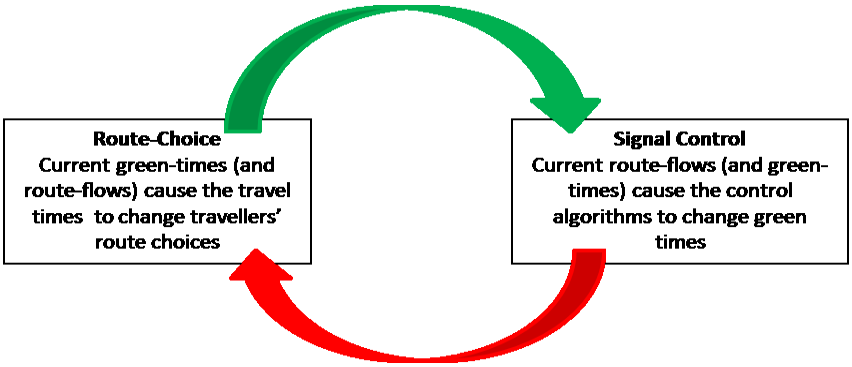

Fig.1.6 Dynamic systems of adaptive signal control (Smith, 2012)

As can be seen from **Fig.1.6**, the green/red time split may cause extra delay, which changes the route flow and route costs. Since drivers always prefer to using quicker routes, such delays cause changes in route choices. This loop vividly shows how adaptive signal control can change flow patterns within the network.

Based on the above descriptions, it is very promising to utilize such control strategies to adjust the route flows to improve robustness and resilience of networks experiencing internal or external disruptions.

Although methods based on traffic assignment such as user equilibrium and system optimization capture many realistic characteristics of systems, they consume a lot of computational effort. Overall, therefore, methods based on complex network theory and those based on traffic assignment each have their own advantages and disadvantages, and, while many measures and indices exist for the measurement of robustness and resilience, there is currently a lack of systematic ways to measure robustness and resilience quantitatively from both topological and operational perspectives. These will be further explored in **Chapter 3**.

1.2 Aims and objectives

Given the background introduced in the previous section, the aim of this research is to develop a systematic methodology quantitatively to assess and analyse the robustness and resilience of urban road networks (URNs) by taking into account network characteristics such as topology, path flows, user behaviours, network capacity and control measures. Several objectives have been formulated to achieve this goal.

A. Define the robustness and resilience of URNs based on a systematic review of the current research into robustness and resilience in order to make sure the definitions facilitate the quantification of robustness and resilience by taking into account the characteristics of URNs such as network topology, path flows, user behaviours and network capacity (achieved in **Chapter 3**).

B. Identify the types of disruptions that URNs may suffer from, and the way in which these affect the networks (achieved in **Chapter 3**).

C. Explore the topological characteristics of URNs from different countries by using topological indices to measure robustness and resilience, and explore the communities and hierarchical structure to identify the underlying characteristics of the URNs (achieved in **Chapter 4**).

D. Model and analyse the robustness of URNs based on topological indices and operational indices that are calculated from both user equilibrium (UE) and system optimal (SO) traffic assignment models, and then explore the potential relationships between topological and operational indices (achieved in **Chapter 5**).

E. Develop a new index, the Relative Area Index (*RAI*), to quantify the robustness of different sizes of URNs with under global/local disruptions (achieved in **Chapter 5**).

F. Develop an agent-based day-to-day (ABDTD) model allowing drivers to communicate within certain groups, which are determined by an information propagation mechanism, so as to capture the irrational behaviour of heterogeneous drivers (achieved in **Chapter 6**).

G. Develop appropriate indices based on the definitions of robustness and resilience to quantify the robustness and resilience of URNs suffering from local disruptions (achieved in **Chapter 7**).

H. Model and analyse the robustness and resilience of URNs based on day-to-day evolutionary dynamics under various control strategies, such as information accessibility, VMS and signal control (achieved in **Chapter 7**).

1.3 Outlines of the Thesis

This thesis consists of eight chapters. Chapter one mainly introduces the background of this thesis, its aim, objectives, and the outline and structure.

In **Chapter 2**, the main methodologies and preliminaries frequently used in this thesis are introduced, such as complex network theory, the main traffic assignment principles and day-to-day evolution dynamic models. For the complex network theory, the definition and topological indices including degree centrality, closeness centrality and betweenness centrality are introduced. Traffic demand, traffic supply and traffic assignment principles, both for user equilibrium (UE) and system optimization (SO), are illustrated as three components of traffic assignment. Day-to-day evolution

dynamic models, including their cost updating process, route choice models and network loading mechanisms are also introduced.

In **Chapter 3**, the applications of complex network theory, robustness and resilience, classification of disruptions, DTD traffic evolution model and traffic control are systematically reviewed from the application side. The review of the applications of complex network theory mainly focuses on social networks, biological networks, resource networks and transport networks. Following this, robustness and resilience are reviewed from the existing definitions and measures so as to define and confirm the focus of robustness and resilience in this thesis. The review of disruptions serves to confirm the way that disruptions influence URNs. Through the review of the applications of DTD dynamic models, the gaps in this field and the advantages of DTD models are presented. Finally, transport control such as variable message signs (VMS) and adaptive signal control are reviewed.

Chapter 4 and **Chapter 5** assess the robustness of URNs based on topological characteristics.

In **Chapter 4**, nine selected urban road networks (URNs) are investigated to explore their topological characteristics. Widely used topological indices, such as indegree/outdegree, weighted closeness, clustering coefficient and weighted betweenness centrality are utilized to assess and analyse the topological properties of URNs from different perspectives. In order to discover the underlying characteristics of URNs, distributions of indegree and outdegree, weighted closeness and weighted betweenness are examined so as to observe the types of such distributions, which may suggest certain dynamic mechanisms of URNs in terms of connectivity. Small world analysis of these URNs are conducted by comparing average path length (*APL*) and clustering coefficient (*CC*) in random networks having the same number of nodes and links. Furthermore, correlation analyses of indegree and outdegree, degree-betweenness and degree-clustering coefficient are investigated so as to find out their inherent structural properties. In order to observe the hierarchical and structural characteristics of these URNs, the Order Statistics Local Optimization Method (OSLOM) is utilized to

detect communities and hierarchies of the URNs. This chapter facilitates a better understanding of URNs.

Following **Chapter 4**, **Chapter 5** explores the robustness of URNs using topological indices and operational indices. These topological indices are all based on complex network theory, while operational indices are based on traditional traffic principles: UE and SO. Such topological indices are able to examine the importance of nodes in the URNs by the magnitude of the indices for each node, and the efficiency measure based on average path length (*APL*) is also able to rank the importance of nodes. Operational indices such as the relative total cost of user equilibrium (RTC_{UE}^{i}) and system optimal (RTC_{SO}^{i}) and the relative price of anarchy ($RPOA^{i}$) are utilized to analyse which nodes are most important in influencing the robustness of URNs by repeatedly calculating when individual nodes are removed. Due to the fact that operational indices take into account many factors, such as road capacity, travel demand and driver behaviours, they take more time to calculate than topological indices. Efforts are therefore made here to look for relationships between topological indices and operational indices. In addition, a new Relative Area Index (RAI) is proposed quantitatively to measure the robustness of URNs suffering from global disruptions.

Chapter 6 and **Chapter 7** assess the robustness and resilience of URNs based on day-to-day dynamic models.

In **Chapter 6**, a novel agent-based day-to-day (ABDTD) traffic evolution model with information percolation is proposed to investigate the impact of communication networks on road traffic networks. The ABDTD model assumes that drivers do not have perfect information of route costs, and they may share the information within a certain group of drivers, which is generated by percolation theory. Information percolation happens at a cyber layer representing communication networks between drivers with bounded rationality, while a physical layer represents day-to-day transport networks with drivers who learn route perceptions not only from their own experience but also from other drivers' in the same group. In this model, all drivers selfishly make routing decisions

to minimize their own route cost. A numerical study is presented to study the relationship between the information percolation rate and the speed of convergence, and further validation is conducted by statistical analysis, taking into account the stochastic nature of the model. Following this, a sensitivity analysis for key parameters is also conducted. This chapter proves that the novel ABDTD model is able to be used to explore quantitative properties of transport networks such as robustness and resilience.

Chapter 7 illustrates how the transport network evolves over time under different control mechanisms, such as VMS and signal control, when the network suffers from different levels of disruptions. Rapidity and the new relative area index (RAI) are proposed to measure the resilience and robustness of the network, respectively. At disaggregate flow levels, information percolation, VMS with different compliance rates (*CR*) and signal control are incorporated into the ABDTD model to observe how resilience and robustness vary as mild, moderate and severe disruptions are imposed on the network. At the aggregate flow level, a continuous flow DTD (CFDTD) model is used to investigate the effects on the robustness and resilience of networks experiencing different levels of disruptions of signal control applying policies such as equi-saturation policy and P0 policy (details can be found in **Section 7.2**), with fixed-time signal control being used as a benchmark. In this context, robustness and resilience can be quantitatively assessed so as to analyse the effectiveness of signal control, and the importance ranking of links of the networks can also be listed in terms of rapidity and RAI.

Chapter 8 confirms the conclusions and contributions achieved in this thesis, points out its limitations and makes recommendations for future research.

Based on above descriptions, the outline of this thesis can be shown in **Fig.1.7.**

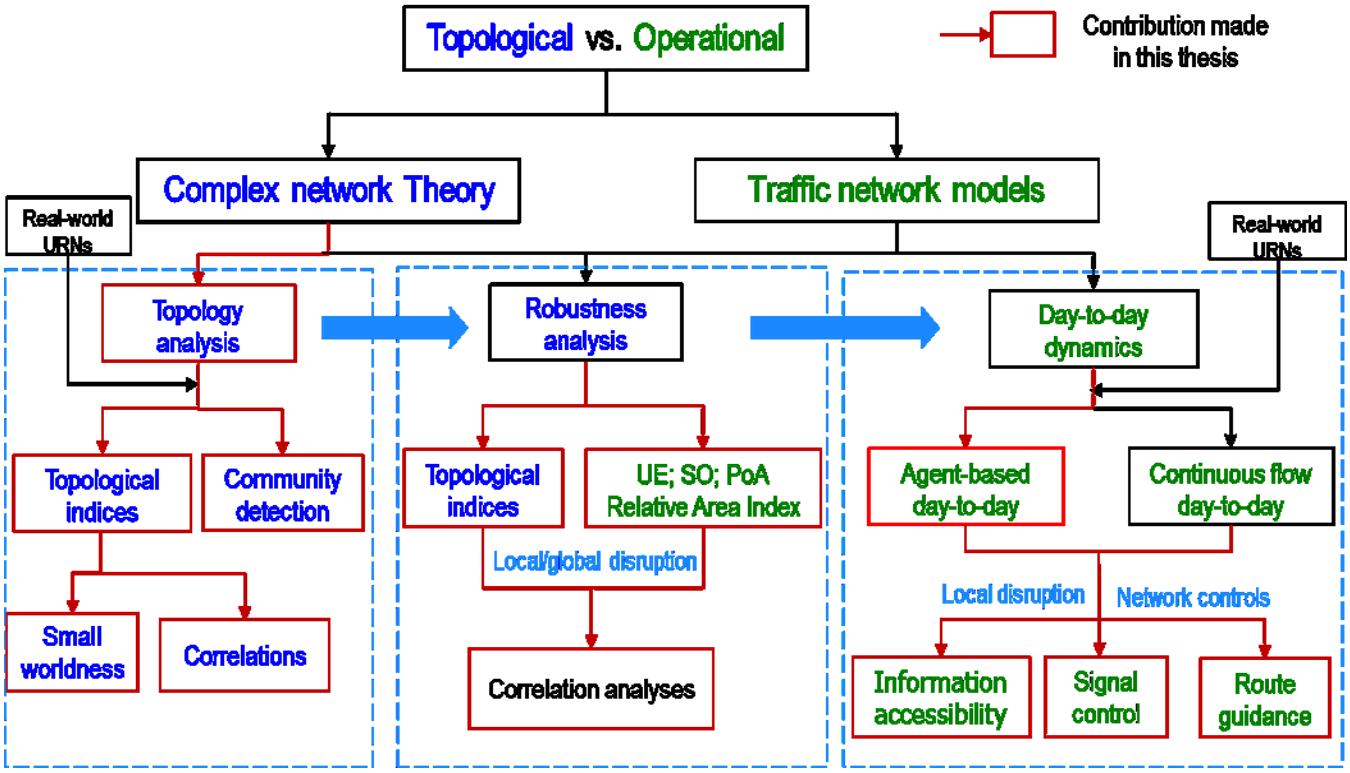

Fig.1.7 Outline of this thesis

As can be seen, the structure of the thesis and the connections between each section are clearly shown in **Fig.1.7.** In addition, contributions made in this thesis are also presented with the red line and box, and the specific-claimed contributions will be discussed in detail in **Chapter 8**.

Chapter 2 METHODOLOGY AND PRELIMINARIES

This chapter introduces the main methodologies and preliminaries frequently used in this thesis, including complex network theory, traffic assignment and day-to-day evolution dynamic models. Commonly used topological indices such as degree centrality, closeness centrality, clustering coefficient and betweenness centrality are reviewed; and relevant mathematical details of methods network science are introduced. Regard traffic network modelling, this thesis reviews some essential components of traffic assignment, in particular network loading and route choice principles (e.g. user equilibrium, system optimal). Finally, day-to-day evolution dynamic models, including their cost updating process, route choice models and network loading mechanisms are also introduced.

2.1 Complex Network Theory

Complex network theory gives rise to a great number of methods and performance indices to explore the topological characteristics of networked systems. Some commonly used topological indices are utilized in this thesis for the analysis of the topological characteristics of urban road networks (URNs).

2.1.1 Definition of complex networks

Kim and Wilhelm (2008) explored the complexity of graphs so as to answer the question of what is a complex graph. They proposed some measures to quantify the complexity of graphs and regarded graph including many different subgraphs as being complex. Regarding complex networks, however, there is no a clear definition so far. The famous Chinese scientist Qian Xuesen adopted a relatively strict conception, that is, a complex network is a network which has all or some of the features of self-organization, self-similarity, small-worldness and scale-freeness (Baidubaike). A complex network is able to be utilized to simulate systems with many interacting components.

2.1.2 Topological indices of complex network theory

2.1.2.1 Degree centrality and its distribution

The degree centrality (*k*) of a node i in an undirected network (i.e. the links are undirecitonal) is the number of links connecting to this node (Barabasi and Albert, 1999), and is formulated as follows:

$$k_i = \sum_j \alpha_{ij} \tag{2.1}$$

where α_{ij} is the connection between node *i* and node *j*; if *i* and *j* are connected αa_{ij} is 1 otherwise it is 0.This is a seemingly simple yet very important index, since it reflects the node's connectivity and its importance in its vicinity. The degree of a network is the average of the degree of all its nodes. A larger network degree implies better connectivity within the network. In some cases, road networks are directional, thus the degree centrality can be divided into indegree and outdegree, which refers to the number of links coming into a given node and those going out from the node, respectively.

The degree distribution of the network $P(k)$ is a ratio of the number of nodes with degree k to the number of all nodes and depicts the connective mechanism of networks.

2.1.2.2 Clustering Coefficient

The clustering coefficient of a node *i* (CC_i) reflects the local feature and clustering effect of the network. It can be written mathematically as:

$$CC_i = \frac{EE_i}{k_i(k_i - 1)/2} \tag{2.2}$$

where EE_i is the actual number of edges between the neighbours of node *i* (nodes connected with node *i* are called its neighbours); k_i is the number of the neighbours of node *i* (Watts and Strogats, 1998). **Fig.2.1** shows an example on the calculation of *CC* of the red node. In social networks, this index tends to measure how close the friends of a given individual are.

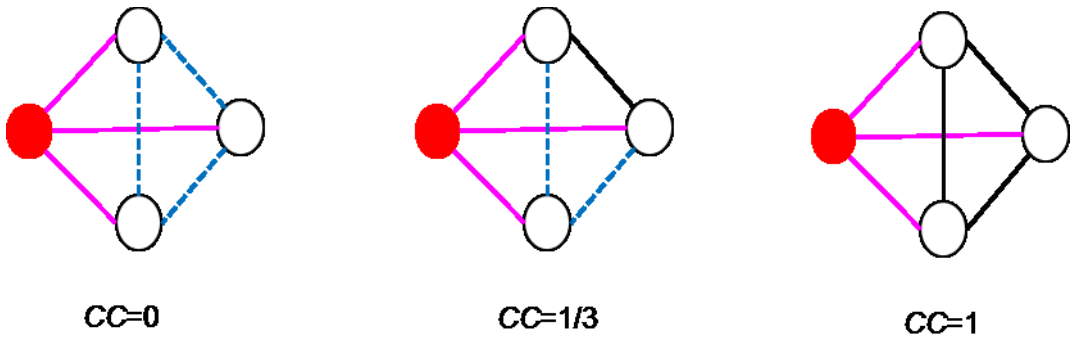

Fig.2.1 Example on clustering coefficient of an undirected network

2.1.2.3 Average Path Length

Average path length (*APL*) is defined as the average length along the shortest paths between any pair of nodes, and can be shown in the following equation:

$$APL = \frac{1}{n(n-1)/2} \sum_{i>j} D_{ij} \tag{2.3}$$

where D_{ij} is the length of the shortest path between *i* and *j.* For un-weighted networks (i.e. every link has equal length of 1), D_{ij} is the number of links of the shortest path between *i* and *j*; while for weighted networks, assuming that the weight is simply physical distance, D_{ij} is physical distance of

shortest path from node *i* to *j*. *APL*, also called the characteristic path length, can be employed to quantify the structural characteristics of networks (Watts and Strogats, 1998). The diameter (*SD*) of the network is the maximum D_{ij} for all node pairs. The *APL* and the *SD* are usually used to measure the efficiency and transport performance of the network.

2.1.2.4 Closeness Centrality

The closeness centrality (Sabidussi, 1966) of a node i is the inverse of the sum of the shortest path distance from node i to other nodes, and is normalized by $n-1$; it is written as:

$$C_i = \frac{n-1}{\sum_{v_j \in V, i \neq j} D_{ij}} \tag{2.4}$$

where *V* is the set of nodes, $V = \{v_j : j = 1,2,\dots,n\}$, *n* is the number of nodes. This index is used to measure the accessibility of the other nodes from the node i.

2.1.2.5 Betweenness Centrality

Betweenness centrality (BC_i) is defined to examine the importance of each node *i*, and can be mathematically expressed as follows:

$$BC_i = \sum_{j,z \in V} \frac{NS_{jz}(i)}{NS_{jz}} \tag{2.5}$$

where $NS_{jz}(i)$ is the number of shortest paths passing through the node *i*, and NS_{jz} is the total number of shortest paths between any pair of nodes. The edge weight is the actual distance of the link, hence it is called weighted Betweenness centrality.

Betweenness measures how frequently a node lies in the critical paths of different networks and thus represents the importance of the nodes in networks. This is beneficial for identifying crucial components so as to assess the robustness of networks experiencing disruption.

2.1.2.6 Efficiency

This index was first proposed by Crucitti et al. (2003) to explore the global efficiency of complex networks and looks very similar to *APL;* for directed and un-weighted networks, it is written as follows:

$$Eff(G) = \frac{1}{n(n-1)} \sum_{i \neq j \in G} \frac{1}{D_{ij}} \quad (2.6)$$

Due to the fact that $sd_{ij} \geq 1$, and the efficiency index (*Eff*) is normalized by the maximum number of links (apparently $\sum_{i \neq j \in G} \frac{1}{D_{ij}} \leq n(n-1)$), so $0 \leq Eff(G) \leq 1$. For undirected networks, the maximum number of links is $\frac{n(n-1)}{2}$, and $i < j \in G$. If the non-weighted network is completely connected, $Eff(G) = 1$. In this thesis, actual distance is assigned to the weight of a link. The greater Eff, the better efficiency.

2.1.2.7 Size of largest connected sub-graph

The largest connected sub-graph of a network is also known as the largest cluster. If a network is connected, the size of the largest connected sub-graph is equal to the number of all the nodes. When the network experiences disruption, it becomes disconnected and several sub-graphs may be formed. The variation of this index is regarded as the simplest indicator by which to measure the resilience of networks, and it is consistent with the giant component of models of percolation theory (Newman, 2003). Observing the evolution of size over time is important to assess the error and attack tolerance of large-scale and homogenous networks.

2.1.3 Classical complex network models

2.1.3.1 Regular Networks

Originally, for the purpose of simplification, mathematicians deemed that all networked systems could be represented by regular networks, whose main feature is that each node has the same number of connections (see **Fig.2.2**).

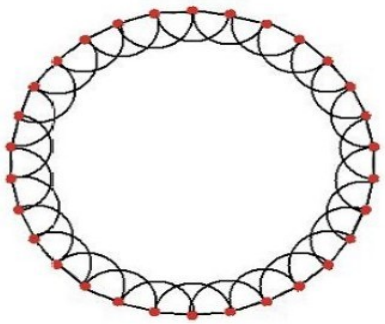

Fig.2.2 Regular network (Hamill and Gilbert, 2009)

For regular networks, the probability of giving rise to connections between arbitrary nodes from networks is the same, the topological characteristics of each node are identical and thus the network is symmetrical and regular.

2.1.3.2 Random Networks

The random network model was proposed by Erdős and Rényi (1960), and hence it is also called the *ER* model. *ER* networks are built as follows: the connections between nodes depend on a probability P_c, if the value of *P* is small, the network is sparse; with the increase of P_c, the network becomes more and more intensive, until when P_c=1, it becomes a complete graph. The whole process is shown in **Fig.2.3**. The degree distribution of *ER* networks follows a Poisson distribution, written as $P_c(k) = \frac{\langle k \rangle^n}{n!} e^{-\langle k \rangle}$, where $\langle k \rangle$ is the average degree of a random network ($\langle k \rangle = \frac{\sum_{i \in n} k_i}{n}$).

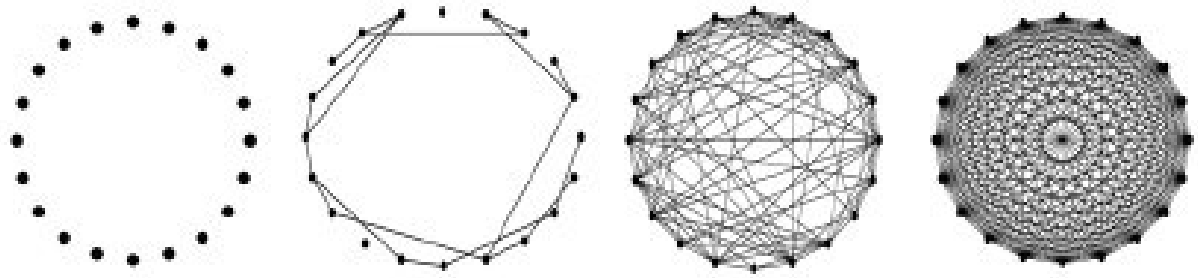

P_c=0 P_c=0.1 P_c=0.5 P_c=1

Fig.2.3 Dynamic evolution of random networks with the increase of P (Barabasi and Albert, 1999)

2.1.3.3 Small world networks

It is believed that the small-world effect was first mentioned by Karkubthy (1929) and mathematically presented by Pool and Kochen (1978). The first experiment was conducted by Stanley Milgram in the 1960s. This experiment was designed to test how many deliveries were on average needed to deliver a package from a person to a targeted individual in another city. The result from this experiment showed that it took on average six deliveries, so it was also called 'six degrees of separation' (Milgram, 1967). Watts and Strogats (1998) constructed networks which lie between regular and random networks, and named these "small-world" networks by analogy with Milgram's conclusion. **Fig.2.4** shows the process through which a complete regular network transforms into a complete random network with the increase of *P* value, which is the probability of rewiring a chosen node with another uniformly chosen node; the middle example in the figure represents a small-world network.

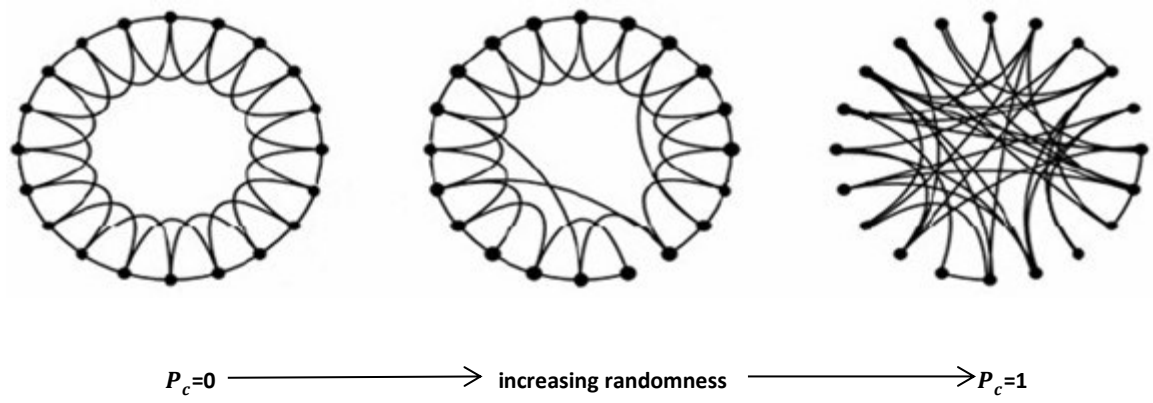

Fig.2.4 WS network model (Watts and Strogats, 1998)

Small-world networks have an *APL* as small as APL_{random} yet $CC \gg CC_{random}$ compared to random networks with the same nodes and edges (Watts and Strogats, 1998). Newman (2003) claimed that the value of the average shortest path scales logarithmically or less with network size for a fixed mean degree. Another way to generate a small world network is by preferentially adding new connections to existing nodes which already have many connections (Fell and Wagner, 2000).

2.1.3.4 Scale-free networks

The earliest published example of scale-free networks are citation networks between scientific papers (Price, 1965). This idea is built on the work by Simon (1955), which states that the effect of 'the rich getting richer' leads to the power laws. In sociology this is called the Matthew effect (Merton, 1968), taking its name from the Bible: *for unto every one that hath shall be given….*(Matthew: 25:29). It is also referred to as a cumulative advantage by Price, and today it is known as preferential attachment.

In recent years many important discoveries concerning complex networks have shown that the degree distribution of networks follows a power law, such as in respect to the Internet (Mitzenmacher, 2004) and metabolism networks (Bellafiore et al., 2005). Due to the fact that the characteristics of individual nodes in such networks are difficult to measure with the same scale used to measure other nodes, they are called scale-free.

The reason for the formation of scale-free networks is that these networks expand by adding new nodes constantly and these new nodes tend to connect those nodes with many connections, in other words, the combination of growth and preferential addition caused such features (Barabasi and Albert, 1999).

Scale-free networks are therefore generally dominated by a few nodes and their behaviour characteristics can be predicted. This means that scale-free networks have both vulnerability and robustness; that is, their endurance to random attack is reasonable but their ability to withstand targeted attacks is poor (Li, 2009).

This section has introduced complex network theory, which is used to explore robustness and resilience from the topological perspective. In next section, traffic assignment, which is applied to the exploration of robustness and resilience from the operational perspective, is introduced.

2.2 Traffic assignment

A traffic assignment model consists of three main components: demand for travel (usually in the form of trip table or matrix), supply for travel (represented as the network, its link parameters, signal control parameters, etc.), and the route choice principle, which allocates available resources (i.e. network capacity) to travel demands. In practice, since simplification and abstraction are used to model such components there will inevitably be some errors that will affect the procedures and results of assignment. The balance between the simplification of various inputs and the degree of accuracy therefore needs to be considered (Heydecker, n.d.).

2.2.1 Demand for travel

Demand is the utility that an economic agent can acquire through a good or service. In the field of transportation, demand is specific to demand for travel, and most travels are purposive and consume time and money. Mokhtarian et al. (2001) stated that travel has intrinsic positive utility and can be valued for its own sake. Travel itself is regarded as a derived demand, which means travels facilitate people to participate in desired activities or to gain access to desired goods or services at a certain destination.

In static traffic models, the demand for travel is usually represented by a trip-matrix or trip table, and the element of this matrix, t_{od} denotes the travel frequency from an *origin* zone *o* to a destination zone *d* within a certain time interval. Here, the term zone refers to a partition of an urban area (Chow, 2007b). Various types of data, such as demographic features and levels of economic activity, can be utilized to calibrate and validate traffic demand (Ortúzar and Willumsen, 2001). The trip-matrix of the network system consists of a trip-end zoning system and the time period. The trip-matrix can be for a whole day or any particular period within the day (such as peak hours) in order to account for the variation of travel demand throughout the day. In this thesis, the traffic assignment model can target any period of a day with a steady flow pattern and fixed trip table. Unless stated otherwise, this thesis always treats the traffic demand as exogenous and

inelastic. Travel demand can be satisfied by appropriate facilities such as buses, trains and roads (Heydecker, n.d.).

2.2.2 Supply for transport networks

Traffic assignment is mainly concerned with allocating network supply (in terms of available road capacity) to travel demands. The supply aspect of a transport system refers to network-specific characteristics and parameters. The transport networks are physical networks and can be represented as a directed graph $G(V, E)$ with a set of nodes *V* and links *E*. For urban road networks, nodes represent the intersections and links representing the road segments between nodes. The representation of intersections in urban road networks struggles to represent turning restrictions (Sheffi, 1985), but since this thesis studies traffic from macro perspective, the flow assignment at junctions at the micro level can be aggregated to a node.

The combinations of nodes and links determine the topology of the transport networks of interest, which provides basic information on the availability of routes that drivers may follow. The following link-specific attributes or variables have a great impact on the route choice and route delays (Heydecker, n.d.):

- Link length (exogenous)
- Link capacity (exogenous)
- Free flow travel time (exogenous)
- Number of stops (exogenous)
- Road type (exogenous)
- Link delay (endogenous)

This thesis assumes that all these quantities except link delay are not able to be influenced by other variables, so they are exogenous. While link delay is endogenous because it depends on the traffic flow on the links, and needs to be calculated based on certain delay functions. A travel time function

for links was proposed by the UK Department of the Environment (1971), and can be shown as follows:

$$t(f) = \begin{cases} {}^{D}/_{S_0} & (0 \le f \le F_{max}) \\ {}^{D}\Big/[S_0 - \frac{(f - F_{max})}{(CP - F_{max})}(S_0 - S_{CP})] & (F_{max} \le f \le CP) \\ {}^{D}/_{S_{CP}} + \frac{f - CP}{8CP} & (CP \le f) \end{cases} \quad \textbf{(2.7)}$$

Where t is the travel delay for the link;

f is the flow on the link;

D is the length of the link;

S_0 is the free flow speed;

CP is the capacity of the link;

S_{CP} is the speed at which capacity is full;

F_{max} is the maximum flow at the free flow speed.

Equation (2.7) is based on the relationship between speed and traffic flow and shows that congestion occurs when the link flow is greater than a threshold, F_{max}, and congestion becomes worse when the flow is above the capacity of the links (over-saturation).

The US Bureau of Public Roads (1964) (BPR) link performance function is another popular choice:

$$t(f) = A_0(1 + \alpha\left(\frac{f}{CP}\right)^{\sigma}) \quad \textbf{(2.8)}$$

where A_0 is the free flow travel time;

α, σ are positive constants.

In general, α and σ are recommended to take 0.15 and 4, which means that travel time will increase by 15% when the flow reaches its capacity and the delay will exponentially increase to the power 4 when the flow exceeds the capacity of the links.

Another function was proposed by Greenshields (1934):

$$t(f) = {2A_0}\Big/{(1 \pm \sqrt{1 - {f}/{CP}})} \quad (2.9)$$

In this function, flow is not allowed to exceed the capacity, so equation (2.9) simply calculates the travel time at low density flow, and this is less practical compared to the other two functions. Equation (2.7) and (2.8) are more realistic and are able to calculate the travel times when flow exceeds capacity. In addition, these two functions both present different sensitivities for travel times at different flow levels. If the flow is low, the sensitivity to the travel time is low as well, while the sensitivity will increase as the flow level increases. In this thesis, the BPR function for the calculation of link travel time is preferred due to the fact that it is simpler than function (2.7) and also captures the sensitivity of travel times to flow levels. Furthermore, the path or route is defined as the set of links sequentially leading one node to another and, accordingly, path cost or route cost is the sum of the travel costs along the links comprising the path or route (Chow, 2007b).

2.2.3 Traffic Assignment Principles

Traffic assignment is one important step in traffic planning models, which are basically divided into four steps: trip generation, trip distribution, mode choice and traffic assignment. This has been discussed in chapter one. Traffic assignment has played an important role in estimating the traffic states in road networks given certain information on the demand and modal choice. Traffic assignment models determine the allocation of trip rates on the routes between O-D pairs. For decades, research in traffic assignment has been largely influenced by Wardrop's first and second principles, namely User Equilibrium (UE) and System Optimal (SO).

2.2.3.1 User Equilibrium (UE)

Wardrop (1952) observed the behaviour of individual drivers selfishly pursuing personal interest maximisation and proposed a modelling principle, which is commonly called Wardrop's first principle (W1) and can be stated as follows:

"The journey times on all routes actually used are equal, and less than those which would be experienced by a single vehicle on any unused route."

UE is based on this principle, and states that *no single driver can reduce travel costs by unilaterally changing route.* UE used in this thesis follows the following assumptions:

1) Drivers have perfect knowledge of all paths. The perfect knowledge means the travel time of paths is known, and it is worth noting that drivers are assumed not only to know the travel costs of paths they have experienced, but also to know the travel costs of those paths they never experienced.
2) Travel time on a given link is a function of the flow on that link only, and travel time is the only criterion of drivers' route choice under identical conditions.
3) Functions of travel time are monotonically increasing.

Assuming there is a general network, $G(V, E)$, where V is a set of nodes and E is a set of arcs. this thesis uses W to denote a set of origin-destination (OD) pairs and $(o, d) \in W$ denotes an OD pair. T_{od} is denoted as a fixed travel demand. In addition, $\bar{u}_{od}$ is defined as the minimum travel cost for an OD pair $(o, d) \in W$, and the set of paths for an OD pair $(o, d) \in W$ is defined as R_{od}, while c_r denotes the unit travel cost over path $r \in R_{od}$. Furthermore, h_r is used to denote the flow on path r, then we are able to say that a user equilibrium is a vector $h = (h_r : r \in R) \geq 0$ obeying the following:

$$h_r > 0, r \in R_{od} \Rightarrow c_r = \bar{u}_{od} \quad \textbf{(2.10)}$$

where $\bar{u}_{od} = \min_{r \in R_{od}} c_r$.

Path costs can be shown in the following way:

$$c_r = \sum_{a \in E} \delta_{ar} c_a(f) \quad \forall r \in R \tag{2.11}$$

where $c_a$is a unit cost function depending on the arc flows $f = (f_a : a \in E)$, here f_a denotes flows on each arc $a \in E$. δ_{ar} is a link-path incident matrix:

$$\delta_{ar} = \begin{cases} 1 & if\ a \text{ belongs to } r \\ 0 & if\ a \text{ does not belong to } r \end{cases}$$

The UE holds the flow conservation:

$$T_{od} - \sum_{r \in R_{od}} h_r = 0 \qquad \forall (o,d) \in W \tag{2.12}$$

Then the set of feasible flows is presented as:

$$\gamma = \left\{ h \geq 0 : T_{od} - \sum_{r \in R_{od}} h_r = 0 \ \forall (o,d) \in W \right\} \tag{2.13}$$

(2.13) describes that demand for O-D pair (o,d) equals to the sum of path flow over all paths of O-D pair (o,d). The above user equilibrium is widely accepted as a variational inequality (*VI*) problem, and can be restated as follows:

Theorem 2.1. *User equilibrium as a variational inequality. The flow pattern* $h^* = (h_r^* : r \in R)$ *is a user equilibrium if and only if*

$$\left. \begin{matrix} h^* \in \Lambda \\ \sum_{r \in R} c_r (h_r - h_r^*) \geq 0 \end{matrix} \qquad \forall h \in \gamma \right\} \quad VI(c, \gamma) \tag{2.14}$$

The proof is divided into two parts (Friesz, 2010):

(a) $\left[UE(c,\gamma) \Rightarrow VI(c,\gamma) \right]$

Note that $c_r(h^*) \geq \bar{u}_{od}$

For any $r \in R$,

$$c_r(h^*)(h_r - h_r^*) \geq \bar{u}_{od}\,(h_r - h_r^*) \tag{2.15}$$

If $(h_r - h_r^*)$<0, for then

$$h_r^* > h_r \geq 0 \Rightarrow c_r(h^*) = \bar{u}_{od}$$

Therefore, summing (2.15) over paths, then *VI* (2.14) is obtained.

(b) $[VI(c,\gamma) \Rightarrow UE(c,\gamma)]$

The Karush-Kuhn-Tucker (KKT) conditions for (2.14) are

$$\begin{aligned} & c_r(h^*) - \bar{u}_{od} - \rho_r = 0 && r \in R \\ & \rho_r h_r = 0 && r \in R \\ & \rho_r \geq 0 && r \in R \end{aligned} \tag{2.16}$$

where ρ_r is Lagrangian multiplier. These are seen to the conditions for $UE(c,\gamma)$.

UE is able to be expressed as the above mathematical formulations. In addition, Beckmann et al. (1956) converted UE into the mathematical optimization program. The link cost functions $c_a(.)$ is separable (i.e. $\frac{\partial c_a}{\partial f_b} = 0 \;\text{ for } b \neq a$) to define an objective *Z*, and these link functions are increasing (i.e. $\frac{\partial c_a}{\partial f_a} > 0$) to make sure the objective be convex(Heydecker, n.d.).

$$Min\ Z = \sum_a \int_0^{f_a} c_a(f_a)df \tag{2.17}$$

Subject to

$$\sum_{r \in R_{od}} h_r = T_{od} \qquad \forall (o,d) \in W \tag{2.18}$$

$$f_a = \sum_o \sum_d \sum_r \delta_{ar}^{od} h_r^{od} \quad \forall a \in E \tag{2.19}$$

$$h_r^{od} \geq 0 \qquad \forall r \in R_{od}, \forall (o,d) \in W$$

$$f_a \geq 0 \qquad \forall a \in E$$

The Lagrangean for (2.17)-(2.19) is

$$L = Z - \sum_{(o,d)\epsilon W} \lambda_{od} \left(\sum_{r \in R_{od}} h_r - T_{od} \right) - \sum_{a \in E} \eta_a \left(f_a - \sum_o \sum_d \sum_r \delta_{ar}^{od} h_r^{od} \right) - \sum_{(o,d)\epsilon W} \sum_{r \in R_{od}} \varsigma_r h_r^{od}$$

Where λ_{od}, η_a and ς_r are Lagrangian multipliers.

The deviation of the optimality conditions (KKT conditions) of UE are well known in transport literature, thus the details are not presented here for brevity, which can be found in page 63-66 of Sheffi (1985). The objective *Z* is artificial, and the value of *Z* has no direct interpretation in term of route choice or traffic (Heydecker, n.d.).

In this case, TC_{UE} is denoted as the total cost when user equilibrium is reached, and is given by:

$$TC_{UE} = \sum_{a \in E} f_a^* c_a(f_a^*) \tag{2.20}$$

The above equations include constraints for flow conservation and nonnegative flows, and the link cost function is monotonically increasing so as to ensure the link flow pattern of UE is unique (Nagurney, 1999) and the objective of the program is convex. Following this, Dafermos and Sparrow (1968) transformed this principle into a Nash Equilibrium of game theory, such that drivers using the road networks are regarded as players. Smith (1979a) also provided another different mathematical formulation.

2.2.3.2 System Optimum (SO)

UE describes how drivers unilaterally choose routes with minimum travel costs, but this approach cannot ensure the best use of road systems, especially in very congested networks, even when

drivers have complete information of all routes and try their best to minimize the travel costs. Assuming there are central controllers, and they take into account the total cost minimization of the whole road system rather than minimizing individual travellers' travel costs, Wardrop (1952) proposed the second principle of traffic assignment (W2), that is:

"the average journey time is a minimum"

This principle describes how drivers are assigned to routes so as to minimize the total travel costs incurred by all drivers. The resulting traffic assignment leads to a minimum cost for the whole system rather than for individual drivers. The Second Wardrop Principle is therefore system optimized, namely, the system optimum is based on this principle. Due to the fact that SO requires some drivers to sacrifice their benefits to achieve systemic minimization this method is not behaviourally realistic. It is important to transport planners and managers, however, because they always try to manage the traffic to make best use of transport infrastructure. The solution of SO is equivalent to the following nonlinear mathematical optimization program:

$$Min\ Z = \sum_{a} f_a c_a(f_a) \tag{2.21}$$

Subject to

$$\sum_{r \in od} h_r = T_{od} \qquad \forall (o,d) \in W \tag{2.22}$$

$$f_a = \sum_{o}\sum_{d}\sum_{r} \delta_{ar}^{od} h_r^{od} \quad \forall a \in E \tag{2.23}$$

$$h_r^{od} \geq 0 \qquad \forall r \in R_{od}, \forall (o,d) \in W$$

$$f_a \geq 0 \qquad \forall a \in E$$

The optimality conditions of SO are presented in page 69-72 of Sheffi (1985).

In this case, TC_{SO} is denoted as the total cost when system optimal is reached, and is given by:

$$TC_{SO} = \sum_{a \in E} f_a^* c_a(f_a^*) \tag{2.24}$$

2.2.3.3 Price of anarchy

The price of anarchy (POA) is proposed to measure the inefficiency of a system caused by the selfish behaviour of individuals. The inefficiency of Nash Equilibria is an old idea (Dubey, 1986), but Koutsoupias and Papadimitriou (1999) first proposed the term POA in the field of computer science. They utilized the ratio between the worst-case Nash equilibria and the social optimal to measure the inefficiency of a system's lack of coordination (Robinson, 2004). In the transport field, POA can be defined as follows:

$$\rho = \frac{TC_{UE}}{TC_{SO}} \tag{2.25}$$

This ratio ρ captures the relationship between costs incurred due to user-oriented behaviour and the system-oriented behaviour rules.

The fixed-point, Frank-Wolfe and Dijkstra algorithms, which are used to solve UE and SO problems and solve shortest paths, are depicted in **Appendix A**.

2.3 Day-to-day evolution model

The day-to-day dynamic evolution model is introduced in detail in this section since this model is able appropriately to capture the variation of network performance daily, and to be incorporated into behaviour rules, levels of aggregation, and various forms of traffic control.

Suppose there is a directed network $G(V, E)$, where *V* and *E* are, respectively, the set of nodes and links of the network. The set of origin-destination (OD) pairs is denoted as *W, and* $R_{o,d}$ is the set of routes connecting OD pairs of the network, where $(o, d) \epsilon\, W$. In this thesis, the discrete time day-to day (DTD) model is utilized and drivers update route perceptions and conduct route decisions on each day. The DTD model has advantages in terms of capturing the evolution of driver behaviours

and network performance with fixed time intervals, in particular as day unit, which may be denoted as t. Two types of DTD models are applied in this research: the detailed introduction and illustration of an agent-based DTD model is presented in **Chapter 6**, and therefore this section mainly introduces the methodology of the continuous flow DTD model that is used in **Section 7.3**. Assuming that the demand of each OD pair is constant and is denoted as $T_{o,d}$, which is non-negative, the flow on link $a\epsilon\ E$ on day t is represented as f_t^a, and f_t is the vector of link flows on day t, $f_t = (f_t^a)_{a\in E}$. h_t denotes route flow vector, $h_t = (h_t^r)_{r\epsilon R_{o,d}}$. Let the cost associated with route r on day t be denoted as c_t^r and c_t represents the vector of route costs on day t, $c_t = (c_t^r)_{r\in R_{o,d}}$. x_t^r is the perceived travel cost along route r on day t with a vector of x_t.

In general, the DTD model consists of two main components: traffic assignment and network loading. The traffic assignment model mainly consists of a cost updating mechanism and a route choice rule, while network loading depicts how to derive route costs based on the assigned link flow.

2.3.1 Assignment of trips

The deterministic discrete time day-to-day (DTD) model consists of two important components: the cost updating model and the flow assignment model. In essence, this type of DTD model is an iterative process (Meneguzzer, 1998). The cost updating model describes how the drivers update the perceived route costs based on the previous experience and actual route cost. In this thesis, the agent-based DTD model learns the perceptions of routes not just from their own experience, but also from other drivers who are in the same group and use the same route, as will be introduced in **Chapter 6** in detail. For the continuous flow DTD model, drivers either just rely on the previous day's experience or depend on the experience of previous several days. The flow assignment model depicts the behaviours of route choice based on the perceived route costs and actual route costs. For the agent-based DTD model in this thesis, individual drivers make decisions based on their own perceptions plus the perceptions of others, which are related to the socio-economic background of these drivers and may involve multidisciplinary subjects. Compared to this, the continuous flow DTD

model ignores the differences between these drivers. The framework of the traffic assignment model of the DTD model is shown in Fig.2.5.

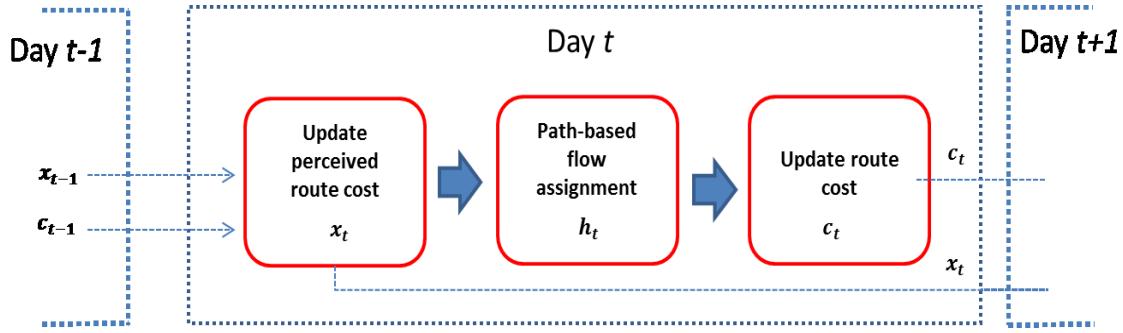

Fig.2.5 The framework of the DTD model

Two main types of function are able to represent the cost update process. The first is that the perceived cost on day *t* relies solely on the perceived cost of the previous one day, and the other depicts the perceived route costs on day *t* depending on the route costs of previous finite days. Other cost update mechanisms are developed based on these two basic functions (Cascetta and Cantarella, 1993). The two types of cost update functions can be shown as follows:

$$\text{a: } x_t = x(c_{t-1}, x_{t-1}) \tag{2.26}$$

$$\text{b: } x_t = x(c_{t-h}, h = 1,2,\dots,m)$$

Horowitz (1984) proposed a cost update process based on individual agents, as shown below:

$$x_t^i = \sum_{k=1}^{t-1} \beta_k(t-1)\, x_{t-1}^i + \varepsilon_i^t \quad i = 1,2,\dots \tag{2.27}$$

Function (2.27) demonstrates that the perceived route cost of driver *i* on day *t* is updated by the sum of the weighted average costs of previous days and an error term. β_k is the weight to decide the magnitude of the impact of a certain day on the route cost for the current day, and it is not fixed since the impact of old days decreases as time goes by. β_k should satisfy the following function:

$$\sum_{k=1}^{t-1} \beta_k (t-1) = 1 \tag{2.28}$$

Function (2.28) also shows the decreasing effect of old days on the current day. In order to simplify function (2.28) so as to reduce the complexity of the model, another cost update function, called the exponential smoothing filter, was developed by Walting (1999). This is independent from time and can be shown as follows:

$$x_t = \beta c(h_{t-1}) + (1-\beta) x_{t-1} \qquad \beta \epsilon (0,1) \tag{2.29}$$

Unlike function (2.27), here, β is constant, enabling the sensitivity of the route cost on the current day to the route cost on the previous day to be shown. A smaller value for β indicates that drivers have a strong habitual tendency. In this thesis, this function is used to represent the learning process.

For the previous model, each individual driver makes route choice decisions based on the perceptions of route costs (the agent-based DTD model that will be discussed in detail in **Chapter 6**). For the continuous flow DTD model, meanwhile, the route choice for aggregate flow can be shown as below:

$$h_t = T_{o,d} P^r(x_t) \qquad \forall r \epsilon R_{o,d}, (o,d) \epsilon W \tag{2.30}$$

According to Daganzo and Sheffi (1977), route flow *h* follows a stochastic user equilibrium (*SUE*) if, and only if, it satisfies function (2.30). This discrete choice model points out what proportion of drivers choose route *r*, which is calculated based on the difference between the perceived route costs of a given route and those of other feasible routes. The proportion is formulated as a logit model (Bie and Lo, 2010), which can be shown as follows:

$$P^r(x_t) = \frac{1}{1 + \sum_{j \epsilon R_{o,d}} e^{\theta (x_t^r - x_t^j)}} \qquad \forall r \epsilon R_{o,d} \tag{2.31}$$

The function shows that the larger the perceived route cost the smaller the proportion of drivers using the route. Parameter θ represents the sensitivity of perceived route cost differences to the proportion of drivers using the route, and this parameter can be related to the quality of information. θ is also termed the *dispersion parameter* by Prashker and Bekhor (2000).

2.3.2 Network loading of DTD models

The processes of calculating route costs based on the route flow vector are known as network loading problems. In this thesis, the link flow is able to be derived from the path flow and is shown below:

$$f_t = \delta_{a,r} h_t \qquad \forall a \epsilon E \tag{2.32}$$

Where $\delta_{a,r}$ is the link-route incident matrix if $a \epsilon r$, equals 1 and equals 0 otherwise. Afterwards, link cost can be obtained by the following function:

$$C_a = C_a(f_t) \qquad \forall a \epsilon E \tag{2.33}$$

Where $C_a(f_t)$ is the link travel cost function, which is assumed to be continuous and monotonically increasing. BPR is used as the link cost function:

$$C_a(f_t^a) = A_a \left[1 + B(\frac{f_t^a}{CP_a})^{\sigma}\right] \qquad \forall a \epsilon E \tag{2.34}$$

Where A_a and CP_a are free flow time and link capacity respectively, and B and σ are parameters. Then Path cost is obtained with the following equation:

$$c_r = \sum_{a \epsilon E} C_a \, \delta_{a,r} \qquad \forall a \epsilon E \tag{2.35}$$

This network loading process is used in this thesis.

2.4 Summary

The main methodologies and preliminaries frequently used in this thesis were presented in this chapter in order to support the discussion in later chapters. As a major tool for exploring the topological characteristics of networked systems, the complex network theory was introduced, including the algorithms and interpretations of widely-used topological indices such as degree centrality, clustering coefficient and betweenness centrality, and classical complex network models such as small-world and scale-free networks. Following this, the main three components of traffic assignment: transport demand, supply and traffic assignment principles, were introduced, and the link cost functions, UE and SO principles and price of anarchy were also presented. In addition, the DTD traffic dynamic is able to capture the evolution of daily traffic, and this process is illustrated, along with the route cost updating rule, route choice model and network loading mechanism, which comprised the complete DTD dynamic models.

The next chapter provides a comprehensive review of the main methodologies from the application side, such as the application of the complex network theory, classification of disruptions, application of day-to-day dynamic traffic models and traffic control.

Chapter 3 LITERATURE REVIEW

In **Chapter 2**, the basic components and formulations of the main methodologies were introduced in detail, such as the topological indices and traffic assignment. In this chapter the existing definitions and measures of robustness and resilience are presented in order to define and confirm the focus of robustness and resilience in this thesis. Following this, the applications of complex network theory are reviewed in different realistic networks such as social networks, biological networks, resource networks and transport networks so as to provide an overview of the developing progress of this method. Then, through a review of the studies on disruptions, the nature of the disruptions influencing urban road networks is made clear. A review of DTD dynamic models confirms the gaps in this field and highlights the advantages of this method of application. Finally, the chapter reviews transport control, focusing mainly on variable message signs (VMS) and adaptive signal control.

3.1 Robustness and Resilience

3.1.1 Definition

3.1.1.1 Robustness

To date, there is no universal definition of the 'robustness' of networked systems, partly due to the diversity in network type, infrastructure, constraints, and objectives. In the *IEEE* standard computer

dictionary (*IEEE*, 1990), robustness is defined as "*the degree to which a system or component can function correctly in the presence of invalid inputs or stressful environmental conditions*". In the study of electrical networks, Holmgren (2007) defines robustness as the ability of a network to keep its structure (function) intact when exposed to perturbations. Immers et al. (2004) regard robustness as "*the degree to which a system is capable of functioning according to its design specifications in the case of serious disruptions*". Boccaletti et al. (2006) define robustness as the ability of a network to avoid malfunctioning caused by the damage of a fraction of its constituents. In addition, Schillo et al. (2011) defined robustness as the ability to maintain 'safety responsibilities' and they pointed out that robustness should be related to the performance measures of the system. In this thesis, robustness is defined as the ability to maintain the original performance of the system.

3.1.1.2 Resilience

Resilience has been studied in different fields, such as social-ecological systems (Carpenter et al., 2001), economics (Hoffman, 2007) and urban infrastructure (Attoh-Okine et al., 2009). Originally, resilience was defined to describe how ecological systems return to a stable state after experiencing a disturbance (Holling, 1973). In general, resilience has overlapping meanings with robustness, but it is remains significantly different from the latter.

Like robustness, resiliency also has a Latin root: *resilire*, which means 'to leap back'. Omer et al. (2013) extends this definition to denote resilience as the ability of systems to bounce back after disruptions. In Webster's Unabridged Dictionary, resilience is defined as "*the ability to bounce or spring back into shape, position, etc., after being pressed or stretched*". In the field of materials, resilience is regarded as the ability of a material to return to its former shaper after a deformation. Manyena et al. (2011) argue that resilience should involve 'bouncing forward' and 'moving on', not just 'bouncing back' after an event. They deem that resilience can be defined as "*the intrinsic capacity of a system, community or society predisposed to shock or stress to bounce forward and adapt in order to survive by changing its non-essential attributes and rebuilding itself*". Sterbenz et al.

(2010), meanwhile, define network resilience as the ability of a network to maintain an acceptable level of service when experiencing various faults and challenges to normal operations.

In the field of infrastructure, Bruneau and Reinhorn (2007) and O'Rourke (2007) describe the resilience of a system through four key characteristics, as follows:

(1) *Robustness: the inherent strength of or resistance in a system to withstand external demands without degradation or loss of functionality;*
(2) *Redundancy: system properties that allow for alternate options, choices, and substitutions under stress;*
(3) *Resourcefulness: the capacity to mobilize needed resources and services in an emergency;*
(4) *Rapidity: the speed with which disruption can be overcome and safety, services, and functionality stability restored.*

In the field of transportation, Freckleton et al. (2012) define resilience as the ability of a transportation network to absorb disruptive events gracefully, maintaining a demonstrated level of service equal to or greater than the pre-disruption level of service within a reasonable timeframe. There are, therefore, many different definitions for resilience, but it can be seen that they all connect with the core part of the concept, namely, recovery after physical disturbances. In reality, it is difficult to find a way to cover the four key characteristics of resilience, so one of these characteristics can be upon for the assessment of resilience. Engineering resilience which has the same definition as rapidity is easier to be calculated and evaluated in terms of the resilience in dynamic traffic models compared to other definitions (Grimme and Calabrese, 2011), in addition Donovan and Work (2015) and Wang et al. (2015) both evaluate the resilience of traffic networks by using the rapidity of recovery. This thesis also follows this approach of exploring the resilience of urban road systems from the perspective of the rapidity of recovery.

3.1.2 Other terms relevant to robustness and resilience and their interrelations

3.1.2.1 Vulnerability

Vulnerability is defined as *"the degree of loss to a given element at risk or set of such elements resulting from the occurrence of a natural phenomenon of a given magnitude and expressed on a scale from 0 (no damage) to 1 (total loss)"* (United Nations Disaster Relief Co-ordinator (UNDRO), 1980). The United Nations International Strategy for Disaster Reduction (UNISDR) (2004) regards vulnerability as *"the propensity of exposed elements such as human beings, their livelihoods, and assets to suffer adverse effects when impacted by hazard events."* This term is closely related to resilience and, indeed, vulnerability and resilience can be viewed as two ends of a spectrum, with resilience representing the positive side (Levina and Tirpak, 2006). Vulnerability is therefore a component of resilience (Maguire and Cartwright, 2008), and resilience can be a function of vulnerability (Brabhaharan, 2006).

3.1.2.2 Reliability

The reliability of networks is very important to engineers, and it is closely related to issues such as disaster management and road space reallocation. A few works (Du and Nicholson, 1997, Bell et al., 1999) focus on this field. In general, reliability has two dimensions, namely, connectivity and performance reliability. Bell (2000) gives an intuitive definition for network reliability:

"A network is reliable if the expected trip costs are acceptable even when users are extremely pessimistic about the state of the network".

The relationship between reliability and robustness is very close, and it is deemed that network robustness plays an important role in ensuring the reliability of the system in terms of travel time for travellers (Immers et al., n.d.). In addition, Husdal (2004) states that a non-linear or reciprocal relationship exists between robustness and reliability.

3.1.2.3 Sustainability

Sustainability is regarded as a measure of the lifespan of a system. It is deemed that relationship between resilience and sustainability is equivalent to that of blood pressure to health, in that resilience is a component of sustainability (McRoberts, 2010). The concept of sustainability overlaps over a time scale with resilience. Resilience can be viewed as a 'subset' or a 'special case' of sustainability. To be more specific, resilience is able to lead into sustainability over the medium term via adaption in the short term, to eventually reach sustainability "*through transformation*"(Seville, 2009). **Fig.3.1** shows the relationship between resilience and sustainability.

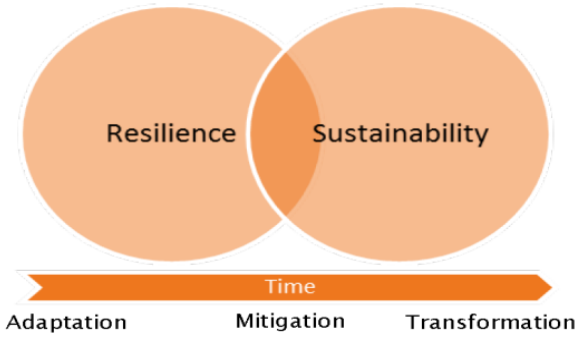

Fig.3.1 Sustainability and Resilience (Grubinger, 2012)

3.1.2.4 Stability

Stability originates from the Latin *stabilis*, which means ability to stand firm or steady. This term has been widely used in many fields and usually refers to the ability of an object to maintain equilibrium (Urruty et al., 2016). In natural science, Justus (2008) defines stability as the constancy of a given performance or attribute when experiencing disturbances. Turner et al. (1993) regard ecological stability as the ability to maintain ecological functions regardless of disruptions. Following this, stability is defined as the ability to return to the initial equilibrium state in the presence of disturbances (Ives and Carpenter, 2007). In the field of transportation, stability refers to whether dynamic systems ultimately approach equilibrium (Horowitz, 1984, Watling, 1999). There is commonality between stability and robustness, that is, both are concerned with persistence (Jen, 2002).

3.2.3 Measure of robustness

There are many indices and measures for the robustness of networked systems. Overall, these indices can be categorized into two classifications. The first can be referred to as topological indices, which are all based on the topology of networks without taking into account the distribution of any quantity transported by the networks. For example, the variations of degree centrality, clustering coefficient, betweenness centrality, the size of the largest connected component, and so on, can be used to represent the ability of a networked system against failures or attacks. This is because these indices are usually related to the robustness of the network and some of these measures are able to reflect the efficiency and functionality of the underlying network (Holme et al., 2002, Crucitti et al., 2003, Crucitti et al., 2004c, Albert et al., 2000a). The second category is operational indices; these take into account the range of more complex factors directly or indirectly affected by disruptions, such as travel demand, user behaviour and link capacity, all of which may greatly influence the distribution of flows. Snelder (2010) makes a similar point in stating that there are two variants: static and dynamic indices.

The robustness of networks can be measured by the size of the largest connected component by removing a percentage of nodes/links. Albert et al. (2000a) explore the robustness of scale-free networks using a simple topological index, diameter, to measure the interconnectedness of networks. Cohen et al. (2001) study the tolerance of Internet networks under intentional attacks, and the average distance between sites in the largest cluster of the network is used to measure the robustness of the network against failures and attacks.

Holme et al. (2002) utilize the size of the largest connected subgroup and the average inverse geodesic length, which is similar to an efficiency measure, to explore network performance under four different attacking strategies, which are all based on the removal of nodes or links according to a descending order of degree and betweenness centrality. Latora and Marchiori (2005), meanwhile, propose a general method based on the efficiency measure of networks to identify the crucial

component of infrastructure networks, and their method can also be used for improvement analysis in the context of network expansion.

In order to quantify the robustness of networks in terms of structural network properties, Demetrius and Manke (2005) proposed a novel representation, network entropy, to assess the robustness of networks. This can be written as:

$$H(m) = \sum_{i=1}^{n} \pi_i H_i \qquad (3.1)$$

$$H_i = -\sum_{j} m_{ij} \log(m_{ij})$$

Where H is the weighted average entropy over all stationary states, and H_i is the Shannon entropy. They assume that the process defining the information source is determined by a Markov matrix $M = (m_{ij})$ ($m_{ij} \geq 0$ and $\sum_j m_{ij} = 1$), which describes the transition rates from state *i* to *j*.

Research on the robustness of transport networks in the presence of disruptions is relatively recent (Nagurney and Qiang, 2007a). Sakakibara et al. (2004) propose a topological index, which was used to classify isomers in molecular chemistry (Hosoya, 1971), to evaluate the dispersiveness/concentration of road networks in the presence of disasters. They define the most robust network as the one that minimizes the isolation of districts when the network experiences a catastrophic disaster.

Scott et al. (2005) present a new Network Robust Index (NRI) that takes into account network flows, link capacity and network topology. This is calculated based on the travel-time cost of removing a given node in order to identify critical links of the network. The results of the NRI demonstrate that this index provides better planning solutions compared to the volume/capacity (V/C) ratio, which is the traditional identification of critical links for congested networks.

Nagurney and Qiang (2007a), meanwhile, propose a network efficiency measure based on travel disutility from a traffic equilibrium model to assess the efficiency of congested networks quantitatively, and to rank the links of networks by capturing demand, flows, costs and user behaviour.

Based on this new measure, Nagurney and Qiang (2007) utilize the relative change of network efficiency as an indicator to study network performance while all link capacities decrease gradually. Following this, Nagurney and Qiang (2009) develop another index, called the relative total cost index, to assess the robustness of networks in the presence of link degradation. This index is calculated based on total travel cost and is able to capture the travel behaviour associated with User Optimization (UO) and System Optimization (SO). Unlike the previous work, they quantify the robustness by gradually decreasing the capacity of all links rather than removing links from the network, thus allowing the research to focus on the degradation of networks.

More literature concerning robustness measures are summarized **Table 3.1.**

3.1.4 Measure of resilience

Resilience can be measured in many ways. Hughes and Healy (2014) propose a qualitative method to assess resilience based on principles such as redundancy and adaptation, which are regarded to better fit the New Zealand Transport Agency's requirements. The method consists of many measures which are scored from 1 (very low) to 4 (very high), and weightings are used to generate aggregate scores. This method is practical and flexible but too subjective.

O'Rourke (2007) measures resilience as the expected loss in quality during the time of recovery, $t_1 - t_0$, as shown in **Fig.3.2**. Resilience (*R*) can be presented mathematically as follows:

$$R = \int_{t_0}^{t_1} [100 - Q(t)]dt$$

Where $Q(t)$ is an infrastructure quality over time, t_0 is the time that disruption occurs, and t_1 is the time the quality is restored.

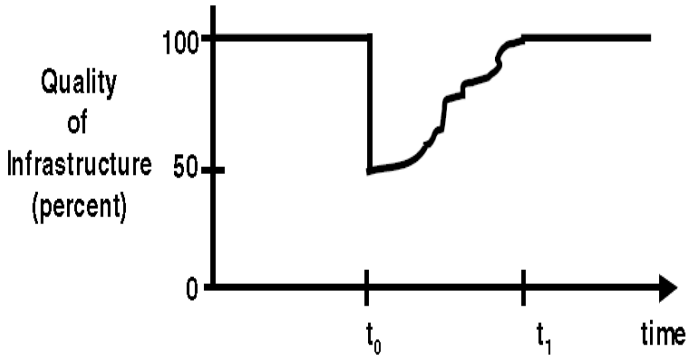

Fig.3.2 Measure of seismic resilience (Bruneau et al., 2003)

Wang et al. (2015) regard rapidity as an important indicator of resilience and develop a day-to-day toll scheme to capture and optimize the resilience of traffic systems after a disruption. Donovan and Work (2015) utilize taxi GPS data between origin-destination (OD) zones to measure the city-scale resilience of transport systems when suffering unusual events. They calculate OD paces, namely, the average travel time per mile between different OD zones in order to observe the pace derivation from typical values. It remains difficult to evaluate the overall resilience of the network, however.

Although there is no universal definition of resilience, peak disruptions and recovery time have been regarded as the main quantities of resilience. In addition, there are other ways to measure resilience of the network.

Omer et al. (2013) propose a Networked Infrastructure Resiliency Assessment (NIRA) framework to assess resilience of networked infrastructure from multiple-perspectives, with travel time resiliency being calculated based on the travel time, and environmental resiliency based on the variation of CO_2 emissions before and after disruptions. Ip and Wang (2011) define the resilience of a node as the weighted sum of the number of reliable passageways of all other nodes in the network, and the sum of the resilience of all nodes is the resilience of the network. Here, so-called reliable passageways are normal operational paths. Bhavathrathan and Patil (2015) utilize an indicator to quantify network's resilience when experiencing recurring capacity disruptions. The indicator is based on the ratio between the minimum possible expected system travel time (ESTT) at the state

without disruption and the ESTT at the critical stage, which measures how much disruptions the system can take in before it shifts from a demand-meeting state to a demand-not-meeting state. A minimax program is used to seek the critical state ESTT. Nogal et al. (2015) investigate the resilience of a traffic network by using the normalized area over the exhaustion curve, which is obtained from a dynamic restricted equilibrium model combined with a cost function using a random parameter following a generalized beta distribution to represent the time-varying hazards of extreme weather. Faturechi and Miller-Hooks (2014) investigate the travel time resilience of the network under different disaster scenarios by proposing a bi-level, three stage stochastic mathematical program with partial user equilibrium constraints. The upper level problem includes decisions in the three stages of mitigation, preparedness and response, while the lower level problem models the user response to the decisions from the upper level.

The number of measures and indices for the robustness and resilience of networked systems are therefore considerable, and the literature related to such indices is summarized in **Table 3.1**. The definitions of operational and topological indices have been interpreted at the beginning of **Section 3.1.3.**

Table 3.1 Summary of measurements of robustness and resilience

Network type	Operational	Topological	Measurement	Performance	Ref.
Scale-free networks		✓	Diameter	Robustness	Albert et al. (2000b)
Scientific collaboration and Internet networks		✓	The average inverse geodesic length and the size of the largest connected subgraph (giant component)	Robustness	Holme et al. (2002)
Virtual networks		✓	The size of the largest connected subgraph (giant component)	Robustness	Callaway et al. (2000)
Scale-free networks		✓	Global efficiency and local efficiency measure	Robustness	Crucitti et al. (2003)
infrastructure		✓	Efficiency	Vulnerability	Latora and

networks					Marchiori (2005)
Communication/transportation networks		✓	Global efficiency measure	Robustness	Crucitti et al. (2004c)
Italian electric power grid		✓	Efficiency measure	Robustness	Crucitti et al. (2004b)
Electrical power grid		✓	Efficiency measure	Robustness	Crucitti et al. (2004a)
communication–transportation network		✓	Efficiency measure	Robustness	Latora and Marchiori (2004)
Air traffic network		✓	The size of the largest connected subgraph (giant component)	Vulnerability	Luca Dall'Asta (2006)
Ecological networks		✓	Average size of the largest connected subgraph	Robustness	Sole and Montoya (2001)
Random geometric network		✓	The size of the largest connected component	Resilience	Kong and Yeh (2010)
Internet networks		✓	The size of the largest connected component	Robustness	Cohen et al. (2001)
Power grids		✓	Betweenness and net-ability	Vulnerability	Bompard et al. (2011)
Power transmission grids	✓	✓	Entopic degree; Net-ability	Vulnerability	Bompard et al. (2009)
Power grid		✓	Efficiency; Net-ability	Vulnerability	Arianos et al. (2009)
North American power grid		✓	Connectivity	Vulnerability	Albert et al. (2004)
Road network		✓	Travel time	Resilience	Werner et al. (2005)
Air transport network		✓	The size of the largest connected component	Robustness	Lordan et al. (2014)
World Wide Web		✓	The size of the largest connected component	Resilience	Brodera et al. (2000)
Airport network		✓	Topological indices	Vulnerability	Chi and Cai (2004)
Airline route networks		✓	Probability based on connected components	Robustness	Di Paolo et al. (2011)
Air transport networks		✓	Algebraic connectivity	Robustness	Wei et al. (2014)
Road networks		✓	Topological indices	Robustness	Jamakovic et al. (2006)
Critical		✓	Node connectivity	Robustness	Dekker

infrastructure networks					(2005)
Road network	✓		Number of cancelled public transport trips	Robustness	Tahmasseby and Van Nes (2007)
Australian Main Road Network		✓	Hansen integral accessibility index; Accessibility/Remoteness Index of Australia	Vulnerability	Taylor et al. (2006)
Road networks	✓		Benefit–Cost Analysis	Robustness	Zhang and Levinson (2008)
Infrastructure networks		✓	Connectivity	Robustness	Dekker and Colbert (2004)
Scale free networks and exponential networks		✓	Topological indices	Robustness	Shargel et al. (2003)
Virtual networks		✓	The size of the largest connected subgraph (giant component)	Robustness	Dong et al. (2013)
Urban road networks		✓	Connected components	Robustness	Masucci and Molinero (2016)
Urban road networks		✓	Clustering coefficient; APL; size of largest and average connected component	Robustness	Duan and Lu (2013)
Air transport network	✓		The sum of the product of all self-excluding importance	Resilience	Janić (2015)
Air Navigation Route networks		✓	Betweenness	Robustness	Sun et al. (2014)
Road networks	✓		A relative total cost index	Robustness	Nagurney and Qiang (2009)
Road networks	✓		Network efficiency based on equilibrium disutility	Robustness	Nagurney and Qiang (2007)
Road networks	✓		Network robust index	Robustness	Scott et al. (2005)
Road networks		✓	Dispersiveness/concentration	robustness	Sakakibara et al. (2004)
Water distribution networks		✓	Algebraic connectivity	Robustness	Yazdani and Jeffrey (2011)

City-scale transportation system	--	--	Average travel time per mile	Resilience	Donovan and Work (2015)
Road Transport Network	✓		Travel time resilience, Environmental resilience	Resilience	Omer et al. (2013)
Road transport network	✓		Rapidity	Resilience	Wang et al. (2015)
Railway network		✓	The weighted sum of the number of reliable passageways	Resilience	Ip and Wang (2011)
Road network	✓		System-optimal total cost	Resilience	Bhavathrathan and Patil (2015)
Road network	✓		The normalized area over the exhaustion curve	Resilience	Nogal et al. (2015)
Roadway networks	✓		Travel time	Resilience	Faturechi and Miller-Hooks (2014)
Air transport network		✓	The size of the largest connected component	Resilience	Cheung and Gunes (2012)
Intermodal Freight Transport	✓		Post-disaster expected fraction of demand	Resilience	Chen and Miller-Hooks (2012)
Surface Transportation Networks		✓	Global efficiency; the relative size of the giant component	Resilience	Osei-Asamoah and Lownes (2014)
Air transport network		✓	Topological indices	Resilience	Li et al. (2014)

As can be seen from **Table 3.1**, although there are a considerable number of robustness measures, most are based on topological characteristics (i.e. connectivity and proximity). Such topological measures are either commonly used topological indices such as degree, closeness, average shortest path length, efficiency and the size of largest connected components (see **Section 2.1.2** for more

details) or the variants or derivatives of these indices. These topological indices have been widely used due to their simplicity and computational efficiency, but they cannot capture the unique flow and operational characteristics on a specific road network (e.g. travel demand, driving behaviour, link capacity, etc.), and therefore do not represent well the system's ability to undergo stress or disruption. Furthermore, studies on the robustness of URNs based on the day-to-day traffic assignment models are very scarce. Regarding the resilience literature, most of the measurements are operational in nature, and in some cases, recovery time is used as an indicator to measure resilience. In this thesis, exploring the resilience characteristic by focusing on the rapidity of recovery time is confirmed as the right approach. In addition, through the review in this section, it is found that there is a shortage of systematic and comprehensive comparisons and analyses between operational indices and topological indices. This thesis addresses this issue.

3.2 The applications of complex network theory

Complex network theory has been widely used to explore the topological characteristics of many networked systems, including transport networks. This section therefore summarizes the application of complex network theory in different fields in order to gain a comprehensive overview of its recent development. According to Newman (2003) review of complex networks, all networks in reality are divided into social networks, information networks, technical networks and biological networks. Furthermore, the technical networks are defined as man-made networks designed for the distribution of resources. In this chapter, on the one hand, transport networks are a central focus, and, on the other hand, information may be regarded as a type of resource. The review of the application of complex networks in this chapter is therefore divided into social networks, biological networks, resources networks and transport networks, with water distribution networks being identified as resources networks. The particular focus is on transport networks considering different types of transport networks including public transport, railways, underground, cargo ships and air transport.

3.2.1 Social networks

Social networks are relationship networks formed by certain connections between individuals or individuals and organizations (Scott, 2013), such as the friendship relationships between individuals (Moreno, 1934, Rapoport and Horvath, 1961), intermarriage relationship between families (Rapoport and Horvath, 1961) and business relationships between companies (Bengtsson and Kock, 2000, Mizruchi, 1982).

Cooperation relationships between scientific researchers have also received attention and scientific co-authorship networks have been investigated (Cardillo et al., 2006) to show how the co-authorship community grew between 2000 and 2005 based on the improvement of connectivity properties, the size of the largest connected component, global efficiency and the clustering coefficient. The correlations between topological properties were also investigated. The drawback in this analysis is that the weighted relations are not discussed.

Complex network theory has been used in the study of the topology of Email networks, with nodes representing email addresses and links denoting emails (Ebel et al., 2002), and BBS (bulletin board system)-reply networks with identifications (*IDs*) as nodes and reply articles as links (Kou and Zhang, 2007). The relationships in social complex networks have also been utilized to develop strategies against terrorism (Latora and Marchiori, 2004). The critical components of complex networks can be identified by a method based on a centrality measure. Two examples were presented to show that the crucial nodes of a communication network can be identified in order to protect the network system from attacks, and, clearly, the identification of key terrorists is also important for governments to destroy a terrorist organization network.

The above work involves the finding of critical components, but other studies have explored the unstable factors within networks in order to strengthen the security of those networks, which is beneficial for the prevention of network viruses (Newman et al., 2002) and human epidemics transmission (Kermack and McKendrick, 1932). Although the links and nodes of social networks tend

to be virtual, while those of transport networks are more likely to be physical, the methods of topological analysis and critical component identification for social networks can also be used for transport networks.

3.2.2 Biological networks

The research scope related to biological networks is broad, from biological cells to micro-organisms, such as metabolic networks (Jeong et al., 2000, Guimera et al., 2007, Fell and Wagner, 2000), protein networks (Bellafiore et al., 2005), neural networks (Sporns et al., 2000, Sporns, 2002) and RNA networks (Lee et al., 2007), to prey relationships between creatures, namely the food web (Sole and Montoya, 2001, Camacho et al., 2002).

Jeong et al. (2000) examine 43 organisms representing all three domains of life in a systematic mathematical analysis. They find that, although there are significant differences in their metabolic pathways and constitutions, these organisms all show similar topological properties in terms of the actual metabolic reactions between substrates. They deem that all living organisms have the same metabolic organizations and obey the same rules for robustness and error tolerance.

The controllability of the complex network is another important issue. Liu et al. (2011) developed a tool to analyse the controllability of arbitrary directed complex networks in order to obtain “drive nodes” which may control the whole system. This method was applied to several real-life networks, with the results showing that the “drive nodes” are decided by the degree distribution, and for sparse networks, the number of “drive nodes” is 80%, while for dense networks the number is approximately 10%.

To date, the research related to biological networks mainly focuses on the analysis of topological structure, but this may provide insights for community and hierarchy detection within transport networks.

3.2.3 Resources Networks

Power grids, as a type of important energy network and a critical infrastructure, play a vital role in underpinning our society and economy.

Crucitti et al. (2004b) point out that an intrinsic drawback of the Italian power grid is large-scale blackouts. A model of cascading failures is proposed by Crucitti et al. (2004a) and used to analyse the vulnerability of the power grids. The model defines a capacity as the maximum load to the node and showed the performance of global efficiency for the network when a certain node with the largest load, or highest degree, was removed. The results show that the removal of the node with the highest betweenness can most likely trigger the cascading mechanism, yet the network is still robust to most failures. The model heavily simplified the actual power grid, and, especially, the assumption that generators send electricity to the substation in the most efficient ways is not realistic.

Sanchez and Caire (2012) propose a new method, a theory of complex numbers, to create a complex network model for two interdependent infrastructures: Information and Communication Technologies (*ICT)* and Power Systems in order to identify the most critical nodes in the model. Node degree and efficiency are regarded as two indices. The significance of this research is to bridge two infrastructures in one model, but whether the method can be used in less correlated systems is not clear.

The World Wide Web (WWW) is an important example of information networks, web pages contain information that can be connected by hyperlinks with other pages (Huberman, 2001). Barabasi et al. (2000a) investigate the topological characteristics of directed networks within the WWW, and the results show that the distributions of incoming and outgoing links both follow power law distribution, and that the WWW has a small-world property. The preferential attachment leads to the scale-free property of the topology, although this network is apparently random. Following this, Barabasi et al. (2000b) further discuss the power law distribution of links within the WWW.

Due to the fact that water is an important resource, water distribution networks have aroused a lot of interest. Yazdani and Jeffrey (2011) apply complex network methods to study the structure and reliability of water distribution networks, which are regarded as spatially organized networks. Four water distribution networks are used as benchmarks to access the structure of networks, their efficiency connectivity and reliability. In the thesis, link density, link-per-node ratio and the central–point dominance are used to describe the structure of the networks, and a meshedness coefficient was considered to reflect the clustering property. Based on the disconnections of nodes from sources, the index of a route factor was better than the conventional assessment of efficiency. Water networks therefore present high efficiency. The spectra of connectivity and Laplacian matrices are used to quantify the level of network tolerance to failures.

3.2.4 Transport networks

Complex network theory has been widely used in exploring topological characteristics of transport networks, ranging from public transport, air transport, railway transport and cargo ship transport.

3.2.4.1 Public transport

Sienkiewicz and Hołyst (2005) explore the public transport network (PTN) systems of 22 cities in Poland. Their analyses of the topological characteristics of these cities, such as degree and degree distribution, average path length and cluster coefficients, show that the degree distribution and average path length distribution of these networks have some similarities in obeying power-law distribution and exponential distribution. The results also show some features of small-world networks, even though the network scale for these 22 cities is different.

Xu et al. (2007) investigate the topological properties of three bus-transport networks in Beijing, Shanghai and Nanjing. The degree distribution and the distribution for the number of lines which provide services to each station in the three cities shows power laws in space *L* (nodes are stations, and links between nodes denote that at least one route exists between corresponding two stations consecutively), while in space *P* (nodes denote stations while links between nodes exist when

corresponding stations are passed by at least one route) that the cumulative degree distribution follows an exponential distribution. They proposed a new topology representation and regarded the routes as the nodes. In this representation, the distributions of degree and strength also obey a power law. Following this, an explanation was given: more and more connections between central and suburban stations influenced the expansion of the routes in the central cities.

von Ferber et al. (2009) explore the public transport networks (PTN) of 14 cities with different geographic, cultural and economic backgrounds and examined the global and local properties of these PTNs when the PTNs are represented in each of an *L*-, *P*-,*B*- and *C*-shape. The results show that these PTNs have high clustering coefficients and relatively low average shortest paths, which are typical small-world characteristics. In the thesis, shortest paths and betweenness centrality are used to present global characteristics, and node degree and clustering coefficient are applied to showing the local properties. A harness concept is proposed to highlight the overlapping routes of PTNs, and this is a recently introduced notion (von Ferber et al., 2007). Geographical coordinates of stations are also considered in the PTN of Berlin and the metro network of Paris to respond to the question of whether the distance between initial and final stations grow linearly with path length. This research, however, did not present reasons regarding the differences in the topological distributions in the different cities, however, nor for their dynamic evolution.

Centrality is crucial for the analysis of public transport. The current transit system is experiencing considerable stress due to increasing demand. Derrible (2012) examines one basic aspect of public transport systems—the network centrality. The author employed betweenness centrality to examine the network centrality of 28 metro systems across the world in order to identify global trends that network expansion causes a lower share of betweenness to most nodes. In the thesis he analysed the relationship between average betweenness centrality and city size, with the results showing there to be a positive relationship. The assumption here is that the terminal and transfer stations are regarded as nodes, enabling the model to focus more on the transferability of the system, but the

influence of other transport modes is not considered and the author also does not point out how to re-distribute the traffic flow as the centrality evolves over time, though he does mention that the centrality of nodes is beneficial for the distribution of traffic flow.

Xiao et al. (2012) investigates a directed and weighted bus transport network in Beijing. This study takes into account the stations as the nodes and regards the bus routes between neighbouring nodes as the edges to enable the nodes to have specific coordinates. The results show that the degree is 2.96, the clustering coefficient is 0.12 and the average path length is 15.5, which suggests that this is a small-world network. The author defined a carrying pressure to analyse the "key nodes" and pointed out that there is a discrepancy between the accessibility of the network and the flow of passengers, and suggested that splitting the central nodes in order to share the flow of other nodes may increase the synchronizing capacity of the network.

3.2.4.2 Air transport

In addition to public transport, aviation networks are also a popular topic for the study of complex networks. The world-wide airport network is a small-world network with power-law distribution` (Guimera and Amaral, 2004). An interesting finding, however, is that the most central nodes are not the most connected nodes in the world-wide airport network (Vázquez et al., 2002). The models with the rule of preferential attachment and geographical distance constraints cannot account for this fact, hence Vázquez et al. (2002) developed a new model with geo-political constraints to explain this phenomenon. In this model, a few cities in each country are allowed to connect with cities in other countries. The model solved the large-betweenness/small-degree puzzle. The results also show, however, that these constraints are not only present in airport networks, but also other critical infrastructures, such as power grids.

Wang et al. (2011) employ complex network theory to explore the network structure and nodal centrality of individual cities in the air transport network of China (ATNC). The results show that degree centrality, closeness centrality and betweenness centrality follow an exponential distribution,

and that the ATNC has a small-world property like the air networks in the USA, India and Italy do. The clustering coefficient in the ATNC (0.69), however, is less than that in the USA (0.73-0.78) and the average path length (2.23) is longer than in the USA, which shows that the ATNC is less mature or efficient than air transport network in the USA. The authors pointed out that all three centrality indices have high correlations with socioeconomic factors of cities such as population, air passenger volume and gross regional domestic product. This represents the first attempt to explore the relationship between topological indices and socioeconomic factors for the ATNC, but the reasons why air passenger volume geometrically grows with degree and closeness but linearly with betweenness are not clear.

3.2.4.3 Railway networks

Li and Cai (2007) study the statistical properties of the directed China Railway Network (CRN) in space *P*. They found the CRN to be a small-world network with an average path length of 3.5 and a clustering coefficient of 0.835. They also studied the anti-correlations of degree-degree and clustering-degree and nonlinear correlation of strength-degree, which shows that the CRN is disassortative, namely, the correlation between the average degree of neighbouring nodes and the degree of a given node is very poor. Degree and weighted degree follow the power-law distribution. The network, consisting of 3915 stations and 22259 railways, has better topological characteristics compared to those of the Indian Railway network.

Since the topological properties of the CRN in space *P* had been explored by Li and Cai (2007), Guo and Cai (2008) investigate the directed CRN in space *L*. The results show that the network is assortative and scale-free in space *L*. In this study, they proposed a new weight and a relative weight to measure the utilized efficiency of stations, which reveals the roles of political, economic and cultural factors to the nodal importance, namely, the stations with better utilized efficiency tend to be built in cities which are political, economic and cultural centres in their local and global regions. In fact, this new weight has similarity with the transport efficiency shown in function (2.6). The

evolution of cumulative distribution concerning shortest path length in space *L* and space *P* are examined, and the results show turning values of 7 and 0.6, respectively in the two-regime exponential decaying distribution.

3.2.4.4 Cargo ship networks

Complex network theory is also applied to the exploration of cargo ship networks. Hu and Zhu (2009) investigate the worldwide container transportation network with the representation of space *L* and *P*. The network shows a similar hierarchical structure and rich-club phenomena, namely, Matthew effect, as the world air network (WAN) . In order to understand global trade patterns and bio-invasion, Kaluza et al. (2010) explore the physical characteristics, the network layers and the network trajectories of different types of ship such as bulk dry carriers, container ships and oil tankers, and utilized the gravity model to estimate the traffic flow so as to forecast the biological invasions. However, the gravity model omits too much information of hierarchical structure.

3.2.5 Other spatial networks

Gastner and Newman (2006b) have studied networks whose nodes are embedded in geographic space in order to look for strong connections between the topological and geographical characteristics of networks. They find an effective way to distinguish the dimension of networks and proposed a simple model of spatial networks to balance the geographic distance and the graph distance based on the preference of users for different networks. This model is utilized to reproduce the qualitative features of real-life networks.

Following this, Gastner and Newman (2006a) investigate the *P* median problem, which is optimal facility location. The problem is to assign locations for a certain number of facilities in a certain area in order to minimize the average distance between residents and the nearest facilities with them. They confirm that the density of facility locations is proportion to the population density as a power law with the exponent 2/3. They also optimized the network configuration with a simple cost model taking into account users' preferences. The model is written as:

$$\mathrm{Min}(T + \chi Z)$$

$$T = \sum_{i<j} a_{ij} l_{ij}$$

$$Z = \sum_{i<j} w_{ij} \tilde{l}_{ij}$$

$$w_{ij} = \int_{V_i} \rho(r) d^2 r \int_{V_j} \rho(r') d^2 r'$$

$$\tilde{l}_{ij} = (1 - \delta) l_{ij} + \delta$$

where *T* is total length of all edges, and proportional with maintenance costs of the network; χ is a constant value to measure the relative importance of two terms; a_{ij} is adjacency matrix , if there is a connection between *i* and *j*, $a_{ij} = 1$, $a_{ij} = 0$ otherwise; l_{ij} is geographic distance; *Z* is total travel cost; $w_{ij}$is amount of traffic, which is proportional to the product of populations in the Voronoi cells V_{i} and V_j; $\rho(r)$ is the population density at position r of facilities; $\tilde{l}_{ij}$ is revised distance and δ determines users' preference.

In another application, Yang Y and Yang HJ (2008) apply complex network theory to time series analysis, utilizing the correlation relationship matrix of a time series to construct networks in order to understand the biological functions of elements in the series. Complex network theory can also provide a new perspective to study spatial economic analysis (Reggiani and Nijkamp, 2007)**.** Based on complex network theory, Latora and Marchiori (2007) introduce a new class measure, delta centrality, that is different from degree centrality, closeness centrality and betweenness centrality. In particular, they focused on a measure called information centrality, based on the transport efficiency of the network. This measure and other centrality measures are applied to both empirical and artificial networks generated by computer for comparisons. They point out that information centrality is more appropriate in exploring community structures and the characteristics of planar graphs.

This review on the application of complex network theory shows that complex network theory is a very active field and also demonstrates its capability to capture network topological characteristics and network dynamics with relatively simple measures. In addition, the review confirms that although the theory has been widely used in many networked systems, studies of urban road networks based on physical road segments and junctions rather than routes of buses or other public transports are insufficient.

3.3 Classification of disruptions

Urban road networks may be affected by various disruptions which are caused by technical problems, natural disasters or man-made incidents. Such disruptions are a major threat for a network's reliability and efficiency (Sullivan et al., 2010). The number of existing studies on transport disruptions is considerable, including transit strikes (Ferguson, 1992, van Exel and Rietveldb, 2001, Lo and Hall, 2006), bridge closure/collapse (Hunt et al., 2002, Clegg, 2007, Zhu et al., 2010), special events (Dimitriou et al., 2006, Hensher and Brewer, 2002) and earthquakes (Giuliano and Golob, 1998, Wesemann et al., 1996). All of these disruptions lead to system and behaviour effects on networks and travellers, and can be categorized as unplanned and planned (Zhu and Levinson, 2012).

To be more specific, the disruptions within urban road networks can be categorized in respect to frequency and predictability (Immers et al., 2004). **Table 3.2** shows the disruptions which may happen in reality.

Table 3.2 Disruptions influencing the urban road networks

	Regular occurrences	**Exceptional occurrences**
Expected	The fluctuation of supply and demand, regular maintenance	Special events, extreme weather conditions, normal facility failures, strikes
Unexpected	Small incidents, facility failures	Natural calamities, man-made sabotage,

terrorist attacks

The normal change of supply and demand and maintenance activities may affect the normal working of road networks, but these are predictable and risks are relatively low. In the context of current technologies and information transparency, extreme weather conditions, normal facility failures and strikes in modern society are also controlled well. The situations that are difficult to anticipate tend to be related to human factors, such as accidents, man-made sabotage and terrorist attacks, which often lead to huge disruption to the network system. Earthquakes are one of the natural disasters that can only be predicted a few seconds before occurring, and are therefore classed as unexpected situations. In general, regular disturbances occur with higher probability and exceptional disruptions happen with less probability. Consequently, exceptional and unexpected situations have more serious effects on the network than expected situations. All of these situations involve technical, economic and political issues.

All these disruptions affect the transport networks in different ways, which can be summarized as follows:

- Capacity reduction

Most disruptions lead to the degradation of network capacity, and the extent and the magnitude of such degradation depend on the types of disruptions. Regular occurrences may cause local and minor capacity loss of road networks, while some exceptional disruptions such as extreme weather conditions may lead to global capacity degradation of the networks.

- Node/link removal

This is an extreme case of capacity reduction. The removal of nodes can lead to the capacity of the network dropping to an extremely low value. In exceptional cases, such as terrorist attacks and

natural calamities, there may be complete destruction of network components, and these can be divided into random/ targeted attacks based on the extent of information completeness.

In fact, a simple and well-known approach to simulate the form of the disruptions impact is to reduce the capacity of the network or the capacity of the links and/or nodes of the network. For example, Aderinlewo and Attoh-Okine (2009) introduced intentional attacks in reality by reducing the capacity of links.

3.4 Day-to-day dynamic traffic models

Day-to-day traffic assignment methods are deemed to be most appropriate for analysing traffic equilibration processes due to their flexibility in accommodating a wide range of behaviour rules, levels of aggregation, and the various traffic models to be integrated within the same modelling framework (Watling and Hazelton, 2003). In this thesis, the robustness and resilience of traffic networks are observed from the perspective of the evolution of day-to-day traffic, and disruptions; control mechanisms and distinct route choice behaviours are also incorporated into the model in order to demonstrate how drivers adapt their behaviours to improve the robustness and resilience when suffering disruptions under different control strategies.

Day-to-Day (DTD) Evolutionary Dynamics are used in this thesis to describe and predict the daily variation of traffic flows and drivers' route adjustment processes. Day-to-day (DTD) models are typically used to accommodate disequilibrium traffic models with embedded drivers' learning processes. Smith (1984b) proposes a deterministic DTD model through the proportional switch adjustment process (PSAP), which stipulates that drivers on a higher-cost path tend to switch to a lower-cost one on the next day at a rate proportional to the cost differences between these two paths. Following this, modelling the path choice dynamics using PSAP becomes a focus. Huang and Lam (2002) model the traffic assignment problem with a queue for simultaneous route and departure time (SDR) choices as a minimization problem, and PSAP is used to iteratively update the

route choice based on route costs and flow. Peeta and Yang (2003) study the stability issues in traffic assignment models of route guidance strategies by combining advanced information systems.

In addition, Zhang and Nagurney (1996) and Nagurney and Zhang (1997) regard the drivers' adjustment process prior to reaching equilibrium as a projected dynamical system (PDS). Friesz et al. (1994) apply a network tatonnement process (NTP) to model the disequilibrium state of DTD dynamics. One type of evolutionary traffic flow dynamics known as the Brown-von Neumann-Nash (BNN) dynamic is used to study how drivers are equally likely to switch strategies with the rate being proportional to the sum of the excess payoffs (Yang, 2005).

While all the above models are based on path flows, He and Liu (2012) propose a link-based day-to-day traffic assignment model to capture the evolution of traffic under network disruptions. The authors describe the traffic equilibrium process with a prediction-correction model rather than relying entirely on their own experiences from previous days. Following this, He and Peeta (2015) develop a marginal utility day-to-day traffic evolution model based on drivers' rationality in their route choices, i.e. by including marginal benefits/costs in the route choice models. In order to capture the characteristics of drivers in terms of route choice within an urban railway network, Wu et al. (2013) propose a day-to-day traffic assignment model taking into account the Bounded Rationality (BR) of drivers. Guo et al. (2015) introduce a general link-based day-to-day dynamic model to facilitate the understanding of the day-to-day adjustment mechanism of traffic flows. Wang et al. (2015) propose a day-to-day congestion pricing scheme to improve the network resilience after transport networks suffers disruptions. Smith et al. (2013) investigate the long term behaviour of deterministic and stochastic day-to-day dynamic models.

In general, the drivers' behaviour in day-to-day models depends on their previous experience on past days. Maio et al. (2013) investigate the influence of previous experience on updating drivers' perceptions regarding route travel time, which may decide route choices. In their model, the route choice and alternative route set both evolve as drivers are aware of new alternatives based on

experience and acquired information. He et al. (2014) develop a day-to-day dynamic model taking into account many drivers' behavioural characteristics such as bounded rationality, risk attitude and forgetting previous route costs. The diversity of route choice behaviours can be illustrated in these models, and both focus on the influence of driver experience on route choice.

The process of evolution within DTD models can be formulated as either a deterministic process or a stochastic process (Walting, 1999). For the deterministic process, initial conditions precisely deicide the evolution of the system. Smith (1984a), Friesz et al. (1994) and Zhang and Nagurney (1996) pay attention to the equilibrium of the system from the perspective of a continuous time process, yet such an approach tends to ignore the heterogeneity of drivers (Watling and Hazelton, 2003). The DTD dynamic models with discrete time have therefore received more attention. Horowitz (1984) investigate the stability of the equilibrium for a simple network, using three route choice decision models and with drivers updating their perceptions based on accumulated knowledge during the most recent days. Cascetta and Cantarella (1993) discuss the theoretical framework of discrete time DTD dynamic model. Following this, Cantarella and Cascetta (1995) and Watling (1999) further discuss the relationship between deterministic and stochastic processes within DTD models with discrete time. Most of the stochastic day-to-day models tend to follow the Markov process (Davis and Nihan, 1993, Watling and Hazelton, 2003, Hazelton and Watling, 2004).

Various constraints, behavioural rules and control strategies can be incorporated into the DTD dynamic models to adjust traffics based on certain circumstances. There are many studies related to the day-to-day model combining Advanced Traveller Information System (ATIS). Han et al. (2011) propose a DTD dynamic system with ATIS to explore the stability of the system, with their results showing that ATIS causes system instability in some cases. Cantarella (2013) investigates the effects of an intelligence transport system (ITS) on total user surplus using a deterministic DTD model. Liu and Smith (2015), meanwhile, focus on the role of different signal control on the traffic evolution of a proposed DTD dynamic model. Wang et al. (2015) employ a toll mechanism in a day-to-day

dynamic evolution model to observe the impact of this mechanism on the traffic evolution after the disruptions. Han et al. (2015a) incorporate variable message sign (VMS) control into a DTD dynamic model to examine the influence of VMS on network performance.

This review of DTD dynamic models shows that, due to their flexibility, DTD models can be incorporated into various control mechanisms, information, and driver behaviours to observe the traffic evolution. In addition, the number of DTD models at disaggregate flow levels is limited.

3.5 Traffic Control

In the daily operation and management of URNs, many forms of control can be utilized to mitigate traffic congestion and delays. The previous section showed the flexibility of DTD dynamic models to incorporate behaviour rules and traffic control, and this section reviews the effect of variable message signs (VMS) and adaptive signal control on transport networks.

3.5.1 Variable Message Sign (VMS)

There are many studies assessing the impact of VMS on traffic performance. Lam and Chan (1996) propose a time-varying traffic assignment model with travel time information relayed by VMS in order to examine the effectiveness of VMS. UE objective value and the mean trip length frequencies are used as two performance indicators to compare cases with and without VMS, and the results show that the effectiveness of the VMS is more significant when congestion occurs.

In order to guide investment and operational decisions, Chatterjeea et al. (2002) employ three questionnaires to examine the impacts of VMS information. Their results show that most drivers hold a positive attitude to more future investment in VMS, and the locations of incidents and the message content are confirmed to be important factors which would affect the diversion probability. In addition, in this study, two thirds of drivers do not notice the VMS information and only one fifth intend to divert.

Chen et al. (2008) develop a simulation model with VISSIM to evaluate the effect of route guidance with and without VMS under common and serious congestion. Their result demonstrates that the effects of VMS on traffic efficiencies are apparent, and VMS has a more significant improvement on serious congestion than that on common congestion.

Wei et al. (2009) point out that traditional VMS designed manually by traffic administers is inefficient and ineffective. Based on this, they develop a dynamic regional traffic guidance model with four layers: resources, information generation, algorithm configuration and VMS applications, to measure the average traveling time and the average waiting time of all vehicles with dynamic, static and non-VMS algorithms, respectively. Results show that the average travel time and average waiting time are better for the dynamic algorithm than for the other algorithms.

To bridge the gap in modelling the traffic dynamics and drivers' learning processes in an analytical way, Han et al. (2015a) propose a dual-timescale dynamic assignment model combining VMS and its compliance rate. The within-day dynamic model mainly captures realistic features such as shock waves and queue spillbacks by a novel dynamic network loading (DNL) procedure, while a day-to-day dynamic model incorporates the bounded rationality of drivers and takes into account route choices and departure time choices. A numerical example located in Glasgow is used to investigate the effects of VMS on route choices and congestion in both the short and long run. The finding shows that VMS has an adverse effect on network performance in the long run.

All these studies show that VMS has great impacts on route choice and network performance, and may play a positive role in mitigating delays and congestion in most of cases.

3.5.2 Adaptive signal control

As a main tool to manage traffic, adaptive signal control is able to improve the performance of URNs and mitigate congestion and delays by adjusting the red/green time split, namely, the signal plan, according to information detected in real-time.

Webster (1958) was one of the first to explore how to model the signal settings and how such settings affect the traffic flow on a single junction. Following this, Robertson (1969) developed a model (TRANSYT) which optimizes the whole network of traffic signals. These are all based on a very unrealistic fundamental assumption, however; that the chosen signal setting does not affect the route choices of drivers. In order to seek mutual interactions of traffic assignment and signal control, many studies related to these have emerged.

Allsop (1974), Gartner (1976), Smith (1979a), Smith (1979b), Smith (1979c), Gartner (1976) and Dickson (1981) are regarded as the earliest scholars who explore combination models of route choice and signal control. Allsop (1974) explores the relationship between the signal control and route choice. The Iterative Optimization and Assignment (IOA) method, which consists of two steps: the signal control setting calculation and traffic flow assignment, is used to represent the interaction between route flow and signal control. He finds that signal settings may influence trip distribution. Gartner (1976) realizes that signal control may influence the demand pattern and thus improve the system-oriented total cost, although the assumption is that the route choice is insensitive to signal control, namely, route choice is fixed in his study. Dickson (1981) investigate how signal settings at signalized junctions influence the route flow at the equilibrium state by taking into account the optimization of total travel cost. They point out that there is mutual relationship between signal settings and traffic flow. The signal settings influence the traffic flow by the adjustment caused by the change of travel time; in the meantime, the signal parameters vary accordingly with the current route flow.

Meneguzzer (1998) combines signal control with Stochastic User Equilibrium (SUE) to study a Combined Traffic Assignment and Control (CTAC) model, which can be solved by the IOA method. The purpose is to develop a methodological framework to evaluate the effectiveness of different adaptive signal control with different levels of user information. One of the distinct features of signal

control here is that the link capacities are not fixed and exogenous, but endogenous and variable with the magnitude of green time at the signalized junctions.

Maher et al. (2001) propose a bi-level program including traffic signal optimization on congested networks and stochastic user equilibrium assignment. The previous is the upper-level and the latter is the lower-level problem. A solution algorithm is presented to solve this bi-level program and the algorithm is tested on several networks.

Nowadays, two main signal control strategies exist. The first is an equi-saturation policy (Webster, 1958) which is one of the oldest signal control used to adjust traffic, and the second one is a P0 policy (Smith, 1979a, Smith, 1979b, Smith, 1979c), which is less conventional and more recent. The core of both signal control is to calculate the green time based on the traffic delays in the assignment models. The aim of the equi-saturation policy is to minimize the delay at the junctions, and thus the green time split is derived from an equalized function in terms of link flow and saturation flow; a detailed introduction of this policy can be found in **Section 7.1.2**. The P0 signal control policy is able to maximize the capacity of the network by adjusting the green time split so as to equalize the product of saturation flow and delay term (Smith, 1979c). The rationale for this policy is to reduce green time split for the approaches with congested traffic, and encourage more drivers to use routes with less flow. In this way, the capacity of the network can be efficiently used. A detailed introduction of the P0 policy can be found in **Section 7.1.3**.

More recently, Mounce (2009.) points out that the signal responsive control may change the traffic route by changing the travel time through the adjustment of junction signal settings, and that the signal system is really at equilibrium when it satisfying the condition of equilibrium with respect to re-routing. Smith and Mounce (2011) develop a within-day and day-to-day dynamic model with splitting rates at nodes or node-exit flows. Their results show that such a dynamic model gives rise to route flow converging to approximate Wardrop equilibrium under certain conditions. Signal green-

times are incorporated into the model, and the responsive signal control with an equi-saturation policy, combined with traffic assignment leads to unpredictable discontinuous behaviour.

Meneguzzer (2012) investigate the mutual interactions of signal settings and traffic assignment under two alternative deterministic, discrete-time DP models, which are compared with the conventional iterative optimization and assignment (IOA) method of combining signal control. Equi-saturation and P0 policies are incorporated in the models, and convergence and equilibrium properties are used to assess the performance of the DP and IOA models.

Liu and Smith (2015) propose a novel day-to-day dynamic model for traffic rerouting, which is based on the restricted proportional-switch adjustment process (RPAP) improved from Smith (1984a)'s proportional adjustment process (PAP) and modified according to the comments from He et al. (2010). This model combined a dynamic model of green-time swapping to illustrate how signal control mutually influences traffic flow on links.

The exploration of the combination of traffic assignment and signal control has been a central focus in the field of traffic control. Adaptive Signal control may facilitate the mitigation of congestion and traffic delay.

3.6 Summary

This chapter has reviewed existing definitions and interpretations of the robustness and resilience in a wide variety of contexts as well as other key notions and methodologies in the field of network theory, infrastructure resilience and traffic network modelling. The successful application of complex network theory in many real-world networks, such as social networks and biological networks, demonstrates its capability to capture profound network dynamics with relatively simple measures. In addition, the review of the application of complex network theory confirms the shortage of studies of urban road networks that focus on physical road segments and junctions.

The review of the existing literature suggests a lack of a systematic and comprehensive examination of different topological and operational indices in the context of network robustness. It seems that the notion of robustness (or resilience for that matter) is used somewhat haphazardly. Although each study employ reasonable network performance indicators for the intended application, these indicators are never assessed on a similar platform and cross-compared with one another. This thesis aims to address this gap through a comprehensive review of different notions of resilience/robustness, a classification of disruptions, followed by extensive comparison of various indices on different networks. The review of DTD dynamic models confirms their suitability to capture the short- and long-term evolution of URNs and, in particular, to study resilience and robustness due to their flexibility to accommodate a wide range of behavioural rules, levels of aggregation and different traffic flow models. Finally, a review of transport control was conducted in order to understand the control mechanisms behind variable message signs and traffic lights, their applicability in different network scenarios, and the mathematical details pertaining to their modelling and simulation.

Chapter 4 TOPOLOGY ANALYSIS OF URBAN TRANSPORT NETWORKS

Urban road networks (URNs) are highly complex systems that not only have a large number of links and nodes but are also characterized by numerous factors such as link capacity, link length and drivers with distinct socio-economic backgrounds. Topology analysis is the first step to explore and understand the structural features of URNs so as to discover the underlying characteristics of these networked systems. Based on this, more complex analyses and comparisons can be conducted. This chapter mainly explores the topological characteristic of nine selected URNs using topological indices such as indegree/outdegree, weighted closeness and weighted betweenness centrality. Based on the calculation of these indices, their distributions are analysed to infer the underlying characteristics of the URNs. Furthermore, small-world analyses and correlation analyses are conducted to look for the common features and inherent structural properties of these URNs, and to make distinctions across different URNs. In order to observe the hierarchical and structural characteristics of these URNs in great depth, community detection (Lancichinetti et al., 2011, Newman and Peixoto, 2015) is also conducted via the Order Statistics Local Optimization Method (OSLOM).

4.1 Description of urban road networks

In this chapter, urban road networks are considered in order to explore the topological characteristics of URNs. Due to the limited scope of our data sources, these URNs are mainly from Europe and North America. It would be a meaningful extension of this thesis to consider URNs from the rest of the world and especially in developed and developing countries, which could provide qualitative insights regarding the inherent network structures in different regions of the globe.

Unlike typical Space *L* and Space *P* representations (von Ferber et al., 2007), the links of all networks used in this section denote the streets or road segments, and the nodes represent the starting, the ending or the intersections of urban street or roads.

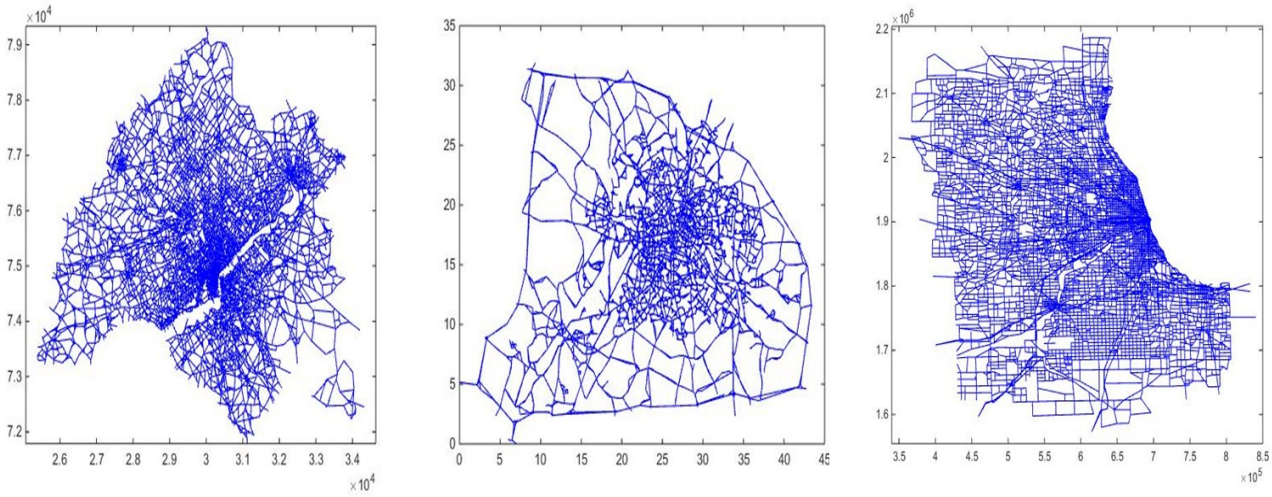

Fig.4.1 Schematic graphs of some urban road networks
a. Chicago; b. central Berlin; c. Philadelphia

The data related to these networks are obtained from the following website http://www.bgu.ac.il/~bargera/tntp/. These network data are frequently used in traffic assignment and modelling. **Table 4.1** presents the number of links, nodes and zones along with short descriptions of the urban road networks analysed in this section. Here, zones are the abstraction of places generating travel demand, namely, sources and destinations of Origin-Destination (OD) pairs. In general, travel demand is generated from within these zones.

Table 4.1 Urban road networks with different scales

City	Nodes	Links	Zones	Descriptions
Austin	7388	18961	7388	The 11th-most populous city in the USA, the capital of the state of Texas, known as the cultural and economic centre of the Austin-Round Rock metropolitan area (Weissmann, 2015).
Chicago	12982	39018	1790	The third most populous city in the USA, an international hub for finance, technology, commerce and transportation, with the largest number of highways and rail road freight (United States Census Bureau, 2015b).
Philadelphia	13389	40003	1525	The economic and cultural anchor of the Delaware Valley with an estimated population of 1560297 in 2014 (Bucks County Quick Facts from the US Census Bureau, 2014).
Anaheim	416	914	38	The second largest city of Orange County in the USA with an economy very reliant on tourism (United States Census Bureau, 2015a)
Winnipeg	1052	2836	147	The capital and largest city of Manitoba province in Canada, with a diversified economy and a hub for railway and

				transportation. It is called the best connected city of Manitoba (Winnipeg Tansportation Master Plan, 2011).
Central Berlin	12981	28376	865	The capital of Germany, with a transportation infrastructure consisting of 979 bridges, 197 km of inner-city water ways, and 5422 km of roadways (Mobile Capital, 2011). The road network used in this chapter is just the central part of Berlin.
Barcelona	1020	2522	110	The second most populous city in Spain (Instituto Nacional de Estadistica, 2009). It is a transport hub with one of Europe's principal seaports, an international airport and an extensive motorway network.
Terrassa	1609	3264	55	A Spanish city with an estimated population of 215517 by 2014 (Statistical Institute of Catalonia, 2014). It is well connected with internal 14 bus lines and connects with Barcelona by external highway and railway.
Hessen	4660	6674	245	A federal state within Germany with one of the best transportation networks in Europe. Many trans-European and German motorways, high speed trains, and waterway lines cross this city (Hessisches Statistisches Landesamt, 2016).

4.2 Analysis of the urban road networks

According to the methodology provided in **Section 2.1**, topological indices of these URNs are calculated in order to facilitate the explorations of topological characteristics, and the discovery of the underlying properties of the urban road networks (URNs) under consideration.

4.2.1 Degree centrality

Degree is used to measure the local centrality of the networks. In the URNs, each intersection of streets/roads is regarded as a node, while the link represents the streets/ roads between the nodes. Due to the fact that the nine URNs are directional, the degree is divided into indegree (the number of links leading to a given node) and outdegree (the number of links leading away from a given node). The average indegree and outdegree of nine URNs have been summarized in **Table 4.4**, and the degree distributions of nine URNs are illustrated in **Fig.4.2.**

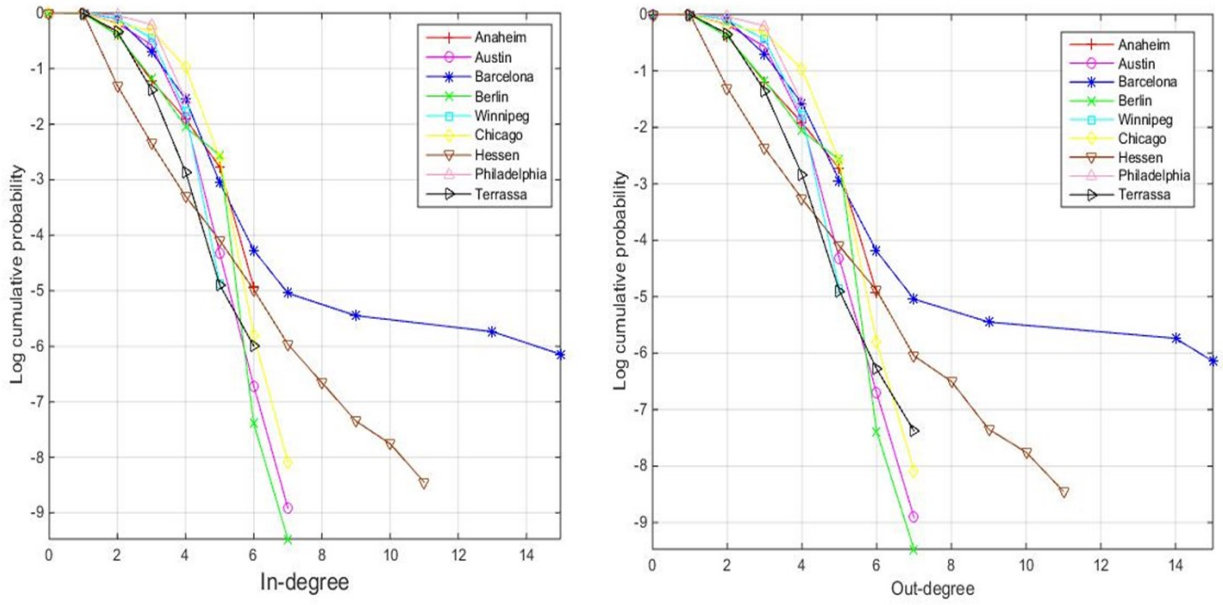

Fig.4.2 Indegree and Outdegree of urban road networks

In **Fig.4.2**, the y-axis represents logarithm of the cumulative probability $P(K \geq k)$, which is the probability that a randomly chosen URN node has indegree/outdegree equal to or more than k. This chapter can observe that the range of indegree and outdegree for nine URNs are limited regardless

of the size of the networks. For example, although the Philadelphia road network has 13389 nodes and 40003 links, the maximum indegree and outdegree are both 4. Among the nine URNs, Barcelona and Hessen have, respectively, the largest and second largest ranges of degree, despite their smaller sizes. The slope of the fitted curve in **Fig.4.2** depicts the speed of descent of the indegree and outdegree distribution curves.

Unlike the rest of the URNs, the indegree/outdegree of Barcelona has significant portions that are larger than 9, and the curves for Barcelona consist of two segments: the first one decreasing quickly while the second decreases slowly. **Fig.4.2** shows that most of nodes in these nine URNs are connected through a few nodes, and that the distributions of indegree and outdegree are qualitatively similar, which suggests that most of streets in these nine URNs are bidirectional.

Table 4.2 shows a regression on the distribution of indegree and outdegree.

Table 4.2 Regressions on indegree and outdegree for nine URNs

City		Degree distribution	Function	R square
Austin	Indegree	Power law	$P(k \geq x) = -0.0648 * x^{2.549}$	0.99
	Outdegree	Power law	$P(k \geq x) = -0.0647 * x^{2.55}$	0.99
Chicago	Indegree	Power law	$P(k \geq x) = -0.0149 * x^{3.253}$	0.99
	Outdegree	Power law	$P(k \geq x) = -0.0149 * x^{3.254}$	0.99
Philadelphia	Indegree	Power law	$P(k \geq x) = -0.0001 * x^{6.981}$	0.99
	Outdegree	Power law	$P(k \geq x) = -0.0001 * x^{7.002}$	0.99
Anaheim	Indegree	Power law	$P(k \geq x) = -0.0753 * x^{2.315}$	0.99
	Outdegree	Power law	$P(k \geq x) = -0.0743 * x^{2.321}$	0.99
Winnipeg	Indegree	Power law	$P(k \geq x) = -0.0032 * x^{4.559}$	0.99
	Outdegree	Power law	$P(k \geq x) = -0.0033 * x^{4.539}$	0.99

Berlin	Indegree	Power law	$P(k \geq x) = -0.0362 * x^{2.879}$	0.97
	Outdegree	Power law	$P(k \geq x) = -0.0368 * x^{2.87}$	0.97
Barcelona	Indegree	Two-regime power law	$P(k \geq x) = -0.1018 * x^{2.037}$ $P(k \geq x) = -3.338 * x^{0.2197}$	0.98 0.89
	Outdegree	Two-regime power law	$P(k \geq x) = -0.0514 * x^{2.471}$ $P(k \geq x) = -3.316 * x^{0.2193}$	0.99 0.91
Terrassa	Indegree	Power law	$P(k \geq x) = -0.1741 * x^{2.002}$	0.98
	Outdegree	Power law	$P(k \geq x) = -0.2464 * x^{1.776}$	0.98
Hessen	Indegree	Power law	$P(k \geq x) = -0.8043 * x^{0.9974}$	0.99
	Outdegree	Power law	$P(k \geq x) = -0.7979 * x^{0.9998}$	0.99

Table 4.2 shows that most of the indegree and outdegree distributions follow the power law well. This result is consistent with previous work relating to public transport networks (von Ferber et al., 2009, Sienkiewicz and Hołyst, 2005), worldwide maritime transportation networks represented in space *L* (Hu and Zhu, 2009) and the Chinese bus-transport network (Xu et al., 2007). It is worth noting that the indegree/outdegree distributions of some URNs also follow other distributions very well, for example, Anaheim, Berlin and Austin can also obey Gaussian distribution: $P(k \geq x) \propto e^{-(\frac{x-b1}{c1})^2}$, and the goodness of for indegree is 0.98, 0.95 and 0.96 respectively. Even so it is still enough to illustrate the decaying tendency of indegree/outdegree. In addition, **Table 4.2** shows that the distribution of indegree and outdegree for these URNs is very similar, and this confirms that most of the links within the nine URNs are once again bidirectional. All node degree distributions are shown to follow the power law well: $P(k \geq x) \propto x^{-\gamma}$ except that Barcelona follows a two-regime power law, and γ is the slope of the fitted curve (in the logarithmic coordinates) which depicts the speed of descent of the indegree and outdegree distribution curves. A distribution curve with a steep slope suggests that the majority of nodes have smaller values of indegree/outdegree given

that it is in the logarithmic coordinates; in other words, the URN overall is less well connected. Philadelphia, with the steepest slope among the nine URNs is overall less well connected than the other URNs.

4.2.2 Clustering Coefficient

The clustering coefficient (*CC*) is used to measure the local compactness of a network, and presents the clustering effect of the network. A larger *CC* of a given node means the neighbours of the node are more likely to attract each other so that the local area of the network is more compact. According to function (2.2), the *CC* for all URNs is calculated. **Fig.4.3** presents the log cumulative distribution $P(CC \geq x)$ of *CC*.

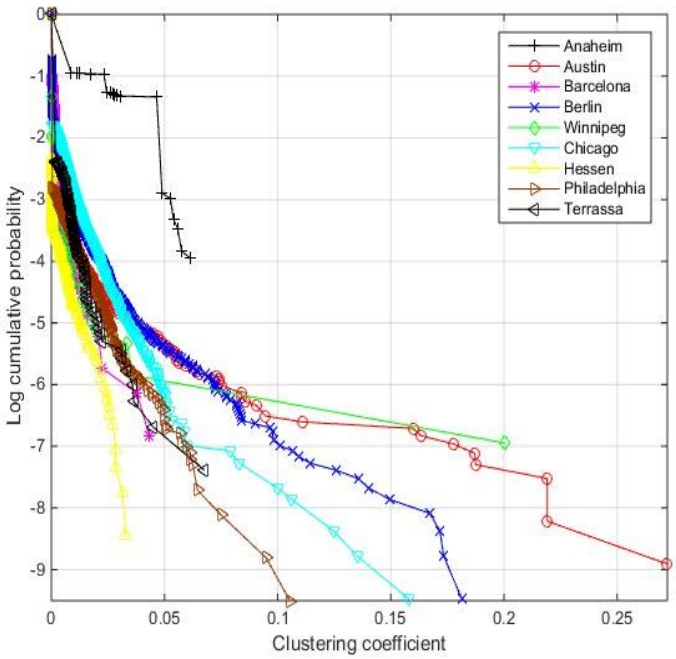

Fig.4.3 Clustering coefficient of URNs

As can be seen from **Fig.4.3**, the distribution for Hessen has the steepest absolute slope, which means the road network of Hessen is the loosest compared to other eight cities due to the fact that most of its nodes have smaller values of *CC*, followed by Winnipeg and Philadelphia. The URN of Terrassa is looser than Barcelona, Chicago, Berlin and Austin, and the nodes of Anaheim tend to attract each other within the local range more than the other urban road networks in this thesis. The

average *CC* for the nine URNs has been summarized in **Table 4.4**, which is normalized by the number of nodes, and also proves the viewpoint observed from **Fig.4.3**. The average *CC* of these URNs is smaller compared to the Chinese airport network (Li and Cai, 2004), the Italian airport network (Guida and Maria, 2007), the world-wide air transportation network (Guimera et al., 2005) and the Boston subway network (Latora and Marchiorib, 2002), possibly because the neighbouring nodes of a given node in the URNs are less likely to be connected to each other. This index is also able to be used to judge whether the network has small-world properties (Watts and Strogats, 1998), and it will be depicted in detail in **Section 4.3.**

4.2.3 Average path length (APL), diameter and efficiency

APL can be categorized as weighted and un-weighted. The weighted *APL* tends to measure the distance travelled from a given node to another node, while the un-weighted *APL* assesses how many links need to be traversed from a given node to another. Both are able to assess the degree of accessibility of the URN. This thesis analyses un-weighted *APL* to explore the structure of these URNs since there are no units for the distance data for the nine urban road networks, which means that comparisons of *APL* between different URNs are meaningless. Furthermore, geodesic distance, namely, the number of links connecting a node pair is more focused in this thesis because of the homogenous characteristics of the physical links of each individual network. Accordingly, the *APL* and the diameter for the nine URNs have been summarized in **Table 4.4**. Anaheim has the smallest *APL*, which means the nodes of this network are connected by the shortest geodesic distance. This is followed Barcelona and Winnipeg, while the three networks with the largest *APL* are Austin, Hessen and Berlin. The diameter and the *APL* of the nine URNs are strongly correlated with the coefficient 0.9714 according to a Pearson correlation. In some cases, *APL* and the diameter of networks are used to assess network performance (Albert et al., 2000a, Crucitti et al., 2003, Crucitti et al., 2004c). The correlations between the size of networks, *APL* and diameter are shown in **Fig.4.4**.

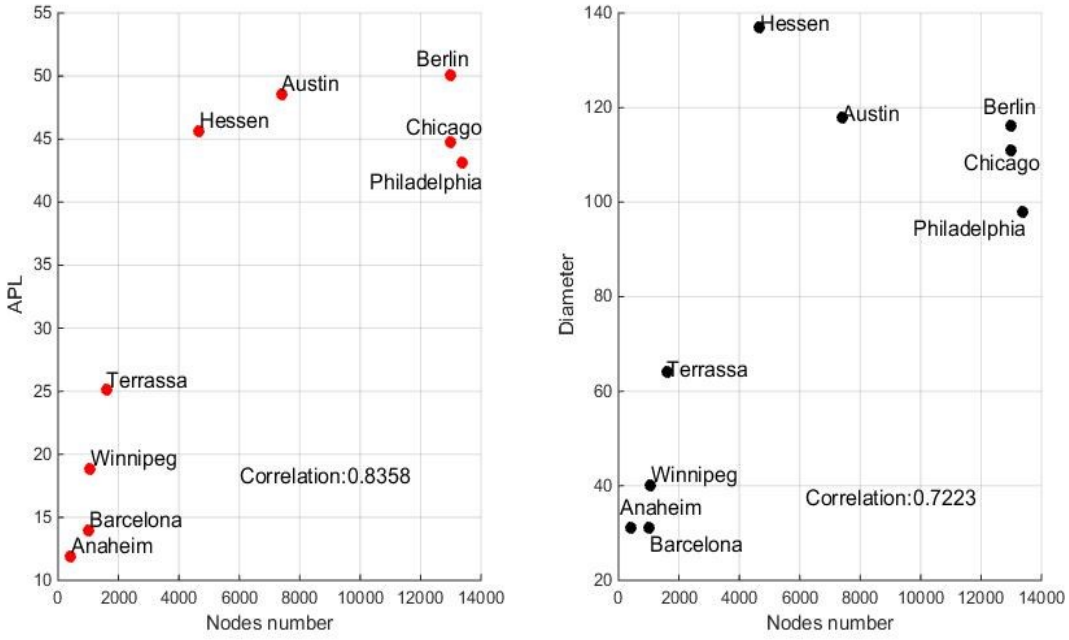

Fig.4.4 Correlations between *APL*, Diameters and the size of nine URNs

As can be seen from **Fig.4.4**, the Pearson correlations between *APL*, diameters and the size of networks are 0.8358 and 0.7223 respectively. This demonstrates that these two indices are positively proportional to the number of nodes to some extent.

In this thesis, *APL* is calculated based on function (2.3). If a network suffers severe disruptions, which may be generated by internal or external disruptions, so that the network is disconnected, an extremely large value is assigned to the disconnected links. While this approach has no effect on the ranking correlations and comparisons the absolute value of *APL* does not make sense. In order to better measure the performance of unconnected networks (Crucitti et al., 2003), an efficiency measure based on the inverse of the shortest path length is proposed in order to better observe the variations in the efficiency of different networks. According to the efficiency function presented in (2.6), the results of efficiency for the nine URNs are calculated and also summarized in **Table 4.4**. As can be seen, the results are consistent with the *APL*; for example, Anaheim has the smallest *APL* (11.87) and, correspondently, its efficiency measure is the largest of all nine URNs, while Berlin has

the largest *APL* (50.09) and the smallest efficiency. In general, efficiency is able to be used to measure the performance of networks when suffering disturbances.

4.2.4 Weighted Closeness Centrality (*WCC*)

As previously discussed in **Section 2.1.2.4**, closeness measures the accessibility of networks. In this thesis, the actual distances of links are taken as the link weights. According to function (2.4), the *WCC* for nine URNs are calculated. The cumulative distributions of *WCC* for these nine URNs are presented in **Fig.4.5** in a logarithmic scale. Given the differences in the size of these URNs, weighted closeness centrality is also normalized.

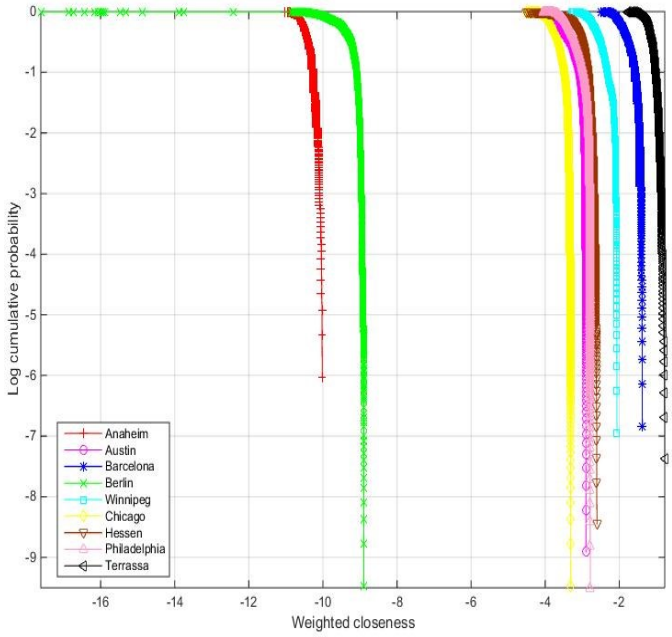

Fig.4.5 Weighted closeness centrality of URNs

As can be seen from **Fig.4.5**, all nodes of Anaheim and Berlin have relatively smaller *WCC* , which demonstrates that these two URNs are less accessible from a given node to other nodes, while Terrassa, Barcelona and Winnipeg have relatively large *WCC*. This conclusion is consistent with the result based on the average weighted closeness shown in **Table 4.4**.

The *WCC* distribution is fitted for the nine URNs , as presented in **Table 4.3**.

Table 4.3 Regressions on weighted closeness centrality for nine urban road networks

City	Degree distribution	Function	R square
Austin	Exponential	$P(WC \geq x) \propto e^{-135.1x}$	0.88
Chicago	Exponential	$P(WC \geq x) \propto e^{-262x}$	0.92
Philadelphia	Exponential	$P(WC \geq x) \propto e^{-118.9x}$	0.88
Anaheim	Exponential	$P(WC \geq x) \propto e^{-167300x}$	0.99
Winnipeg	Exponential	$P(WC \geq x) \propto e^{-48.93x}$	0.90
Berlin	Exponential	$P(WC \geq x) \propto e^{-72080x}$	0.96
Barcelona	Exponential	$P(WC \geq x) \propto e^{-34.03x}$	0.95
Terrassa	Exponential	$P(WC \geq x) \propto e^{-20.27x}$	0.99
Hessen	Exponential	$P(WC \geq x) \propto e^{-112.7x}$	0.99

As observed from **Table 4.3**, most URNs follow an exponential distribution, i.e. $P(WC \geq x) \propto e^{-\alpha x}$, yet Austin, Philadelphia and Winnipeg do not fit this exponential distribution as well as other networks. From this distribution, it can see that Anaheim and Berlin have the largest α parameter values, which suggests that most of the nodes in these two URNs have smaller *WCC,* followed by Chicago, Austin, Philadelphia and Hessen, and Terrassa and Barcelona have a smaller α value. This is consistent with what **Fig.4.5** describes.

The average closeness centrality for nine URNs is summarized in **Table 4.4**. The nodes with the largest *WCC* are generally thought as being located in the geographic centre of the city, since these nodes are easier to access than other nodes.

Table 4.4 Indices of nine urban road networks

City	Average Indegree	Average Outdegree	Average Betweenness	Closeness	Clustering coefficient	*APL*	Diameter	Efficiency
Austin	2.5658	2.5658	0.0099	0.0393	0.0010	48.58	118	0.0284
Chicago	3.0062	3.0062	0.0053	0.0273	0.0017	44.71	111	0.0297
Philadelphia	2.9878	2.9878	0.0059	0.0446	0.0007	43.17	98	0.0290
Anaheim	2.1971	2.1971	0.0316	0.00003	0.0157	11.87	31	0.1098
Winnipeg	2.7269	2.7269	0.0253	0.0897	0.0007	18.85	40	0.069
Berlin	2.1855	2.1855	0.0075	0.0001	0.0017	50.09	116	0.0242
Barcelona	2.7118	2.7118	0.0203	0.1853	0.0009	14.00	31	0.0765
Terrassa	2.0362	2.0362	0.0181	0.3441	0.0009	25.09	64	0.0533
Hessen	1.4322	1.4322	0.0160	0.0516	0.0003	45.60	137	0.0282

4.2.5 Weighted Betweenness Centrality (WBC)

Betweenness is a very important topological index in that it indicates that how frequently a given node is passed through by the shortest paths between all node pairs. In this thesis, the length of links is used as the edge weight, and *WBC* is calculated according to the function (2.5). The log cumulative distribution of *WBC* for the nine URNs is presented in **Fig.4.6**. In order to mitigate the effect of the size of different networks to betweenness, the weighted betweenness is normalized by dividing $n(n-1)$, where n is the node number of the network. **Fig.4.6** exhibits that most of the nodes for the nine URNs have small *WBC*, and among all URNs, by intuition, Chicago overall shows the fastest decaying behaviour, followed by Philadelphia, and Austin; while Anaheim presents a relatively flat decaying tendency, followed by Winnipeg and Barcelona. As discussed, the larger betweenness centrality of a given node means the node is more important due to the fact that more of the shortest paths in the URN pass through this node. According to Sun et al. (2014), a network is less robust if the proportion of nodes with large betweenness centrality is higher. The slopes of the

curves in **Fig.4.6** show this proportion statistically, in other words, the steeper the slope is the more robust the URN is.

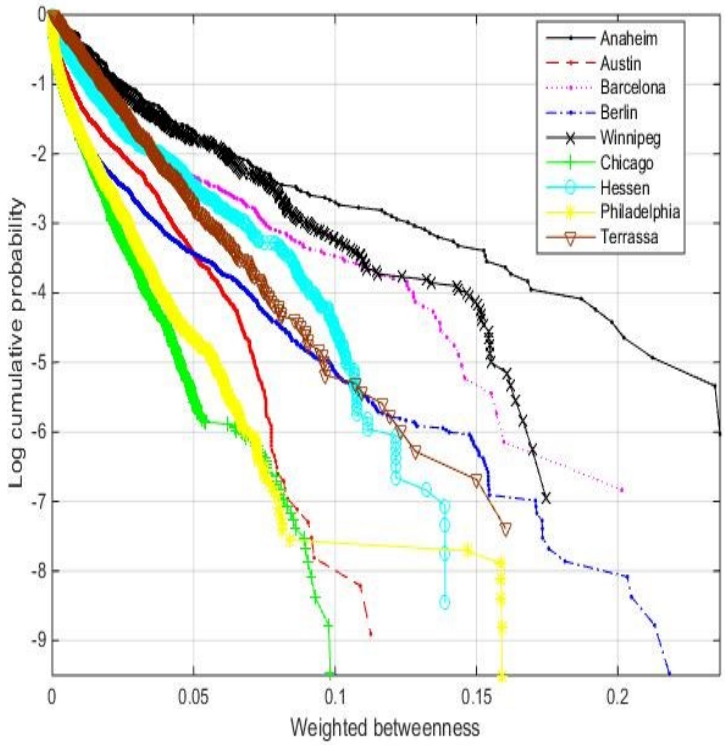

Fig.4.6 Weighted betweenness centrality of nine URNs

The log cumulative distribution of *WBC* can be also fitted by a power law function: $P(BC \geq x) \propto x^{-\alpha}$, and the results for this are summarized in **Table 4.5**. In this case, normalized *BC*$\in (0,1)$, thus the larger α the slower the rate of decay.

Table 4.5 Regressions on weighted betweenness for nine urban road networks

City	Degree distribution	Function	R square
Austin	Power law	$P(BC \geq x) = -24.79 * x^{0.6536}$	0.98
Chicago	Power law	$P(BC \geq x) = -32.02 * x^{0.6195}$	0.99
Philadelphia	Power law	$P(BC \geq x) = -26.49 * x^{0.5901}$	0.99
Anaheim	Power law	$P(BC \geq x) = -15.2 * x^{0.7496}$	0.99
Winnipeg	Power law	$P(BC \geq x) = -19.82 * x^{0.7811}$	0.98
Berlin	Power law	$P(BC \geq x) = -14.32 * x^{0.4645}$	0.99
Barcelona	Power law	$P(BC \geq x) = -20.13 * x^{0.7356}$	0.99
Terrassa	Power law	$P(BC \geq x) = -20.13 * x^{0.7356}$	0.99
Hessen	Power law	$P(BC \geq x) = -22.41 * x^{0.7174}$	0.98

Comparing all α, Berlin exhibits the quickest decaying characteristic of *WBC* distribution, followed by Philadelphia, Chicago and Austin, which is against the intuitive observation. The reason could be that the distributions tend to overestimate or underestimate the decaying tendency of the curves in this case. The average weighted betweenness centrality (*AWBC*) of these URNs, however, which are presented in **Table 4.4**, show that Chicago has the smallest value, followed by Philadelphia, Berlin and Austin, and that Anaheim has the largest value, followed by Winnipeg and Barcelona. Statistically, the lower the *AWBC* the network has the more robust the network is (Sun et al., 2014). The conclusion related to the robustness of these networks based on *AWBC* is therefore roughly consistent with that of observations from **Fig.4.6**.

WBC depicts how a given node of the network is passed by the shortest paths, and this information may be used to allocate important resources. Hence this index is sometimes used to assess the robustness and vulnerability of the network (Sun et al., 2014). In **Chapter 5**, this index will be

depicted in detail in order to compare this measure of the robustness of networks with other methods.

4.3 Small-worldness of urban road networks

A definition and detailed descriptions of small world networks was presented in **Section 2.1.3.3**. As a quick recap, small-world networks have *APL* as small as APL_{random} yet $CC \gg CC_{random}$ compared to random networks with the same number of nodes and edges, and a general feature of many complex networks is their small-world property (Watts and Strogats, 1998), meaning that two nodes in the network can be connected with shorter paths. In order to explore whether these URNs have significant small-world properties, random networks which have the same number of nodes and the same average degree as these networks are generated using the **Pajek** software so as to calculate their average path length (*APL*) and clustering coefficient (*CC*). The comparisons between the generated random networks and the corresponding urban road networks are shown in **Table 4.6**:

Table 4.6 *APL* and *CC* comparisons between nine URNs and corresponding random networks of the same size

City	*APL*	*CC*	APL_{random}	CC_{random}	*Ln(N)*
Austin	48.58	0.0010	9.2	0.0002	8.8940
Chicago	44.71	0.0017	8.6	0.0002	9.4713
Philadelphia	43.17	0.0007	8.6	0.0002	9.5022
Anaheim	11.87	0.0157	7.3	0.0032	6.0307
Winnipeg	18.85	0.0007	6.9	0.0018	6.9584
Berlin	50.09	0.0017	12	0.0001	9.4712
Barcelona	14.00	0.0008	7.4	0.0013	6.9276
Terrassa	25.09	0.0009	9.3	0.0007	7.3834
Hessen	45.60	0.0003	18.9	0.0003	8.4468

As can be seen from **Table 4.6**, the *APL* of the nine real-life urban road networks (URNs) are much larger than those of the random networks with the same size. Although the *APL* of Anaheim is the closest to that of the corresponding random network, it still takes 4.5 more. In the meantime, most of the *CCs* for these nine URNs are larger than that for the corresponding random networks, but they are still in the same magnitude-level, except for Berlin. The *CCs* of the URNs for Berlin and Winnipeg, meanwhile, are smaller than those for the corresponding random networks. In addition, the last column shows that *APL* does not scale logarithmically with network size, $Ln(N)$, where *N* is the number of nodes. The above observations show that the small-world property is not significant among these nine URNs. In many studies of realistic networks, however, such as metabolic networks (Guimera et al., 2007), the Chinese airport (Li and Cai, 2004), the Italian airport network (Guida and Maria, 2007), the world-wide air transportation network (Guimera et al., 2005), the Boston subway network (Latora and Marchiorib, 2002), the worldwide maritime transportation network (Hu and Zhu, 2009) and public transport networks (Sienkiewicz and Hołyst, 2005) small-world properties are evident. This may be due to the fact that these URNs are spatial and that all links are directional, which may increase the average geodesic distance between any node pairs and reduce the clustering effect in any given local area. This finding shows that these URNs are different from other networked transport systems in the real world, and this may imply more profound impacts of other characteristics of these networks.

4.4 Correlation analysis

Many topological indices for the nine selected URNs have been calculated and analysed in **Section 4.1**. Based on this, a correlation between these topological indices can be conducted in order to explore the relationship between the topological indices and the underlying structural properties of these URNs. In addition, many interesting intuitive questions in the field of network science can be answered by correlation analyses of topological indices, for example, whether the most connected nodes are most central ones or those that are most compact at the local level (Guimera et al., 2005).

4.4.1 Indegree and outdegree correlation

Degree is used to measure which nodes are most connected so as to observe the vulnerability of urban road networks in terms of their connectivity. In the previous section, calculations of indegree and outdegree were performed, and their distribution analysed, with the results showing that although the links of the urban road networks (URNs) are not all bidirectional, the distribution of indegree and outdegree is very similar and indeed the average indegree and average outdegree are almost exactly the same. If the outdegree and indegree are the same, it would show that the links within these URNs are all bidirectional, but it is difficult to judge this simply through the previous degree analysis. In order to check the relationships between indegree and outdegree, the correlations between normalized indegree and normalized outdegree were calculated and plotted for the nine URNs, as shown in **Fig.4.7**.

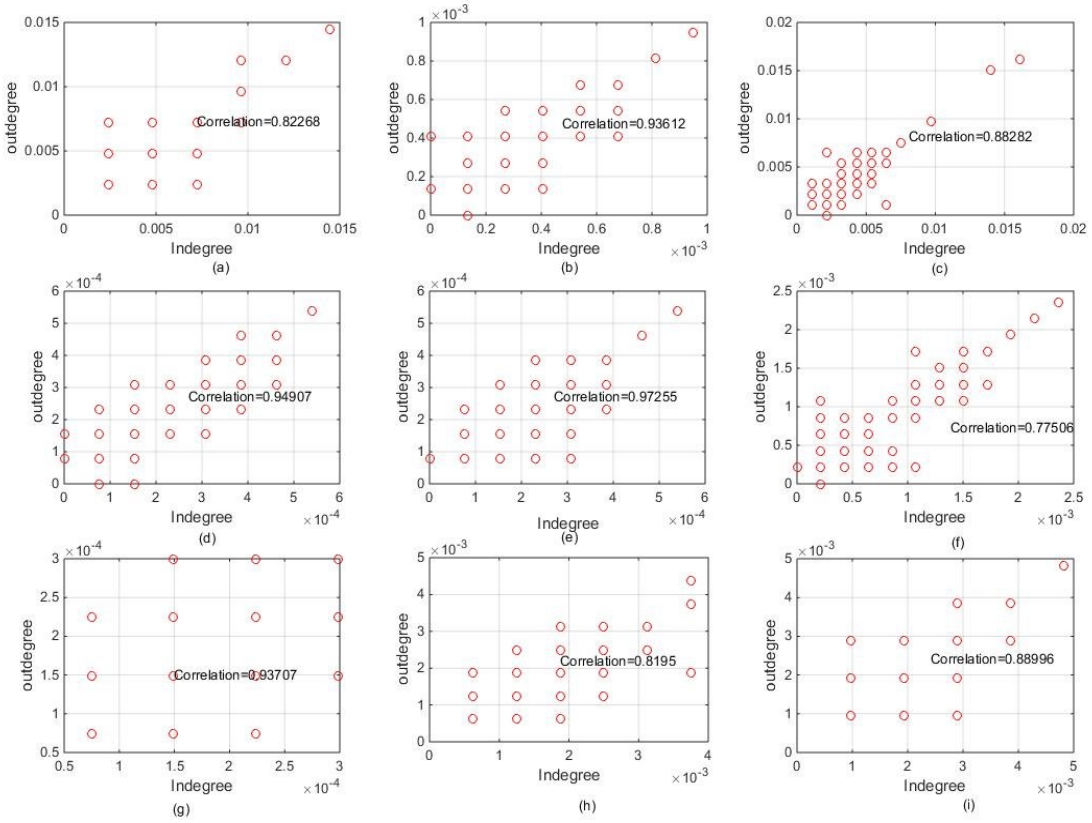

Fig.4.7 The correlation between normalized indegree and normalized outdegree
(a) Anaheim; (b) Austin; (c) Barcelona; (d) Berlin; (e) Chicago; (f) Hessen; (g) Philadelphia; (h) Terrassa; (i) Winnipeg

As can be seen, for the nine URNs, although the distribution of indegree and outdegree are very similar and average indegree and average outdegree are exactly the same, the correlations of these URNs are different, and, indeed, some, such as Anaheim, Barcelona, Hessen and Terrassa, are not highly correlated. This shows that some portion of the links within these URNs are unidirectional. Chicago with the largest correlation demonstrates that the proportion of unidirectional links is very low, followed by Berlin, Philadelphia and Austin. It seems that large-scale URNs tend to have a lower proportion of unidirectional links. The interesting phenomenon concerning indegree and outdegree is that the average indegree and average outdegree of such URNs are exactly the same, but the correlations between them are less than the expected 1. This may be due to the unique topological characteristics of URNs compared to public transport networks and airport transport networks.

4.4.2 Degree-betweenness correlation

The nodes with large degree are most connected, and the nodes with large betweenness are most central in the network. Nodes with large/small betweenness and small/large degree are regarded as anomalies (Guimera et al., 2005). In fact, it is easy to design networks in which nodes have large betweenness and small degree. For example, if there are two communities connected by a single node with just two links, the node must have large betweenness due to the fact that it is frequently passed by routes which are going to one community from the other. This node plays an important role in such a network system. In order to check whether nodes with large degree have large betweenness for these URNs, this chapter calculates correlations between betweenness and indegree and plots them as shown in **Fig.4.8**.

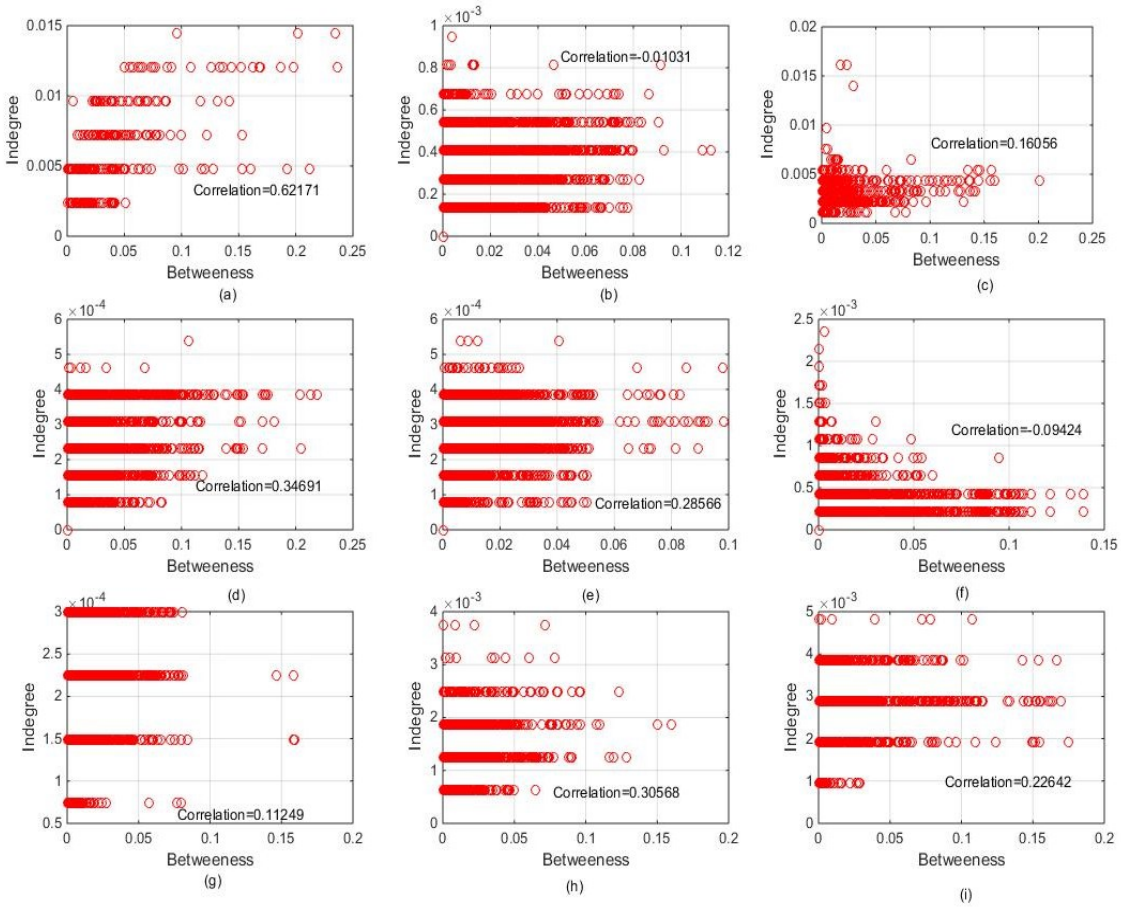

Fig.4.8 The correlation between normalized indegree and betweenness
(a) Anaheim; (b) Austin; (c) Barcelona; (d) Berlin; (e) Chicago; (f) Hessen; (g) Philadelphia; (h) Terrassa; (i) Winnipeg

Many complex networks, such as the Internet network (Vázquez et al., 2002), show that nodes with large betweenness also have a large degree, while the worldwide airport network presents anomalous behaviour in this regard (Guimera et al., 2005). As can be seen from **Fig.4.8**, the correlations between betweenness and indegree are weak, with neither presenting highly positive relationships or showing anomalous behaviour, but instead exhibiting more complex relationships. Anaheim has the highest correlation, 0.62, which means most of the city's nodes are well connected as well as central. Such relationships are almost non-existent for Austin, Barcelona, Hessen and Philadelphia, however, as shown by the low correlations (0.01, 0.16, 0.09 and 0.11, respectively). Such correlations may be caused by the distinct community characteristics of URNs. Although the indegree and outdegree are not exactly correlated for these URNs, the correlations between

outdegree and betweenness are identical to those between indegree and betweenness, as shown in **Fig.4.9**.

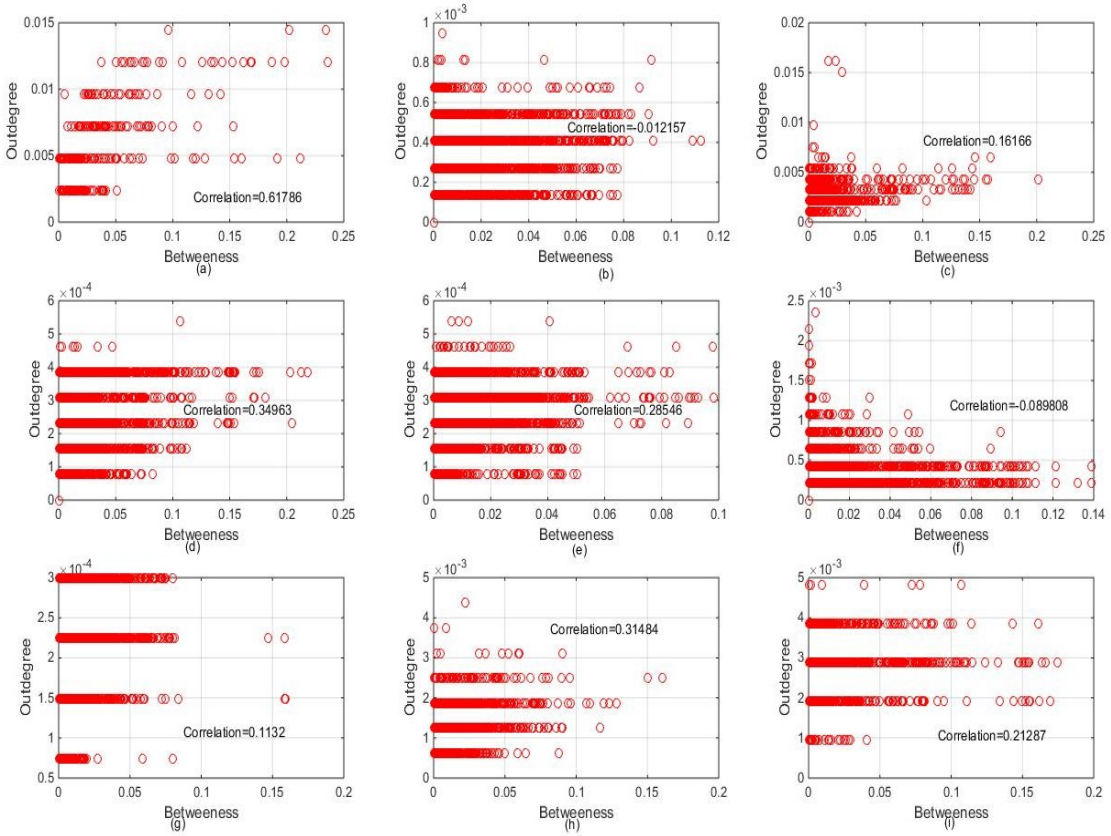

Fig.4.9 The correlation between normalized outdegree and betweenness
(a) Anaheim; (b) Austin; (c) Barcelona; (d) Berlin; (e) Chicago; (f) Hessen; (g) Philadelphia; (h) Terrassa; (i) Winnipeg

4.4.3 Degree-clustering coefficient correlation

In order to examine whether the well-connected nodes in these URNs still have a large clustering coefficient (*CC),* the correlations between *CC* and indegree are calculated and plotted, as shown in **Fig.4.10**. It is not surprising that the correlations between them are very low, in fact all lower than 0.25, since this is identical to the analyses of *CC*. For these URNs, the neighbouring nodes are less connected with each other. The correlations below confirm this viewpoint.

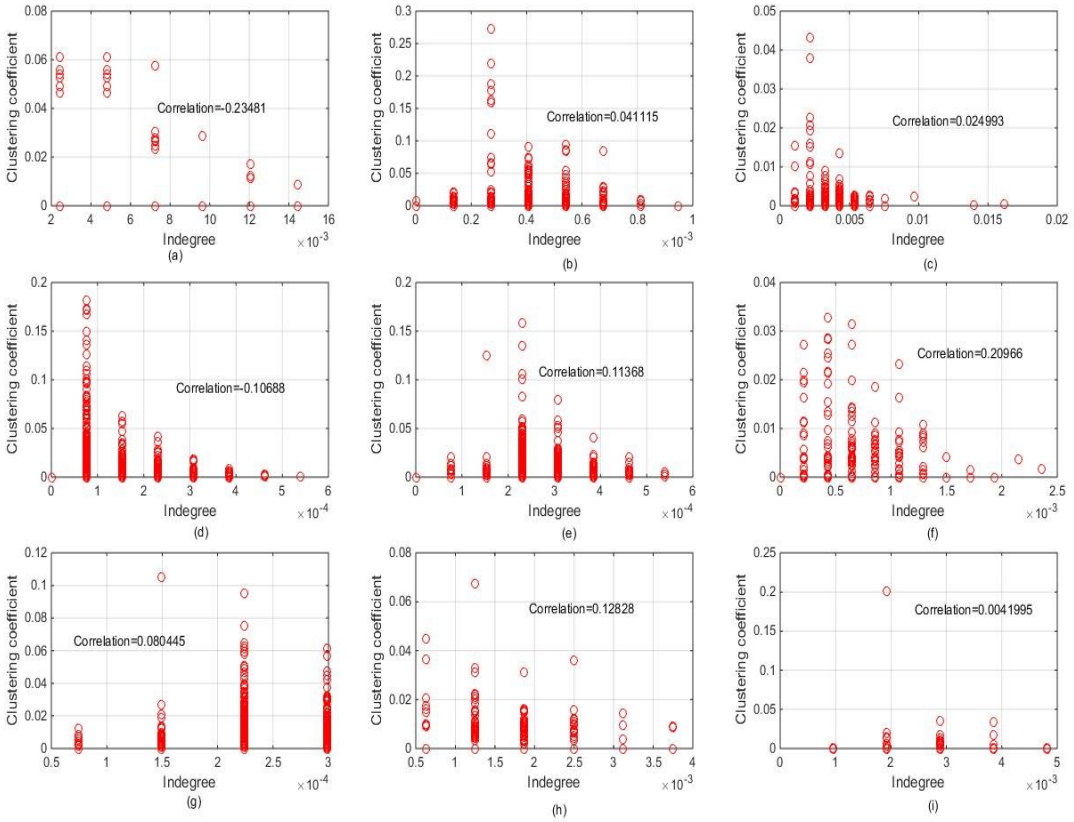

Fig.4.10 The correlation between normalized indegree and clustering coefficient (a) Anaheim; (b) Austin; (c) Barcelona; (d) Berlin; (e) Chicago; (f) Hessen; (g) Philadelphia; (h) Terrassa; (i) Winnipeg

The correlations between *CC* and outdegree are similar to that between *CC* and indegree, and against consistently very poor and lower than 0.25. The reason why urban road networks with many links have such poor correlations is that these networks are directional, and that the nodes in urban road networks tend to constitute quadrangles rather than triangles, which implies the neighbouring nodes of a given node are less likely to be connected with each other. This also explains why the clustering coefficients in these URNs are not very high.

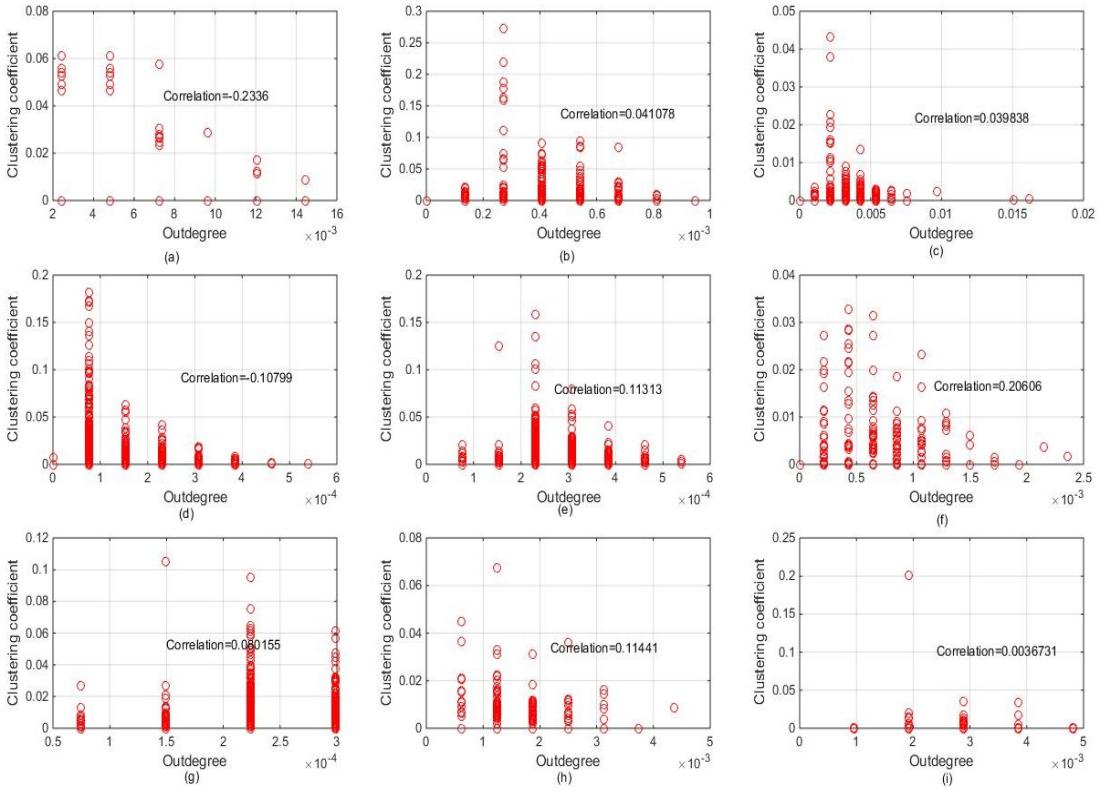

Fig.4.11 The correlation between normalized outdegree and clustering coefficient (a) Anaheim; (b) Austin; (c) Barcelona; (d) Berlin; (e) Chicago; (f) Hessen; (g) Philadelphia; (h) Terrassa; (i) Winnipeg

4.5 Communities of urban road networks

The previous sections have performed topological analysis, small-worldness and correlation analysis between some topological indices. Building on these analyses, this section detects and analyses community structures within these networks in order to explore the topological characteristics of the URNs more fully.

The detection and analysis of the community structures within large-scale networks has been a focus of research in recent years. The quantitative definitions of communities within networks are diverse. Fortunato (2010) defined a community as a groups of nodes which play a similar role or share common features or properties within those groups. Lancichinetti et al. (2011) regarded 'highly cohesive sub-graphs' of networks as communities, clusters or modules. In biological and social

networks (Fortunato, 2010), community structure is a common feature, and it is thought of as a division of networks into densely connected subgroups (Newman and Peixoto, 2015). Lancichinetti et al. (2011) proposed that a community is one pattern of node connections in realistic networks, and if a node is in one community, it means that this node has a higher probability of connecting to nodes in the same community than to those in other communities.

Detecting communities has important applications in reality. World Wide Web clients who have similar interests and are near to each other in terms of geographical distance may be provided with a better service due to the fact that the World Wide Web is able to designate a dedicated mirror server to clusters of clients (Krishnamurthy and Wang, 2000). Identifying communities of relationship networks between customers and online retailers, meanwhile, is helpful to provide efficient purchase recommendations to customers and marketing analyses to retailers (Reddy et al., 2002). The identification of clusters in large networks are good for data storage due to the fact that path searches can be efficiently conducted (Wu and Huberman, 2004). In computer science, community detection facilitates the improvement of efficiency for parallel computing due to the fact that it can guide the computers to allocate tasks to a processor in such a way as to minimize the calculation. In addition, community and cluster detection can be used to control and stabilize networked systems since the nodes classified as the core nodes of the clusters may play an important role to the system, and nodes which are located between different communities can be mediators to build communications for these communities. The community structure of a network also offers a better way to understand networked systems more completely in that it is a powerful visualization tool to present the representation of networks rather than simply showing all the nodes and links of the network. In the transport field, in order to make clear the role of human collective behaviour phenomena across time and space in London transport, intertwined communities of traffic across the whole city are investigated by Petri et al. (2013) to prove that this human spatial system is able to reach a self-organized critical state. Community detection has therefore been a hot topic in the modern science of complex systems (Fortunato, 2010).

There are many methods and algorithms to detect communities in graphs, such as graph partitioning, hierarchical clustering and spectral clustering (Fortunato, 2010), but they all have limitations in handling edge weights, edge directions or overlapping communities. In this chapter, Order Statistics Local Optimization Method (OSLOM), which is calculated based on the connectivity of networks and optimizes locally the statistical significance of clusters, is used to detect the community structure of these URNs. This was first proposed by Lancichinetti et al. (2011) and is capable of handling directional and weighted networks, overlapping community structure, hierarchical structure, pseudo-communities, and so on, due to the fact that OSLOM focuses on optimizing locally the statistical significance of clusters. The detailed algorithm can be found in Lancichinetti et al. (2011) work.

The word 'community' is derived from social science, recognizing that society provides various organizations such as friendship circles, families, enterprises and nation states, and that these organizations naturally derive many communities and complex hierarchical structures, which are crucial to the sustainable development and daily operation of human society. As a lifeline infrastructure, URNs can be regarded as one type of self-organized system, which means that they are similar to other systems in nature to some extent. In order to examine this natural property, community detection and analyses are conducted, based on the OSLOM method, and the results are shown in **Fig.4.12**.

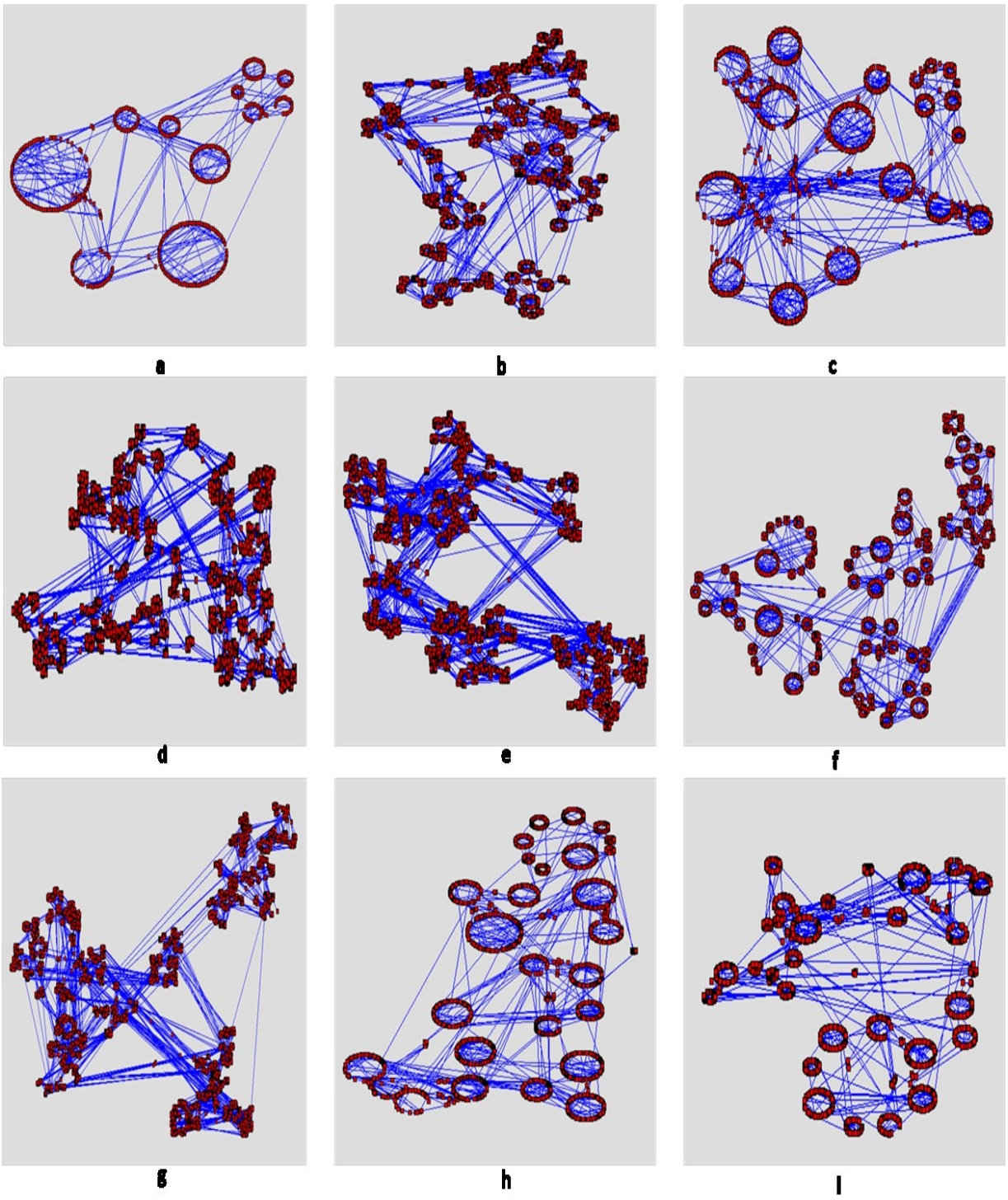

Fig.4.12 Schematic graphs of communities for nine urban road networks
a. Anaheim; b. Austin; C. Barcelona; d. Berlin; e. Chicago; f. Hessen; g. Philadelphia; h. Terrassa; i. Winnipeg

The communities of all nine URNs are presented in **Fig.4.12**. The first impression of these communities is that the bigger the URNs the more the complex community structure they have. For example, Austin, Berlin, Chicago and Philadelphia are the larger networks, and the number of communities for these URNs are apparently more than those in the smaller networks. In addition, it seems that these bigger URNs have a significant hierarchical structure, namely, the bigger clusters consist of several smaller ones. The smaller networks, such as Anaheim, Terrassa and Winnipeg, meanwhile, present a clearer community structure. In addition, some nodes which look like not belonging to any communities in these URNs are overlapping ones, which suggests that these nodes are shared by several communities and they may assist the mutual communications for these communities.

The number of hierarchical layers and the number of communities in each hierarchical layer are presented in **Table 4.7**.

Table 4.7 Structure of hierarchy and communities in each hierarchical layer for nine URNs

City	Nodes	Hierarchy layers	Communities in each hierarchy(from low to high)
Austin	7388	5	151; 46; 13; 7; 5
Chicago	12982	5	266; 81; 22; 7; 2
Philadelphia	13389	6	343; 100; 29; 11; 6; 3
Anaheim	416	2	11; 2
Winnipeg	1052	3	30; 8; 7
Berlin	12981	5	457; 112; 34; 14; 5
Barcelona	1020	3	20; 6; 4
Terrassa	1609	3	27; 5; 3
Hessen	4660	4	104; 25; 8; 5

Identifying the modules and structure of the hierarchy using the topology information encoded in the networks is the main purpose of detecting communities (Fortunato, 2010). As can be seen from **Table 4.7**, larger URNs are more likely to have more communities and hierarchical layers. For example, Philadelphia, Berlin and Chicago have 6, 5 and 5 hierarchy layers respectively, and the number of communities in the lowest layers is 343, 457 and 266 respectively. Anaheim, with just 416 nodes, however, has just two hierarchical layers and the number of communities at the lowest layer is just 11.

All these URNs consist of many communities, with each community consisting of many individual nodes, and hence the size of communities varies. To some extent, these communities may follow a certain distribution rule. In order to identify this point, histograms can be plotted, as shown in **Fig.4.13**.

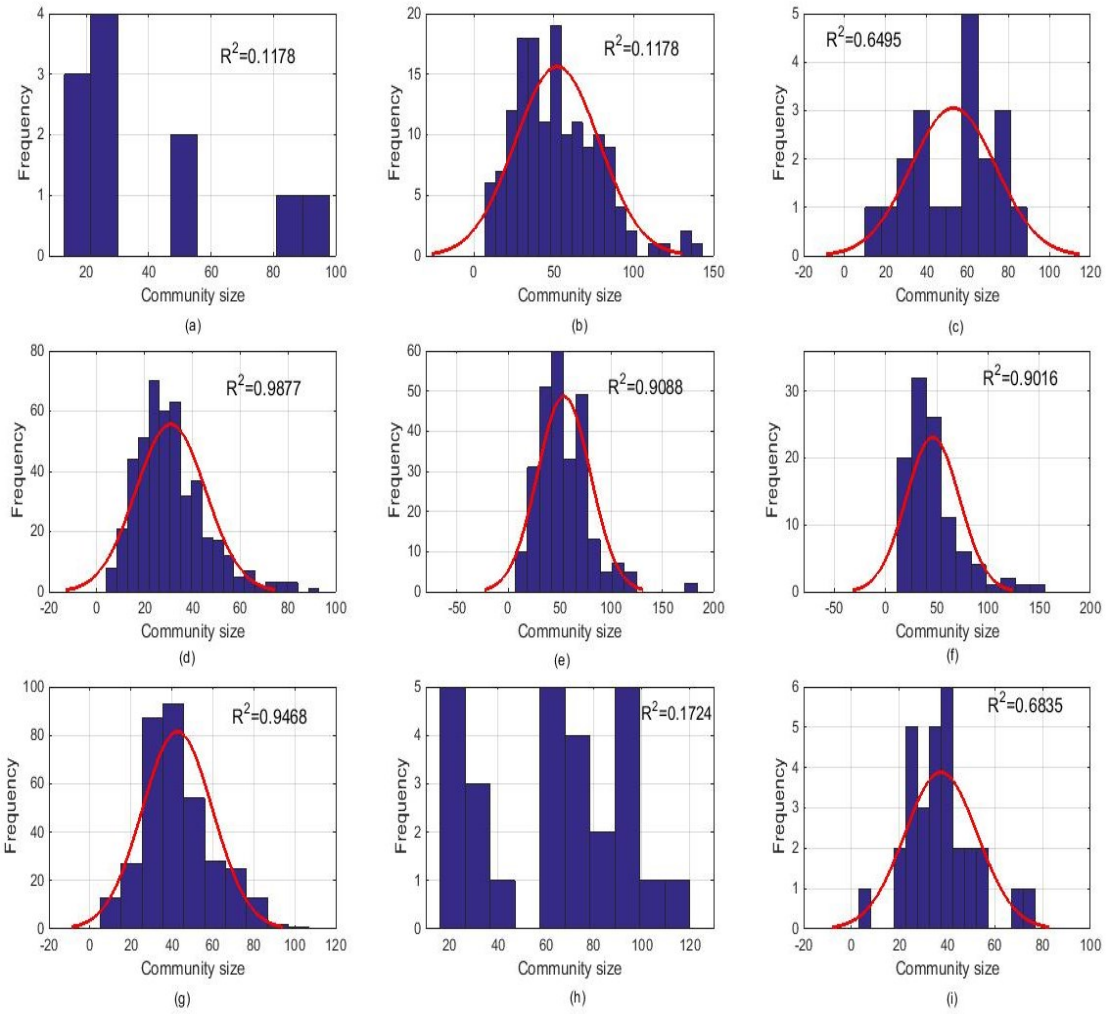

Fig.4.13 Histograms for nine URNs
a. Anaheim; b. Austin; C. Barcelona; d. Berlin; e. Chicago; f. Hessen; g. Philadelphia; h. Terrassa; i. Winnipeg

As can be seen from **Fig.4.13**, the larger URNs, such as Austin, Berlin and Chicago, tend to follow a normal distribution. Among these URNs, the left side of sub-figures regarding Austin, Berlin and Chicago does not fit well with normal distribution compared to their right side. The red lines in the graphs are the normal distribution fitting lines and clearly identify this point. $\boldsymbol{R^2}$, meanwhile, which is calculated based on the maximum likelihood method, represents the goodness of the communities of the URNs following normal distribution. Conversely, those URNs with a smaller size apparently have worse normal distribution, and it seems that Anaheim and Winnipeg do not follow any distribution rules due to the fact that these URNs are relatively small so they are not too many

hierarchical layers and communities. Through the above analysis, a rough conclusion is able to be summarized; that is, the larger the URNs are the better the normal distribution fitting they have.

The detection of communities for URNs may provide insightful views for the management and planning of transport within urban areas. For example, installing detectors or any other electronic facilities based on the distribution of communities may efficiently collect data such as traffic flows, driver behaviours and traffic incidents to improve network safety or mitigate traffic congestions. In addition, through the detection and analysis to communities and hierarchies of URNs, we may say that the URNs also tend to follow general nature rules in natural systems, such as a hierarchical structure and a normal distribution.

4.6 Summary

This chapter has investigated the topological characteristics of a number of nine urban road networks (URNs) for the first time. Widely used topology indices based on complex network theory were used in this chapter to explore the topological characteristics of the nine URNs, and relatively new notions such as community detection were also applied to supplement the understanding of these topological networks. The results can be summarized as follows:

- The average indegree and average outdegree of these URNs are exactly the same, and the distribution of indegree and outdegree are very similar, despite the fact that these URNs are directional. In addition, the distributions of indegree and outdegree for these URNs follow power law, showing that most of nodes have small indegree and outdegree.
- The clustering coefficients (*CC*) of the URNs are very low, suggesting the URNs are less compact in local areas.
- *APL* and diameters are proportional with the size of the URNs, and efficiency measures are consistent with *APL*. The results show that Berlin has the worst efficiency, while Anaheim has the best efficiency in terms of *APL*.

- Most of the weighted closeness of these URNs also follows an exponential distribution, and Anaheim and Berlin are the URNs in which most of the nodes have worse accessibility to other nodes.
- The weighted betweenness centrality (*WBC*) of all URNs follows a power law distribution well, and the parameterα ($P(BC \geq x) \propto x^{-\alpha}$) for the distributions is between 0.4 and 0.8.
- Unlike other transport networks, these URNs do not have significant small-world properties.

Based on this, the relationships among indegree, outdegree, *WBC* and *CC* have been examined, the correlations reveal that indegree and outdegree are positively correlated but are less than the expected 1, and the correlations between degree, *WBC* and *CC* are not significant; neither highly positive relationships nor anomalies exist in these URNs.

Following this, community detections for the URNs were conducted using the OSLOM method, and the results show that the larger the URNs were, the more communities and hierarchical layers they had. In addition to this, the distributions of communities at the lowest hierarchical layer for the URNs tend to fit a normal distribution better if the URNs are larger. These findings are compatible with common phenomena in natural and social science (Casella and Berger, 2001).

The purpose of this chapter has been to explore the topological characteristics of the URNs. This work also helps to prepare the ground for further analyses of robustness and resilience in the following chapters, however. The topological indices shown in this chapter are usually related to the robustness of networks due to the fact that some of these measures are able to reflect the efficiency and functionality of those networks (Holme et al., 2002, Crucitti et al., 2003, Crucitti et al., 2004c, Albert et al., 2000a), and this feature can be used for the assessment of robustness and resilience.

Chapter 5 ROBUSTNESS ANALYSIS OF URBAN ROAD TRANSPORT NETWORKS

This chapter builds on the topology analysis of urban road networks (URNs) presented in **Chapter 4**, and mainly focuses on complex networks with heterogeneous user behaviour. The User Equilibrium (UE) and System Optimal (SO) principles are considered in order to explore the robustness of selected urban road networks. Analysing topological indices may help to pin down the most important nodes for URNs from the perspective of connectivity, while more sophisticated operational indices (such as those introduced in this chapter) are helpful to examine the importance of nodes for URNs by taking into account link capacity, travel demand and drivers' behaviour. The first method is calculated in a static way, which reduces the computation times and increases the efficiency for a quick assessment of the robustness of URNs, while the latter is calculated in a dynamic way based on removal of individual nodes; this is more likely to capture realistic meanings but consumes a huge amount of computational effort. These calculations attempt to find the relationship between topological indices and operational indices so as to assist the assessment of the robustness of URNs to local disruptions.

In addition, this chapter proposes a new Relative Area Index (RAI), which is based on UE and SO, to measure the robustness of urban road networks quantitatively under global capacity degradation.

Weighted betweenness centrality is used to compare with RAI, and the results show that RAI is able better to measure the robustness of urban road networks of different sizes. This index is able to provide a benchmark for understanding and improving network robustness for the planning and management of URNs.

5.1 Operational indices for Urban Road Networks

This chapter utilizes topological and operational indices to analyse the robustness of urban road networks (URNs). Topological indices based on complex network theory have been introduced in **Section 2.1**, and the relative total costs based on UE and SO are detailed in the following section.

5.1.1 Relative total UE cost, Relative total SO cost and Relative price of anarchy (RPOA)

The descriptions and basic formulations of UE and SO have been given in **Chapter 2**. In this case, the relative total UE and SO cost are denoted as RTC_{UE} and RTC_{SO}. Specifically, this chapter proposes new robustness indices in **Section 5.2** based on Nagurney and Qiang (2007a) and Nagurney and Qiang (2009), and their index has been introduced in detail in **Section 3.1.3**. The relative total UE can be presented in the following way:

$$RTC_{UE}^{i} = \frac{TC_{UE}^{i} - TC_{UE}}{TC_{UE}} \times 100\% \tag{5.1}$$

Here, TC_{UE}^{i} is the total cost under the *UE* principle when node *i* in the network is removed.

Similarly, the relative total *SO* can be shown as follows:

$$RTC_{SO}^{i} = \frac{TC_{SO}^{i} - TC_{SO}}{TC_{SO}} \times 100\% \tag{5.2}$$

Where TC_{SO}^{i} is the total cost under the *SO* principle when node *i* in the network is removed.

In addition, aiming to analyse the robustness of URNs under global capacity degradation, this chapter uses other relative total UE and SO cost indices originally proposed by Nagurney and Qiang

(2007), which are important components of the calculation of a new relative area index (RAI) and can be shown as follows:

$$RTC_{UE}^{\gamma} = \frac{TC_{UE}^{\gamma} - TC_{UE}}{TC_{UE}} \times 100\% \quad (5.3)$$

$$RTC_{SO}^{\gamma} = \frac{TC_{SO}^{\gamma} - TC_{SO}}{TC_{SO}} \times 100\% \quad (5.4)$$

Where γ is the capacity retention parameter, TC_{UE}^{γ} and TC_{SO}^{γ} are the total cost under UE and SO principles, respectively, when all the link/node capacities in the network are uniformly reduced by $\gamma\%$ of their original values.

According to function (2.25), *RPOA* can be formulated as follows:

$$RPOA^{i} = \frac{TC_{UE}^{i}}{TC_{SO}^{i}} \times 100\% \quad (5.5)$$

5.1.2 Relative Area Index (RAI)

A new Relative Area Index (RAI) is developed from an original *RAI* which was first proposed by Shang et al. (2014) and Pien et al. (2015) to explore robustness. The original *RAI* is presented below.

Various levels of degradation in the nodal capacity are taken into account, which may be due to recurring activities such as maintenance, or non-recurring events such as weather, accidents and terrorist attacks. Here u represents capacity degradation of a given node ranging from 0 to 1. $MF^{i}(u)$ is further denoted as the maximum flow obtained from linear programming assuming a degradation of capacity by *u* at node *i*, and unchanged nodal capacities elsewhere. The superscript *i* indicates that such degradation is applied to node *i*. Some examples of this function are shown in **Fig.5.1** below.

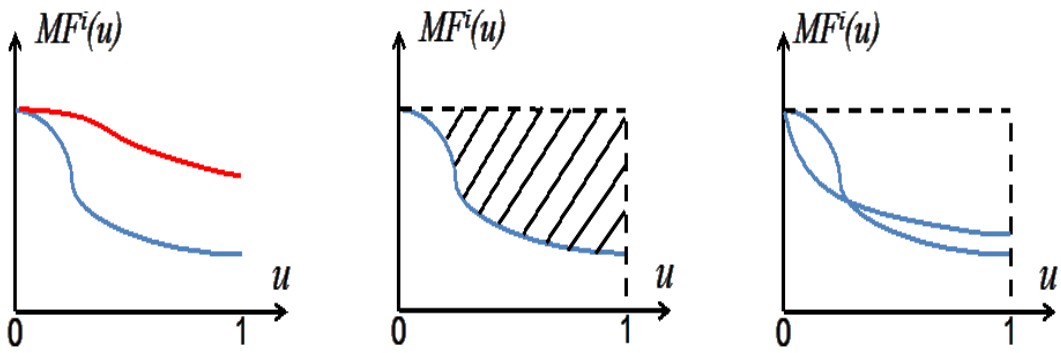

Fig.5.1 Illustrative examples of the $MF^i(u)$ function
Left: two examples of the function $MF^i(u)$: the upper (red) one shows better robustness than the lower (blue) one. Middle: using area as an indicator of the deterioration of network maximum flow. Right: two different curves may correspond to the same area, thus a weight is needed.

In order to capture and quantify the deterioration of network maximum flow, the area formed by the $MF^i(u)$ curve is considered, and the two line segment corresponding to *u=1* and $MF^i = MF^i(0)$; see **Fig.5.1** (middle). This area reflects how fast the network efficiency is decreasing as the capacity at node *i* is reduced. The smaller this is, therefore, the more robust the network is with respect to node *i*. Two different *MF* curves may yield the same area, however (**Fig.5.1**, right). A weighting parameter $w^i(u)$ is introduced, and the original Relative Area Index (RAI) for node *i is* considered:

$$RAI^i = \frac{\int_0^1 w^i(u).\left[MF^i(0) - MF^i(u)\right]du}{\int_0^1 w^i(u).MF^i(0)du} \qquad (5.6)$$

The numerator of Equation (5.6) is the weighted area with different weights $w^i(u)$, assigned to different levels of capacity degradation, namely, *u*. The adoption of the weighting function $w^i(u)$, serves to highlight a particular scenario or emphasize certain aspects of the network performance. In the case study of the air traffic network that follows, higher weights are assigned to smaller values of *u*; that is, the issue of concern is more focused on the network robustness with minor local perturbations. Here, the generality of the proposed original *RAI* is marked by noting that the choice of the weighting functions is arbitrary and can be tailored to suit different needs and objectives.

The weighting function can be used to accommodate different degrees of capacity reduction, depending on the cause of that reduction. It can be also be used to emphasize the performance and robustness of the network at a specific stage of deterioration.

The denominator of Equation (5.6) serves to normalize the area to enable the study of the trend of the network deterioration relative to its unperturbed performance. For a given node, the larger the original *RAI*, the more flow reduction it brings when its capacity drops, thus the network is less robust with respect to this node.

In this thesis, the weighting parameter $w^i(u)$ always takes 1, hence it is impossible to distinguish the following cases (shown in **Fig.5.2**) by using the original *RAI* to measure the robustness of urban road networks. Here, red and blue curves are the total cost at which the networks reach equilibrium.

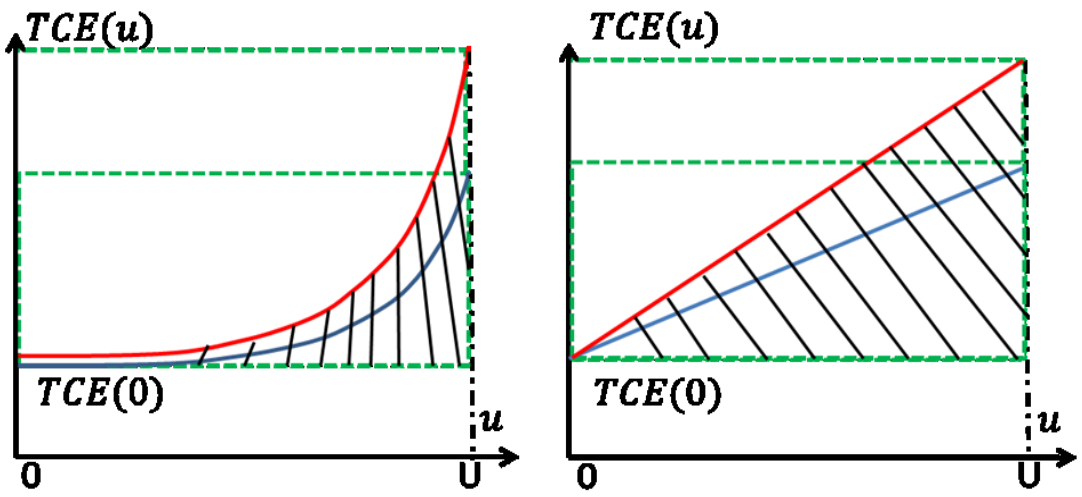

Fig.5.2 Two cases which are apparently counter-intuitive but have the same *RAI*

The new *RAI* is therefore used to measure the robustness based on the total cost when the network reaches equilibrium. Based on UE and SO principles, it can be divided into *RAI-UE* and *RAI-SO* respectively. In this context, the cases presented in **Fig.5.2** are able to be generated via the original RAI expressed in function (5.6). In these cases, the original *RAI* values for these two curves are the same (i.e. the ratio between the areas under the red and blue curves and the corresponding square areas is the same). Apparently, however, the red curve deviates from the original performance at

the equilibrium state by more than that of the blue curve; in other words, the red curve has worse robustness than the blue line. The right graph of **Fig.5.2** is a more significant case in terms of proving the limitation of the original *RAI* (values of the original *RAI* are both 0.5 due to the fact that the areas under the red and blue curves are half of the corresponding square areas).

In short, the limitation of the original *RAI* is that it is possible mistakenly to distinguish the robustness when the weight parameters are the same. A new *RAI* is therefore proposed, based on Equation (5.6), to overcome this weakness and can be presented in the following equation.

$$RAI = \int_0^U w(u).\frac{[TCE(u) - TCE(0)]}{TCE(0)}du \tag{5.7}$$

Where TCE is the network performance based on the equilibrium state of the network, *u* is able to represent the proportion of capacity degradation or the time step during the disruptions (which is discussed in **Chapter 7**). Both the original *RAI* and the new *RAI* measure the change in the network performance, as expressed by SO or UE solutions. Whereas the original *RAI* is calculated based on the normalization of areas, however, the new *RAI* is the area based on a normalized performance curve; that is, the ratio of the total cost entailed for the network to reach equilibrium *after the disruptions* to the total cost to reach equilibrium *before the disruptions*.

5.2 Robustness analysis of urban road networks experiencing local disruptions

This section mainly presents the robustness performance of some urban road networks from topological and operational perspectives, and further explores the relationship between relatively simple topological indices and relatively complex operational indicators based on the analyses. Examples of URNs at Sioux Falls and Anaheim are depicted in detail, and other networks, which are parts of Berlin, such as Tiergarten centre, Mitte centre and Prenzlauburg centre are analysed briefly. The detailed information is shown in **Appendix B**. Due to the fact that the calculation of the UE and

SO solutions for large scale networks is computationally highly intensive, only these seven networks are selected.

5.2.1 Sioux Falls network

Sioux Falls is located in the east of South Dakoda and has a total area of 190.29 square kilometres(United States Census Bureau, 2010). The actual and abstract road networks of Sioux Falls are presented in **Fig.5.3** (*http://www.bgu.ac.il/~bargera/tntp/*).

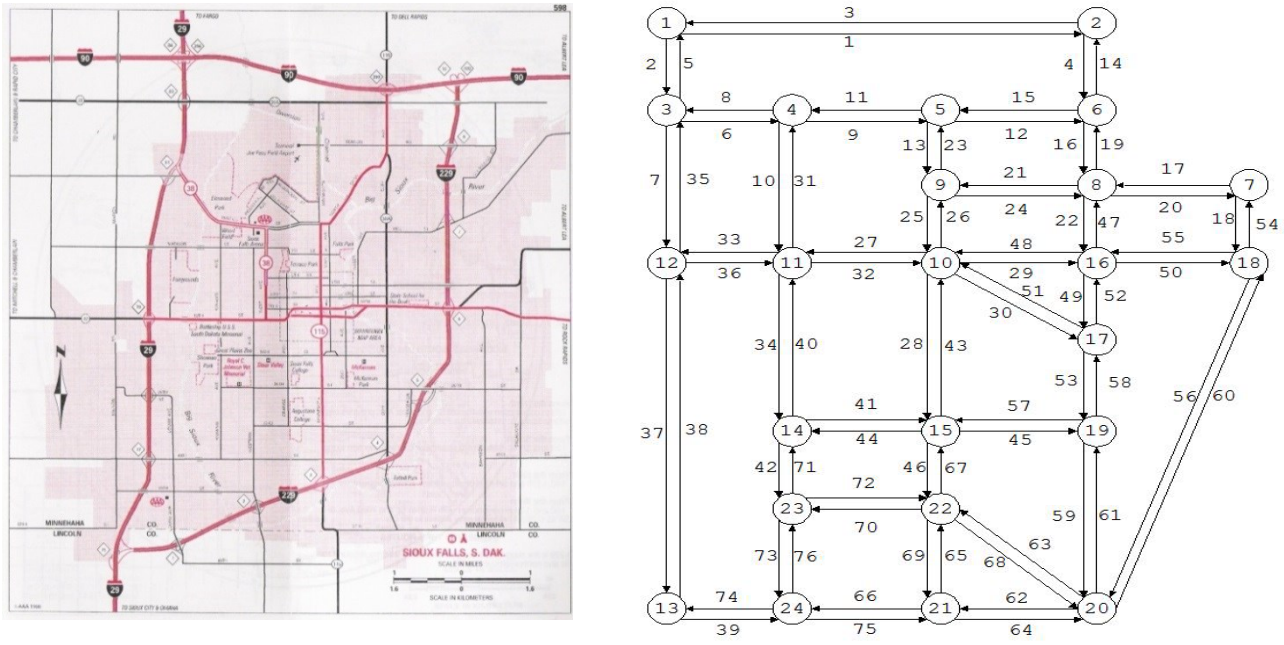

Fig.5.3 Sioux Falls Urban Road Network
Left: realistic Sioux Falls network; Right: abstract Sioux Fall network

The abstract Sioux Falls network depicted above consists of 24 nodes and 76 links. Assuming that the network is subject to local disruptions, which can be simulated by removing nodes or links from the abstract network plan, employing function (5.1), (5.2) and (5.5), the relative total cost of user equilibrium (RTC_{UE}^{i}) and system optimal (RTC_{SO}^{i}) and the relative price of anarchy ($RPOA^{i}$) are calculated after each node is removed. Detailed information is summarized in **Table 5.1**, and **Fig.5.4** shows the total costs under UE and SO, as well as the POA when individual nodes are removed from the network.

Table 5.1 Topological indices and operational indices of all nodes for the Sioux Fall network (Topological indices: degree (*D*), weighted closeness centrality (*WCC*), clustering coefficient (*CC*) weighted betweenness centrality (*WBC*) and efficiency measure are all defined in Section 2.1.2)

Indices / Node	*D*	*WC*	*CC*	*WBC*	*Eff'*	*WEff'*	RTC^{i}_{UE}	RTC^{i}_{SO}	$RPOA^{i}$
1	0.0870	0.0667	0	0.0198	0.3965	0.1117	2.3588	2.4590	1.0088
2	0.0870	0.0691	0	0.0316	0.3961	0.1116	1.0941	1.1454	1.0140
3	0.1304	0.0799	0	0.1146	0.3878	0.1078	1.1437	1.2187	1.0038
4	0.1304	0.0895	0	0.1252	0.3871	0.1067	3.3681	3.5178	1.0044
5	0.1304	0.0920	0	0.1344	0.3888	0.1060	2.0273	2.1329	1.0039
6	0.1304	0.0906	0	0.1838	0.3863	0.1044	2.3281	2.4351	1.0065
7	0.0870	0.0909	0	0.0889	0.3955	0.1071	3.3825	3.5044	1.0107
8	0.1739	0.0927	0	0.1798	0.3814	0.1041	5.0474	5.2643	1.0029
9	0.1304	0.0898	0	0.0277	0.3878	0.1096	4.7399	4.9516	1.0019
10	0.2174	0.1018	0.0400	0.1067	0.3693	0.1062	14.3559	14.9324	1.0013
11	0.1739	0.0962	0	0.0982	0.3731	0.1085	6.7353	7.0059	1.0037
12	0.1304	0.0839	0	0.1120	0.3839	0.1080	4.1157	4.2802	1.0065
13	0.0870	0.0807	0	0.0817	0.3924	0.1086	4.0706	4.2363	1.0060
14	0.1304	0.0888	0	0.0567	0.3886	0.1091	4.2972	4.4696	1.0061
15	0.1739	0.0962	0	0.1344	0.3842	0.1060	6.3645	6.6235	1.0036
16	0.1739	0.1013	0.0667	0.1779	0.3821	0.1033	7.5824	7.9025	1.0015
17	0.1304	0.0970	0.1333	0.1028	0.3889	0.1053	11.7029	12.1898	1.0005
18	0.1304	0.0966	0	0.1304	0.3855	0.1053	1.8496	1.9364	1.0081
19	0.1304	0.0931	0	0.0968	0.3901	0.1056	3.6382	3.7820	1.0076
20	0.1739	0.0902	0.0652	0.0771	0.3809	0.1083	5.3172	5.5382	1.0037
21	0.1304	0.0885	0.1305	0.1014	0.3895	0.1076	3.1435	3.2669	1.0088
22	0.1739	0.0931	0.0652	0.1074	0.3874	0.1060	7.5057	7.8065	1.0034
23	0.1304	0.0858	0	0.0257	0.3917	0.1080	4.4205	4.6018	1.0052
24	0.1304	0.0855	0	0.1094	0.3887	0.1057	2.3496	2.4518	1.0081

As can be seen from **Table 5.1**, topological indices such as degree (*D*), weighted closeness (*WC*), clustering coefficient (*CC)* and weighted betweenness (*WBC*) centrality are included in the analysis. These topological indices each reflect a certain characteristic of the network topology of URNs that

may be used to assess the robustness and resilience of the networks. As for detailed definitions for these topological indices, these have been discussed in **Section 2.1**. Here, *Eff'* denotes efficiency measure (see function (2.6)) after individual nodes are removed, and link length in function (2.6) is 1 if two nodes are connected otherwise 0. *WEff'* represents a weighted efficiency measure when individual nodes are removed, treating realistic link length as the weight of the links. Both of these indices examine the performance of the network in terms of average path length. The 8th, 9th and 10th columns are operational indices: RTC_{UE}^{i} and RTC_{SO}^{i} are total costs of UE and SO respectively when individual nodes are removed, and $RPOA^{i}$ is the ratio of RTC_{UE}^{i} to RTC_{SO}^{i}, which assesses the closeness of a UE network state from the system optimal state.

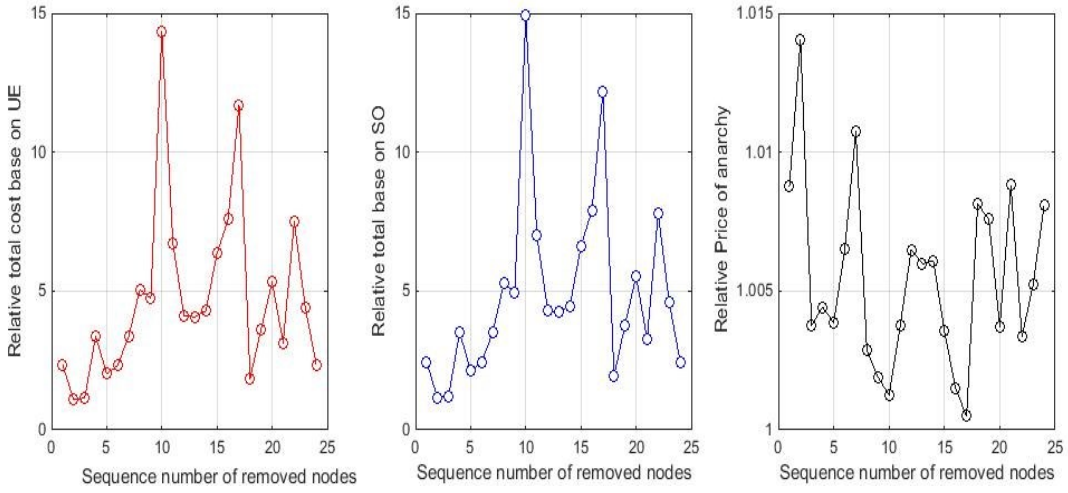

Fig.5.4 Evolution of RTC_{UE}^{i}, RTC_{SO}^{i} and $RPOA^{i}$ of Sioux Falls when nodes are removed

As can be seen from **Fig.5.4**, the RTC_{UE}^{i} and RTC_{SO}^{i} curves have a similar tendency, and node #10 is the most important node in this network, since removing it brings the largest increase in the network-wide cost. Node #10 happens also to have the largest degree in the network. The right graph of **Fig.5.4** shows that the node #10 is located in the central position of the network, but $RPOA^{i}$ tends to show that node #2 has the greatest impact on the network, even though this node is located at the edge of the network. It is worth noting that RTC_{UE}^{i} and RTC_{SO}^{i} curves may follow different trend when individual nodes are removed. The reason that such trend of the network is similar is due to its parameters of the network and demand distribution.

According to these quantitative topological and operational indices, all the nodes in the network are ranked and the results are shown in **Table 5.2**. Of the nine indices, *Eff'* and *WEff'* are ranked in an ascending order, which means nodes with lower efficiency values have the greatest impact on the network. For the remaining indices, the nodes are ranked in descending order; that is, nodes that can cause the greatest deterioration of relevant network performance are most important, and also require more resources when such disruptions happen.

Table 5.2 Ranking of all nodes based on topological and operational indices for Sioux Falls

Indices / Node	*D*	*WC*	*CC*	*WBC*	*Eff'*	*WEff'*	RTC_{UE}^{i}	RTC_{SO}^{i}	$RPOA^{i}$
1	21	24	--	24	10	16	18	18	3
2	22	23	--	21	11	8	24	24	1
3	8	22	--	8	20	6	23	23	15
4	9	15	--	7	8	17	16	15	13
5	10	10	--	4	16	18	21	21	14
6	11	12	--	1	12	19	20	20	8
7	23	11	--	17	15	24	15	16	2
8	2	9	--	2	18	5	8	8	20
9	12	14	--	22	6	15	9	9	21
10	1	1	6	12	4	22	1	1	23
11	3	5	--	15	22	10	5	5	16
12	13	20	--	9	3	4	12	12	9
13	24	21	--	18	9	7	13	13	11
14	14	16	--	20	14	21	11	11	10
15	4	6	--	5	24	3	6	6	18
16	5	2	3	3	5	12	3	3	22
17	15	3	1	13	17	23	2	2	24
18	16	4	--	6	21	20	22	22	5
19	17	7	--	16	19	11	14	14	7
20	6	13	4	19	23	13	7	7	17
21	18	17	2	14	13	14	17	17	4
22	7	8	5	11	7	9	4	4	19

23	19	18	--	23	2	2	10	10	12
24	20	19	--	10	1	1	19	19	6

'—' means these nodes' ranking is meaningless since the values are zero due to the fact that the neighbours of the given node are not connected with each other.

Based on **Table 5.1** and **Table 5.2**, the relationships between those topological indices and operational indices are analysed as follows.

The Spearman correlation method, also named ranking correlation, is used to explore this relationship. **Table 5.3** depicts the significance of the correlation between each pair of indices.

Table 5.3 Spearman correlations between pairs of any indices for Sioux Falls

	D	*WC*	*CC*	*WBC*	*Eff'*	*WEff'*	RTC_{UE}^{i}	RTC_{SO}^{i}	$RPOA^{i}$
D	1	0.6762	0.4329	0.4376	-0.8614	-0.4187	0.6890	0.6972	-0.7336
WC	0.6762	1	0.4199	0.4505	-0.5608	-0.6612	0.6085	0.6050	-0.5910
CC	0.4329	0.4199	1	0.0469	-0.2110	-0.2654	0.5415	0.5415	-0.4341
WBC	0.4376	0.4505	0.0469	1	-0.5485	-0.8034	-0.0283	-0.0196	-0.2803
Eff'	-0.8614	-0.5608	-0.2110	-0.5485	1	0.3475	-0.4966	-0.5071	0.6054
WEff'	-0.4187	-0.6612	-0.2654	-0.8034	0.3475	1	-0.1489	-0.1498	0.2906
RTC_{UE}^{i}	0.6890	0.6085	0.5415	-0.0283	-0.4966	-0.1489	1	0.9991	-0.7746
RTC_{UE}^{i}	0.6972	0.6050	0.5415	-0.0196	-0.5071	-0.1498	0.9991	1	-0.7842
RTC_{UE}^{i}	-0.7336	-0.5910	-0.4341	-0.2803	0.6054	0.2906	-0.7746	-0.7842	1

As can be seen from **Table 5.3**, *D* has a high negative correlation with the non-weighted efficiency index (*Eff'*) , -0.8614, and also has relatively high correlations with $RPOA^{i}$, RTC_{UE}^{i} and RTC_{SO}^{i}. *WC* has the highest correlation with *D* and the weighted efficiency index, while the correlations between *WC* and operational indices are not very high. Since many nodes have *CC* as 0, the correlations between *CC* and other topological indices are rather low. *WBC* is used to measure how frequently the shortest paths pass through a given node, so the weighted efficiency measure has the best correlation with it, and *WBC* has poor correlations with operational indices. The non-weighted

efficiency index has a low correlation with $RPOA^i$, RTC^i_{UE} and RTC^i_{SO}, but the weighted efficiency index is worse, with correlations of -0.1490, -0.1489 and -0.2906 respectively.

5.2.2 Anaheim

Anaheim is located to the south-east of downtown Los Angeles, California. **Fig.5.5** presents the layout of the Anaheim road network (*http://www.bgu.ac.il/~bargera/tntp/*).

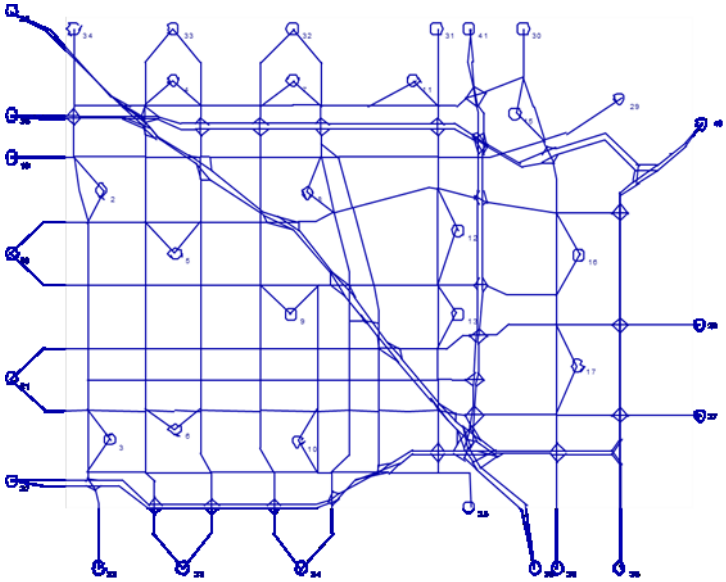

Fig.5.5 Anaheim network

As for the Sioux Falls network, nine topological and operational indices are calculated to indicate the network performance when suffering from local disruptions. Due to the large number of nodes, the detailed presentation of these indices' values for the top 30 nodes is shown in **Table B.1**. Here, as previously, with the exception of *Eff'* and *WEff'*, nodes are ranked in descending order. **Table 5.4** shows the top 20 nodes of these indices for Anaheim.

Table 5.4 Top 20 nodes based on topological and operational indices for Anaheim

Indices / Rank	*D*	*WC*	*CC*	*WBC*	*Eff'*	*WEff'*	RTC^i_{UE}	RTC^i_{SO}	$RPOA^i$
1	303	303	151	308	299	308	62	62	195
2	330	27	152	337	266	337	63	63	194

3	337	302	224	29	277	29	233	233	193
4	266	319	225	303	305	303	2	2	187
5	267	28	241	361	358	304	4	4	188
6	269	304	242	33	273	299	232	232	189
7	273	301	245	302	321	302	87	87	190
8	299	317	246	304	407	307	234	234	191
9	302	330	334	299	333	361	86	86	192
10	304	31	228	378	269	28	235	235	140
11	308	329	229	27	308	267	89	89	141
12	317	300	239	28	390	294	88	88	204
13	329	286	240	307	375	306	74	74	203
14	332	311	222	267	267	269	25	25	236
15	333	312	223	269	384	300	73	73	196
16	341	305	226	268	265	305	1	1	198
17	361	299	227	266	399	330	398	398	197
18	369	42	243	394	319	378	397	397	142
19	373	331	244	305	264	394	116	116	143
20	378	316	247	36	357	33	117	117	231

Fig.5.6 depicts how the total UE cost, SO cost, and $RPOA^i$ change as certain nodes are removed from the network. As can be seen from the evolution of RTC_{UE}^i and RTC_{SO}^i, the node #62 causes the most deterioration when removed, which highlights its importance, and $RPOA^i$ shows that node #195 has the greatest impact on the price of anarchy. It seems that that the rankings based on topological indices, however, are not directly related to those based on operational indices.

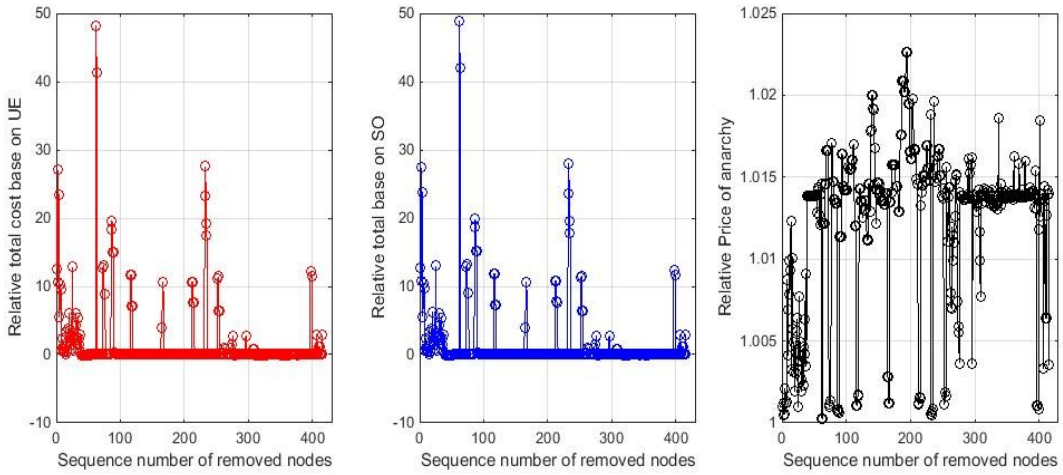

Fig.5.6 Evolution of RTC^i_{UE}, RTC^i_{SO} and $RPOA^i$ of Anaheim when nodes are removed

In order to quantify the ranking correlations between these indices, Spearman correlation method is employed. **Table 5.5** presents the correlation coefficients between any pair of indices.

Table 5.5 Spearman correlations between pairs of any indices for Anaheim

	D	*WC*	*CC*	*WBC*	*Eff'*	*WEff'*	RTC^i_{UE}	RTC^i_{SO}	$RPOA^i$
D	1	0.3273	-0.1363	0.5477	-0.3227	-0.4445	-0.4025	-0.3819	-0.0272
WC	0.3273	1	0.0646	0.4808	-0.2002	-0.5073	-0.4737	-0.4766	0.1948
CC	-0.1363	0.0646	1	-0.0435	-0.0988	-0.0388	-0.0422	-0.0533	0.3189
WBC	0.5477	0.4808	-0.0435	1	-0.5208	-0.7688	-0.0703	-0.0341	-0.0267
Eff'	-0.3227	-0.2002	-0.0988	-0.5208	1	0.4698	-0.0965	-0.1008	0.0022
WEff'	-0.4445	-0.5073	-0.0388	-0.7688	0.4698	1	0.1025	0.0836	-0.1026
RTC^i_{UE}	-0.4025	-0.4737	-0.0422	-0.0703	-0.0965	0.1025	1	0.9917	-0.3260
RTC^i_{SO}	-0.3819	-0.4766	-0.0533	-0.0341	-0.1008	0.0836	0.9917	1	-0.3869
$RPOA^i$	-0.0272	0.1948	0.3189	-0.0267	0.0022	-0.1026	-0.3260	-0.3869	1

As can be seen from **Table 5.5**, RTC^i_{UE} and RTC^i_{SO} have very poor correlations with topological indices, even with degree the correlations are just -0.4025 and -0.3819 respectively. $RPOA^i$ has no discernible correlations with these topological indices. In comparison, RTC^i_{UE} and RTC^i_{SO} have better

correlations with degree, partially due to the homogeneity of the network; that is, nodes with more connections are more important in terms of both topological and operational perspective.

Node rankings and correlations between any pair of indices of other networks such as Tiergarten centre, Mitte centre and Prenzlauburg centre are presented in **Appendix B**.

Examining the tables for these URNs, it is clear that there are still no significant correlations between topological indices and operational indices, although the correlations between topological indices and operational indices are much better than those of Sioux Falls and Anaheim. In particular, the average weighted betweenness centrality (*WBC*) has the largest correlation with RTC_{UE}^{i} and RTC_{SO}^{i} out of all the topological indices used in this thesis, with values uniformly above 0.63, and correlations for Mitte and Mitte-Prenzlauerberg-Friedrichshain (MPF) even up to 0.76 and 0.77, and 0.74 and 0.74, respectively. For these networks, therefore, although the correlations are not significant enough, which is expected, *WBC* seems to be relatively highly related to the total costs under UE and SO principles when networks suffer from local disruptions. A possible explanation is that the nodes that are frequently passed by shortest paths between all O-D pairs carry more flows, so the removal of the nodes with large *WBC* is more likely to cause a significant increase in drivers' total travel times. In addition, the relationship between the correlation and the distribution of demand is also considered. If the demand is very low, according to the UE and SO principle, the traffic tends to be assigned to shortest paths, and the correlation between UE cost, SO cost, and *WBC* could be high. However, the dependence of the conclusion on the network configuration (including demand, supply) is the point here. One of the main findings is that the topological and operational indices are not necessarily aligned, which depends on numerous factors typically ignored by complex network science. This finding motivates a branch of the complex network theory to account for information specific to the nature of the network, whether it is a traffic network, a pipeline network, or a social network.

5.3 Robustness comparisons of different urban road networks suffering from global disruptions

The previous section examines the robustness of the networks under local node removal and explores the relationships between topological indices and operational indices. This section will mainly explore the robustness performance across a number of different urban road networks experiencing global capacity degradation. The networks of Sioux Falls, Anaheim, Friedrich centre, Prenzlauerberg centre, Tiergarten centre and Mitte centre, and Mitte-Prenzlauerberg-Friedrichshain (MPF) centre are chosen for the robustness comparison of the robustness. Although, as discussed in **Section 3.1.3** and **3.1.4,** there are many measures to assess the robustness of the network, these are limited to quantitatively examining and comparing the robustness in the performance of urban road networks with different sizes by taking into account travel demand, link capacity, drivers' behaviour, and so on, when the network experiences certain types of disruptions. Here, a new relative area index (RAI) is proposed to make robustness comparisons of robustness for different URNs.

According to the methods presented in **Section 5.1**, the results are summarized in **Table 5.6**, and the curves of relative total UE cost (TUE) and total SO cost (TSO) when the networks suffer from global capacity deterioration are presented in **Fig.5.7**.

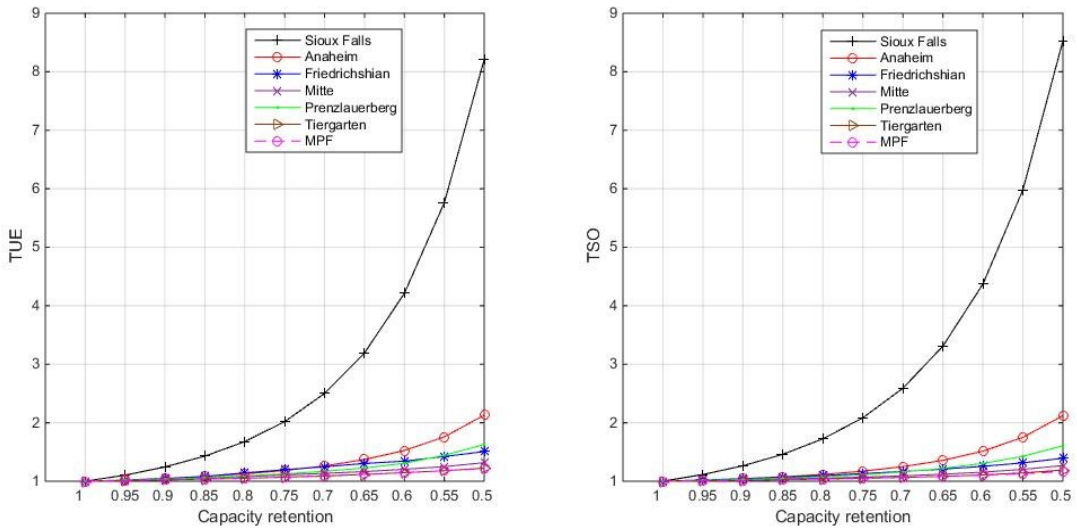

Fig.5.7 Normalized TUE and TSO under global capacity degradation of urban road networks

As can be seen from **Fig.5.7**, the global capacity reduction ranges from 0% to 50% (i.e. a 50%-100% retention rate). The graphs show the normalized total cost of UE and SO under different levels of global capacity degradation for selected urban road networks. The normalized TUE and TSO for the Sioux Falls network seems to deviate from the original total cost most significantly as capacity reduction increases. In other words, the robustness of Sioux Falls is the worst when the network suffers from global capacity degradation. This is followed by Anaheim. The reasons are probably that, one the one hand, Sioux Falls network is much smaller than other 6 URNs, and the smaller the network is the less alternative paths the network has (but the ranking correlation between RAI and the scale of URNs is not significant); on the other hand, the significant deviation is also caused by the demand distribution and parameters of Sioux Falls network. For the remaining road networks, however, it is difficult to tell which has the greater deviation from the original total cost since most of the curves are overlapping or crossing. In order accurately to quantify the magnitude of deviations for these URNs, the new RAIs are calculated based on Equation (5.7), and all these new RAI values are summarized below in **Table 5.6**.

Table 5.6 Summaries of RAI and WBC for urban road networks
(*N* denotes the number of nodes and *L* represents the number of links.)

Networks	*n*	*L*	*RAI-UE*	*RAI-SO*	*WBC*
Sioux Falls	24	76	1.0675	1.1214	0.1010
Anaheim	416	914	0.1754	0.1709	0.0316
Friedrichshain	224	523	0.1155	0.0846	0.0406
Prenzlauerberg	352	749	0.1052	0.1002	0.0364
Tiergarten	361	766	0.0472	0.0361	0.0352
Mitte	398	871	0.0681	0.0514	0.0309
MPF	975	2184	0.0472	0.0339	0.0124

As can be seen from **Table 5.6**, RAI-UE and RAI-SO are new RAIs based on User Equilibrium (UE) and System Optimal (SO) principles respectively. Due to the fact that WBC is able to measure how frequently the shortest paths pass through a given node, it is used to measure the robustness of networks (Sun et al., 2014).

Based on **Table 5.6**, the network robustness ranking is presented in terms of RAI-UE, RAI-SO and WBC. The robustness rankings of these networks are shown in **Table 5.7**.

Table 5.7 Robustness rankings of urban road networks

Rank	*RAI-UE*	*RAI-SO*	*WBC*
1	MPF *	MPF	MPF
2	Tiergarten *	Tiergarten	Mitte
3	Mitte	Mitte	Anaheim
4	Prenzlauerberg	Friedrichshain	Tiergarten
5	Friedrichshain	Prenzlauerberg	Prenzlauerberg
6	Anaheim	Anaheim	Friedrichshain
7	Sioux Falls	Sioux Falls	Sioux Falls

'*' means these two URNs have tied in the ranking list.

Table 5.7 shows that MPF and Tiergarten are the most robust of the seven networks to global capacity degradation as measured by RAI-UE since the degree of deviation is the least, followed by Mitte, Prenzlauerberg and Friedrichshain respectively; Anaheim and Sioux Falls are assessed to have the least robust networks. The ranking based on RAI-SO is approximately the same as RAI-UE except the fourth and the fifth places are reversed. The coefficient of ranking correlation between RAI-UE and RAI-SO is very high (0.9550), and the *P* value is 0.004, which suggests this correlation is significant. The ranking based on WBC, however, is quite different from that from RAI-UE and RAI-SO, the most (MPF) and least (Sioux Falls) robust networks remain the same. The ranking correlation coefficients between [RAI-UE, WBC] and [RAI-SO, WBC] are 0.6667 and 0.6786, which are not

significant enough to suggest strong correlations between RAI-UE and RAI-SO and the topological index WBC. In addition, although people tend to believe that the larger networks have more alternative routes, and the result also show that Sioux Falls with the least number of nodes and links is also the least robust, and that MPF with largest scale has the best robustness, it is difficult to conclude that the robustness of URNs depends on the scale of the networks, since a clear positive correlation between the robustness of URNs and the scale of the networks. For example, Anaheim is the second largest among seven networks, yet it ranks the sixth in terms of RAI-UE and RAI-SO.

Although betweenness is able to measure how important a given node is in a network, it is insufficient to capture more realistic and sophisticated characteristics of urban road networks, such as capacity, flow propagation and driving behaviours. The new index proposed in this section take into account all these features, in addition to network topology, and is able to better quantify the robustness of URNs when these networks are subject to global/local capacity degradation. RAI is therefore a more realistic approach to capturing the inherent robustness characteristics of networks.

Through the robustness comparisons among selected urban road networks, their rankings according to the robustness against global-scale disruptions are presented and analysed, which may shed light on the planning and management of network traffic.

5.4 Summary

Following the topological analysis of urban road networks presented in **Chapter 4**, this chapter has introduced a few new operational indices based on UE and SO principles, which take into account traffic flow characteristics, link capacity, travel demand and travel behaviour, in order to assess the robustness of URNs suffering from local and global disruptions. Comparisons of these operational indices with some widely used topological indices have been conducted. In the search for potential relationships between all these indices, Spearman ranking correlations have been employed to explore whether the relatively simple topological indices can reveal aspects of the complex structure of the networks, as predicted by the traffic network flow models (e.g. UE, SO). The results show that

although some individual nodes in some URNs have the same importance in both topological and operational terms (e.g. node #10 in Sioux Falls network), overall, the ranking correlations between these indices are weak. There are, however, a few specific networks such as Mitte, Prenzlauerberg and Tiergarten, for which the correlations between operational and topological indices were much higher than other networks.

This chapter has also proposed a new relative area index (RAI) to analyse quantitatively the robustness of URNs suffering from global capacity disruptions. Average weighted betweenness centrality was used here as the baseline. The results suggest a weak ranking correlation between WBC and RAI-UE/RAI-SO, although the Sioux Falls (MPF) networks are consistently the least (most) robust for all three indices. Results also show that the size of URNs has no significant relationship with robustness.

After the robustness analysis based on topological and operational indices, the following chapters will model robustness and resilience in dynamic traffic models. In the next chapter, a novel agent-based day-to-day dynamic evolution model with information percolation is proposed for the exploration of robustness and resilience, and its formulations and numerical study is presented.

Chapter 6 EVOLUTION OF DYNAMIC NETWORK TRAFFIC WITH INFORMATION SHARING

This chapter mainly focuses on the effect of information sharing on the day-to-day evolution of network traffic. To achieve this, the chapter introduces an agent-based day-to-day traffic evolution model with information percolation that explores the impact of communication networks on road traffic networks. The main model consists of two layers: a cyber layer representing the communication network among travellers in which travel information can be shared based on a certain structure; and then a physical layer expressing the traditional day-to-day transport network with individual travellers routing selfishly in order to minimize their own travel costs. This model assumes that, instead of having perfect information, travellers form *groups* such that travel information is shared within the same group, and that travellers' routing decisions are influenced by travel experiences not only of their own, but also of others in the same group. One novel aspect of this model is that the groups are formed in the cyber layer according to *percolation theory*, which describes the formation of connected clusters (groups) in a random graph. Such a clustering mechanism could potentially represent the market segregation of travel information services. This model is suitable for studying different qualitative properties of transport networks such as resilience, robustness and stability, when information-sharing mechanisms fall within the purview of

transport planners. This chapter presents a numerical study that focuses on the convergence of the transport network when a range of *percolation rates* are considered in the cyber layer. The findings suggests a positive correlation between the percolation rate and the speed of convergence, which is validated through statistical analysis taking into account the stochastic nature of the agent-based simulation and the random percolation graph. Sensitivity analysis related to key parameters is also conducted in this chapter.

6.1 Modelling travelling information sharing in traffic assignment

Travel information plays an increasingly vital role in shaping travel behaviour and network dynamics. In the literature on traffic assignment, the user equilibrium (UE) principle assumes that travellers have perfect information (Wardrop, 1952), whereas the stochastic user equilibrium (SUE) allows the information to be incomplete (Daganzo and Sheffi, 1977). Intrinsic to both approaches, however, is a strong relationship between the availability and quality of travel information and network performance.

Data quality has already been acknowledged as a key concern in much of the existing work on traffic assignment. The effects of data quality were initially studied by Mahmassani (1990), where it was found that travel times in simulated networks would converge to an equilibrium state regardless of the completeness of travel information. In a later study, Friesz et al. (1994) examined the evolution of traffic flow patterns when users are provided with complete or incomplete information through Advanced Traveller Information Systems (ATIS). It was found that perfect information leads to faster convergence and lower travel costs during the adjustment period leading to the equilibrium. Similarly, Zheng et al. (2013) emphasize that incomplete network information and insufficient communication have a negative impact on traveller's route behaviour. The authors use simulations to show that network performance and convergence speeds increase as the numbers of travellers receiving up-to-date information increase. Studies exist that suggest otherwise, however:

Balakrishna et al. (2013) point out that information does not necessarily improve network performance for day-to-day traffic learning models.

A common characteristic of these studies is that they all focus on travel information provided by exogenous sources (e.g. network operators, ATIS, Google Maps, etc.). There is, however, another source of information, which is generated among travellers themselves through their daily commute, and disseminated and used through certain information sharing structures[1] and learning processes. Furthermore, studies so far have not considered the possible segregation of travellers in terms of information access and sharing. This chapter seeks to address this literature gap by proposing a two-layer, agent-based, day-to-day traffic model that captures the imperfect nature of travel information.

The model developed in this thesis consists of two layers: a cyber layer that represents the communication network among travellers in which travel information can be shared based on certain structure; and a physical layer expressing the day-to-day transport network with individual travellers routing selfishly in order to minimize their own travel costs. This model assumes that, instead of having perfect information,[2] travellers form groups where travel information is internally shared. As such, routing decisions are not only influenced by the travellers' own experiences, but also by choices made by their group peers.

The novelty of the model lies in the fact that these processes are represented using two distinct but interacting networks. A physical network is used to capture the underlying traffic network (along with links, nodes and users), while the transmission of travel decisions and experiences among users is modelled through the application of percolation theory (Newman, 2003) to a conceptual communication network (the cyber layer). In this context, percolations refer to the formation of

[1] Examples include internet-enabled navigation devices (such as those offered by TomTom or Garmin) or smartphone apps with social networking features (such as Waze).

[2] In this chapter, having perfect travel information means that exact route travel times/costs are known to all drivers using the network.

connected node clusters (user groups) in a random graph, where there is a certain probability that node (user) pairs establish a link (connection to exchange travel info). Using this approach, different passenger groups can be generated, representing the market segregation of travel information provision.

In the physical layer of the model, a day-to-day route adjustment process is proposed based on an agent-based routing game in which individual travellers make rational routing decisions in order to minimize their travel costs. Such a process may be represented using an agent-based model that captures the actions and interactions of autonomous travel agents. In the proposed model, such interaction occurs on both the cyber and the physical layers.

Relationships among travel agents give rise to emerging and collective behaviours at network level; this chapter is mainly concerned with the convergence of the traffic network to an approximate equilibrium state.[3] To the best of our knowledge, this is the first study to use percolation theory to capture the disaggregated and distributed nature of travel information sharing. It also addresses imperfect travel information since the model assumes that travellers can only perceive the travel cost along a certain path if at least one traveller in the same group uses that path. When the network is sufficiently large such that the number of viable paths is significantly larger than the number of agents in the same group, that group undergoes a learning process with very limited information on the entire network.

With the application of information percolation in the agent-based, day-to-day traffic model, this chapter is able to describe and quantify the effects of the percolation rate on the travellers' collective driving behaviour, and the convergence of the resulting network to an approximate equilibrium state. The significance of this model is that it manages to parameterize the imperfectness of travel information using a single variable (the percolation rate), which has not

[3] As shall subsequently be seen, due to the stochasticity inherent in the traffic model, an exact equilibrium is difficult to achieve. Thus a definition of approximate equilibrium is needed.

hitherto been achieved in the literature. It also proposes a measure for the convergence of the resulting traffic system in the presence of a variety of stochasticities (e.g. the random connections in the cyber layer and the logit route choice sub-model).

6.2 Relevant background

This section provides an in-depth review of two subjects: agent-based simulation and percolation theory.

Agent-based simulation (ABS) is a popular approach for modelling complex systems composed of autonomous, interacting agents, and is able to reveal relevant characteristics such as self-organization, emergence of order, and resilience, by compiling information about entities at a lower level (Macal and North, 2010). ABS was originally applied in the study of complex adaptive systems (Kauffman, 1993) and artificial life (Langton, 1989).

In the field of transportation, a range of agent-based models have been applied to study driving and travel behaviours at microscopic/mesoscopic/macroscopic levels. Nagel and Schreckenberg (1992) apply ABS to set up a stochastic discrete automation model to simulate car motions of individual vehicles. Following this, agent-based modelling in transportation received increased scholarly attention. Node, arc and traveller are regarded as three types of agents by Zhang and Levinson (2004). Following this, Zou and Levinson (2006) develop an agent-based model. Nagel and Flötteröd (2009) propose studying traffic assignment from an individual agent's perspective in order to address the complexity of choice dimensions such as the departure time and mode choices. The influence of spatial information on user behaviour is addressed by Zhu et al. (2007), who propose an agent-based route choice model to simulate how travellers make route choices over time by using a route choice set. Although the model is able to account for the presence of exogenous information, how such information is propagated among agents is not addressed. Zheng et al. (2013) explicitly introduce basic concepts and general modelling frameworks of ABS. The authors point out the close relationship between ABS and social science models, behaviour models, route choice models, land

use models and activity-based travel demand models. In addition, ABS is employed to explore the parking search and decision process (Levy et al., 2013), and container transport business (Sinha-Ray et al., 2003).

Percolation theory seeks to link connectivity and information transport in geometrically complex systems (King et al., 2002) – it has been branded as the science of 'clumping' in random environments (Gastner, n.d.). A percolation process is one in which a vertical or edge in a network is randomly marked either 'occupied' or 'unoccupied' (Newman, 2003). Its origins can be traced back to World War II, when Flory and Stockmayer applied it to the study of the chemical processes by which small molecules form large macromolecules (Stauffer and Aharony, 1994). Percolation theory was first used in an epidemiological study by (Broadbent and Hammersley, 1957) to model the spread of diseases – this was the first study that involved real-world networks. Sahini (1994) attempted to summarize the applications of percolation theory to the modelling of phenomena in disordered systems, and stated that porous media problems such as oil recovery processes may benefit from such research.

Many other problems can also be mapped by percolation models. Brodera et al. (2000) and Albert et al. (2000a) deem that the resilience of web graphs to random failures of nodes is equivalent to the site percolation process; and Sander et al. (2002) point out that the models of epidemic diseases can be mapped through percolation in which the percolation rate is correspondent to the "epidemic threshold" of epidemiology. Summarizing, percolation theory is a widely accepted tool for the exploration of critical phenomena, and is crucial to understanding important aspects of network topology (Albert and Barabasi, 2002).

6.3 Preliminaries

This section introduces some basic concepts, notations and models. How percolation theory can be applied to traffic modelling is also described.

6.3.1 Notation for network traffic assignment

In this section some standard assumptions and notations employed in static traffic assignment and discrete choice models are briefly reviewed. Since this chapter focuses on the day-to-day evolution of traffic, some variables presented below have explicit dependence on the time index t, which represents one "day". Here, the notion of day is arbitrary, and can represent any portion of an actual day for which there is a discernible, significant fluctuation in travel demand. In the context of our traffic evolution modelling, one "day" can also represent multiple calendar days, such as a week or a month.

$G(V,E)$	Graph representation of a network with node set V and link set E
W	Set of origin-destination (OD) pairs
$R_{o,d}$	Set of routes connecting OD pair $(o,d)\ \epsilon\ W$
R	Set of routes in the network
f_t^a	Flow on link $a\ \epsilon\ E$ on day t
f_t	Vector of link flows on day t, $f_t = (f_t^a)_{a\in E}$
h_t^r	Flow along route r on day t
x_t^{ir}	Perceived travel cost on route r by agent $i \in I$ on day t
$Y_t^{ir}\epsilon(0,1)$	Random route choice index: equals 1 if i takes route r on day t; equals 0 otherwise.
$C_a(f_t)$	Link travel cost function (possibly non-separable)
c_t^r	Cost associated with route r on day t
c_t	Vector of route costs on day t, $c_t = (c_t^r)_{r\in R}$

$\delta_{a,r}$ Link-route incidence index: equals 1 if $a \in r$; equals 0 otherwise

δ Link-route incidence matrix: $\delta = (\delta_{a,r})_{a\in E, r\in R}$

N^i Travel group to which traveller i belongs

In a road network, a route r is represented as a set of links it traverses. The flow f_t^a on link $a \in E$ on day t is the sum of relevant route flows h_t^r; that is,

$$f_t^a = \sum_{r\in R} \delta_{a,r} \cdot h_t^r \quad \text{for all } a \in E, t \tag{6.1}$$

or, in matrix notation, $f_t = \delta h_t$. Given the link loads f_t, the cost for using link a is assumed to be a function: $C_a(f_t)$. The route travel cost is the sum of relevant link travel costs:

$$c_t^r = \sum_{a\in E} \delta_{a,r} \cdot C_a(f_t) \quad \text{for all } r \in R \tag{6.2}$$

The process of calculating route travel costs for a given vector of route flows is known as the *network loading* problem. Mathematically, the network loading can be expressed as:

[Network loading] $c_t = (c_t^r)_{r\in R}$, $f_t = (f_t^a)_{a\in E}$, $c_t^r = \sum_{a\in E} \delta_{a,r} \cdot C_a(f_t)$ for all $r \in R$ **(6.3)**

x_t^{ir} is denoted as the perception of driver i on the cost of route r on day t; it represents the *subjective* and *expected* travel costs of driver i. In some literature (Davis and Nihan, 1993, Cominetti, 2013), the perception is based on the driver's past travel experience and is updated on a daily basis as:

$$x_t^{ir} = x_{t-1}^{ir} + \alpha \cdot Y_{t-1}^{ir}(c_{t-1}^r - x_{t-1}^{ir}) \quad \alpha\epsilon(0,1) \tag{6.4}$$

It can be seen from Equation (6.4) that the perception of a driver about a route on a particular day is jointly affected by his/her previous perception, and the travel cost experienced on that route on the

most recent day (day $t-1$). Here, the parameter α measures the impact of the most recent travel experience (on day $t-1$) on the perception, which varies between 0 and 1 to make sure that the perception always stays positive.

The logit model is utilized to describe drivers' random route choices under the influence of their own perceptions. In particular, the probability of choosing a route $r \in R_{o,d}$ is

$$P\left(Y_t^{ir}=1\right)=\frac{exp(-\beta \cdot x_t^{ir})}{\sum_{r' \in R_{o,d}} exp(-\beta \cdot x_t^{ir'})} \tag{6.5}$$

This stochastic route choice model assumes that there may be some irrationality involved in the route choice process; that is, the route with the minimum cost may not necessarily be chosen by all the travellers, due to imperfect travel information and drivers' predictive behaviour.

The main novelty of the proposed agent-based, day-to-day traffic flow model lies in the incorporation of imperfect travel information through the cyber layer. It will be assumed that travellers form groups; and that within each group travel information is shared according to a mechanism that is an extension of Equation (6.4); namely, the perception of one driver will be influenced by the travel experience not only of his/her own, but also of the others within the same group. Such an extension will be elaborated in **Section 6.4.1.3**. In general, however, the way the travellers form groups is arbitrary and difficult to capture using parameterization; percolation theory is employed to overcome this issue. A brief introduction of the application of percolation theory in the context of information sharing will be presented in the next section, while the proposed learning process based on information percolation will be detailed in **Section 6.4.1.3**.

6.3.2 Random graph and percolation

This chapter invokes the notion of random graph to describe and quantify the connectivity among drivers and the degree of information accessibility. In particular, the nodes in the random graph are defined to be all the drivers within the same O-D pair. Then, for an arbitrary pair of nodes, the link

between them, which represents the communication channel between the two drivers, is randomly generated according to a fixed probability $p \in (0,1)$, called the *percolation rate*. In addition, the events of link generation between different node pairs are independent. As a result of this random generation of links, a graph will be obtained. **Fig.6.1** shows three realizations of the random graph, with different percolation rates. As can be seen from this figure, when the percolation rate is rather low (e.g. **Fig.6.1.a**), the links are unlikely to be established and the nodes are completely disconnected; when the percolation rate becomes high, however (e.g. **Fig.6.1.c**), the entire graph becomes connected.[4]

Here, a few basic terminologies and notions in graph theory are introduced. Two graphs are considered, $G(V_1, E_1)$ and $G(V_2, E_2)$, where V_1, V_2 and E_1, E_2 denote the sets of nodes and links, respectively.

Definition 1. (Sub-graph and maximum connected sub-graph) $G(V_1, E_1)$ can be said to be a *sub-graph* of $G(V_2, E_2)$, denoted $G(V_1, E_1) \subset G(V_2, E_2)$, if $V_1 \subset V_2, E_1 \subset E_2$. $G(V_1, E_1)$ can be said to be a maximum connected sub-graph of $G(V_2, E_2)$ if for any connected graph $G(V_3, E_3)$ such that $G(V_1, E_1) \subset G(V_3, E_3) \subset G(V_2, E_2)$ it must be the case that $G(V_1, E_1) = G(V_3, E_3)$.

In prose, a graph is the maximum connected sub-graph provided no bigger and connected sub-graph exists. For an arbitrary realization of the random graph with a percolation rate p, all of its maximum connected sub-graphs are considered, each one corresponding to a *driver group*. By definition, any two drivers in the same driver group can be connected through a finite number of communications (links); see **Fig.6.1** (second row) for the determination of the driver groups.

[4] A graph is said to be connected if any node is connected to any other node through a finite number of links.

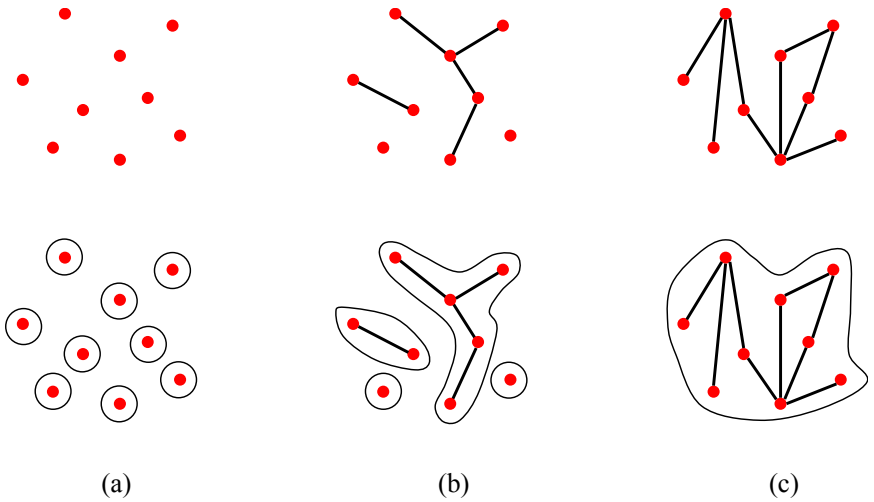

Fig.6.1 Illustration of random graph and percolation.
Form (a) to (c), the percolation rate increases, causing fewer maximum connected sub-graphs (driver groups), which are encircled by dark curves.

According to percolation theory, there exists a certain percolation rate threshold p^* beyond which the entire network becomes fully connected. In other words, as the percolation rate p increases, the number of driver groups decreases; and when $p > p^*$, there is a very high probability that the driver group number is equal to 1.

The study described here relies on the theory of percolation allowing random connections to be established between drivers, and assuming that information sharing can occur within the extent of the same driver group (i.e., the maximum connected sub-graph of the communication network). Moreover, the day-to-day learning process of a given travel agent is influenced by the knowledge obtained from other members in the same group, creating a complex learning dynamic that is coupled with the actual traffic evolution on a daily basis.

Note that the random graph approach considered here is not an attempt to capture the real-world information sharing structure, which is affected by numerous factors and is difficult to estimate due to the complex nature of social interaction and the lack of relevant data. Instead, for the ease of mathematical representation and parameterization, a greatly simplified version that relies on the random connectivity of travellers at the information (cyber) layer is considered. This has given rise to a specific network configuration that falls within the scope of percolation theory. In particular, the

range of connection probabilities, including the critical probability p^* stipulated by the percolation theory, results in different degrees of network connectivity in the cyber layer, which manifest themselves in the traffic layer in terms of qualitative behaviours such as convergence.

6.4 An agent-based day-to-day traffic evolution model

This section presents details of the agent-based day-to-day traffic assignment model underpinned by information percolation. A method of quantifying convergence through the stochastic traffic model is also proposed.

Each travel agent in this model is associated with a perception for each route in the network, which may change over time as the network evolves. Unlike the existing literature on this approach (Davis and Nihan, 1993, Cominetti, 2013), our model also stipulates that an agent's perception about a given route may also be influenced by others in the same communication group even if he/she does not take that route.

6.4.1 Details of the agent-based simulation

6.4.1.1 Route choice model

Recalling that the perception of agent i regarding route r on the t-th day is denoted x_t^{ir}. The probability of choosing a particular route is thus given by the logit model:

$$P(Y_t^{ir} = 1) = \frac{exp(-\beta x_t^{ir})}{\sum_{l \in R_{o,d}} exp(-\beta x_t^{il})} \quad \beta > 0 \tag{6.6}$$

where the binary variable $Y_t^{ir} = 1$ if agent i selects route r on day t, and equals 0 otherwise. In the context of stochastic user equilibrium (Prashker and Bekhor, 2000), β is termed the *dispersion parameter,* which is used to indicate the sensitivity of drivers to route costs.

The resulting route choice model relies on the premise that agent travel choices depend on their subjective perceptions rather than the actual and objective route costs, due to a variety reasons including imperfect information, driving experience, and drivers' socio-economic characteristics. This

direction of research mainly focuses on relaxing the perfectly rational behaviour when it comes to route choices with perfect travel information; this is especially relevant when decisions are made based on their predictions (He and Peeta, 2015, Heath, 2000).

It should be noted that this route choice model may be insufficient to capture the heterogeneity of road users and their complex and realistic decision-making processes; and that there are many more advanced models for route choices, such as the mixed logit model (Ben-Elia and Shiftan, 2010), the nested logit model (Ben Akiva and Lerman, 1985), and the paired-combinatorial logit model (Chu, 1989, Koppelmana and Wen, 2000). This chapter, however, is a theoretical investigation of the information-sharing paradigm, and thus, instead of employing complicated route choice models in an attempt to replicate reality, simplified route choice assumptions are utilized in order to highlight the role played by information sharing/percolation.

6.4.1.2 Bounded rationality

A fundamental assumption in most deterministic DTD models is that drivers' route-choice behaviour is completely rational, and they always have the tendency to switch to routes with lower travel costs. As a result, in the steady (equilibrium) state of the route switching process all the experienced travel costs for the same O-D pair are the same and minimum. In reality, however, drivers do not always choose the least costly routes (Zhu and Levinson, 2015) due to a variety of reasons such as imperfect information and behavioural inertia. Rather, if the difference between the perceived travel cost of the current route and the cost of an alternative route is below a threshold, then drivers are not incentivized to switch to the alternative route. This notion is termed *bounded rationality* (BR) in the travel behaviour, and has been extensively studied in the traffic assignment literature (Simon, 1957, Mahmassani and Chang, 1987, Han et al., 2015b). As part of the route choice model, a sub-model that incorporates the BR user behaviour is introduced. The BR model used here is presented in Zheng et al. (2013) and works as follows.

If the difference between the actual travel cost of a driver i along route r on day $t-1$ (c_{t-1}^{ir}), and his/her minimal perceived travel cost among all routes for the next day $\left(\min_r x_t^{ir}\right)$ is less than a threshold (tolerance) e, this driver would stick to the same route as the previous day; otherwise, with the following probability, the agent will consider all routes based on the logit model (6.6).

$$\frac{c_{t-1}^{r} - \min\limits_{r} x_t^{ir}}{c_{t-1}^{r}} \tag{6.7}$$

(6.7) is the probability that drivers consider to switch routes, which means the probability that drivers do not consider to change routes is $\frac{min_r\, x_t^{ir}}{c_{t-1}^{r}}$. Mathematically, recalling **Section 6.3.1**, if $Y_{t-1}^{ir} = 1$, then

If $c_{t-1}^{r} - \min_r x_t^{ir} < e$:

$$Y_t^{ir} = 1$$

Else:

(6.8)

$$\begin{cases} Y_t^{ir} = 1 \quad \text{with probability} \quad \dfrac{\min\limits_{r} x_t^{ir}}{c_{t-1}^{r}} + \dfrac{c_{t-1}^{r} - \min\limits_{r} x_t^{ir}}{c_{t-1}^{r}} \times \dfrac{\exp\left(-\beta x_t^{ir}\right)}{\sum_{l \in R_{o,d}} \exp\left(-\beta x_t^{il}\right)} \\ Y_t^{ir} = 0 \quad \text{with probability} \quad \dfrac{c_{t-1}^{r} - \min\limits_{r} x_t^{ir}}{c_{t-1}^{r}} \times \dfrac{\exp\left(-\beta x_t^{ir'}\right)}{\sum_{l \in R_{o,d}} \exp\left(-\beta x_t^{il}\right)}, \quad r' \in R_{o,d} \end{cases}$$

The first case of (6.8) represents the drivers still using route r, and the second case expresses the drivers using other routes. The sum of the probabilities for these two cases should be one, so the mathematical validity of (6.8) can be proved by showing that the sum of probabilities for choosing all the routes between OD pair (o, d) is equal to one for each driver. Indeed, given the current route $r \in R_{o,d}$, when the second case (indicated by 'Else' in (6.8)) occurs, we have:

$$P\left(Y_t^{ir}=1\right)+\sum_{r'\in R_{o,d}}P(Y_t^{ir}=0)$$

$$=\frac{\min\limits_r x_t^{ir}}{c_{t-1}^r}+\frac{c_{t-1}^r-\min\limits_r x_t^{ir}}{c_{t-1}^r}\times\frac{\exp\left(-\beta x_t^{ir}\right)}{\sum_{l\in R_{o,d}}\exp\left(-\beta x_t^{il}\right)}$$

$$+\sum_{r'\in R_{o,d}}\frac{c_{t-1}^r-\min\limits_r x_t^{ir}}{c_{t-1}^r}\times\frac{\exp\left(-\beta x_t^{ir'}\right)}{\sum_{l\in R_{o,d}}\exp\left(-\beta x_t^{il}\right)}$$

$$=\frac{\min\limits_r x_t^{ir}}{c_{t-1}^r}+\frac{c_{t-1}^r-\min\limits_r x_t^{ir}}{c_{t-1}^r}\times\left(\frac{\exp\left(-\beta x_t^{ir}\right)}{\sum_{l\in R_{o,d}}\exp\left(-\beta x_t^{il}\right)}+\sum_{r'\in R_{o,d}}\frac{\exp\left(-\beta x_t^{ir'}\right)}{\sum_{l\in R_{o,d}}\exp\left(-\beta x_t^{il}\right)}\right) \quad (6.9)$$

$$=\frac{\min\limits_r x_t^{ir}}{c_{t-1}^r}+\frac{c_{t-1}^r-\min\limits_r x_t^{ir}}{c_{t-1}^r}$$

$$=1$$

In this thesis, both scenarios with and without bounded user rationality will be considered and tested later in the numerical study in **Section 6.5**. As will be seen, the convergence to a steady state is significantly improved in the bounded rationality case, which is in line with similar studies on bounded rationality (Mahmassani and Chang, 1987).

6.4.1.3 Updating route perceptions based on information sharing

Equation (6.10) below expresses the learning mechanism in the proposed model. It differs from the traditional formulation (6.4) in that it has an additional term that represents the influence of drivers in the same group. In the proposed model, the perception of driver i towards route r on day t is defined as:

$$x_t^{ir}=x_{t-1}^{ir}+\alpha_1 Y_{t-1}^{ir}\left(c_{t-1}^r-x_{t-1}^{ir}\right)+\sum_{j\in N^i}\alpha_2^{jr}Y_{t-1}^{jr}\left(c_{t-1}^r-x_{t-1}^{jr}\right)\quad \alpha_1\epsilon(0,1) \quad (6.10)$$

where α_1 weighs the influence of the driver's own experience, and $\alpha_{2,j}^r>0$ measures the impact of driver j's experience about route r. The parameters $\alpha_{2,j}^r$ is normalized by stipulating that:

$$\alpha_2^{jr} = \frac{\alpha_2}{\sum_{k \in N^i} Y_{t-1}^{kr}} \quad \text{for all } j \in N^i \text{ such that } Y_{t-1}^{jr}=1 \tag{6.11}$$

where $\alpha_2 \in (0,1)$ is a constant. Eqn (6.11) means that, all the drivers j in the same group as i, and who used route r on the previous day $t-1$ have equal weights which sum up to be α_2. The parameters α_1 and α_2 combined determine how much a driver's perception is influenced by his/her own experience and by others in the same group. Here it is worth noting that the communication between drivers is captured by the notation N^i in the third term of (6.10), that is, travel group to which traveller i belongs, and the group is formed on the cyber layer according to percolation theory. Within such group, a given driver *i* is able to communicate travel information with other drivers.

Remark 1. *In general,* α_1 *and* α_2 *may be dependent on time* t *and/or a specific traveller* i*. For example, the degree of influence by oneself and others may be related to the driver's age, gender, socio-economic status (in which case* i *is relevant), and familiarity with the network (in which case* t *may be relevant). Here, due to the lack of relevant real-world data and without a loss of such generality, the simplified formulation* (6.10) *and* (6.11) *is employed.*

The first summation term on the right hand side of (6.10) is the perception of agent i on route r on the previous day $(t-1)$, which encapsulates the driver's past driving experience. The second term expresses a self-correction process where the perception on the same route is updated based on the actual driving experience on the previous day $(t-1)$. The third term is another correction process that is based on the actual experience of other drivers in the same group. This third term expresses how other drivers' perceptions cumulatively affect those of the subject driver.

Equation (6.10) can be seen an extension of the following learning process (Cominetti, 2013), which relies solely on the agent's own travelling experience without any communication with others.

$$x_t^{ir} = x_{t-1}^{ir} + \alpha_1 Y_{t-1}^{ir}\left(c_{t-1}^{r} - x_{t-1}^{ir}\right) \tag{6.12}$$

In fact, the learning process described in (6.12) can be regarded as a special case of the model presented here; namely, if no connections are present in the cyber layer, each agent will constitute a group and (6.10) immediately reduces to (6.12).

Remark 2. *This chapter employs an agent-based simulation (ABS) in which each traveller's trip and decision-making process is modelled individually. In addition, the realization of one's route choice is stochastic with probabilities given by the logit model. Therefore, regardless of the state of the system, it is entirely possible that travellers' route choices differ on any two consecutive days as a result of the aforementioned stochasticity. In this sense, the proposed day-to-day ABS has no stationary/steady state. However, one could relax the model by assuming that travellers are "infinitely splittable" (i.e. non-atomic), then the stochasticity can be eliminated. The steady state of this relaxed problem is a stochastic user equilibrium with bounded rationality.*

6.5.1.4 The complete model

The three modelling components illustrated in the previous three subsections are integrated to form the complete agent-based day-to-day model as follows. Beginning with day one drivers' route perceptions are randomly generated (which is usually taken as the free-flow times). Then the route choice probabilities are determined according to (6.6), and the actual route choices are randomly generated accordingly. After the network loading procedure, which determines the actual (experienced) route costs, (6.10) is invoked to update the perceptions of all the routes for all the travel agents based on the information sharing structure. Finally, function (6.8) is used to determine whether or not the agent should stick to the previous route or select new ones for the next day's travel. The aforementioned procedure is repeated on a day-by-day basis. The pseudo code for this process is provided in **Table 6.1**.

Table 6.1 Pseudo code for the agent-based day-to-day model.

Pseudo code. The agent-based day-to-day model

Input: Information percolation rate. Randomly establish connections within the communication network according to the percolation rate, and form groups of travellers.

- **Step 0**: Assign the free-flow costs of all paths as the initial path perceptions of agents. Then determine their route choice probabilities according to the logit model (6.6). Perform network loading to obtain each agent's actual travel costs. Set $t = 0$.
- **Step 1:** Set $t = t + 1$. Update each agent's perception about all the routes according to the learning process (6.10) and the established information sharing structure.
- **Step 2:** Determine the route choice or route choice probabilities using formula (6.8), based on the agent's updated perceptions and the travel costs experienced on day $t - 1$.
- **Step 3:** Perform the stochastic network loading (6.3) according to the route choice probabilities determined in **Step 2**, and obtain the travel costs. Return to **Step 1**.

Remark 3. *To perform the simulation without bounded rationality, one may simply replace the formula* (6.8) *in* ***Step 2*** *with the model* (6.6)*.*

Remark 4. *The proposed model implies that only drivers within the same O-D pair can share route information, since drivers belonging to different O-D pairs have no route in common. In reality, this may not be the case. For example, for drivers whose origins and destinations are close to each other, or whose travel routes have substantial overlap, may have closely related route experiences or perceptions. The model proposed here may be extended to treat these scenarios as well, by allowing drivers (or network operator) to share information regarding only a portion of a complete route, such as a highway segment or a major arterial. In this case, the route choice model would need to be modified to incorporate only partial information regarding a complete route. This would allow drivers of different O-D pairs to share information and interact with each other in both the cyber and physical layers of the transportation network.*

6.4.2 Quantifying convergence of the network

The proposed ABDTD model contains two types of stochasticity. The first one arises from the random connections that are established due to the percolation rate in the cyber layer. The second one is inherent to the stochastic, logit-based route choice model. Notice that the latter introduces no stochasticity to the model if the latter is non-atomic (i.e. the flows are continuous), which is not the case for agent-based approaches. With this in mind, the resulting model performance will be subject to a great deal of uncertainty, making qualitative analysis regarding convergence difficult.

In order to characterize the convergence of the system properly in the presence of random noise, the following criterion for convergence in an approximate sense is proposed. Let us consider the curve illustrated in **Fig.6.2**. Such a curve could be regarded as a generic state variable (with given travel costs, or volumes, on a given path). As the iteration goes on, the curve may stabilize around a certain value, albeit with minor local oscillations due to the presence of random route choices.

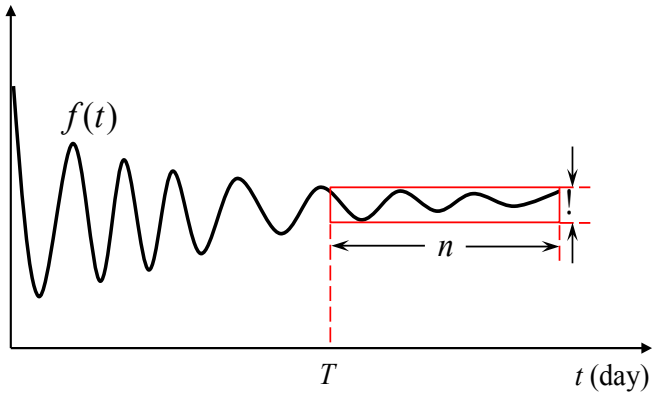

Fig.6.2 Illustration of approximate convergence.

In order reasonably to declare the convergence of such a state variable with quantifiable and tuneable measures, a region with length n and width ε is considered; see **Fig.6.2**. The following definition of convergence is employed.

Definition 2. (Approximate convergence). Consider a region with length n and width ε. A time-trajectory of a certain quantity is said to converge at time $t = T$ if the trajectory starting from T and

ending at $T+n$ is entirely within such a region; in addition, T should be the earliest time such that this property holds. We therefore have:

$$T = min\left\{t: \max_{s\in(t,t+n)} f(s) - \min_{s\in(t,t+n)} f(s) < \varepsilon\right\} \quad (6.13)$$

In prose, the above definition means that a given quantity can be regarded as convergent on day $t = T$ if in the next n days the oscillations of this quantity are all within a given threshold ε. Clearly, this is a reasonable criterion for declaring approximate convergence. Moreover, the strictness of this convergence measure can be adjusted by changing the values of n and ε. Here the defined approximate convergence is similar but different from Lyapunov stability, which describes how the trajectory of a function starting out near the equilibrium x_e point stays near x_e forever (Hokayem and Gallestey, 2015).

It is also noted that this definition of approximate convergence is closely related to the notion of *stability in the Lagrange sense*.

Remark 5. *the notion of stability in the Lagrange sense refers to the situation where the time-trajectory of the state variable remains bounded beyond a certain point in time (Nemytskii and Stepanov, 1960). This is an important notion for studying traffic equilibria as a real-life traffic network rarely operates at perfect equilibrium; instead, it is more likely to 'orbit' around one while exhibiting the Lagrange stability.*

6.5 Numerical study

This section presents some simulation results for the proposed model, and illustrates the qualitative behaviour of the network with different degrees of information transparency and accessibility. The argument will illustrate how the travel information shared across a number of agents affects the qualitative behaviour of the network (i.e. its convergence to an approximate equilibrium state), through a comparison of network performances associated with different percolation rates in the cyber layer. In particular, it will show flow patterns, users' route choices, route cost, as well as the

convergence of these quantities, in association with the proposed information sharing paradigm and different percolation rates. Confidence intervals for the speeds of convergence are calculated in order to address the uncertainties inherent in the model, and the results are presented in **Section 6.5.2**. A comparison of the network performance with and without bounded user rationality is also presented in **Section 6.5.2**. The model involves several exogenously defined parameters, which may have potentially significant effects on the performance of the network; and therefore a sensitivity analysis of these parameters is carried out in **Section 6.5.3.**

The proposed agent-based day-to-day traffic model is implemented on a three-by-three grid network (shown in **Fig.6.3**) consisting of 9 nodes and 12 links. One origin-destination pair (node a and node *i*, respectively) is considered, between which six paths are enumerated. The O-D demand is 1000.

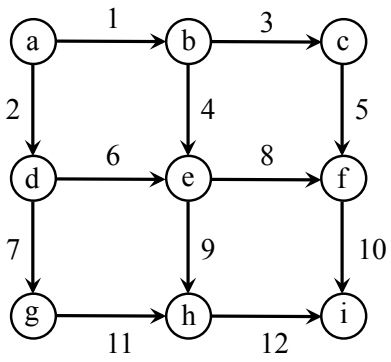

Fig.6.3 The test network.

In this numerical example, the following BPR functions are used to describe the link travel cost:

$$C_a(h) = A \cdot \left[1 + B \cdot \left(\frac{f^a}{CP_a}\right)^{\sigma}\right] \tag{6.14}$$

Where f^a is the flow on link a, CP_a is the flow capacity of link a, and A, B, σ are positive parameters. The numerical values for these parameters are summarized in **Table 6.2.**

Table 6.2 Link parameters of the test network

Link ID	A	B	σ	CP_a
1	15	0.15	4	500
2	15	0.15	4	500
3	15	0.15	4	500
4	15	0.15	4	500
5	15	0.15	4	500
6	15	0.15	4	500
7	15	0.15	4	500
8	15	0.15	4	500
9	15	0.3	4	500
10	15	0.15	4	500
11	15	0.15	4	500
12	15	0.15	4	500

In the numerical example, the drivers' perceptions of different routes are initially set to be equal to their free-flow times. Then, the pseudo code presented in **Table 6.1** is followed to carry out the simulation.

6.5.1 Different percolation rates

This section investigates how the proposed information sharing structure, which is parameterized by the percolation rate, plays a role in the day-to-day traffic evolution. Notice that the widely studied case in which drivers learn their routes based solely on their own past experience (without sharing information, e.g. (6.4)) is just a special case of the investigation here, namely when the percolation rate is zero and each driver constitutes a group.

In view of the discussion of the random graphs in **Section 6.3.2**, due to the fact that the driver groups are randomly formed with a given percolation rate, the clustering of drivers varies even with

the same percolation rate. To ensure the statistical significance and reliability of the investigation, for each given percolation rate, 36 independent simulations are conducted. Within each such simulation, driver groups in the cyber layer are randomly generated, and this information sharing structure is used to conduct day-to-day simulation of traffic.

This section begins by illustrating the relationship between the percolation rate and the average number of driver groups (maximum connected sub-graph) formed in the cyber layer. **Fig.6 4** clearly shows that as the percolation rate p increases, the average number of driver groups decreases as the proliferating connections between agent-pairs lead to group redundancies. This decrease is more drastic for $p \in (0, 0.004)$. In addition, when $p > 0.005$, the average group number is almost 1, which means that all the drivers are connected.

The curve shown in **Fig.6 4** follows an exponential trend with the best fit $y = 1103 \cdot exp(-887.4 \cdot x)$ with $R^2 = 0.99$. The fitting is shown in **Fig.6.5**.

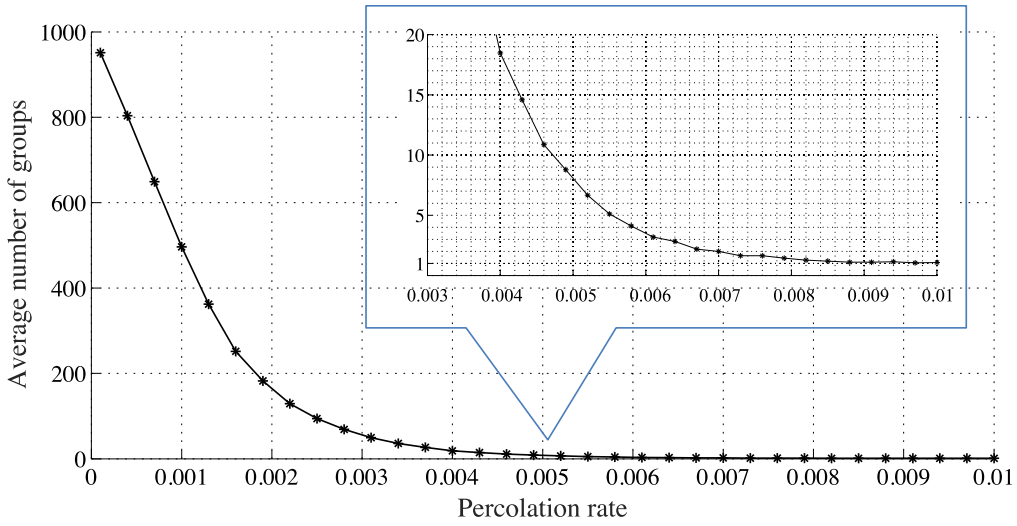

Fig.6 4 The average number of groups as a function of the percolation rate. The sub-figure is a close-up of the graph for $\mathbf{p} \in [0.003, 0.01]$.

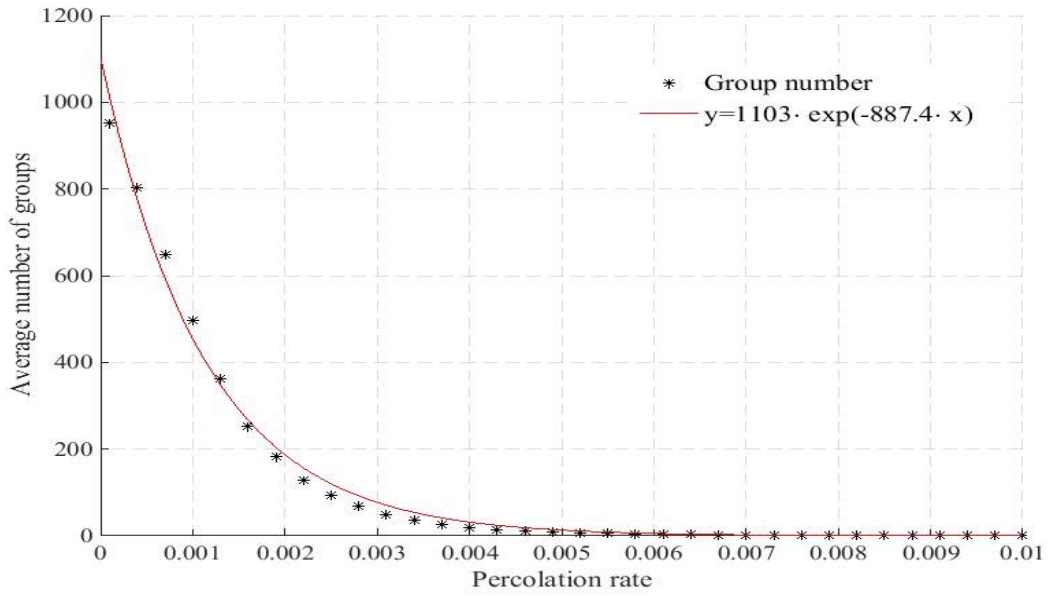

Fig.6.5 Exponential fit of the trend of the group number.

In particular, with 1000 agents and $p = 0.0001$, there are on average 100 connections in the communication network, leading to 951 groups on average. This means that when $p = 0.01$ only 1.08 groups are formed on average, and hence almost the entire population of agents is within one group.

In view of **Fig.6 4,** several representative percolation rates: 0.0001, 0.0007, 0.0013, 0.0025 and 0.01, are considered for the following experiments. This chapter also considers the base scenario where individual drivers make routing decisions based solely on their own perception and past experience without the influence of others; which is easily realized by setting $p = 0$, as discussed above. The following parameters are chosen for the day-to-day learning process (6.8), (6.10), and (6.11):

$$\alpha_1 = 0.25, \ \ \alpha_2 = 0.25, \ \ \beta = 1$$

This choice of parameters will have a quantitative impact on the results, but the main qualitative insights regarding the percolation rate and the resulting network's convergence remain valid. This will be confirmed by the sensitivity analysis conducted later in **Section 6.5.3**.

Fig.6.6, **Fig.6.7** and **Fig.6.8** present, respectively, the day-to-day evolution of route travel costs, route flows, and network-wide total costs for a range of percolation rates. Note that all quantities displayed here are based on an average over 36 independent experiments.

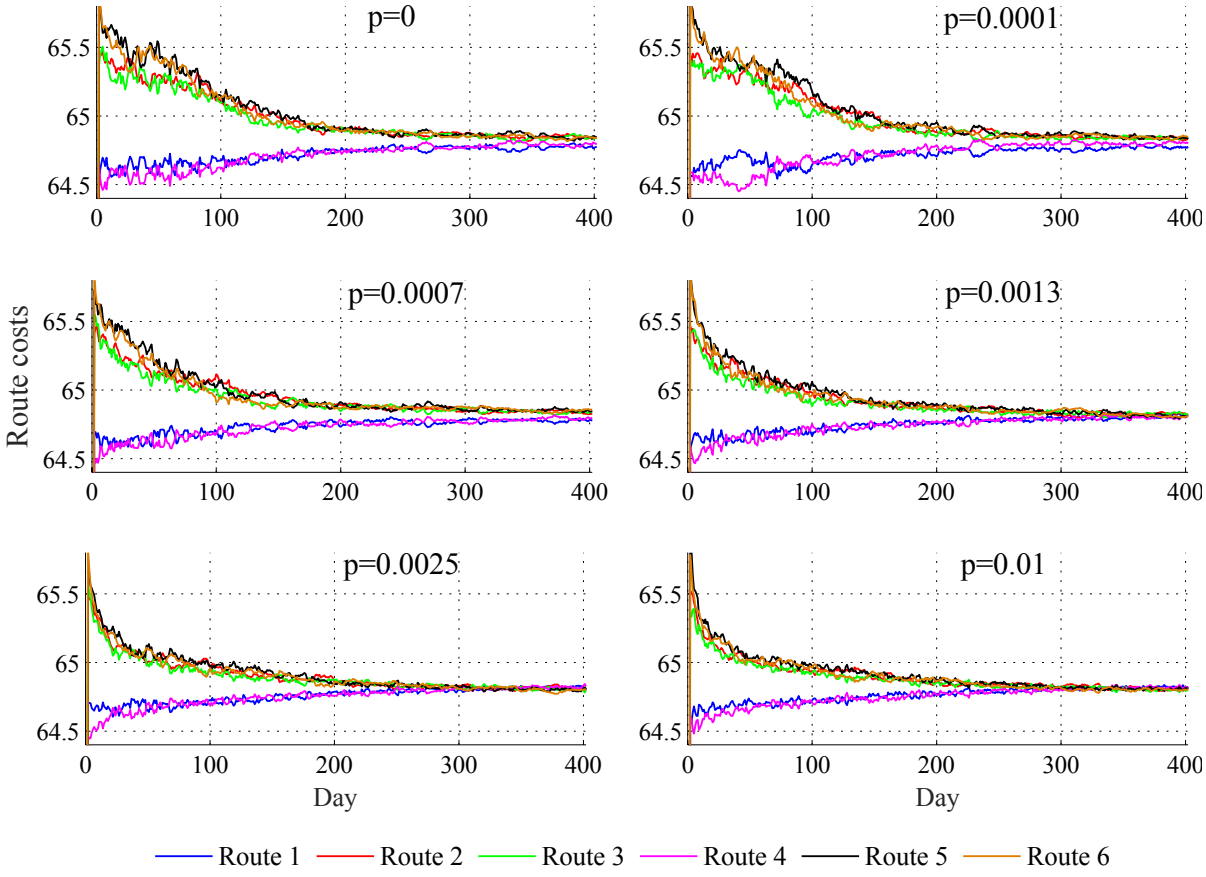

Fig.6.6. Average route costs over time for different percolation rates.

As can be seen from **Fig.6.6**, for all the percolation rates, the route travel costs converge within the time horizon in the approximate sense articulated in Definition 2. The speed and precision of the convergence varies, however. In particular, the rate of convergence increases with the percolation rate, and the gap between the route costs when convergence is declared is smaller for larger percolation rates.

Similar observations about the route flows can be made from **Fig.6.7**, although the effect of the percolation rate seems less obvious than on the route costs. A quantified assessment of the convergence will be provided later in **Table 6.3.**

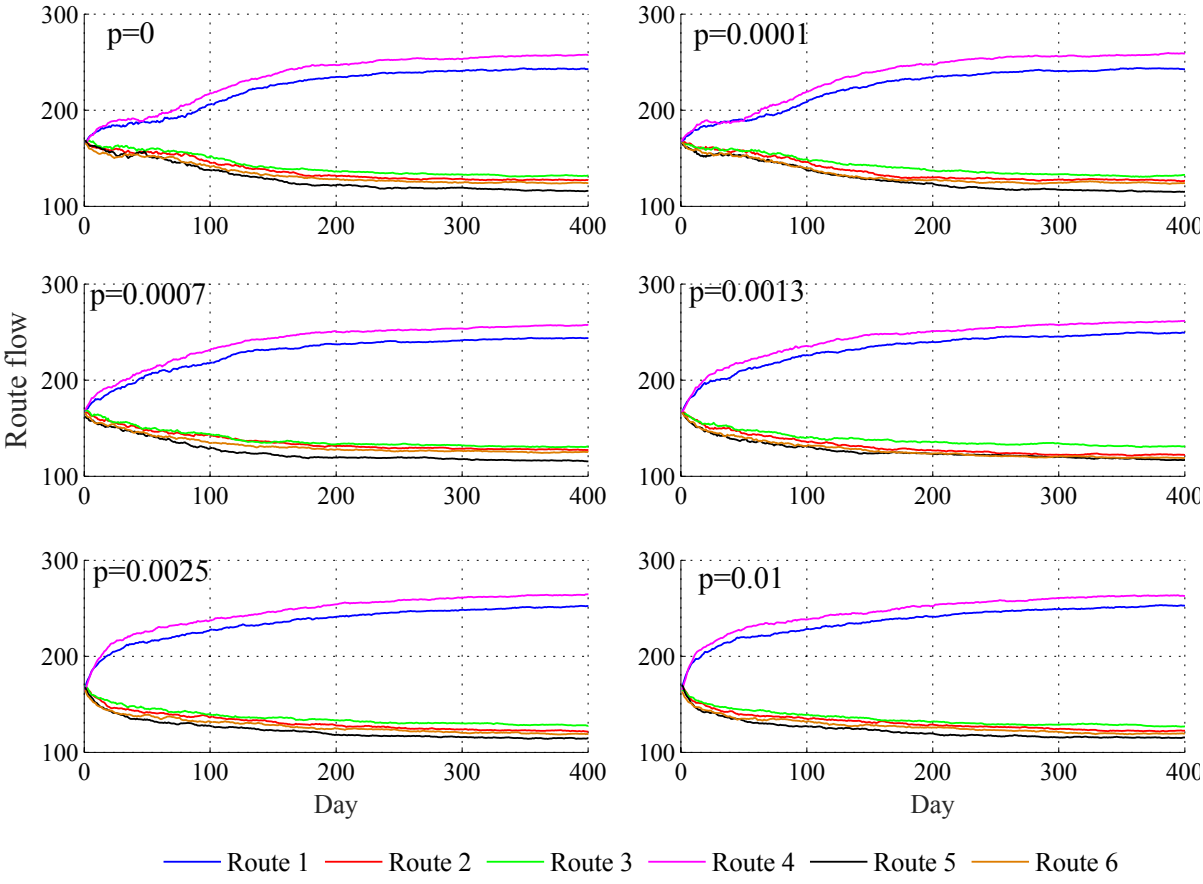

Fig.6.7 Average route flows over time for different percolation rates.

In order to demonstrate and quantify the effect of percolation rate on the overall network efficiency, **Fig.6.8** plots the day-to-day evolution of network-wide total travel costs for different percolation rates. It can be seen that the percolation rate has a significant effect on the cost-effectiveness of the traffic network, in that the costs incurred before convergence are lower with higher percolation rates. This suggests that, under the proposed network and learning dynamic, information transparency and accessibility among drivers has a positive impact in terms of reducing traffic congestion; this finding is in line with some of the existing studies (Friesz et al., 1994, Zheng et al., 2013).

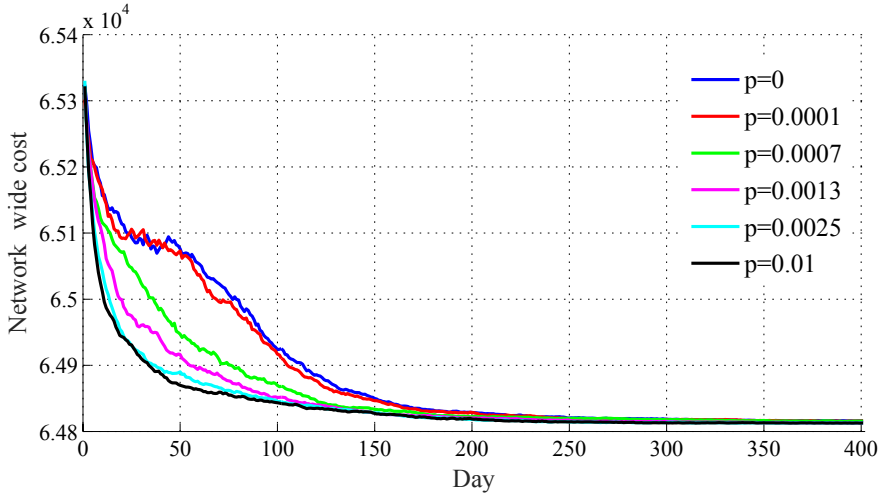

Fig.6.8 Average network total costs over time for different percolation rates.

In order to further quantify convergence for different percolation rates, the definition of approximate convergence described in (6.10) is invoked, where *n* is fixed to be 100. It should be noted that the value ε shown in (6.10) is an indication of the precision of the convergence, and **Table 6.3**, below, considers values of ε ranging from 0.3 to 1.0. The numbers in this table represent the average number of 'days' taken for the network to reach convergence in the sense of Definition 2. In this experiment the time horizon is 1000 days, and in **Table 6.3** a value of 1000 indicates that convergence was not reached within the prescribed time horizon.

Table 6.3. Number of days taken to reach convergence.

	$\varepsilon = 0.3$	$\varepsilon = 0.4$	$\varepsilon = 0.5$	$\varepsilon = 0.6$	$\varepsilon = 0.7$	$\varepsilon = 0.8$	$\varepsilon = 0.9$	$\varepsilon = 1.0$
$p = 0$	1000	920.58	603.64	218.72	188.03	160.17	141.36	125.78
$p = 0.0001$	1000	938.5	440.81	239.92	179.53	149.61	130.59	117.58
$p = 0.0007$	980.56	797.64	303.89	189.33	157.97	130.28	105.92	93.86
$p = 0.0013$	940.78	484.06	234.17	154.83	128.58	110.08	84.78	75.72
$p = 0.0025$	940.28	403.47	192.97	153.64	120.31	94.92	75.31	56.72
$p = 0.01$	858.97	320.5	188.03	146.81	118.08	91.56	62.44	47.17

As expected, **Table 6.3** shows that larger ε yields faster convergence. In addition, across different percolation rates, the convergence trend is consistent with those shown in **Fig.6.6** and **Fig.6.7**; that is, higher percolation rates always facilitate convergence to the approximate equilibrium.

Fig.6.9 is used to illustrate the relationship between the number of traveller groups and the convergence rate of the network. The right panel shows the decreasing trend of the group number as the percolation rate increases. This trend is reflected in the convergence rate on the left panel, through the network dynamics. In addition, for both cases, a critical percolation rate $p^* \approx 0.002$ clearly exists, across which both quantities display qualitatively different behaviours.

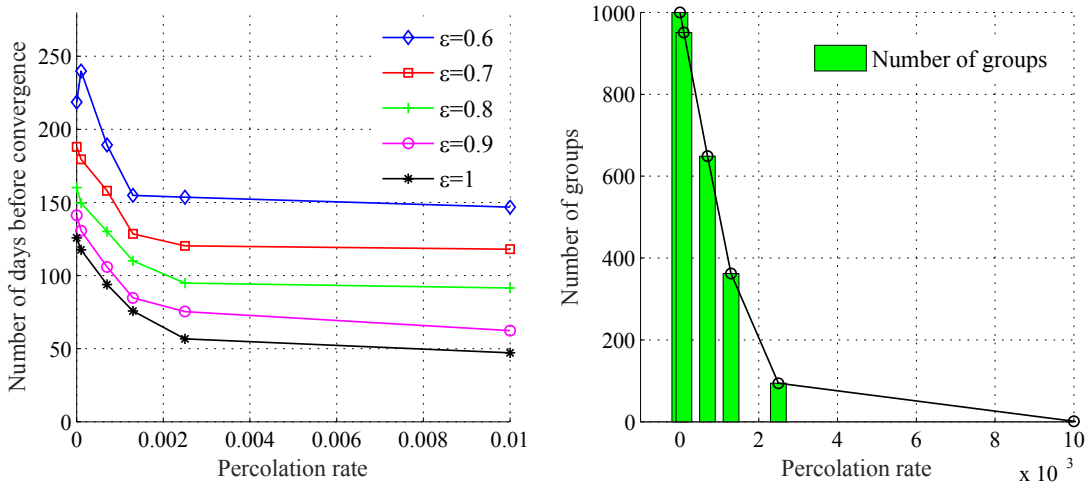

Fig.6.9 Percolation in the communication layer (right) and its effect on convergence in the traffic layer (left).

Finally, the 95% confidence intervals for the convergence rate (the number of 'days' taken to reach convergence) are computed, for a range of percolation rates. The results are summarized in **Table 6.4** and visualized in **Fig.6.10**.

Table 6.4 95% confidence interval for the convergence rates.

	$\varepsilon = 0.6$	$\varepsilon = 0.7$	$\varepsilon = 0.8$	$\varepsilon = 0.9$	$\varepsilon = 1.0$
$p = 0$	[206,231]	[178,198]	[150,170]	[134,149]	[120,132]
$p = 0.0001$	[194,285]	[169,190]	[141,158]	[125,136]	[112,123]
$p = 0.0007$	[179,199]	[149,167]	[123,138]	[100,111]	[88,100]
$p = 0.0013$	[146,164]	[122,135]	[104,116]	[81,89]	[71,80]
$p = 0.0025$	[145,162]	[113,128]	[87,103]	[68,83]	[52,62]
$p = 0.01$	[138,156]	[110,126]	[85,98]	[56,69]	[41,54]

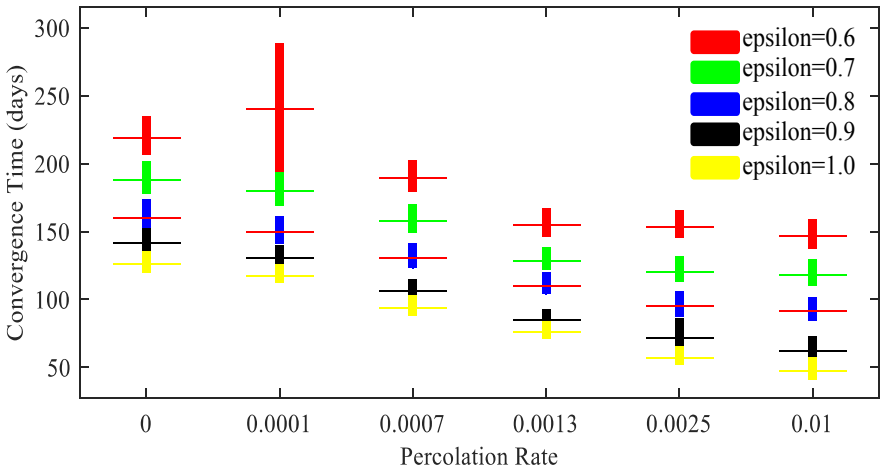

Fig.6.10 95% confidence intervals for the convergence rate with different percolation rates and convergence thresholds ε.

Fig.6.10 illustrates graphically the confidence intervals shown in **Table 6.4**. Although one box under Pr=0.0001 and $epsilon$=0.6 is different others due to the stochasticity of the ABDTD model with information percolation, overall, these box plots further illustrate that increased percolation rate accelerates the convergence of the traffic network.

6.5.2 Effect of bounded rationality

As described in **Section 6.4.1.2**, the concept of *bounded rationality* (BR) is a relevant aspect of route choice behaviour that enjoys wide empirical support. This section considers the agent-based day-to-

day model with and without the BR notion, and compares their simulation results. The simulation method without bounded rationality is described in Remark 3.

In **Fig.6.11** and **Fig.6.12** two scenarios without BR are examined, for percolation rates 0.0001 and 0.01, respectively. The other model parameters remain the same as those presented in **Fig.6.6** and **Fig.6.7**. For $p = 0.0001$, both route costs and flows oscillate considerably. Although one may still observe the converging trend, the precision of the convergence is quite low due to the local variations; that is, the difference in the route costs for the same O-D pair is around 0.8, whereas the route cost difference with BR is around 0.2 (see **Fig.6.6**). For $p = 0.01$, although the various quantities eventually become stabilized, there is a discernible gap between the costs experienced on different routes, indicating a non-convergent state. On the other hand, the cost gap for the BR case with the same percolation rate is below 0.05 upon convergence.

These results show that the BR route choice behaviour helps to improve the convergence of the network. Indeed, with an indifference band, drivers are less incentivized to switch to lower-cost routes, and the network is more likely to stabilize with less switching of flows among routes. Due to the fact that, without BR, it is difficult to observe convergence within the prescribed time horizon, in the following presentation of the numerical experiments, those without the BR route choice sub-model are omitted.

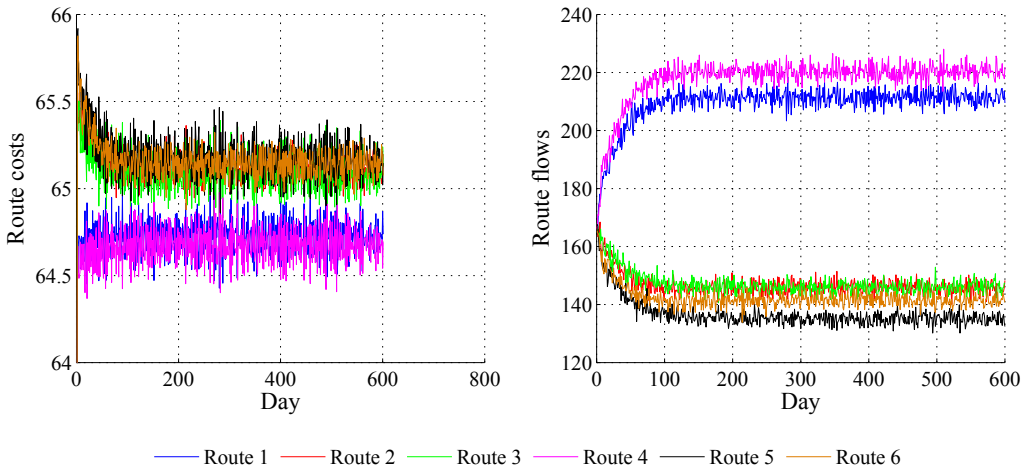

Fig.6.11 Evolution of route costs and flows with a percolation rate 0.0001 and without bounded rationality.

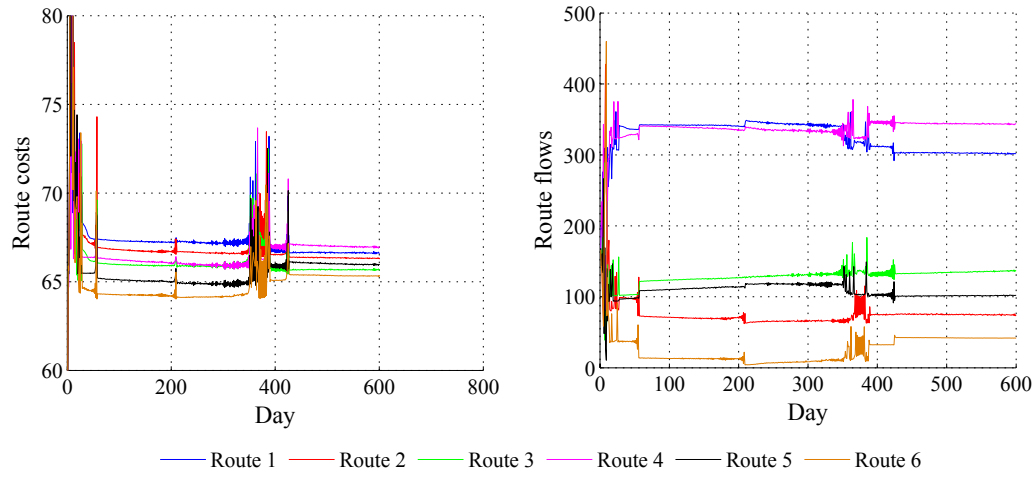

Fig.6.12 Evolution of route costs and flows with a percolation rate 0.01 and without bounded rationality.

6.5.3 Sensitivity analysis

The numerical results presented so far are based on a fixed set of model parameters. In order to investigate the effect of these choices on the validity of the experimental conclusions, a preliminary sensitivity analysis is conducted in this section. The main parameters of interest are: β defined in the route choice model (6.6) and (6.8), and α_1 and α_2 defined in the learning process (6.10) and (6.11).

The analysis begins with β, in order to adjust the sensitivity of drivers, in terms of route choice, to the difference in route costs. Then α_1 and α_2 are fixed to be 0.25, and the percolation rate to be 0.0025. Following the agent-based day-to-day model with 36 independent simulation runs, the convergence results are shown in **Table 6.5**.

Table 6.5 Sensitivity analysis for β.
The numbers are the average days taken to reach convergence.

	$\varepsilon = 0.3$	$\varepsilon = 0.4$	$\varepsilon = 0.5$	$\varepsilon = 0.6$	$\varepsilon = 0.7$	$\varepsilon = 0.8$	$\varepsilon = 0.9$	$\varepsilon = 1.0$
$\beta = 0.5$	1000	960.78	545.58	220.61	162.86	133.61	105.97	74.86
$\beta = 1.0$	940.28	403.47	192.97	153.64	120.31	94.92	75.31	56.72
$\beta = 1.5$	755.97	267.06	165.47	132.75	110.67	86.86	69.53	50.19
$\beta = 2.0$	532.47	202.06	156.94	129.36	105.25	81.03	62.42	47.72

As shown in **Table 6.5**, when β increases, the convergence of the network improves accordingly. The positive impact of β on the convergence diminishes as ε becomes larger. This is apparent from **Fig.6.13**.

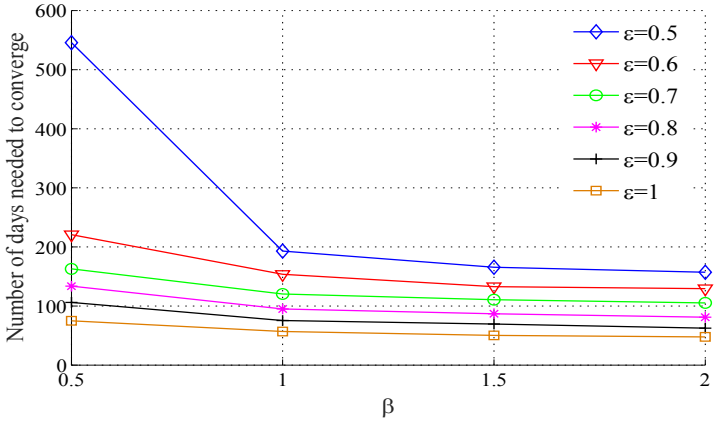

Fig.6.13 Sensitivity analysis of β.

Next, the model sensitivity is tested with regards to α_1 and α_2. These two parameters represent, respectively, weights assigned to the travel cost experienced by oneself and others, during the

update of one's route perception; see (6.10) and (6.11). In **Fig.6.6**, β is set to be 1 and the percolation rate remains 0.0025. It can be seen from this table that regardless of the choice of α $(= \alpha_1 = \alpha_2)$, the convergence trends are similar to those shown earlier.

Table 6.6 Sensitivity analysis of $\alpha = \alpha_1 = \alpha_2$.
The numbers are the average days taken to reach convergence.

	$\varepsilon = 0.3$	$\varepsilon = 0.4$	$\varepsilon = 0.5$	$\varepsilon = 0.6$	$\varepsilon = 0.7$	$\varepsilon = 0.8$	$\varepsilon = 0.9$	$\varepsilon = 1.0$
$\alpha = 0.05$	1000	757.83	349.47	224.28	161.33	130.78	106.42	87.64
$\alpha = 0.10$	960.06	585.5	210.92	180.83	144.28	115.92	84.83	69.92
$\alpha = 0.25$	940.28	403.47	192.97	153.64	120.31	94.92	75.31	56.72
$\alpha = 0.50$	940.39	367.97	182.64	153.08	120.72	90.22	70.17	47.81

Fig.6.14 provides a visualization of the convergence results. Overall the convergence becomes faster when α_1 and α_2 increase. Similar to **Fig.6.13**, however, the effects of α_1 and α_2 become less significant when ε increases.

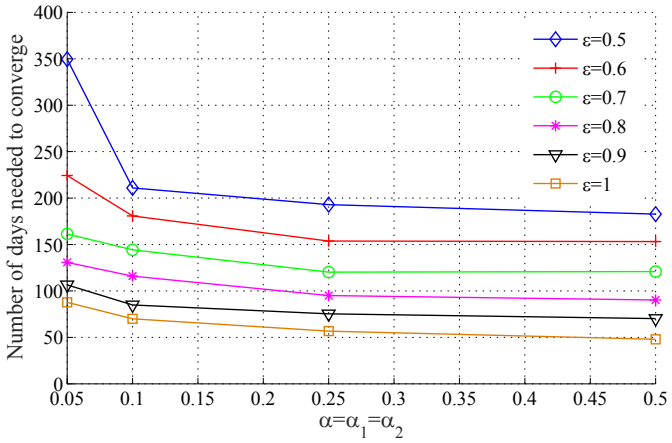

Fig.6.14 Sensitivity analysis of $\alpha = \alpha_1 = \alpha_2$.

In

Table 6.6 and **Fig.6.14** both α_1 and α_2 are set to the same value. In the following, however, both parameters are allowed to vary independently with the goal of identifying the effect of the individual parameters. In **Fig.6.15** and **Fig.6.16** shows several combinations of α_1 and α_2, each varying from

0.05 to 0.75, along with the change in the convergence rates. Interestingly, for different percolation rates qualitatively different convergence trends are observed. For smaller percolation rates (i.e. fewer drivers in the same group), such as $p = 0.0001$, the convergence is facilitated by having larger values of α_2, which corresponds to the information transmitted from other group members. When the percolation rate gets very large, however (more drivers in the same group), for instance $\mathrm{p} = 0.01$, having large values of α_2 seems to hinder convergence, and conversely fast convergence is observed mostly for very small α_2 values. For percolation rates that are less extreme, i.e. $p \in (0.0007, 0.0013, 0.0019, 0.0025)$, the situations are less straightforward and seem to exhibit some kind of transitional states. In particular, there seems to be a bifurcation point ($p = 0.0013$), which separates two qualitatively different convergence trends. This observation is confirmed in both **Fig.6.15** and **Fig.6.16**.

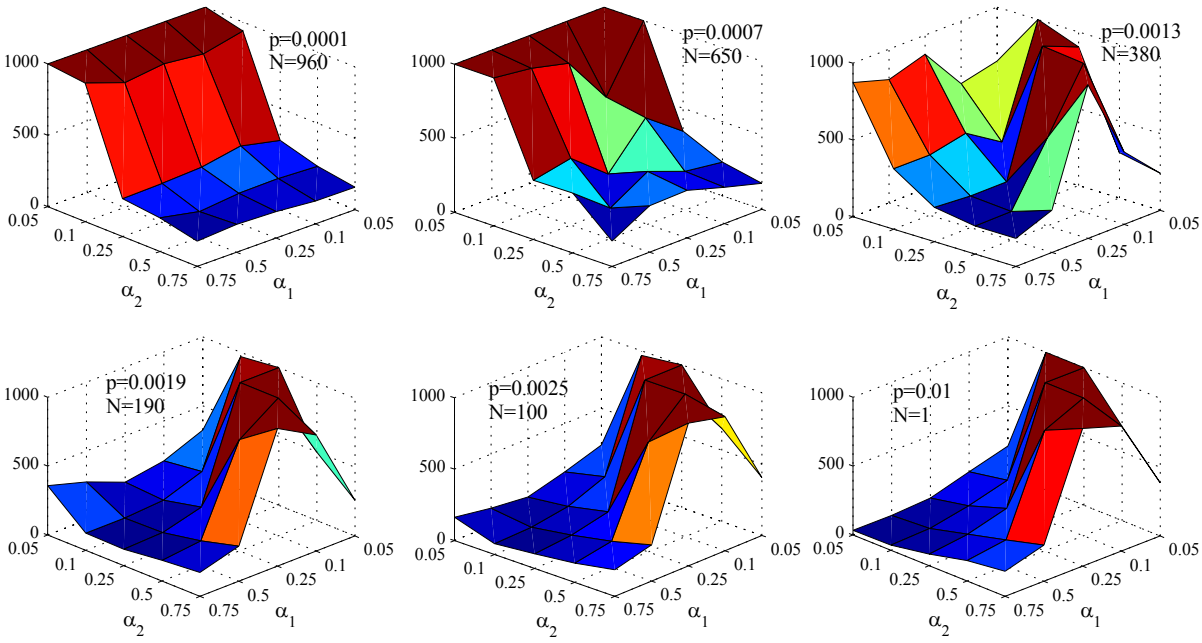

Fig.6.15 Sensitivity analysis of individual α_1 and α_2.
The z-axis represents the number of days taken to reach convergence with $\varepsilon = 0.5$. p and N denote the percolation rate and average group number, respectively.

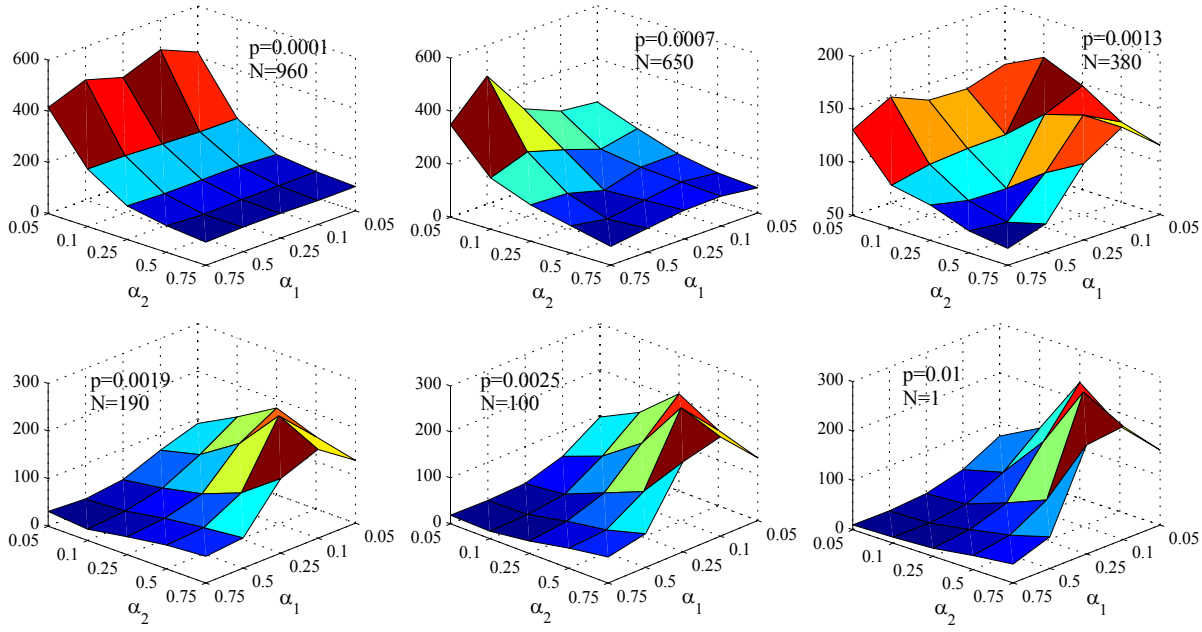

Fig.6.16 Sensitivity analysis of individual α_1 and α_2.
The z-axis represents the number of days taken to reach convergence with $\varepsilon = 1$. p and N denote the percolation rate and average group number, respectively.

Our explanation for the aforementioned two extreme cases are as follows. When p is very small, there is very little extra information available to a driver since the groups tend to be very small. Thus if the driver relies more on such information, as represented by a large α_2, the network is more likely to converge. On the contrary, if p is very large, a driver receives a lot of information from many group members, and relying too much on it would introduce much disturbance and noisy influence to the dynamics, thus slowing down convergence.

Overall, regardless of the values of α_1 and α_2, the convergence improves as the percolation rate gets higher, which is consistent with the main finding of this chapter.

As a summary of this section, the sensitivity analyses show that the effects of α_1, α_2, and β are minor on the convergence for a certain range of ε ($[0.6, 1]$). Similar results hold for different percolation rates, although, for brevity, these are not shown here. Moreover, the conclusion regarding the relationship between the percolation rate and the convergence remains qualitatively valid.

6.5.4 Network with multiple O-D pairs

The proposed model with an information sharing structure is also applicable to networks with multiple O-D pairs, such that the heterogeneity in percolation rate and travel choice behaviour parameters can be modelled. To demonstrate this, the Sioux Falls network, shown in **Fig.6.17**, is considered, with 4 O-D pairs (1, 20), (2, 13), (13, 2), and (20, 1) and a demand of 1000 per O-D pair. Moreover, ten paths are considered per O-D pair.

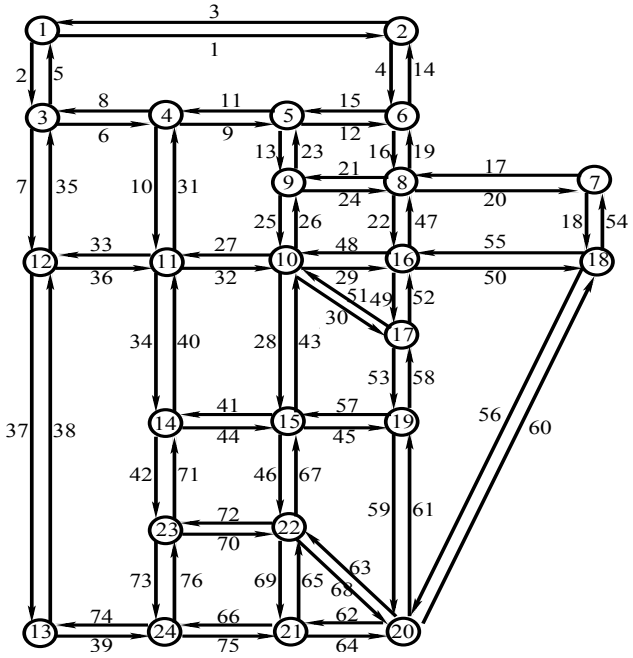

Fig.6.17 The Sioux Falls network

The modelling parameters are chosen as $\alpha_1 = 0.25, \alpha_2 = 0.25, \beta = 1$. For simplicity, the same percolation rate is used for all four O-D pairs. Due to the significant number of paths, the following relative difference in the path flow vectors is used to measure the convergence of the network:

$$\frac{\| \mathrm{h}_{t+1} - \mathrm{h}_t \|_2}{\| \mathrm{h}_t \|_2} \leq \varepsilon \qquad (6.15)$$

where $\|\cdot\|_2$ is the Euclidean norm, ε is threshold and takes 0.01 in this case. Results for this quantity are presented in **Fig.6.18** for three percolation rates: $p = 0.0001, p = 0.0025, p = 0.01$. It can be

seen that the convergence follows a similar pattern as the smaller network shown before, where larger percolation rates lead to improved convergence.

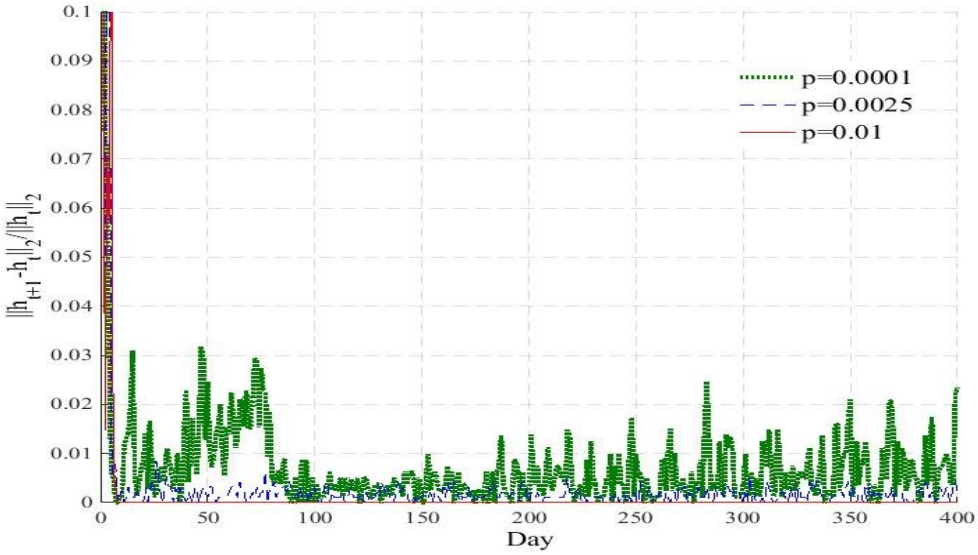

Fig.6.18 Convergence of path flows in the Sioux Falls network.

Fig.6.19 shows the daily evolution of network-wide travel costs for all four O-D pairs. Interestingly, unlike in **Fig.6.8**, higher percolation rates lead to higher total cost, even after the network has converged. This suggests that more information provision could lead to a loss of efficiency.

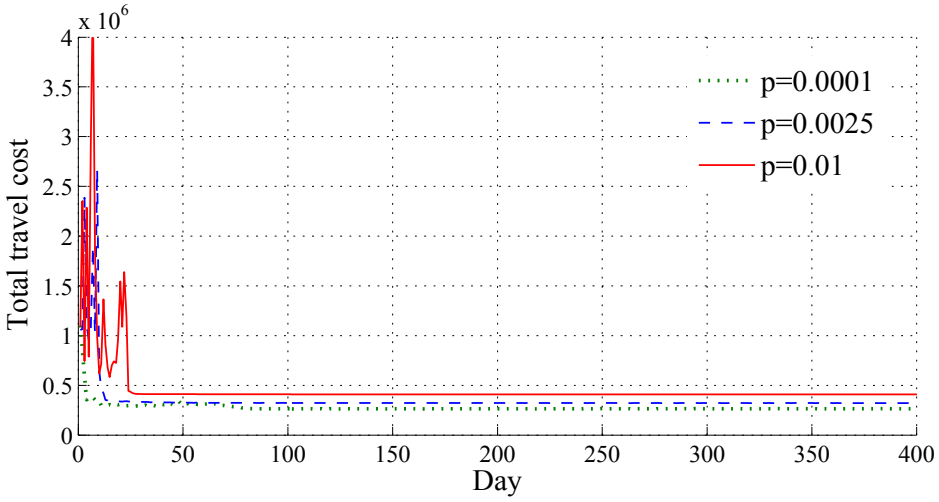

Fig.6.19 Network-wide travel cost on the Sioux Falls network.

6.7 Summary

This chapter has proposed an agent-based day-to-day (ABDTD) model, which, for the first time in the literature, incorporates percolation theory in order to capture and quantify the impact of information sharing structures on the convergence of the traffic network. A physical network was used to capture the underlying traffic network (along with links, nodes and users), while percolation theory was used in conjunction with a conceptual communication network (the cyber layer) to model the transmission of travel decisions and experiences among users.

An agent-based simulation was used to study the daily evolution of the traffic network and drivers' route choices, under the influence of imperfect information and users' bounded rationality. The results suggest a strong positive correlation between the percolation rate, which reflects the connectivity of the communication network, and the convergence of the network. This finding is further confirmed through statistical validation and sensitivity analysis. The ABDTD model developed in this chapter is able to capture information accessibility and decision making at an individual level, and is general and flexible enough to support the simulation of network traffic under a variety of scenarios, including local or global network disruptions and intelligent transport system (ITS) control. These different scenarios, as well as the robustness and resilience of networks, are studied in detail in **Chapter 7**.

Chapter 7 ROBUSTNESS AND RESILIENCE OF NETWORKS UNDER DIFFERENT CONTROL

This chapter investigates the robustness and resilience of urban road networks (URNs) under disruptions, when certain control mechanisms, including Variable Message Signs (VMS) and signal control are applied, singly and in combination. Two traffic flow modelling approaches are employed in this chapter: the agent-based simulation approach described in Chapter 6, and a continuous-flow day model. In this thesis, two key performance indicators (KPIs), namely rapidity and the new relative area index (RAI), are used to represent the resilience and robustness respectively. Compared to DTD models that rely on aggregate and continuous flow variables, an agent-based day-to-day (ABDTD) model captures the learning processes of individual drivers, and automates their interactions in such a way as to give rise to collective and complex behaviours at the macroscopic level. Based on the ABDTD framework it is also possible to test a range of traffic control tools (variable message signs, signal control strategies) and assess their effects on network resilience or robustness when the network experiences disruption. A small network is used for the numerical studies to show the evolution of network performance under these control when the network is subject to mild (25%), moderate (50%) and severe (75%) local capacity degradation. Based on this, a quantitative analysis of robustness and resilience is conducted in order to compare the effectiveness of different control under varying levels of disruption.

Similarly, these control measures are incorporated in the continuous-flow day-to-day (CFDTD) model. The small network and the Sioux Falls network are considered in the numerical examples to observe the evolution of robustness and resilience under different levels of capacity reduction. In addition, all the links in these networks are ranked based on their relevant resilience and robustness indices to understand which links have the greatest effects on the resilience and robustness of the network.

7.1 Modelling urban road networks with traffic control

This section details the VMS and signal control as means to manage traffic when the network is subject to local disruptions. This chapter also articulates the two key performance indicators to quantify the robustness and resilience of URNs suffering from local capacity degradation. For the agent-based modelling framework, information percolation is also incorporated, as described in **Chapter 6**.

7.1.1 Variable message signs (VMS)

Variable Message Signs (VMS) are widely used to provide real-time traffic information pertaining to congestion, incidents, roadworks and speed limits (Transport Bureau, 1998) as well as to make route suggestions (Mascia et al., 2016). As an instrument for the temporal and spatial management of congestion, these facilities may suggest that drivers take alternative routes, indicate the duration and location of incidents, or show general traffic conditions. VMS are able to divert traffic when incidents occur, such as in the case of the local capacity reduction considered in this thesis.

In this thesis, disruptions are modelled as global or local capacity degradation of road links or node. A VMS facility starts working after the disruption occurs. The capacity degradation of the link suffering from the disruption leads to a decrease in travellers using the corresponding routes, including the affected link. In the meantime, alternative routes are used more frequently than before the disruption. During the disruption, the VMS makes recommendations to travellers regarding alternative routes. In this context, for each O-D pair, drivers will adapt their route choices

with an exogenously defined compliance rate (CR), and switch to the alternative routes by following a logit route choice model:

$$switch\ rate_r = \frac{\exp(-\beta * c_t^r(\mathrm{h}_t^r))}{\sum_{r' \epsilon RL} \exp(-\beta * c_t^{r'}(\mathrm{h}_t^{r'}))} \quad (7.1)$$

where RL is the set of alternative routes that drivers may choose from if they comply with the VMS recommendation. Here, c_t^r refers to the route *r* cost on day *t*.

For a given O-D pair, the total amount of flow that needs to be switched can be expressed as:

$$\Delta H = \sum_{r \epsilon RS} h_t^r \times CR \qquad CR \in [0,1] \quad (7.2)$$

where *RS* is the set of paths affected by the disruptions for a given O-D pair. Then, the routes directly affected by the disruption update their flows as:

$$h_t^r \leftarrow h_t^r - h_t^r \times CR, \ \ r \in RS \quad (7.3)$$

Where $' \leftarrow '$ represents assignment of values. Alternative routes update their flows according to:

$$h_t^{r'} \leftarrow h_t^{r'} + \Delta H \times switch\ rate_{r'} \quad r' \in RL \quad (7.4)$$

7.1.2 Equi-saturation signal policy

Equi-saturation is one of the most widely adopted conventional signal-setting methods used in traffic engineering to handle *combined traffic assignment and control* (CTAC) problems (Meneguzzer, 2012). Webster (1958) originally proposed the equi-saturation signal control policy, which stipulates:

$$\text{Link red time cost} = \frac{f_a}{g_a s_a} = \frac{f_a}{(1-\bar{r}_a)s_a} = \frac{f_a}{s_a - \bar{r}_a s_a} \quad (7.5)$$

where s_a is the saturation flow on link *a*, g_a and $\bar{r}_a$ are green-time split and red-time split on link *a* respectively (they are dimensionless), f_a is the flow on the link *a*.

For a general road junction with $\bar{n}$ incoming links controlled by the signal, (7.5) can be generalized as follows:

$$p_1 = \frac{f_1}{s_1 g_1}, p_2 = \frac{f_2}{s_2 g_2}, \dots, p_{\bar{n}} = \frac{f_{\bar{n}}}{s_{\bar{n}} g_{\bar{n}}} \tag{7.6}$$

and the equi-saturation policy implies that:

$$p_1 = p_2 = \cdots = p_{\bar{n}}$$

This is equivalent to:

$$\frac{f_1}{s_1 g_1} = \frac{f_2}{s_1 g_2} = \cdots = \frac{f_{\bar{n}}}{s_{\bar{n}} g_{\bar{n}}} \tag{7.7}$$

Assuming $\frac{x_{\bar{n}}}{s_{\bar{n}}} = M_{\bar{n}}$, then (7.7) becomes:

$$\frac{M_1}{g_1} = \frac{M_2}{g_2} = \cdots \frac{M_{\bar{n}}}{g_{\bar{n}}}$$

Then assuming：

$$\frac{g_1}{M_1} = \frac{g_2}{M_2} = \cdots = \frac{g_{\bar{n}}}{M_{\bar{n}}} = \tau \tag{7.8}$$

Also, the total proportion of green time split for a given junction must be equal to 1 (Liu and Smith, 2015):

$$g_1 + g_2 + \cdots + g_{\bar{n}} = 1 \tag{7.9}$$

Based on (7.8), function (7.9) becomes:

$$(M_1 + M_2 + \cdots + M_{\bar{n}})\tau = 1 \tag{7.10}$$

Due to the fact that $M_{\bar{n}}$ can be calculated, hence τ can be derived, then green time split is obtained as $g_{\bar{n}} = M_{\bar{n}}\tau$. The red time split is :

$$\bar{r}_i = 1 - M_i\tau, \quad i\epsilon(1,..,n) \quad \bar{r}_i\epsilon[0,1] \tag{7.11}$$

Then the link flow is updated by adding extra flow in terms of red time split (Liu and Smith, 2015).

$$f_i \leftarrow f_i + \vartheta\bar{r}_i f_i, \quad i\epsilon(1,..,\bar{n}) \tag{7.12}$$

where ϑ is a constant multiplier, and in this thesis ϑ takes 1.

7.1.3 P0 signal policy

Compared to the equi-saturation policy, the P0 policy, introduced by Smith (1979a), (1979b), is more recent and specifically designed for use in CTAC modelling (Meneguzzer, 2012). The P0 policy also assumes that red times may cause additional link delays that may be captured through some extra flow units on the relevant links. Let the augmented link flow be $x_i + s_i\bar{r}_i$, the link red time cost can be shown as follows.

$$\text{Link red time cost} = s_i b_i(f_i + s_i\bar{r}_i) \tag{7.13}$$

where $b_i(.)$ is the non-decreasing link delay function (such as the BPR function).

For a signalized junction with *n* incoming links, the P0 policy chooses the red time splits to make sure that:

$$s_1 b_1 = s_2 b_2 = \cdots = s_{\bar{n}} b_{\bar{n}} = \mu \tag{7.14}$$

In this thesis, the delay function is chosen to be the BPR function, which is described in **Section 2.1.2**. Recalling the BPR function, according to (7.14), the P0 policy becomes:

$$s_i A_i \cdot \left[1 + B_i \cdot \left(\frac{f_i + \bar{r}_i s_i}{CP_i}\right)^{\sigma}\right] = \mu \tag{7.15}$$

where A_i is free flow time on the link *i*, B_i is the parameter for link *i*, σ is the power parameter, CP_i is the capacity of link *i* and here is equivalent to saturation flow, and $\bar{r}_i$ is the red time split for link i.

According to the P0 policy, the red time split can be deduced in the following way, and (7.15) can be rewritten as follows:

$$1 + B_i \cdot \left(\frac{f_i + \bar{r}_i s_i}{CP_i}\right)^{\sigma} = \frac{\mu}{s_i A_i} \Rightarrow$$

$$B_i \cdot \left(\frac{f_i + \bar{r}_i s_i}{CP_i}\right)^{\sigma} = \frac{\mu - s_i A_i}{s_i A_i} \Rightarrow$$

$$\frac{f_i + \bar{r}_i s_i}{CP_i} = \sqrt[\sigma]{\frac{\mu - s_i A_i}{s_i A_i B_i}}$$

Then $\bar{r}_i$ is obtained as follows:

$$\bar{r}_i = \frac{CP_i \sqrt[\sigma]{\frac{\mu - s_i A_i}{s_i A_i B_i}} - f_i}{s_i}, \forall i = 1, 2, 3, \cdots, \bar{n}, \quad \bar{r}_i \epsilon [0,1] \tag{7.16}$$

Assuming that the signal light for a given incoming link has two phases: red and green, then we must have $\bar{r}_i = 1 - g_i$, according to (7.9), we have:

$$\sum_{i=1}^{\bar{n}} \bar{r}_i = \sum_{i=1}^{\bar{n}} (1 - g_i) = \bar{n} - 1 \tag{7.17}$$

Then (7.17) can be written as:

$$\sum_{i=1}^{\bar{n}} \frac{CP_i \sqrt[\sigma]{\frac{\mu - s_i A_i}{s_i A_i B_i}} - f_i}{s_i} = \bar{n} - 1 \tag{7.18}$$

This is recognized as an algebraic equation with unknown $\boldsymbol{\mu}$, which can be resolved numerically by following root-search algorithms.

7.1.4 Key Performance Indicators (KPI)

The main goal in this chapter is to investigate the robustness and resilience of urban traffic networks when suffering from disruptions. In order to present the evolution of robustness and resilience quantitatively in terms of these different control strategies, relevant KPIs need to be defined.

7.1.4.1 Resilience KPI: Rapidity

As presented in **Section 3.1.1**, one aspect of resilience may be defined as the rapidity of recovery. Here, recovery means that the network reaches a new equilibrium that is not necessarily the same as the previous one if the disruption is not removed and/or the network capacity is not restored. Rapidity, therefore, can be quantified as the time between the day of the disruption and the time when new equilibrium state is reached.

The system evolution is illustrated in **Fig.7.1**, where a hypothetical disruption occurs on day t_1. Before the disruption, the network traffic is at equilibrium with a constant total travel cost across different days. Immediately after the disruption, the network-wide travel cost is likely to increase (as seen from the figure) before traffic reaches a new equilibrium on day t_3. In the simple case of **Fig.7.1**, the rapidity can be presented as the duration of the period between t_1 and t_3.

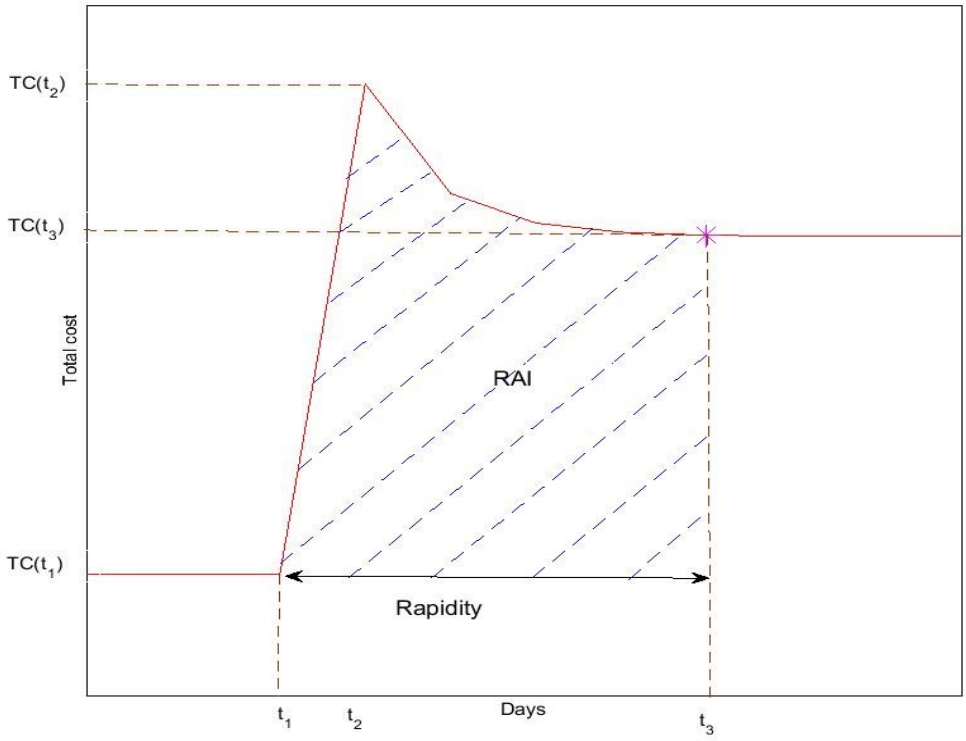

Fig.7.1 The evolution of total travel cost before and after the disruption

7.1.4.2 Robustness KPI: new Relative Area Index (RAI)

In some of the literature, robustness is defined as the network's capability to maintain its functionality after disturbance occurs. In this study, however, the network functionality is equated to the system-wide total travel cost. When the traffic network suffers from disruptions, the total cost of the network will evolve accordingly. As indicated in **Fig.7.1**, right after the disruption the cost increases but is then likely to reduce as a result of adaptive routing of travellers and improved system efficiency thereafter.

Here, the time-varying total cost can be measured by the relative area during the recovery time; that is, the area under the total cost curve from the time of the disruption (t_1) to the time when the new equilibrium is reached (t_3), which is the shaded area in **Fig.7.1**. This RAI can be calculated based on the function (5.7), and can be written as follows:

$$RAI = \int_{t1}^{t3} w(t).\frac{[TC(t) - TC(t_1)]}{TC(t_1)}dt \tag{7.19}$$

In some studies (Shang et al., 2014), the weight ranges from 10 to 1 based on the consideration of the cascading effects caused by consecutive capacity reductions. This thesis mainly focuses on the local capacity degradation occurring on a certain day, and the effects of the disruption are assumed to be consistent during the period of capacity degradation. Here, therefore, all weights *w* take 1.

RAI represents the running cost during recovery. This index assesses the cumulative loss of efficiency as a result of the disruption, and is used in this thesis to measure the network's robustness. A larger RAI implies a less robust traffic network.

7.2 Robustness and resilience analysis from agent-based day-to-day dynamic model

This section incorporates different control mechanisms (e.g. Variable Message Signs, traffic signal control) into an agent–based day-to-day (ABDTD) dynamic model to describe and quantify the

network resilience and robustness under a range of local disruptions. The ABDTD dynamic model and its characteristics have been described in detail in **Chapter 6**. Based on this, quantitative analysis and assessment of robustness and resilience can be conducted. The numerical results, despite their simplistic nature, reveal some highly interesting and complex phenomena that provide valuable insights regarding the design and management of urban traffic networks.

7.2.1 Numerical example on the small network

For the small network as shown in **Fig.6.3**, link 9 is assumed to be subject to 25%, 50% and 75% capacity degradation. There are 1000 travel agents using the network, and the other modelling parameters remain the same as in **Section 6.5**. There are six routes in the networks: $a \rightarrow b \rightarrow c \rightarrow f \rightarrow i$ (route 1), $a \rightarrow d \rightarrow e \rightarrow f \rightarrow i$ (route 2), $a \rightarrow b \rightarrow e \rightarrow f \rightarrow i$ (route 3), $a \rightarrow d \rightarrow g \rightarrow h \rightarrow i$ (route 4), $a \rightarrow d \rightarrow e \rightarrow h \rightarrow i$ (route 5) and a $\rightarrow b \rightarrow e \rightarrow h \rightarrow i$ (route 6). The network will experience two stages: pre-disruption and post-disruption. Before the disruption, the network system is assumed to be at equilibrium, which represents the normal state of the network. Three different scenarios involving traffic control are presented in the remainder of this section. In the first scenario (**Section 7.2.1.1**), no external control are imposed except for the information sharing mechanism (i.e. percolation) discussed in **Chapter 6.** In the second scenario (**Section 7.2.1.2**), the traffic is assumed to be under the influence of a variable message sign (VMS) at a relevant location in respect to the disruption. In the third scenario (**Section 7.2.1.3**), two types of adaptive traffic signal control policies are implemented: equi-saturation and P0. These different scenarios are tested with network disruptions, and the resulting network performance, as well as the resilience /robustness indicators, are analysed in detail.

7.2.1.1 Scenario1: Traffic Evolution with information percolation

In this scenario, different degrees of capacity degradation caused by different levels of disruption are imposed on link 9. Before the disruption the network is assumed to be at (approximate) equilibrium, (see **Chapter 6** for more details on approximate equilibrium for agent-based simulation). When

disruption occurs, travel information sharing through the theoretical paradigm of percolation discussed in **Chapter 6** is utilized to mitigate the impact of the disruption. Two different percolation rates (Pr), 0.0025 and 0, are considered in this thesis. These two cases are conducted to demonstrate the effect of information sharing on the resilience/robustness of the network.

Based on the description above, the case with $Pr = 0$ is conducted, and the results of route costs, route flow and total cost under mild, moderate and severe disruptions are shown in **Fig.7.2**.

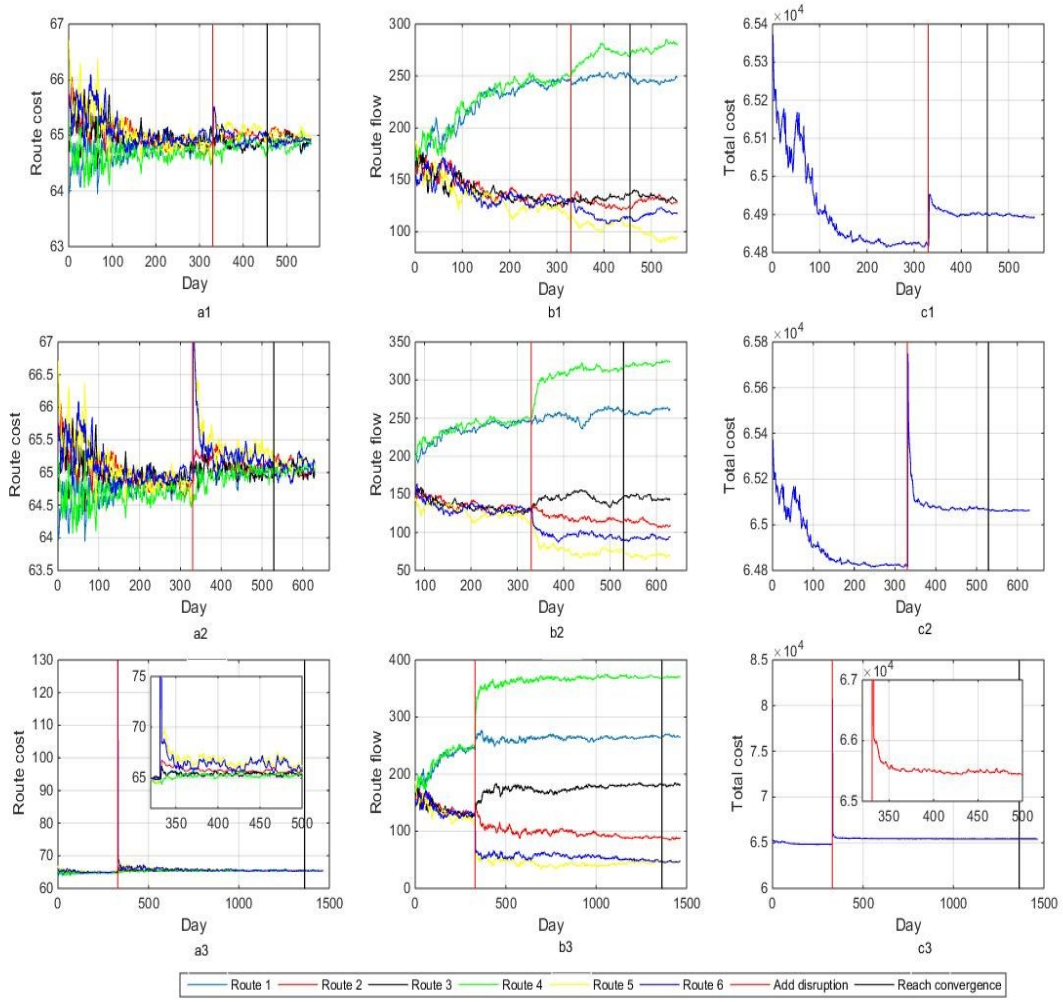

Fig.7.2 Route costs, route flow and total cost under mild, moderate and severe disruption with no communication between drivers.
First row (from a1 to c1): route costs, route flow and total cost evolution when the capacity of link 9 of the network reduces by 25% with $Pr = 0$; second row: (from a2 to c2): route costs, route flow and total cost evolution when the capacity of link 9 reduces by 50% with $Pr = 0$; third row: (from a3 to c3): route costs, route flow and total cost evolution when the capacity of link 9 reduces by 75% with $Pr = 0$.

As can be seen from **Fig.7.2**, the network starts with an arbitrary configuration of route flows and reaches an approximate equilibrium state (indicated by the red vertical line). The red vertical lines also mark the time of the disruption. On the other hand, the black vertical lines represent the attainment of a new approximate equilibrium.

The first column of **Fig.7.2** shows that route costs evolve over time when the network suffers from different levels of disruptions. There is an insignificant increase in the route costs when mild disruption (25%) occurs, and it takes 125 days to reach a new convergence. When the network suffers from moderate disruption (50%), the route costs can be seen to increase and daily fluctuations in the route costs become more significant. The network reaches a new equilibrium 199 days after the disruption. Route costs drastically increase when the network is subject to severe disruption (75%), and, as expected, it takes more days to reach a new equilibrium, 1033 days.

The second column of **Fig.7.2** shows the daily evolution of route flows after the disruption. Due to the capacity degradation of link 9, flows on the two paths, route 5 $(a \to d \to e \to h \to i)$ and route 6 $(a \to b \to e \to h \to i)$, which are directly affected, decrease greatly, as expected, while the flows on route 4 $(a \to d \to g \to h \to i)$ and route 1 $(a \to b \to c \to f \to i)$ increase due to the low perceptions of drivers. In the model, lower perception of travel cost implies that more drivers will switch to these routes. In addition, it seems that the more serious the disruption is, the more significant the changes in route flows are. Route 4 and route 6 have the most significant increase and decrease in route flow, respectively.

The third column of **Fig.7.2** depicts the total cost of the network as it evolves over time before and after the disruption. In the case of 25% capacity reduction, the total cost climbs up to 64950 from the initial approximate equilibrium (64819), and then it goes down to 64903 upon new convergence. As expected, the network does not retain its initial performance in terms of total travel cost. When the capacity decreases by 50%, the total cost first jumps to 65750 then bounces back to 65060. It is,

again, higher than the total cost at the equilibrium before the disruption. When the most serious disruption occurs (75%), the total cost goes up to 80965, then gradually climbs down to stability.

In order to examine the performance of the network with a certain level of communication between the drivers, the agent-based simulation with $Pr = 0.0025$ is once again conducted. The resulting route costs, route flows and network-wide total cost under different levels of disruptions are shown in **Fig.7.3**.

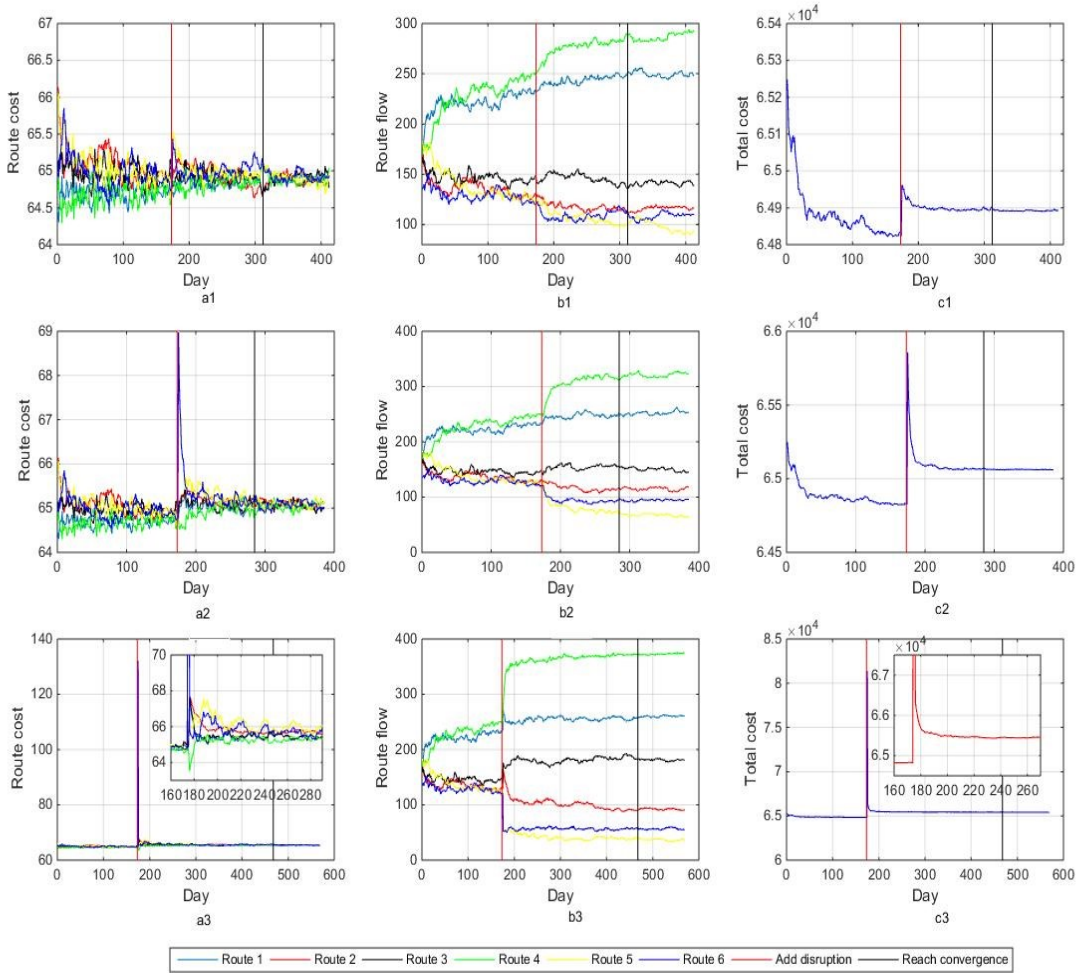

Fig.7.3 Route costs, route flow and total cost under mild, moderate and severe disruption with communication between drivers.
First row (from a1 to c1): route costs, route flow and total cost evolution when the capacity of link 9 of the network reduces by 25% with $Pr = 0.0025$; second row: (from a2 to c2): route costs, route flow and total cost evolution when the capacity of link 9 reduces by 50% with $Pr = 0.0025$; third row: (from a3 to c3): route costs, route flow and total cost evolution when the capacity of link 9 reduces by 75% with $Pr = 0.0025$.

As a general trend, **Fig.7.3** shows that the convergence of the network before or after the disruption is faster than the case with $Pr = 0$, which is consistent with the findings presented in **Chapter 6**. The first column of **Fig.7.3** shows how route costs evolve over time. There is no significant increase in the route costs under mild disruption (25%), and it takes 139 days to reach a new equilibrium. When the network suffers from moderate (50%) and severe disruption (75%), the increase in route costs becomes more significant, and the network reaches a new approximation equilibrium after 112 and 295 days, respectively. The second column of **Fig.7.3** shows the evolution of route flows over time. The flows on route 5 $(a \to d \to e \to h \to i)$ and route 6 $(a \to b \to e \to h \to i)$ decrease greatly as expected, and the flows on route 4 $(a \to d \to g \to h \to i)$ and route 1 $(a \to b \to c \to f \to i)$ increase accordingly. In addition, the more serious disruption causes more significant changes of route flows. Under the severe disruption (75%), the flow on route 5 and route 6 decreases more significantly while the flow on route 4 increases by more than other routes, which demonstrates that the flows affected by the disruption propagated to route 4, and that route 4 is capable of taking the extra flows. The third column of **Fig.7.3** depicts how information percolation influences the evolution of total cost over time. The total cost tends to jump to a higher position if the more serious disruption occurs. To be more specific, the total cost bounces to 64961, 65858 and 81362 respectively when the network suffers from minor, moderate and severe disruptions. Afterwards, the total cost is unable to revert to its original state, even though it is able to reach a new approximate equilibrium. Overall, this case is much better than that with $Pr = 0$ in terms of the speed of convergence and the significance of fluctuations.

7.2.1.2 Scenario2: Traffic evolution with VMS control

For the small network (shown in in **Fig.6.3**), only route 5 and route 6 are affected, and the other 4 routes are potential alternative paths for drivers instead of the affected routes. In this study, the VMS simply displays information regarding the disruption ahead without supplying any additional information such as suggested alternative routes, real-time travel information, etc. It is used as a

means to divert traffic away from the location of the disruption. As a result of the VMS, the route flows of the all routes are updated according to **(7.20)**.

In addition, the compliance rate (CR) directly influences the performance of the network since a larger compliance rate implies more drivers' route choices are affected by the information provided by the VMS. The *CR* is varied (0.2, 0.1 and 0.05) to observe the sensitivity of the network performance to the compliance rate, which is usually very difficult to estimate in a real-world environment. The following re-assignment of route flows are instances of the more general modelling approach presented in **Section 7.1.1**.

$$h_t^5 \leftarrow h_t^5 - h_t^5 \times CR$$

$$h_t^6 \leftarrow h_t^6 - h_t^6 \times CR$$

$$\Delta H = \sum_{r\epsilon(5,6)} h_t^r \times CR$$

$$h_t^i \leftarrow h_t^i + \Delta H \times switch\ rate_i \qquad i\epsilon(1,2,3,4) \tag{7.20}$$

Where ′ ← ′ denotes assignment of values.

In this scenario, VMS is applied as a main tool for the mitigation of congestion caused by disruptions. In addition, the effect of the combination of information percolation and VMS is also investigated.

VMS control with information percolation, $P_r = 0$

In this case, the VMS control is employed when the network is under the disruption, and during the day-to-day evolution process, none of the travel agents communicate with each other but rely only on their own perception of route costs in their route choices. The agent-based simulation incorporating both information percolation and VMS route diversion is conducted according to the following procedures.

1. At each iteration (day), the route choices of agents are first generated according to their perception of the routes, following the procedure described in **Chapter 6**.

2. After the initial route choices have been assigned, the route choices are revised according to (7.20), where the drivers initially following the affected routes will switch to alternative routes with a fixed probability (*CR*). The probability of choosing a specific alternative route is specified by the switch rate in (7.1).

Following this simulation procedure, the resulting route costs, route flows and network-wide total cost over time are presented in **Fig.7.4**, **Fig.7.5** and **Fig.7.6**, one for each compliance rate of the VMS (i.e. 0.05, 0.1 and 0.2).

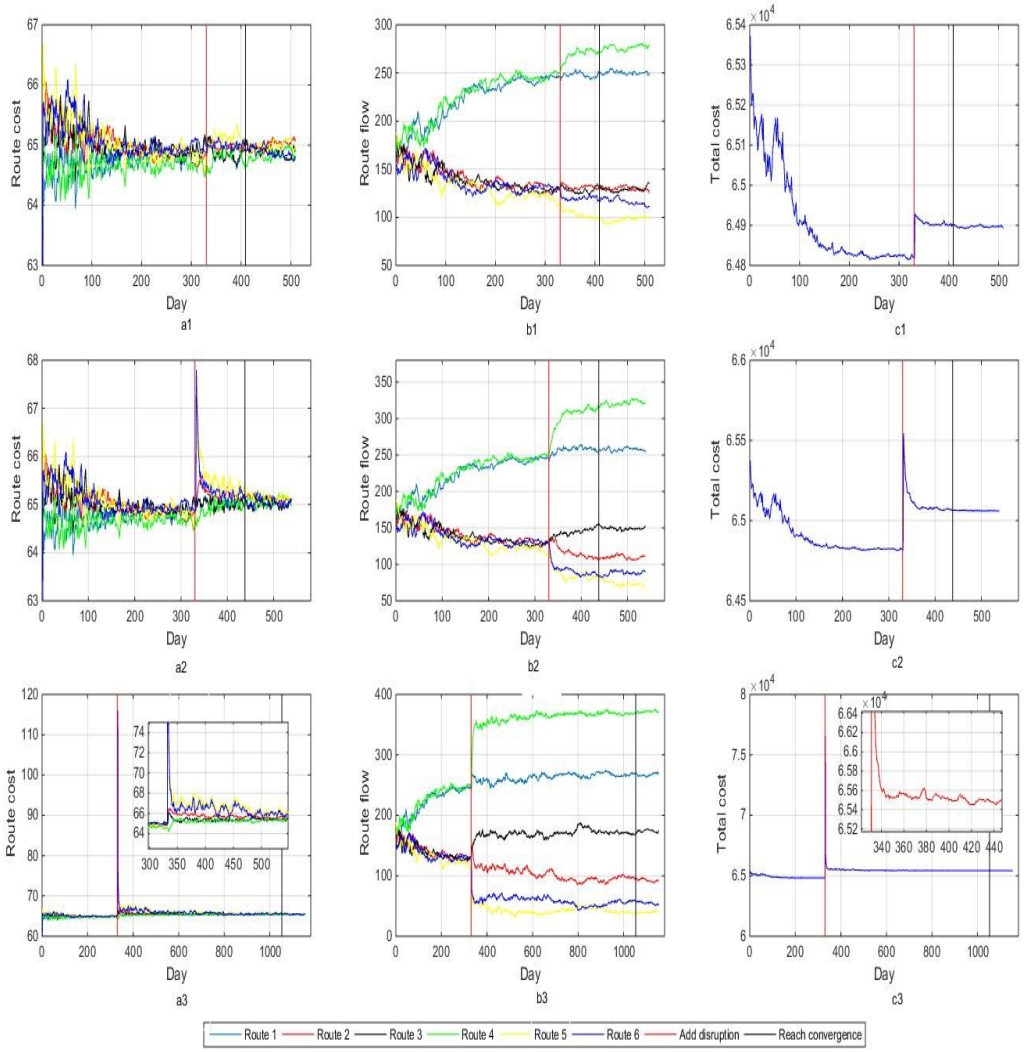

Fig.7.4 Route costs, route flow and total cost evolution under VMS control with *CR =0.05* and *Pr=0* First row (from a1 to c1): the evolution of route costs, route flow and total cost when the capacity of link 9 reduces by 25% with $Pr = 0$; second row: (from a2 to c2): the evolution of route costs, route flow and total cost when the capacity of link 9 reduces by 50% with $Pr = 0$; third row: (from a3 to c3): the evolution of route costs, route flow and total cost when the capacity of link 9 reduces by 75% with $Pr = 0$.

Fig.7.4 shows how the route costs, route flows and network-wide total costs evolve when a VMS with a *CR*=0.05 is used to manage the traffic. In this case, where *Pr*=0, drivers adjust their route perception and choices based solely on their own travel experience. As can be seen from **Fig.7.4**, with this compliance rate, the route costs do not react significantly to the minor disruption (25% capacity reduction), and the network takes approximately 70 days to reach a new approximation equilibrium. For the moderate and severe disruptions, the route costs and route flow both significantly fluctuate over time, and the network also takes longer to reach an equilibrium. The increase in the total cost is more significant when more severe disruption occurs, and the total cost at the new approximate equilibrium is further deviated from the original approximate equilibrium.

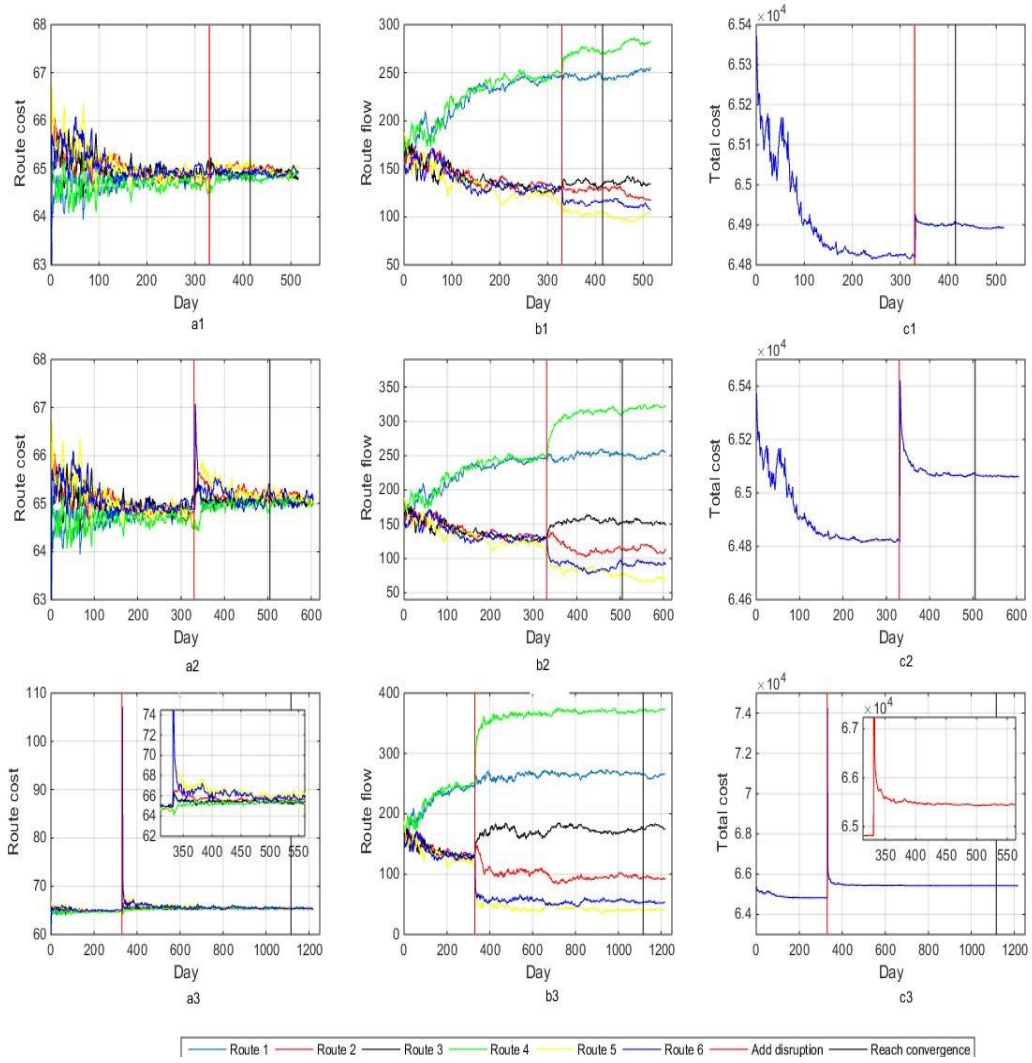

Fig.7.5 Route costs, route flow and total cost evolution under VMS control with *CR* =0.1 and *Pr=0* First row (from a1 to c1): the evolution of route costs, route flow and total cost when the capacity of link 9 reduces by 25% with $Pr = 0$; second row: (from a2 to c2): the evolution of route costs, route flow and total cost when the capacity of link 9 reduces by 50% with $Pr = 0$; third row: (from a3 to c3): the evolution of route costs, route flow and total cost when the capacity of link 9 reduces by 75% with $Pr = 0$.

Fig.7.5 shows the evolution of route costs, route flows and network-wide total cost over time when a VMS with a *CR*=0.1 is employed to mitigate the congestion caused by different levels of disruptions. It seems that the network is less affected by the minor disruption (25%), and the network takes 85 days to reach a new equilibria, which is longer than that with *CR*=0.05. For 50% and 75% capacity reduction, the route costs abruptly increase then gradually reach stability, and the fluctuations on route flows are significant. Compared to the case where *CR*=0.05, the networks take longer to reach equilibria in these scenarios. Through the observation and analysis from

Fig.7.4 and **Fig.7.5**, it may be concluded that it may not always lead to the best outcome if the compliance rate is greater.

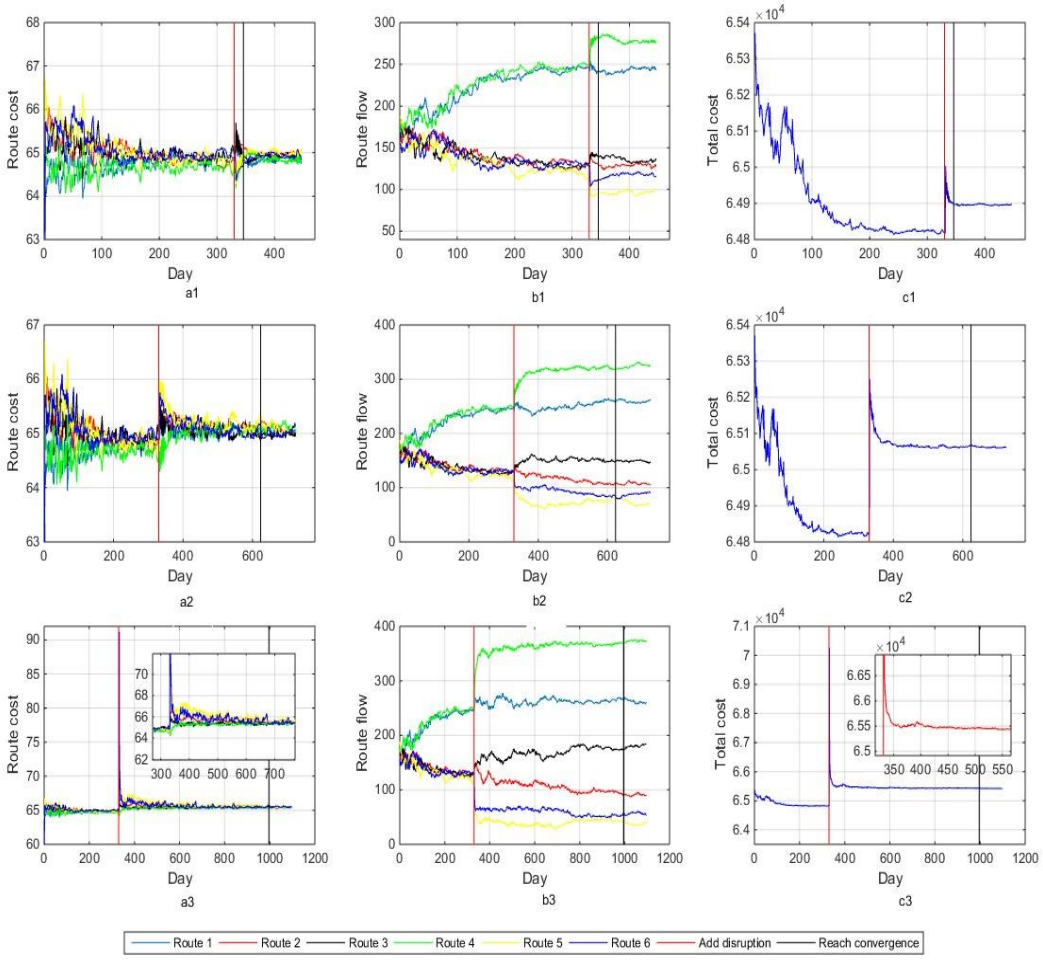

Fig.7.6 Route costs, route flow and total cost evolution under VMS control with *CR* =0.2 and *Pr=0* First row (from a1 to c1): route costs, route flow and total cost evolution when the capacity of link 9 reduces by 25% with $Pr = 0$; second row: (from a2 to c2): route costs, route flow and total cost evolution when the capacity of link 9 reduces by 50% with $Pr = 0$; third row: (from a3 to c3): route costs, route flow and total cost evolution when the capacity of link 9 reduces by 75% with $Pr = 0$.

As can be seen from **Fig.7.6**, the utilization of VMS with *CR*=0.2 causes significant fluctuations of route flows, but also facilities the networks suffering from minor and severe disruptions to reach new approximate equilibria faster than the case where *CR*=0.05 and 0.1. The explanation for this is that more drivers follow the information provided by VMS to use other alternative paths, and it quickly stabilizes traffic after the disruption. Interestingly, however, it does not speed up the convergence of the network when suffering from moderate capacity degradation, since at this level

CR overestimates the impacts caused by the disruption. For severe disruption, on the other hand, this level of *CR* improves the rapidity compared to the case where *CR=0.01* and *0.05*.

Through the observations of **Fig.7.4**, **Fig.7.5** and **Fig.7.6**, it can see that the route costs, route flows and network-wide total costs evolve over time as the *CR* of VMS takes 0.05, 0.1 and 0.2, respectively. For minor and severe disruption, the case of VMS with *CR*=0.2 shows the fastest convergence, while the case where *CR*=0.1 presents the worst rapidity. This clearly demonstrates that the larger value of *CR* does not necessarily facilitate the network to reach convergence faster. It is even worse for moderate disruption; the larger *CR* hinders the convergence of the network. The quantitative results are presented in **Table 7.2**.

VMS control with information percolation, $P_r = 0.0025$

In this case, the positive percolation rate allows the drivers to form groups and communicate with each other in their learning processes. Through the analyses in **Chapter 6**, it is shown that extra information obtained from others does not necessarily facilitate the convergence speed of the system (as shown in **Fig.6.15** and **Fig.6.16**). It is unclear, however, whether the VMS with different *CR* and information percolation can improve the robustness and resilience of the system under different levels of disruptions, so it is worth investigating how the combination of VMS and information percolation works when the network suffers from capacity degradation. The results are presented in **Fig.7.7**, **Fig.7.8** and **Fig.7.9**, one for each compliance rate (i.e. 0.05, 0.1, and 0.2).

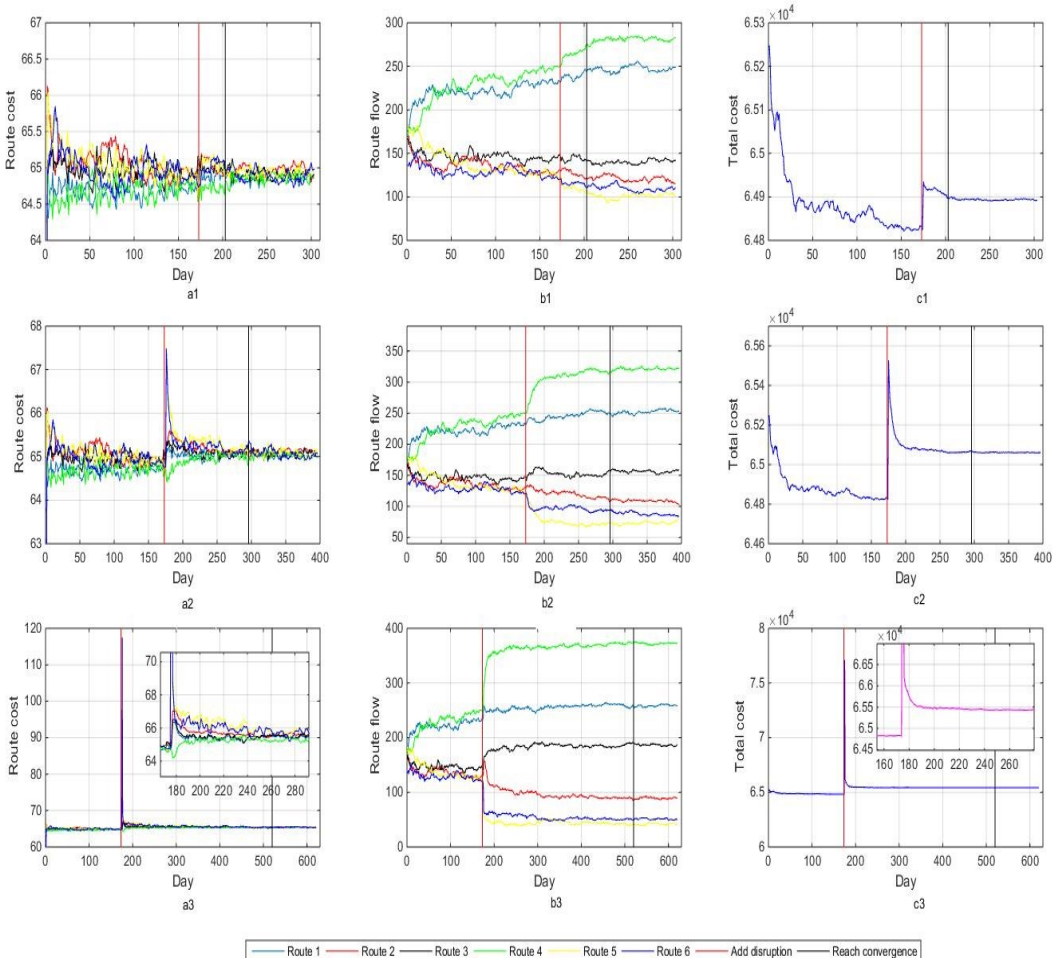

Fig.7.7 Route costs, route flow and total cost evolution under VMS control with *CR =0.05* and $Pr = 0.0025$

First row (from a1 to c1): the evolution of route costs, route flow and total cost when the capacity of link 9 reduces by 25% with $Pr = 0.0025$; second row: (from a2 to c2): the evolution of route costs, route flow and total cost when the capacity of link 9 reduces by 50% with $Pr = 0.0025$; third row: (from a3 to c3): the evolution of route costs, route flow and total cost when the capacity of link 9 reduces by 75% with $Pr = 0.0025$.

When the combination of information percolation and VMS is employed, overall, the rapidity of the network is improved under minor, moderate and severe disruptions compared to the case purely using VMS with *CR*=0.05. For minor disruption, the route costs and the route flows are relatively smooth after the disruption, and the total cost increases to a bit more than 64930 from 64819. This control facilitates the network to converge much faster than the case purely using VMS, although the fluctuations of the route costs and the route flow are still significant. In this case, the utilization of VMS plus information percolation is effective in improving the resilience of the network.

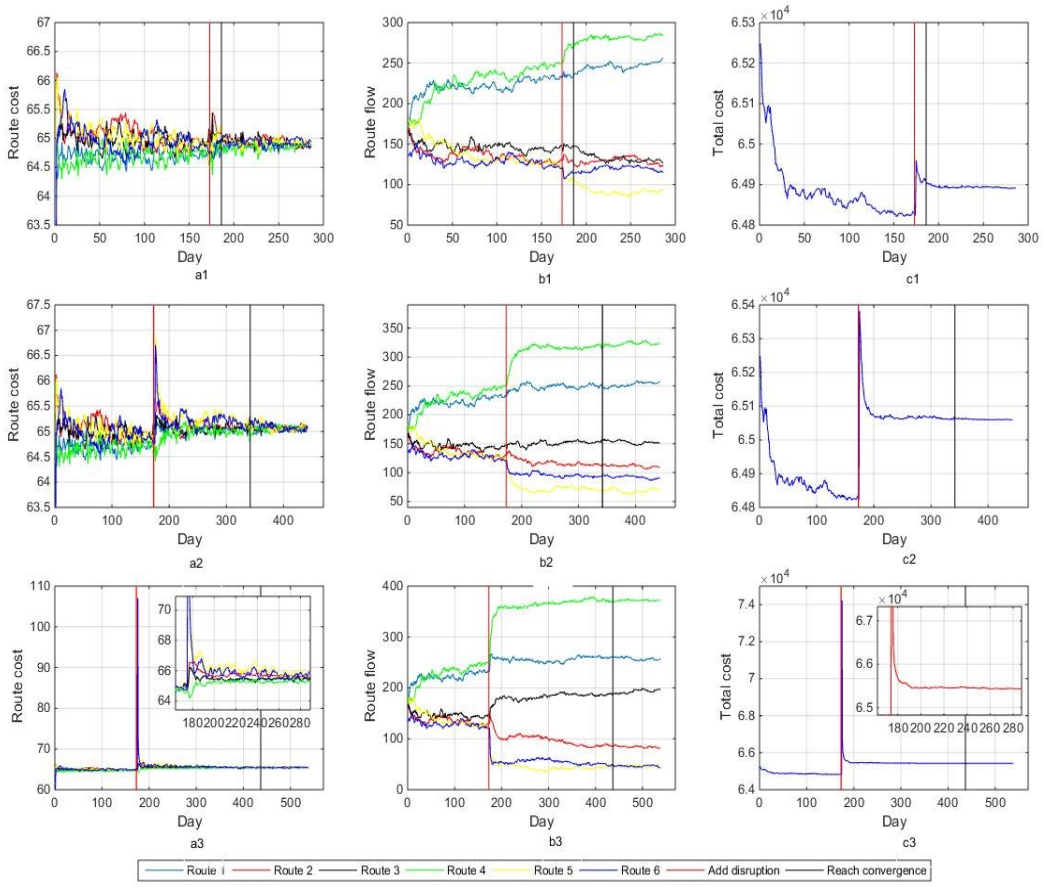

Fig.7.8 Route costs, route flow and total cost evolution under VMS control with *CR* =0.1 and $Pr = 0.0025$
First row (from a1 to c1): the evolution of route costs, route flow and total cost when the capacity of link 9 reduces by 25% with $Pr = 0.0025$; second row: (from a2 to c2): the evolution of route costs, route flow and total cost when the capacity of link 9 reduces by 50% with $Pr = 0.0025$; third row: (from a3 to c3): the evolution of route costs, route flow and total cost when the capacity of link 9 reduces by 75% with $Pr = 0.0025$.

In this case, drivers are allowed to obtain the route perceptions from others formed in the same group and the compliance rate (CR) also increases to 0.1, namely, every day 10% of drivers who are supposed to use the routes passing through link 9 switch to other alternative paths. Under this mechanism, the route costs and the route flows demonstrate gentler fluctuations when experiencing minor disruption and the network tends to converge very quickly. For 50% capacity reduction, the network reaches a new approximate equilibrium more slowly than the case using VMS and information percolation with *CR*=0.05, which demonstrates that larger *CR* cannot always play a positive role again in terms of rapidity of the network. This control mechanism, however,

facilitates the network to reach convergence faster when the network is subject to serious disruption.

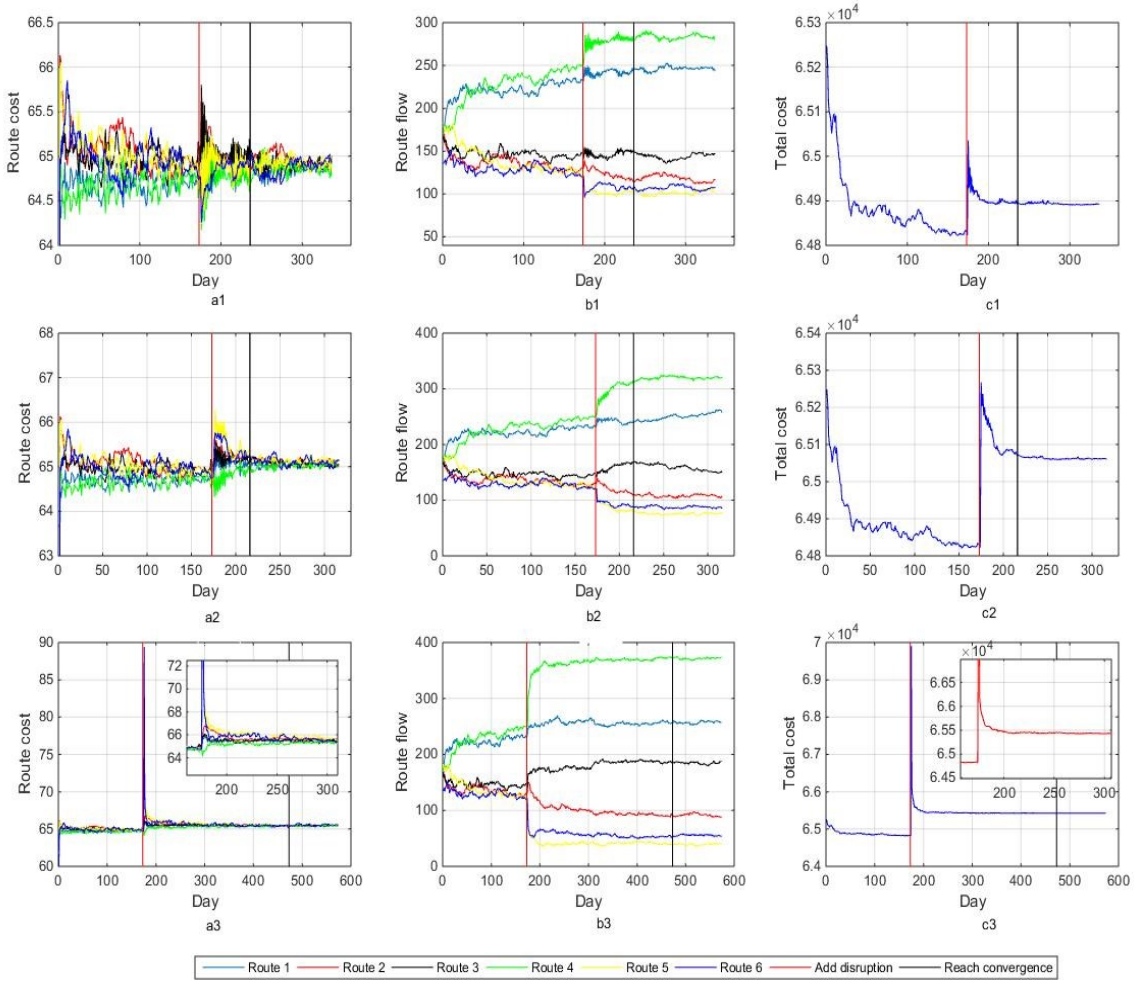

Fig.7.9 Route costs, route flow and total cost evolution under VMS control with *CR* =0.2 and $Pr = 0.0025$
First row (from a1 to c1): the evolution of route costs, route flow and total cost when the capacity of link 9 reduces by 25% with $Pr = 0.0025$; second row: (from a2 to c2): the evolution of route costs, route flow and total cost when the capacity of link 9 reduces by 50% with $Pr = 0.0025$; third row: (from a3 to c3): the evolution of route costs, route flow and total cost when the capacity of link 9 reduces by 75% with $Pr = 0.0025$.

As can be seen from **Fig.7.9**, when 20% of drivers on the routes passing through link 9 switch to other alternative paths every day, it seems that VMS in this case overestimates the impacts caused by the minor disruption. Significant fluctuations in the route flows and the route costs therefore appear, and the rapidity of the network is worse than the cases shown in graphs a1 to c1 of **Fig.7.7** and **Fig.7.8**. In addition, the extra information provided by information percolation also hinders the

convergence of the network suffering from 25% capacity degradation compared to the case without information percolation. The second row of **Fig.7.9** shows that VMS control in the case of moderate (50%) disruptions leads to fewer fluctuations and faster convergence compared to other cases. Moreover, for 75% capacity reduction, information percolation plus VMS where *CR* =0.2 significantly improves the rapidity of the network compared to the cases without information percolation, but it has worse rapidity than the case shown in the third row of **Fig.7.8**.

Table 7.2 presents a quantitative analysis of the effect of VMS on the network for the three cases shown in **Fig.7.7**, **Fig.7.8** and **Fig.7.9**.

7.2.1.3 Scenario 3: Traffic evolution with signal control

In this section, a network controlled by traffic lights is considered. As shown in **Fig.7.10**, two adaptive traffic signal control strategies are employed to react to the daily variation of network traffic flows. This is done by adjusting the green/red split for different approaches at relevant junctions. The rationale for this mechanism is that the time splits can respond to the delays caused by the disruptions, thereby reducing the flow fluctuation as well as the network-wide delay. Given that a signal control is needed only when there are conflicting approaches at a junction, in the case of the small network signals are only considered at nodes e, f and h (see **Fig.7.10**). Regarding the adaptive signal control strategies, the equi-saturation control policy and the P0 control policy are employed.

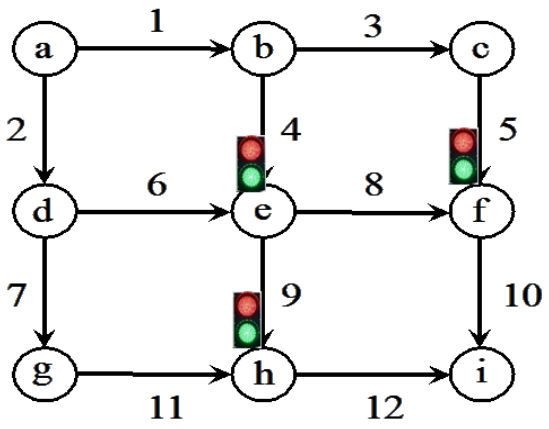

Fig.7.10 Signal control used in the intersection of the network

Signal control

Adaptive traffic signals respond to current traffic situations in ways that reduces the total congestion and travel time as time (day) evolves. In this thesis, the network is controlled by adaptive signal lights before and after the disruption. Due to the capabilities of both equi-saturation and P0 signal control policies in minimizing network delay, it is expected that they could help improve the network performance in terms of resilience and robustness.

The incorporation of adaptive signal control and drivers' route choices has been investigated in a number of studies (Allsop, 1974, Smith, 1979c, Smith, 1984a, Dickson, 1981); the combination of adaptive signal control and day-to-day traffic assignment is studied in Meneguzzer (1996) and Wong et al. (2001). Two well-known signal control policies are equi-saturation and P0 policies (Webster, 1958, Smith, 1979a). Both policies are employed in this study, and the combinations of such signal control and information percolation are also investigated.

Traffic evolution with an Equi-saturation policy

The simulations with an equi-saturation signal policy and information percolation with $P_r = 0$ and $P_r = 0.0025$ are conducted according to the methodology introduced in **Section 7.1.2**. The evolution of route costs, route flows and network-wide total costs are shown in **Fig.7.11** and **Fig.7.12**, for $P_r = 0$ and $P_r = 0.0025$, respectively.

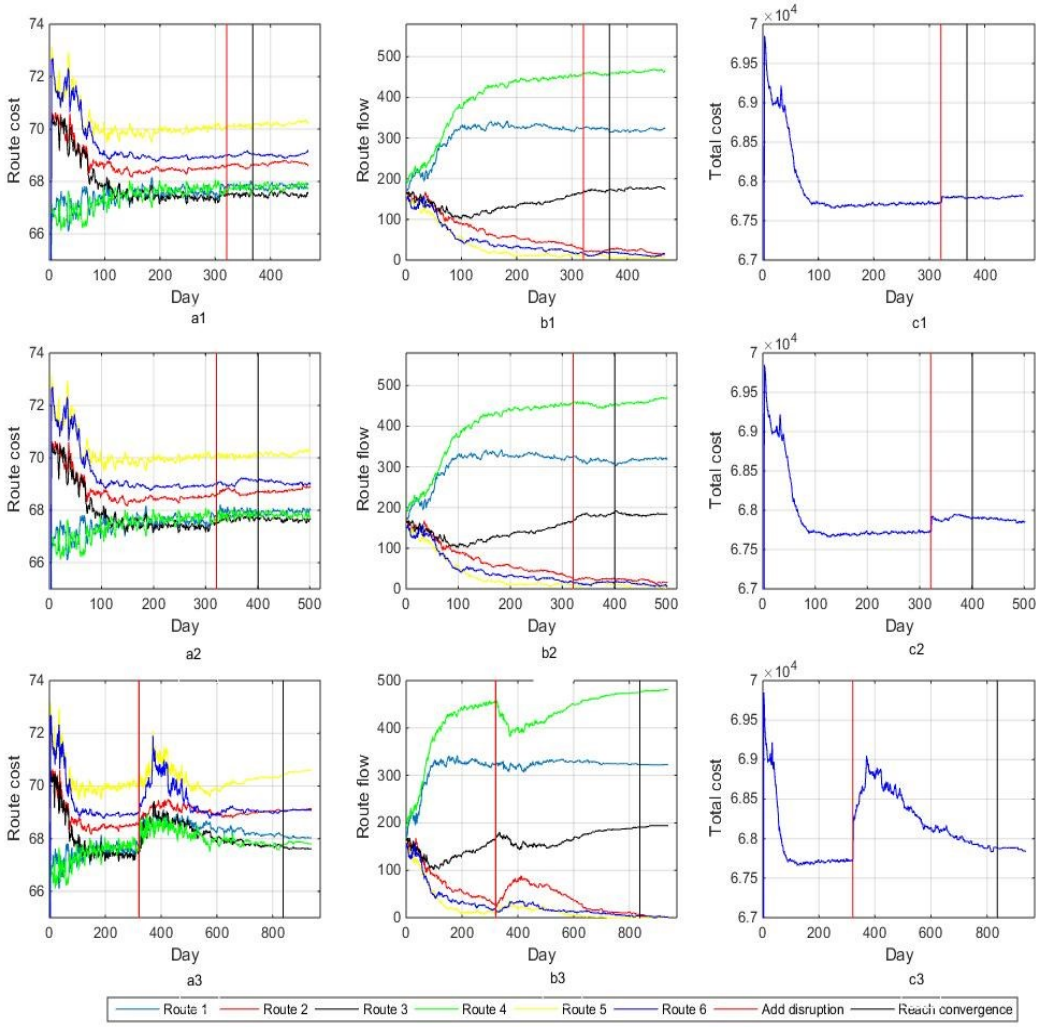

Fig.7.11 Route costs, route flow and total cost evolution with an equi-saturation signal policy and $Pr = 0$

First row (from a1 to c1): route costs, route flow and total cost evolution when the capacity of link 9 of the network reduces by 25% with $Pr = 0$; second row: (from a2 to c2): route costs, route flow and total cost evolution when the capacity of link 9 reduces by 50% with $Pr = 0$; third row: (from a3 to c3): route costs, route flow and total cost evolution when the capacity of link 9 reduces by 75% with $Pr = 0$.

As can be seen from **Fig.7.11**, route costs are relatively stable when 25% and 50% capacity degradation occur under the equi-saturation signal policy. When 75% disruption is imposed on the network, however, the route costs fluctuate considerably and the number of days before convergence is much more than the previous two cases. Route flows and total cost under different levels of disruptions have quantitatively similar performances as the route costs. Moreover, the network-wide total cost with 75% capacity reduction continues to increase for 20 days after the

disruption, before it finally decreases. This reveals that the equi-saturation policy does not perform well in tending the network towards equilibrium under severe network disruption (75% capacity reduction).

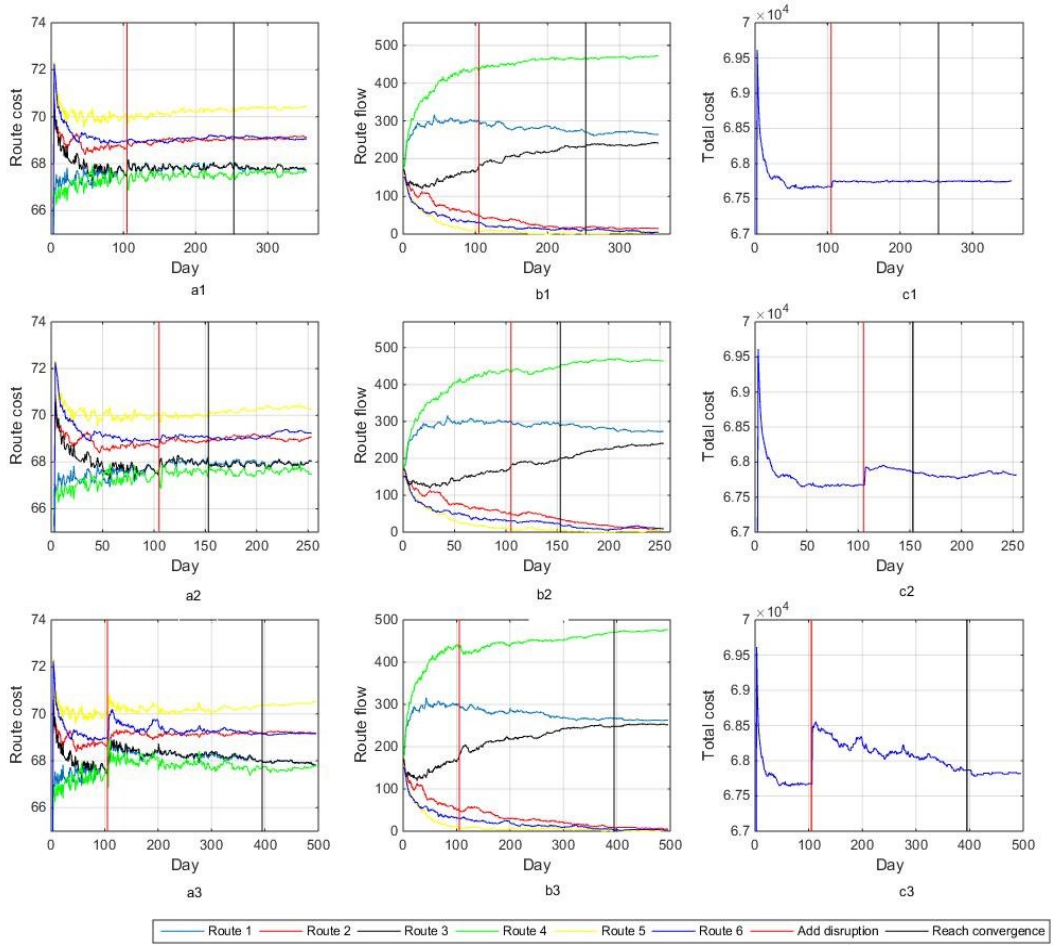

Fig.7.12 Route costs, route flow and total cost evolution with an equi-saturation signal policy and $Pr = 0.0025$
First row (from a1 to c1): route costs, route flow and total cost evolution when the capacity of link 9 of the network reduces by 25% with $Pr = 0.0025$; second row: (from a2 to c2): route costs, route flow and total cost evolution when the capacity of link 9 reduces by 50% with $Pr = 0.0025$; third row: (from a3 to c3): route costs, route flow and total cost evolution when the capacity of link 9 reduces by 75% with $Pr = 0.0025$.

Compared to the equi-saturation policy with $Pr = 0$, although route costs, route flows and total cost under 25% and 50% capacity degradation evolve over time in a similar way, the network takes longer to reach a new convergence, which may be due to the extra information provided by the information percolation mechanism. In addition, the fluctuations of the route costs and the route

flows under severe disruptions become much less, and the network also takes fewer days to reach a new convergence after the disruption. It seems that the equi-saturation signal policy with information percolation facilitates the system to return to stability more quickly when suffering from severe disruption. It does not work very well when the network is subject to minor disruption, however. Moreover, the combination of the equi-saturation policy and information percolation shows a good stability against the disruptions in that the route costs and the route flows do not show a significant increase or decrease in response to the disruption.

Traffic evolution with a P0 control policy

The simulations regarding P0 signal control policy with $P_r = 0$ and $P_r = 0.0025$ are conducted based on the method introduced in **Section 7.1.3**, and evolution processes of route costs, route flow and total costs are presented in **Fig.7.13** and **Fig.7.14**.

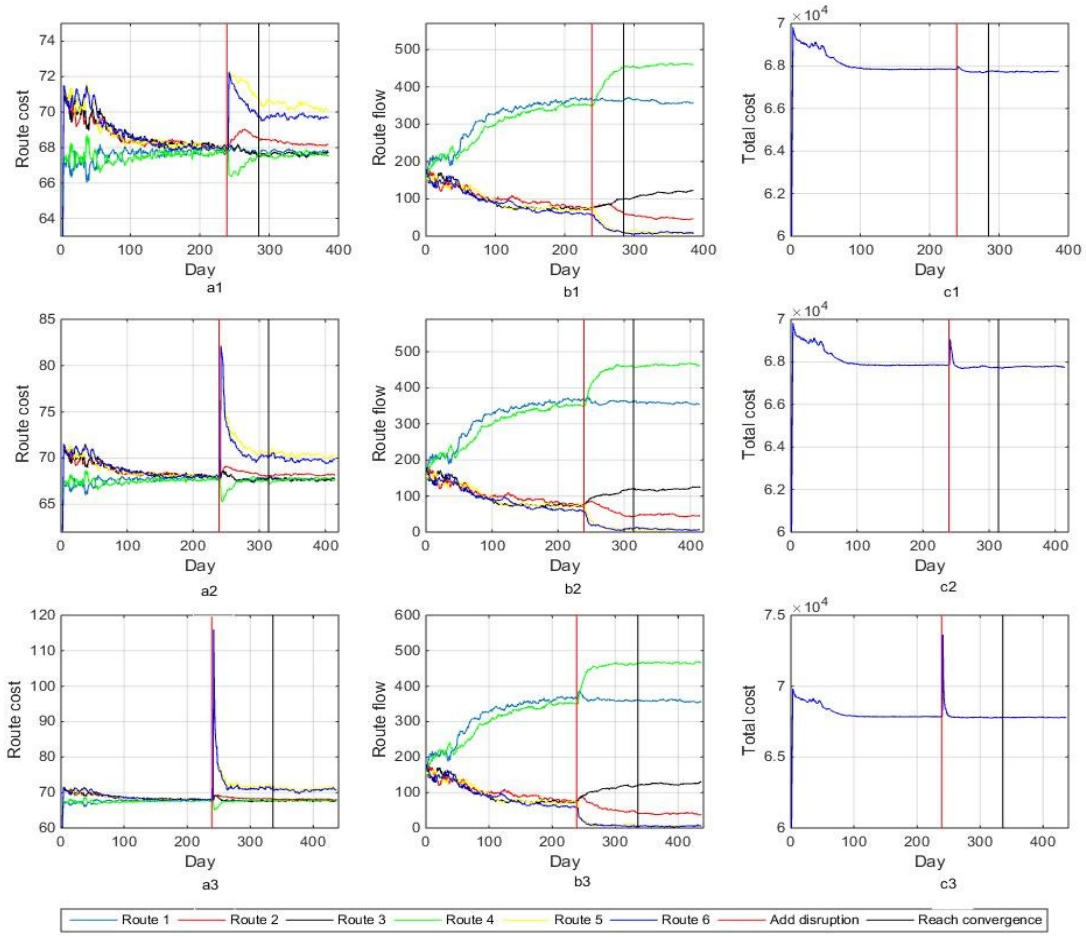

Fig.7.13 Route costs, route flow and total cost evolution with a P0 signal policy and $Pr = 0$ First row (from a1 to c1): route costs, route flow and total cost evolution when the capacity of link 9 of the network reduces by 25% with $Pr = 0$; second row: (from a2 to c2): route costs, route flow and total cost evolution when the capacity of link 9 reduces by 50% with $Pr = 0$; third row: (from a3 to c3): route costs, route flow and total cost evolution when the capacity of link 9 reduces by 75% with $Pr = 0$.

Under the P0 policy, the evolution of route costs, route flow and total cost deviates significantly from the equi-saturation policy. The vertical red lines and black lines clearly depict that the P0 signal control facilities fast convergence of route flows to equilibrium. In particular, it seems that the flow is able to reach convergence more quickly than with the equi-saturation policy with $Pr = 0$ when more serious disruptions occur. As can be seen from the third column of **Fig.7.13**, the network-wide total costs to reach equilibria before and after the disruption differ by a very small margin. This indicates that the network controlled by the P0 policy is highly robust. This may be partially due to the bounded rationality embedded in the network model, which introduces inefficiencies to the

network even at equilibrium. The bounded rationality also induces non-uniqueness of equilibrium solutions, which increases the chance of network paradoxes such as the Braess paradox.

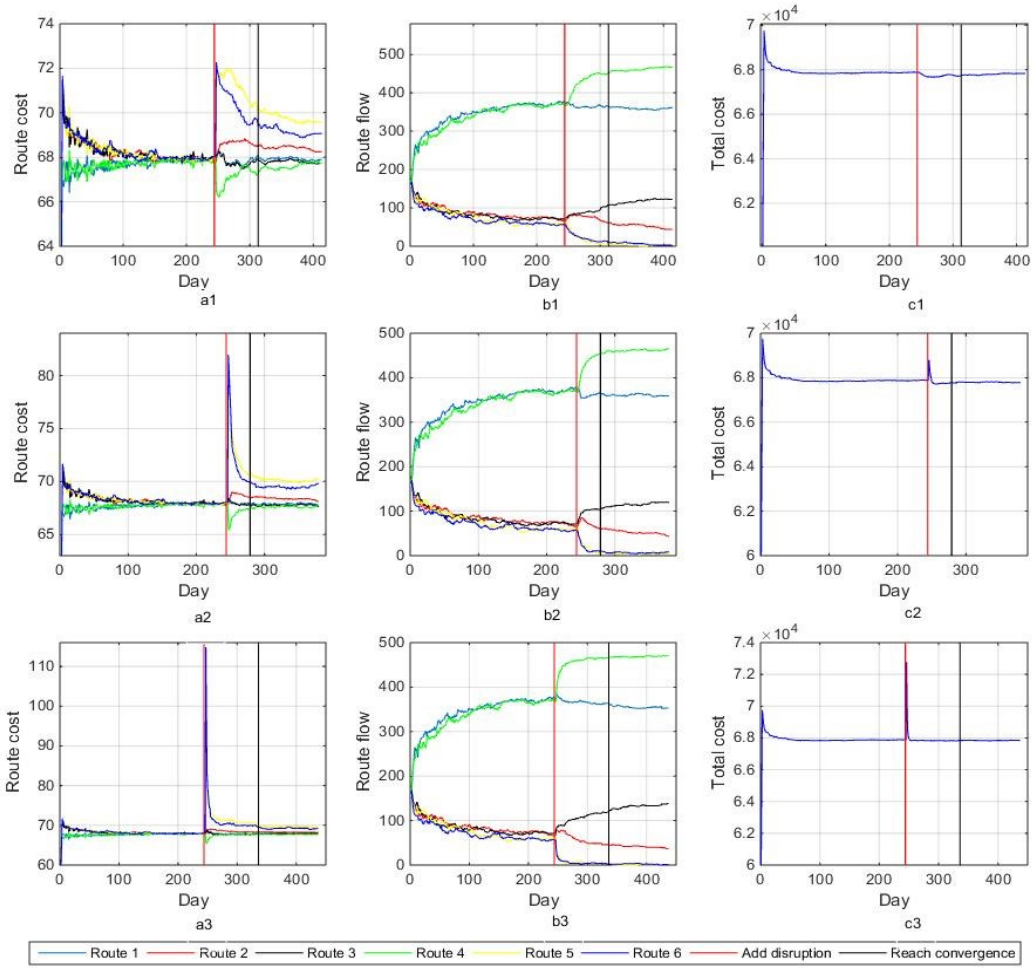

Fig.7.14 Route costs, route flow and total cost evolution with a P0 signal policy and $Pr = 0.0025$ First row (from a1 to c1): route costs, route flow and total cost evolution when the capacity of link 9 of the network reduces by 25% with $Pr = 0.0025$; second row: (from a2 to c2): route costs, route flow and total cost evolution when the capacity of link 9 reduces by 50% with $Pr = 0.0025$; third row: (from a3 to c3): route costs, route flow and total cost evolution when the capacity of link 9 reduces by 75% with $Pr = 0.0025$.

As can be seen from **Fig.7.14**, the route costs abruptly increase when the disruption occurs, and peak route costs are larger if the disruption is more serious. The route flow exhibits similar performance to route costs, and the third column of **Fig.7.14** clearly shows that more severe disruption leads to larger peak total cost. The total cost curves of the network also exhibit the phenomenon that the total cost is lower than original total cost when the network reaches new

convergence. In particular, when the network suffers from 50% disruption, this phenomenon is very significant, and also the network reaches new convergence much faster under this level of disruption. It is difficult to say exactly whether the combination of the P0 policy and information percolation is better than the case purely using the P0 policy in terms of resilience and robustness, so the quantitative analysis for signal control is given in **Section 7.2.2.3**. In addition, the combination of information percolation and P0 is better than the combination of information percolation and an equi-saturation control policy. This observation will be further corroborated in the detailed quantitative analyses presented next in **Section 7.2.2**.

7.2.2 Robustness and resilience analysis for the small network

The previous section mainly depicts how route costs, route flow and total cost of the network evolve over time under information percolation control, VMS control and signal control when the network is subject to local capacity reduction. The results presented in **Section 7.2.1** indicate a positive effect of control strategies (including information percolation) on the resilience and robustness of the underlying network. This section further confirms this observation by presenting some quantitative, and rigorous, measures of network performance in terms of resilience and robustness. Following the methodology introduced in **Section 7.1.4**, a quantitative characterization of resilience and robustness are conducted here, and all the quantitative results for different control strategies are presented in **Table 7.1**, **Table 7.2** and **Table 7.3**.

7.2.2.1 Information percolation

Under information percolation, drivers are able to gain extra information from others within the same group and thus reduce personal bias towards relevant routes. Such an information sharing mechanism may facilitate convergence of the network as well as more efficient recovery. The description of route costs, route flows and total cost are presented in **Section 7.2.1**. According to the quantitative method introduced in **Section 7.1.4**, the recovery time and RAI are calculated and shown in **Table 7.1**. Here $TC(t_2)$ denotes the maximal total cost caused by the disruption on day t_2,

and is also called peak total cost. $TC(t_3)$ is the total cost when traffic reaches a new equilibrium on day t_3.These quantitative indicators, including rapidity and RAI, are shown in **Table 7.1**.

Table 7.1 KPI of robustness and resilience for the small network under the control of information percolation

	Pr=0				***Pr=0.0025***			
Capacity reduction	***TC(t_2)***	***TC(t_3)***	**Rapidity**	**RAI**	***TC(t_2)***	***TC(t_3)***	**Rapidity**	**RAI**
25%	64953	64903	125	0.1673	64961	64899	139	0.1542
50%	65751	65065	199	0.8345	65858	65067	112	0.4686
75%	80695	65429	1033	10.2177	81362	65424	295	3.0713

Table 7.1 quantitatively depicts the rapidity of recovery time and RAI of the network suffering from different levels of disruptions. After the disruption, it takes 125 (25%), 199 (50%) and 1033 (75%) days to reach a new equilibrium. The corresponding RAI are 0.1673, 0.8345 and 10.2177, respectively. Based on the observations from **Table 7.1**, it seems that the system is less robust and resilient to severe disruptions than to minor and moderate disruptions, since the rapidity and RAI are the smallest among all three levels of disruption. In the scenarios in which the system allows all drivers to learn from others, the rapidity of the system suffering from the minor disruption is similar to the case where *Pr=0*, and the rapidity under the moderate and severe disruptions is smaller than the corresponding cases where *Pr=0*. In particular, the rapidity under 75% local capacity loss (295) is much smaller compared to the corresponding case where *Pr=0* (1033). RAIs with *Pr*=0.0025 are overall smaller than the cases with *Pr*=0, despite the fact that RAI under minor disruption is a bit larger than the corresponding case with *Pr*=0. This shows that the role of information percolation becomes more significant as the level of the disruption increases. Furthermore, the RAIs with *Pr*=0.0025 under 50% and 75% disruptions are 0.47 and 3.1, respectively, which are both much smaller than the cases with *Pr*=0.

To summarize, information percolation improves the resilience and robustness of the network, especially under moderate and severe local disruptions.

7.2.2.2 VMS control

VMS is widely used to provide information related to incidents and disruptions to drivers in order to change their route decisions. The brief discussions regarding how route costs, route flow and total cost of the network evolve under VMS with different compliance rates (*CR*) are presented in **Section 7.1.1**, and a quantitative evaluation and analysis of robustness and resilience under the VMS control is conducted here based on the method introduced in **Section 7.1.4**. The results are shown in **Table 7.2.**

Table 7.2 KPI of robustness and resilience for the small network under the VMS control

		Pr=0				***Pr=0.0025***			
CR	**Capacity reduction**	***TC(t_2)***	***TC(t_3)***	**Rapidity**	**RAI**	***TC(t_2)***	***TC(t_3)***	**Rapidity**	**RAI**
0.05	25%	64929	64900	79	0.1042	64935	64898	30	0.0383
	50%	65545	65064	108	0.4715	65858	65067	123	0.4964
	75%	76620	65428	723	7.2890	77117	65423	347	3.4748
0.1	25%	64926	64904	85	0.1072	64960	64909	13	0.0166
	50%	65421	65068	175	0.7218	65381	65063	169	0.6435
	75%	74230	65425	786	7.7789	74232	65424	264	2.6591
0.2	25%	65004	64897	16	0.0229	65036	64897	63	0.0738
	50%	65251	65068	294	1.1420	65267	65070	43	0.1846
	75%	70263	65426	666	6.6098	69905	65423	300	2.9135

As can be seen from **Table 7.2**, if VMS alone is employed after the disruptions, in most cases, the network takes longer to recover to reach a new equilibrium compared to corresponding cases with

Pr=0.0025, except for the two scenarios where *CR* is 0.05 and capacity reduction is 50%, and where *CR* is 0.2 and capacity reduction 25%. Similarly, all the RAIs of the network with information percolation are smaller than those without information percolation, except for these two cases. This demonstrates that, in most cases, the extra information obtained from information percolation does facilitate the network to recover more quickly and leads to smaller running costs during the recovery.

For *Pr*=0.0025, in most cases, as the level of the disruption increases the rapidity and RAI also increase, which means the resilience and robustness of the network deteriorate as the disturbances become severe. There is only one exception to this; when *CR* is 0.2 and capacity reduction is 50%, the rapidity is smaller than that with a 25% capacity degradation but the robustness of the network in this case is still worse.

As compliance rate (CR) increases from 0.05 to 0.2, rapidity and RAI under *Pr*=0 and *Pr*=0.0025 are not necessarily improved or worsened corresponding to the level disruption. Under *Pr*=0, for moderate disruptions, resilience and robustness both become worse, but when *CR* takes values from 0.05 to 0.1 they first become worse but are then improved. The larger *CR* does not necessarily always play a positive role in improving recovery time and running costs since the combination of VMS with higher *CR* may lead drivers to overestimate or underestimate the real impacts of the disruption. The magnitude of the *CR*, therefore, must be related to many factors such as the degree of disturbances, the quality of extra information and the socio-economic background of the drivers and so on, and this means that efforts to make drivers follow the VMS must be balanced carefully. This may be an interesting optimization problem for future research.

7.2.2.3 Signal control

Relevant quantitative results are illustrated in **Section 7.2.1**, and based on the quantitative methods introduced in **Section 7.1.4** the rapidity and RAI are calculated and shown in **Table 7.3**.

Table 7.3 KPI of robustness and resilience for the small network under signal control

		Pr=0				Pr=0.0025			
Signal policy	**Capacity reduction**	***TC(t_2)***	***TC(t_3)***	**Rapidity**	**RAI**	***TC(t_2)***	***TC(t_3)***	**Rapidity**	**RAI**
Equi-saturation	25%	64803	67795	47	0.0511	67748	67739	148	0.1746
	50%	67920	67909	80	0.2122	67919	67868	48	0.1669
	75%	68289	67894	516	4.1915	68466	67779	304	2.0439
P0	25%	67983	67743	46	-0.0688	67900	67743	69	-0.1607
	50%	69060	67720	75	-0.0498	68793	67773	35	-0.0397
	75%	73632	67803	97	0.0986	72766	67841	93	0.0346

As can be seen from **Table 7.3**, as the level of disruptions increases, the rapidity and RAI of the cases purely using equi-saturation signal control become steadily worse. In contrast, the rapidity and RAI of the networks with a combination of information percolation and signal control do not follow this trend, and for the minor disruption, it has worse rapidity and RAI. Overall, however, the pure equi-saturation signal control is less effective in improving the rapidity of recovery time and the running cost during the disruption compared to the cases with a combination of an equi-saturation policy and information percolation, in particular for the network suffering from moderate and severe disruptions. For *Pr*=0.0025, however, the extra information in this context may not play a positive role in cases of minor disturbance, possibly since the extra information leads to drivers overestimating the effects of the minor disruption.

The P0 signal control policy performs in a similar way to the equi-saturation policy. When a P0 policy is utilized in isolation, the recovery time becomes steadily worse as the disruption level increases, while a combination of a P0 policy and information percolation overestimates the impacts of mild disruption, with worse rapidity compared to the pure P0 policy, in a similar pattern to that seen

above with the equi-saturation policy. The quantitative results for the P0 policy confirm the initial conclusion made in **Section 7.2.1.3**, however, that is, the P0 policy not only better facilitates convergence compared to the equi-saturation policy, but also improves the network-wide total cost of the network compared to before the disruption when suffering from mild and moderate disturbances due to that corresponding RAIs are negative.

To summarize, for the equi-saturation policy, information percolation combined with signal control overestimates the effects of minor disruption and leads to worse resilience and robustness. The P0 policy, meanwhile, has an apparent advantage in improving the resilience and robustness of the network suffering from all levels of disruptions, and even facilitates the robustness of the network better than before the disruption due to that it forces drivers to overcome bounded rationality.

7.3 Robustness and resilience analysis based on Continuous flow day-to-day dynamic model

7.3.1 Continuous flow based day-to-day dynamic model

In order to further investigate the evolution of the robustness and resilience of urban road networks, and to provide a different modelling perspective, a continuous flow DTD model is considered as a means of capturing the daily variations of network-related quantities. Due to the continuous (non-separable) nature of the flow, information percolation is not considered in this model and the focus is instead placed on signal control strategies as a means to mitigate congestion after disruption. As test networks, both the small network and the Sioux Falls network are considered.

Assuming that the flow is a continuous variable, a proportion of drivers will switch from routes with higher perceived costs to routes with lower perceived costs until drivers cannot reduce their travel costs by unilaterally changing routes, and the network thus reaches user equilibrium (UE). It is worth noting that deterministic UE is based on the assumption that all drivers have perfect information of the network; here, however, this assumption is relaxed so the state the system can reach in this

model is stochastic UE (SUE). For SUE, drivers choose paths to minimize the perceived cost instead of actual cost.

The formulation of the DTD model with continuous flow is presented in **Section 2.3**.

7.3.2 Numerical example

Two networks, the small network shown in **Fig.6.3** and the Sioux Falls network are considered in this section. In addition to the equi-saturation and P0 signal polices, a fixed-time signal control, which assigns green/red time splits equally for all the approaches, is also used as a benchmark. Here, and as before, the traffic is at equilibrium when the disruption occurs, and the evolution of traffic after the disruption is the subject of our analysis before the network reaches a new equilibrium. The expression (6.15) is used here to examine when the network reaches equilibrium; that is, if the path flow vector satisfies function (6.15) for *N* consecutive days, then the network is seen to be at equilibrium. Different levels of disruptions are also considered, namely, 25%, 50% and 75% capacity reductions are imposed at relevant links.

For both networks, the signal control strategies are used during the whole process, including before and after disruptions.

7.3.2.1 Small network

For the small network, it is assumed that link 9 is subject to 25%, 50% and 75% capacity reduction, and that signal control are present at the same junctions as shown in **Fig.7.10**. Network evolution corresponding to the fixed-time signal control, P0 signal control and equi-saturation control are computed, and the resulting route costs, route flows and network-wide total costs are presented in **Fig.7.15**, **Fig.7.16** and **Fig.7.17**, respectively.

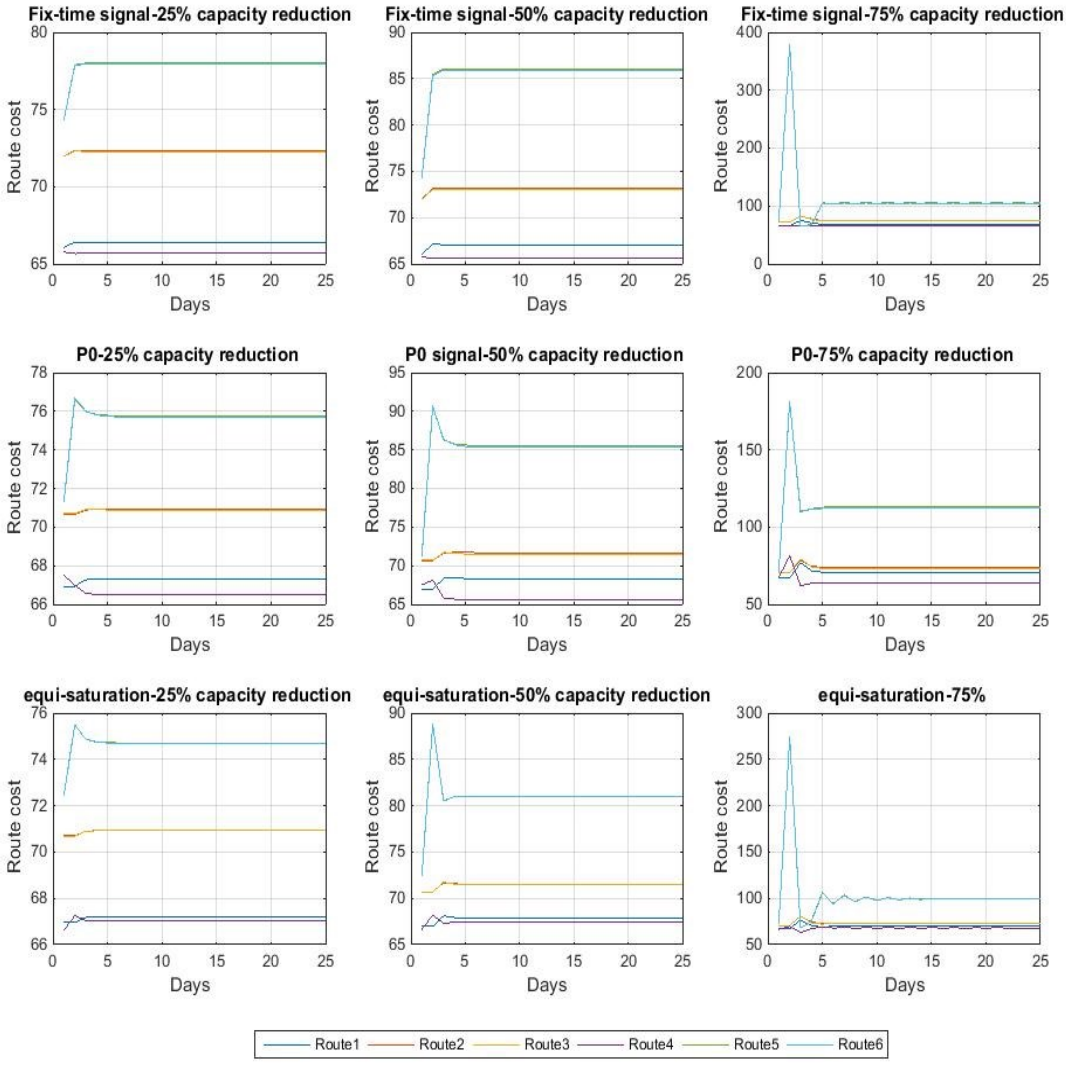

Fig.7.15 Evolution of route costs under fixed-time P0 and equi-saturation control policies when the network experiences different levels of disruption

As can be seen from **Fig.7.15**, the route costs evolve under the different control policies. For minor and moderate disruptions, the route costs under fixed-time signal control are broadly similar after the disruption to those under P0 and equi-saturation policies. For example, for all three signal polices, the cost of route 1 abruptly climbs due to the capacity reduction on link 9, which makes many drivers move to other routes, and the signal control tends to adjust drivers to move to routes with lower cost. For severe disruption, however, there are more significant fluctuations when disturbance occurs. The P0 policy control the route costs better than the other two polices, and it suppresses the cost of route 1 to be less than 200 under severe disruption; the equi-saturation

policy is the next best performing policy, while the fixed-time signal policy is the worst performing in this scenario.

In addition, the route costs at equilibrium vary for different signal control policies. The explanation for this is that the route choices of drivers are influenced by different signal policies in different ways. Moreover, under different levels of disruption, the route costs at equilibrium also vary, which suggests that the magnitude of the disruption affects the route choices of drivers.

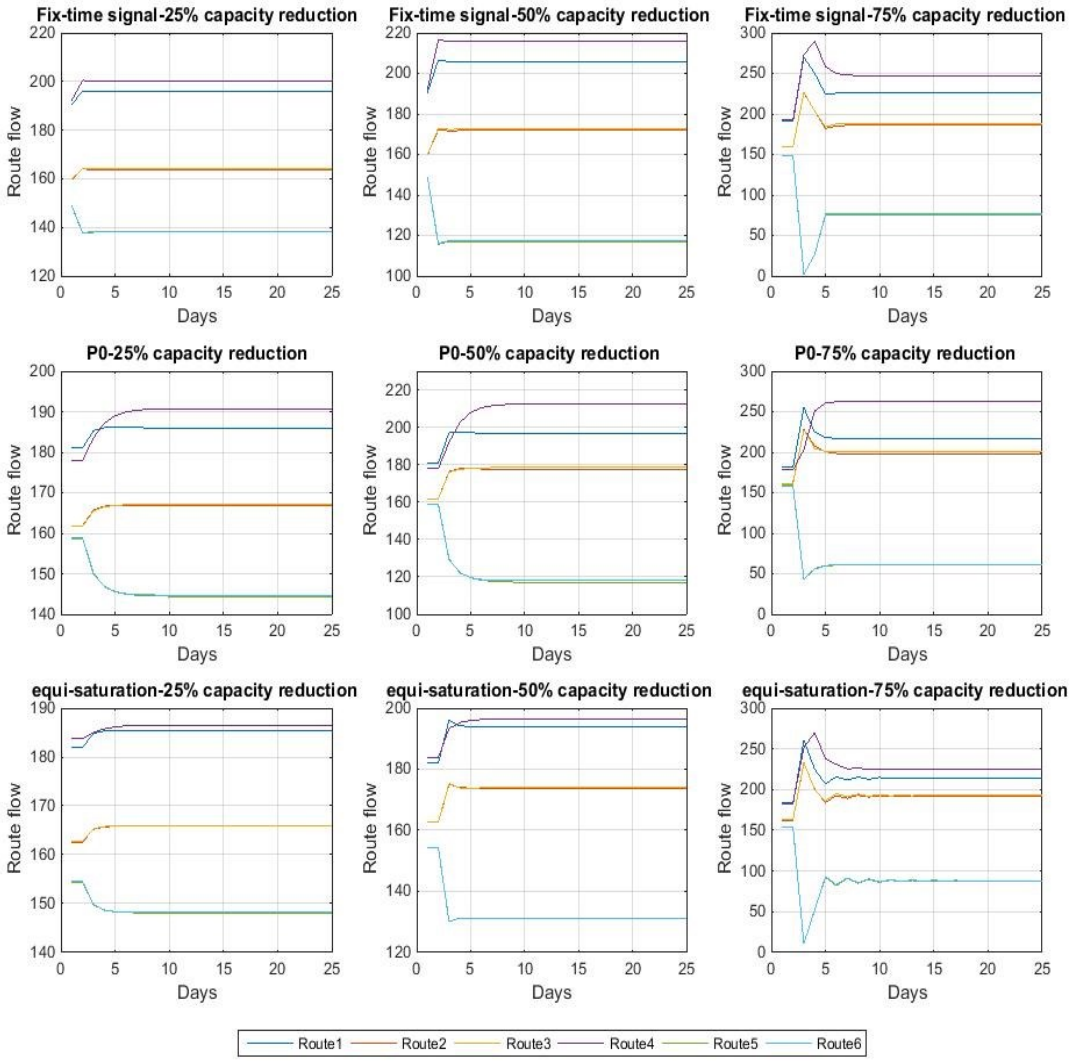

Fig.7.16 Evolution of route flow under fixed-time, P0 and equi-saturation control policies when the network experiences different levels of disruption

Fig.7.16 demonstrates how route flow evolves over time given different signal control. For these three levels of disruption, the flow on route 5 and 6 decreases, while that on route 4 increases greatly. As can be seen from the third column of **Fig.7.16**, the severe disruption causes drivers to over-react, as reflected in the flow on all routes. For example, route 5 and route 6 decrease abruptly to near 0 after the disruption, thereafter, the flow increases to a stable state given the influence of the adjustment of signal control.

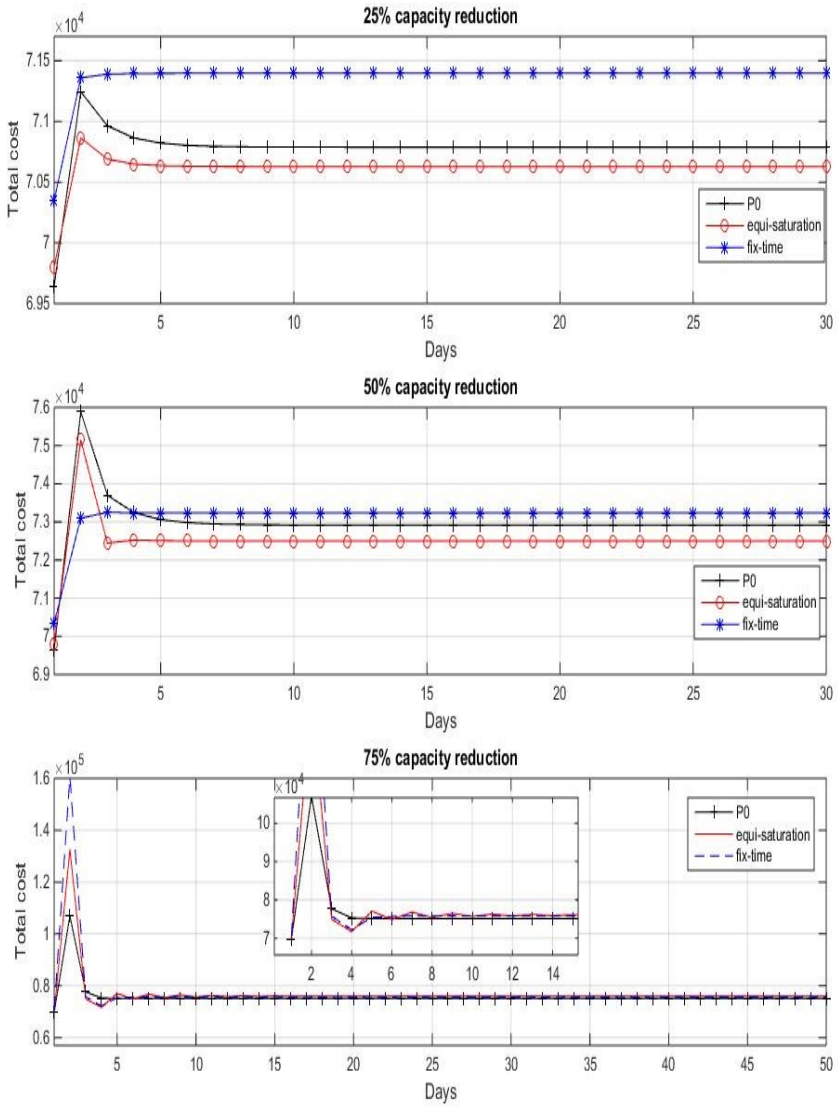

Fig.7.17 Evolution of total cost under fixed-time, P0 and equi-saturation control policies when the network experiences different levels of disruption

Fig.7.17 depicts the evolution of network-wide total cost over time. When the disruption initially occurs, the total cost abruptly goes up from the previous SUE state. With the exception of the case for 50% capacity reduction, the P0 signal and equi-saturation signal policies lead to lower peak cost on the day the disruption occurs, which suggests that these two policies may mitigate the congestion caused by the disturbance in most cases. In addition, except for the moderate disruption, the P0 and equi-saturation signal control perform better overall than the fixed-time signal control. The quantitative analysis of this is presented in following section.

Robustness and resilience analysis of the small network with signal control

Here, rigorous quantitative analysis of robustness and resilience is conducted by assessing relevant key performance indicators (KPIs) related to these two notions. According to the methods presented in **Section 7.1.4**, rapidity and RAI are calculated, and **Fig.7.18** shows the outcomes corresponding to different levels of capacity reduction.

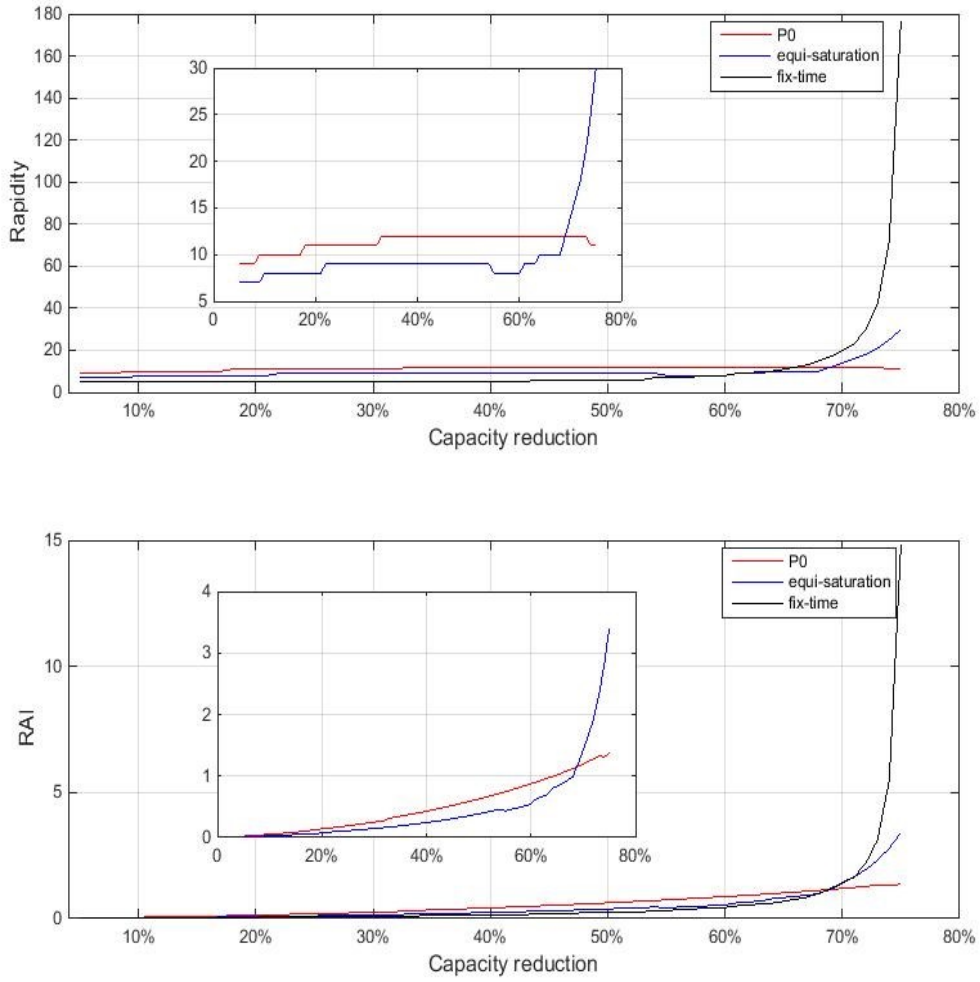

Fig.7.18 Evolution of rapidity and RAI as capacity reduction increases

Fig.7.18 demonstrates how the rapidity and RAI evolve as the capacity reduction ranges from 5% to 75%. It is apparent that when the network suffers from a 75% capacity reduction the fixed-time signal control lead to relatively worse resilience and robustness since the rapidity and RAI are 177 and 14.87 respectively, which is much worse than the results for the P0 and equi-saturation signal control scenarios. On the other hand, the fixed-time signal control seems to exhibit better resilience and robustness when the network suffers from moderate and minor disruptions, as can be confirmed from **Table 7.4**. In addition, when the capacity reduction is above 68%, the network with a P0 policy is most robust and resilient. The sub-graphs inside **Fig.7.18** show that the equi-saturation policy leads to better robustness and resilience compared to the P0 policy when the network

experiences moderate and minor disruptions, but causes worse resilience and robustness when the network is subject to severe disturbance. The P0 and equi-saturation signal control policies therefore each work well in improving resilience and robustness under severe disruptions, while the fixed-time signal control may lead to better resilience and robustness for minor and moderate disruptions. The reason for this may be that the less complex control mechanisms like fixed-time signal control are better able to handle less complicated situations, although the stability of P0 and equi-saturation signal control in handling all levels of disruptions is an advantage in managing urban road networks, which encounter many unpredictable disturbances all the time. Particularly, the P0 policy seems to have the best stability in handling the widest range of disruptions.

All the rapidity and RAI values for the network experiencing capacity reductions ranging from 5% to 75% are shown in **Table C.3**, while **Table 7.4** just presents the rapidity and RAI under 25%, 50% and 75% disruption so as to facilitate the explanation of **Fig.7.18**.

Table 7.4 Rapidity and RAI for the small network suffering 25%, 50% and 75% capacity reduction

	Fix-time		P0		Equi-saturation	
Capacity reduction	**Rapidity**	**RAI**	**Rapidity**	**RAI**	**Rapidity**	**RAI**
25%	5	0.0737	11	0.1922	9	0.1111
50%	6	0.2444	12	0.6267	9	0.3851
75%	177	14.8662	11	1.3670	30	3.4126

In order to rank the importance of all links of the network based on RAI and rapidity, calculations of RAI and rapidity are conducted while reducing a certain amount of capacity in each link one-by-one. The results with 50% capacity reduction applied to each and every one of the links are presented in **Table 7.5.**

Table 7.5 Rapidity and RAI under 50% capacity degradation when links are degraded one-by-one

	Rapidity			RAI		
Link No.	**Fix-time**	**P0**	**Equi-saturation**	**Fix-time**	**P0**	**Equi-saturation**
1	10	9	9	1.2096	1.0667	1.0593
2	11	9	9	1.6601	1.0414	1.0647
3	9	8	8	0.0403	0.0136	0.0140
4	9	12	10	0.3328	0.5803	0.4113
5	10	12	8	0.1200	0.3139	0.1215
6	9	12	10	0.3361	0.5889	0.4101
7	10	8	8	0.0154	0.0123	0.0144
8	8	12	9	0.3541	0.5879	0.3141
9	10	12	9	0.5011	0.6267	0.3851
10	12	11	11	1.7311	1.4090	1.4718
11	10	12	8	0.1650	0.2645	0.1662
12	11	10	10	1.2262	1.1727	1.1509

Table 7.5 presents the rapidity and RAI when a 50% capacity degradation is imposed on each link one-by-one. The disruption on different links under different signal control leads to distinct robustness and resilience outcomes for the network. In this table, a link with higher rapidity and RAI is more important in terms of the resilience and robustness of the network. Based on this rationale, the ranking of links is shown in **Table 7.6**.

Table 7.6 Ranking of link importance based on rapidity and RAI under 50% capacity degradation

	Rapidity			RAI		
Ranking	**Fix-time**	**P0**	**Equi-saturation**	**Fix-time**	**P0**	**Equi-saturation**
1	10	4	10	10	10	10
2	2	5	4	2	12	12
3	12	6	6	12	1	2
4	1	8	12	1	2	1
5	5	9	1	9	9	4
6	7	11	2	8	6	6
7	9	10	8	6	8	9
8	11	12	9	4	4	8
9	3	1	3	11	5	11
10	4	2	5	5	11	5
11	6	3	7	3	3	7
12	8	7	11	7	7	3

As can be seen from **Table 7.6**, the second, third and fourth columns rank different links in descending order of their importance in terms of rapidity and according to the signal policy applied. Link 10, link 2, link 12 and link 1 are most important links when the network has a fixed-time signal control policy, since these four links are more frequently used by routes. When a P0 control policy is applied, however, link 4, link 5, link 6 and link 8 are most important since these links are located at the junctions at which signals are installed. For the equi-saturation signal control paradigm, link 10, link 4, link 6 and link 12 have the greatest impact on the convergence of the network given a 50% capacity reduction.

The last three columns of the **Table 7.6** rank the links in descending order of their importance in terms of RAI. The result shows that link 10, link 2, link 12 and link 1 are consistently the most important under the three signal control policies. There are differences in the specific link rankings, however; for example, link 12 is the third most important under fixed-time signal control while it is the second most important under P0 and equi-saturation signal policies. The importance of links in terms of RAI is related to the frequency with which a given link is passed by routes.

7.3.2.2 Sioux Falls network

The Sioux Falls network is presented in **Fig.6.17,** and includes 552 OD pairs (detailed OD information is presented in **Table C.2**). According to the analysis from **Section 5.2.1**, node 10 is the most important in terms of degree centrality (*D*), weighted closeness centrality (*WC*), total cost based on user equilibrium (RTC_{UE}^{i}) and system optimal (RTC_{SO}^{i}). Building on this insight, it is assumed that links connecting with node 10 will experience different levels of disruption given a capacity reduction. These links are: 25, 26, 27, 28, 29, 30, 32, 43, 48 and 51. In the Sioux Falls network, all the nodes, with the exception of node 1, node 2, node 7 and node 13, are equipped with signal control to resolve conflicts between different traffic streams.

This Sioux Falls network has 552 OD pairs, and within each OD pair a number of routes are generated *a priori*. In order to illustrate the system's performance, just one O-D pair (10,20) is selected here, the travel demand of which is 2500, in order to explore the corresponding evolution of its route flows and route costs. The results for OD (10,20) are shown in **Fig.7.19** and **Fig.7.20.**

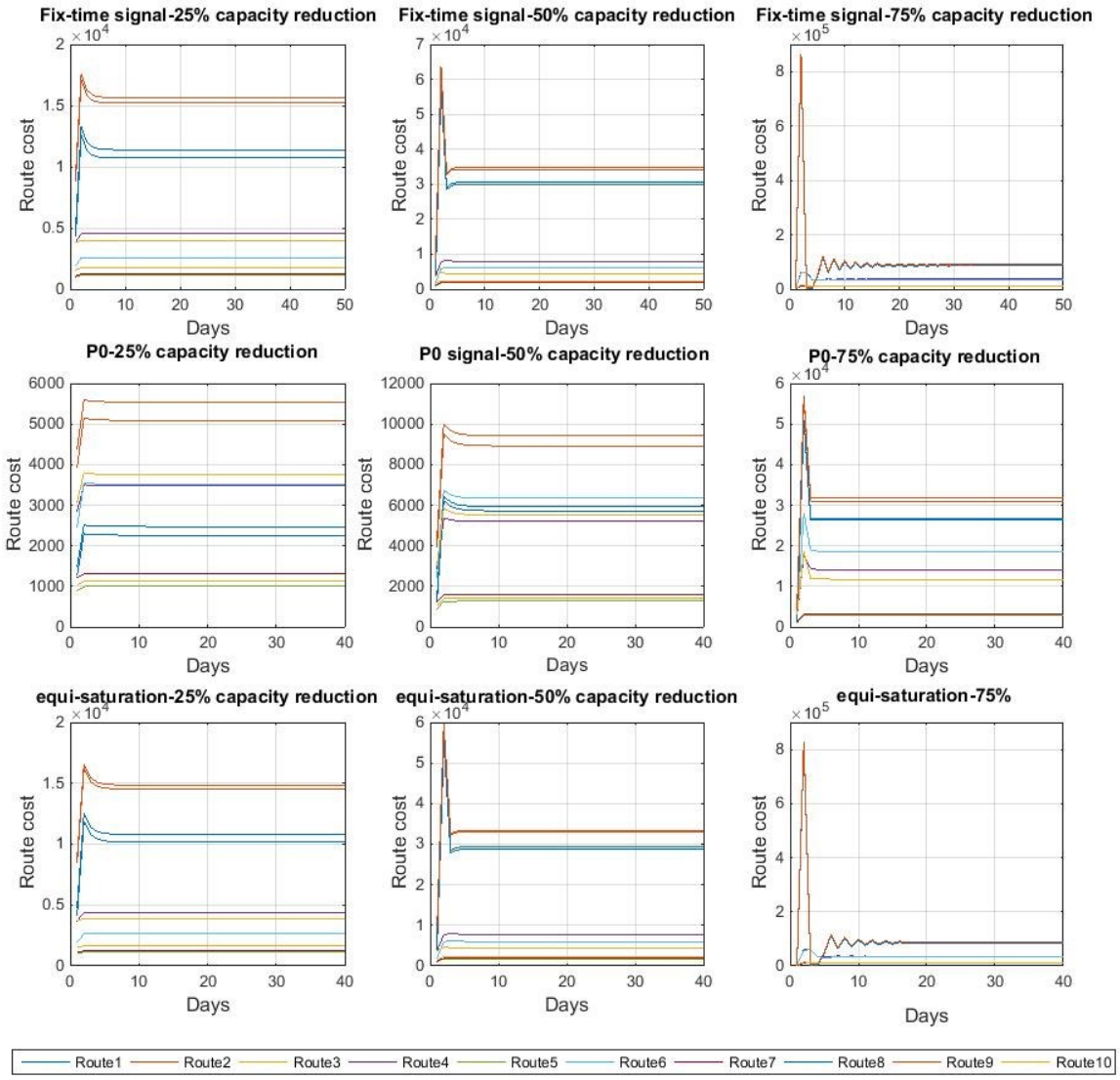

Fig.7.19 Evolution of route costs for the Sioux Falls network under fixed-time, P0 and equi-saturation signal control policies when the network experiences different levels of disruption

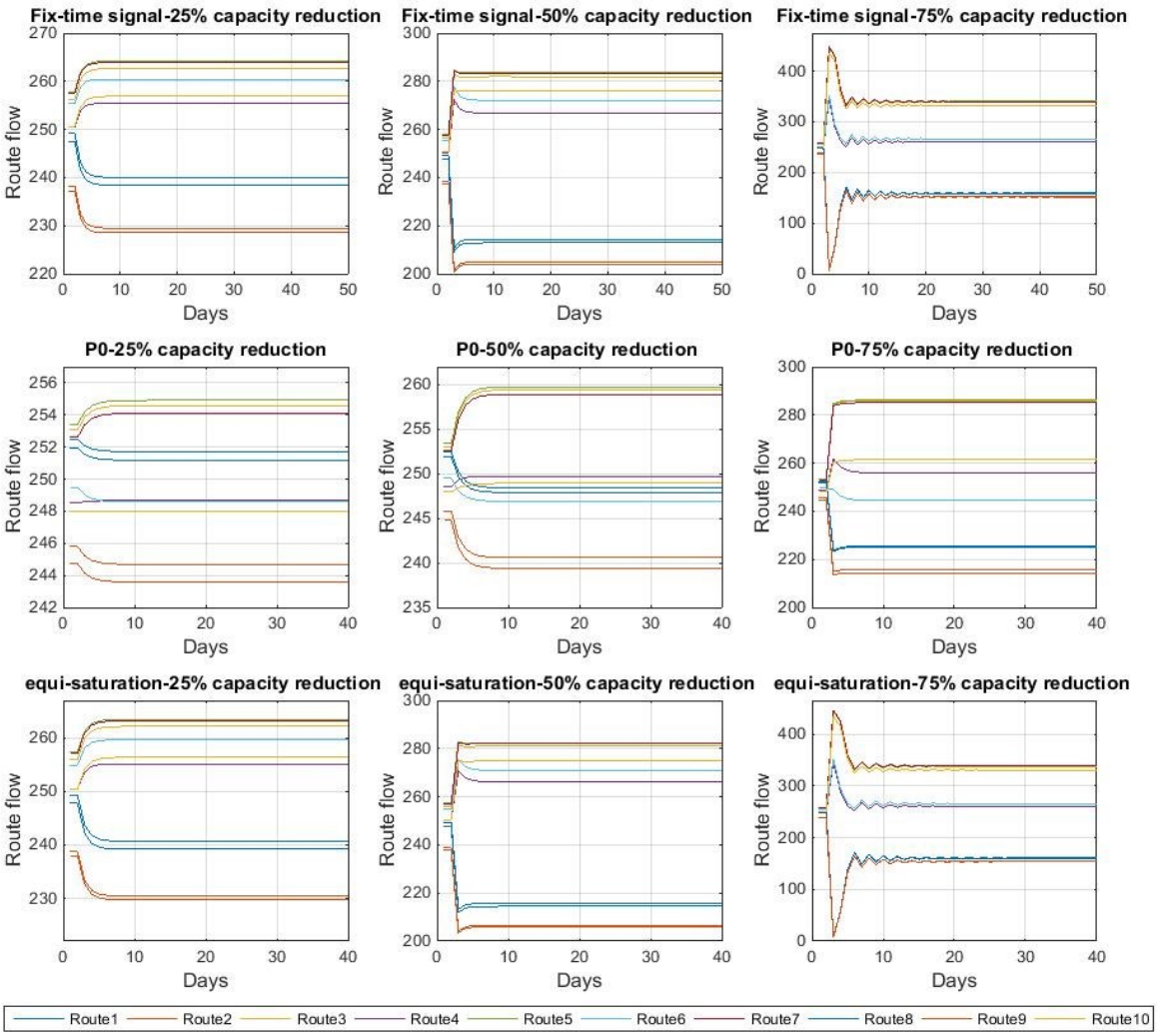

Fig.7.20 Evolution of route flow for the Sioux Falls network under fixed-time, P0 and equi-saturation signal control policies when the network experiences different levels of disruption

Fig.7.19 and **Fig.7.20** show how route costs and route flow evolve over time under different signal control policies. All levels of disruption can be seen to lead to an abrupt increase in route costs and a significant fluctuation of route flows for this OD pair; with more serious disruption leading to more severe fluctuations in the network flows. It seems that route costs under the P0 signal control policy performs very well: the peak in the route costs caused by the disruptions tends to be much lower than with the other two signal control scenarios, and the convergence is also quicker, especially when the disruption is severe. The situation regarding route flow is quantitatively similar. Furthermore, the P0 signal control policy also maintains good stability in the system against all levels of the disruption. This observation is consistent with those from the study on the small network.

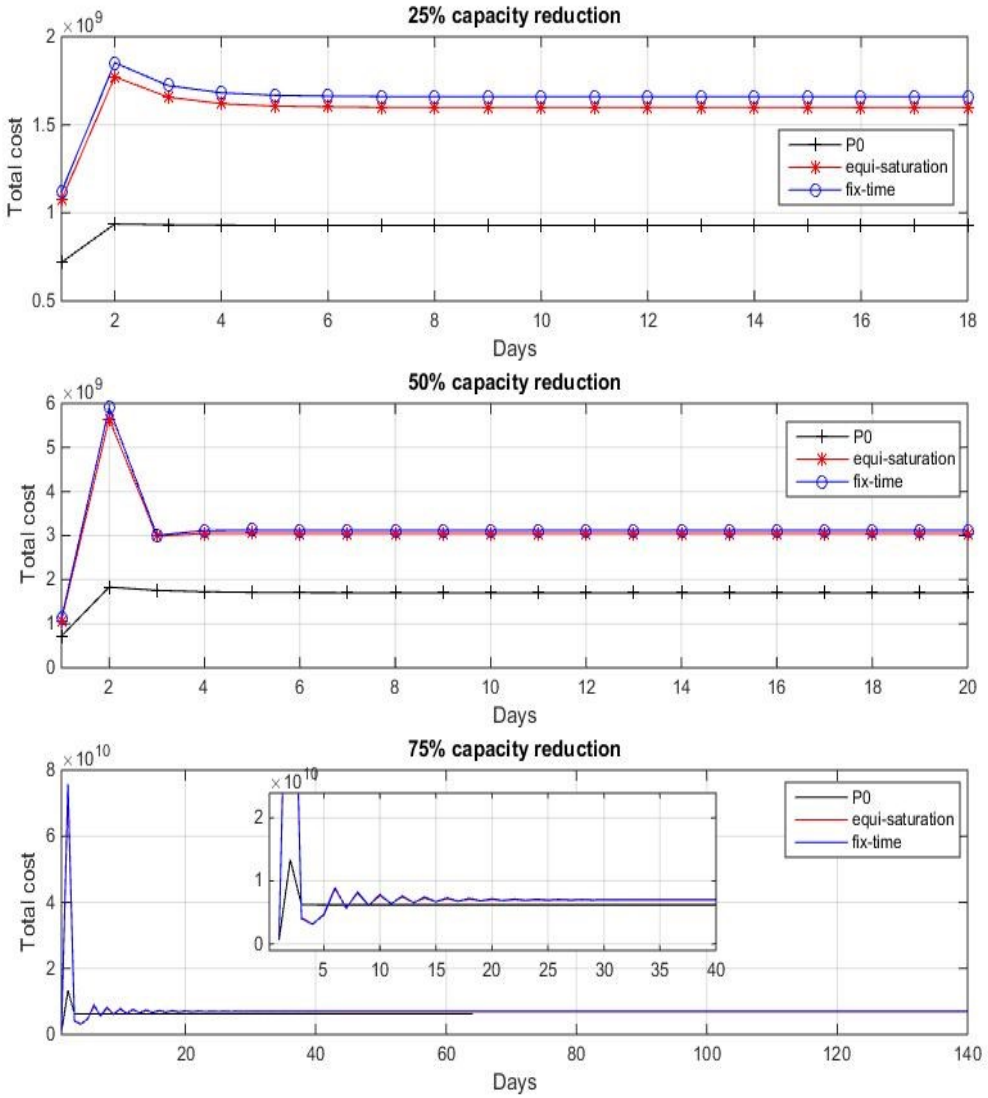

Fig.7.21 Evolution of total cost in the Sioux Falls network under fixed-time, P0 and equi-saturation signal control when the network experiences different levels of disruption

Fig.7.21 shows the network-wide total cost when the network experiences different levels of disruption under fixed-time, equi-saturation and P0 signal control policies. Unlike the case for the small network presented earlier, in the Sioux Falls network the P0 control policy has a considerable advantage over the other two policies for all levels of disruption, in that the total network cost is maintained at a very low level. In addition, the P0 policy also facilitates faster convergence than the others. As can also be seen from **Fig.7.21**, the performances of the equi-saturation and fixed-time policies are very similar.

Robustness and resilience analysis of Sioux Falls network

A further quantitative assessment is conducted regarding the resilience and robustness of the Sioux Falls network under different signal control. According to the methods presented in **Section 7.1.4,** the rapidity and RAI of the network suffering from different levels of disruption are calculated, and **Fig.7.22** shows the rapidity and RAI corresponding to different capacity reductions.

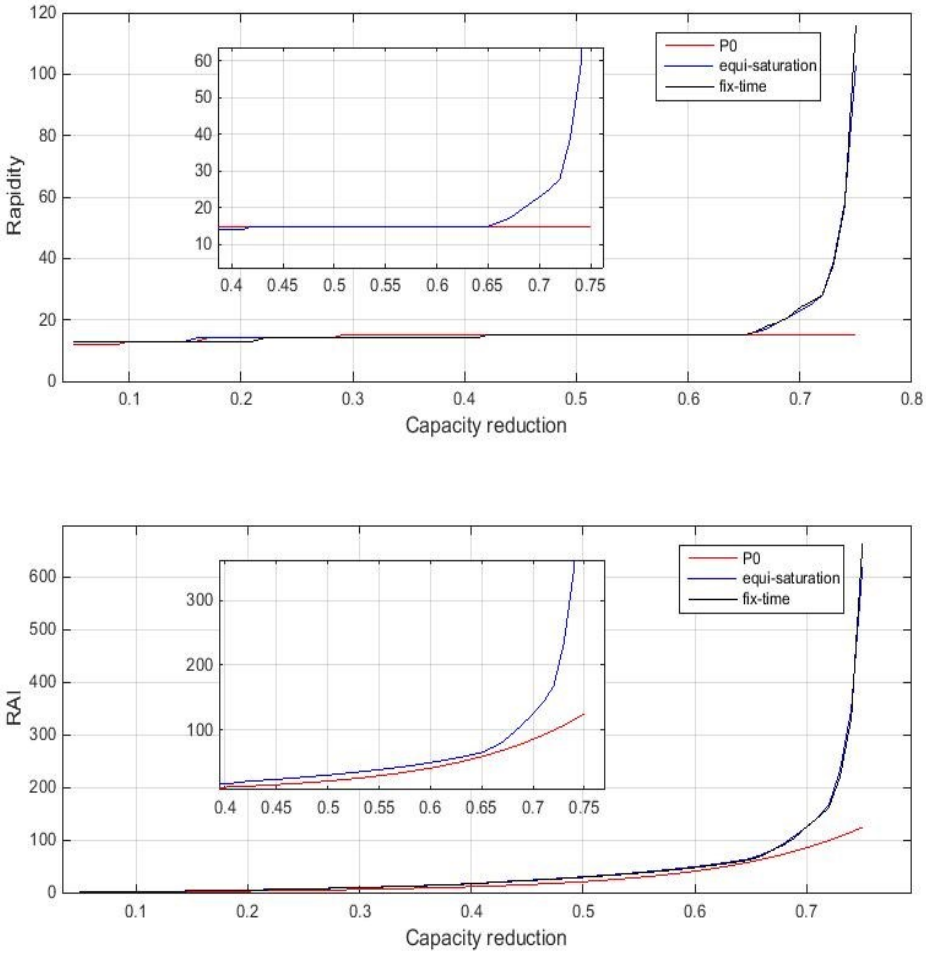

Fig.7.22 Evolution of rapidity and RAI as capacity reduction increases

The comprehensive assessment presented in **Fig.7.22** supports the observation made in the previous section; that is, P0 signal control lead to better resilience and robustness when the network experiences different levels of disruption. In particular, when the network suffers from severe disruption, the P0 signal control shows a considerable advantage in keeping the network robust and

resilient compared to fixed-time and equi-saturation control. The sub-graphs in **Fig.7.22** show that rapidity and RAI with the P0 policy are also better than those with equi-saturation signal control under moderate and minor disruptions, albeit rapidity with P0 policy is a bit higher than equi-saturation policy when capacity reduction is approximate 40%. In addition, the P0 policy also shows good stability to all levels of disruption in terms of improving the robustness and resilience of the network.

All the rapidity and RAI values of the Sioux Falls network with capacity reductions ranging from 5% to 75% are shown in **Table C.4**. Here, in **Table 7.7,** due to space limitations, just the rapidity and RAI associated with 25%, 50% and 75% capacity disruption are presented.

Table 7.7 Rapidity and RAI for the Sioux Falls network suffering from 25%, 50% and 75% capacity reduction

	Fix-time		P0		Equi-saturation	
Capacity reduction	**Rapidity**	**RAI**	**Rapidity**	**RAI**	**Rapidity**	**RAI**
25%	14	7.0264	14	4.1036	14	7.1080
50%	15	29.2143	15	20.7971	15	30.0215
75%	116	665.2010	15	124.3413	103	618.8533

In order to investigate the relative importance of the 76 links in the Sioux Falls network based on RAI and rapidity, their values are computed based on a 50% capacity reduction. The results are presented in**Table C.5**.

Table C.6 illustrates the ranking of 76 links for the Sioux Falls network based on rapidity and RAI under moderate disruption. As can be seen from **Table C.6**, for rapidity, the ranking of links based on fixed-time signal control is very similar to that based on an equi-saturation policy, with a Spearman ranking correlation coefficient of 0.97. For RAI, the ranking based on P0 signal control, meanwhile, has a very high-ranking correlation with that based on fixed-time and equi-saturation signal control policies, with a ranking correlation coefficient of 0.95 and 0.96, respectively. It is worth nothing that

the ranking for rapidity based on the P0 policy is very similar to that for RAI based on the P0 policy, with a ranking correlation coefficient of 0.98.

7.4 Summary

This chapter has investigated how networks perform under different control mechanisms such as information percolation, VMS and signal control, when certain links of those networks are subject to different levels of disruption. Rapidity and RAI have been used as two primary KPIs to measure the resilience and robustness of the subject networks quantitatively. The proposed agent-based day-to-day (ABDTD) model and continuous flow day-to-day (CFDTD) model were integrated with the control mechanisms to observe how such control improve or impede the resilience and robustness of the networks.

In particular, when applied to ABDTD model of the small network, information percolation, VMS and signal control demonstrate the following:

1. Information percolation tends to improve the resilience and robustness of the network, especially with moderate to severe local disruptions;
2. For VMS, a larger compliance rate (*CR*) does not necessarily play a positive role in improving the resilience and robustness of the network because a high *CR* in respect to route guidance may cause traffic to overreact to network situations, impeding convergence of the network. The actual values of *CR*, however, are often related to numerous factors such as the nature and degree of disturbances, the quality of real-time information and the socio-economic characteristics of the drivers and so on. It is critical to come up with an accurate estimation of the *CR* in order to understand the impact of VMS on the network performance. In addition, the combination of VMS and information percolation also shows that information percolation does act to strengthen the positive role of VMS in most cases, although occasionally information percolation can offset the positive impacts of VMS to worsen the resilience and robustness, such as when *CR*=0.2 and capacity reduction is 25%.

3. The combination of information percolation and signal control leads to worse resilience and robustness when the network suffers from minor disruption (as shown in **Section 7.2.2.3**). Compared to the equi-saturation policy, however, the P0 policy has a considerable advantage in improving the resilience and robustness of the network for all levels of disruptions, and P0 may even render a post-disruption network with a lower system-wide cost than before the disruption for mild and moderate disruptions.

This chapter has also considered continuous-flow models to add more insights to the analysis. Three types of signal control were incorporated in the CFDTD model, and the results show that, compared to fixed-time and equi-saturation signal control, the P0 policy plays a more effective role in improving the robustness and resilience of the Sioux Falls network. In addition, the P0 policy also yields good rapidity and stability against all levels of disruptions in the small network and the Sioux Falls network.

Chapter 8 CONCLUSIONS AND FUTURE WORK

This thesis has conducted a systematic investigation into the quantitative assessment of the resilience and robustness of urban road networks (URNs). The scope of this research encompasses the topological characteristics of networks, including connectivity and proximity. A hallmark of the original research presented here is the consideration of the complex network flow dynamics and behavioural rules that arise in a realistic urban traffic network, and their collective effect on the network's performance in reaction to internal or external disturbances. The notions of resilience and robustness are reviewed and rigorously defined, followed by interpretation from the perspectives of network science and traffic network modelling.

This chapter summarizes the results obtained from the previous chapters, identifies the contributions made in this thesis, and provides a few concluding remarks regarding on-going research and future research directions.

8.1 Summary of results

This thesis has investigated the robustness and resilience of urban road networks (URNs) based on their topological characteristics and operational aspects. The latter refer to the modelling of URNs taking into account the flow characteristics, travel demand distribution, network supply

characteristics, user behaviour, and network control mechanisms. The analyses based on topological characteristics explore robustness and resilience from a static and aggregate perspective by ignoring flows and drivers' behaviour, while the study on the operational aspect of URNs focuses on the network's functionality to carry flows and increase accessibility to different locations. The conclusions obtained from this thesis can be divided into several parts and are listed below.

8.1.1 Topological characteristics of the nine URNs

Complex network theory is widely applied to the analysis of the topological characteristics of networked systems. The topological characteristics of the URNs are explored initially by commonly used topological indices such as degree centrality, clustering coefficient and betweenness centrality. The results show that:

1. The distributions of indegree and outdegree for these URNs follow power law, suggesting that most of the nodes have smaller indegree and outdegree. Although the distribution of the indegree and outdegree of the URNs are very similar and indeed the average indegree and outdegree for all the URNs examined are the same, the URNs are not bi-directional since the Pearson correlation between indegree and outdegree is less than 1.
2. The URNs are less compact in local areas compared to other transport networks because of the low clustering coefficient (*CC*).
3. In addition, it is shown that the size of the URNs is positively correlated with average path length (*APL*) and diameters (*D*). Moreover, among the nine URNs under consideration, Berlin shows the largest *APL* (50.09), which suggests worse efficiency, while Anaheim (11.87) has the best. The efficiency measure is consistent with *APL*.
4. Furthermore, Anaheim and Berlin are shown to have smaller average weighted closeness centrality (*WCC*) than the other URNs, which suggests that the nodes in these two URNs are relatively more difficult to access from other nodes. Most of the *WCC* distributions for these URNs are exponential.

5. The analysis of weighted betweenness centrality (*WBC*) shows that the *WBCs* of the URNs follow the power law distribution, which suggests most of the nodes of the URNs have smaller *WBC*, and the parameter α ($P(BC \geq x) \propto x^{-\alpha}$) for the distributions is between 0.4 and 0.8. According to the average and distribution of *WBC*, Chicago and Philadelphia are most robust while Anaheim and Winnipeg are less robust in terms of the frequency of the shortest paths passing through a given node.

The Pearson correlations of all URNs between indegree, outdegree and *WBC* and *CC* were calculated, and the correlations show that indegree is positively correlated with outdegree. In addition, poor correlation between degree and *WBC* suggests there are no anomalies in these URNs, and *CC* is also not correlated with degree well.

8.1.2 Small-worldness and communities of the nine URNs

Small-worldness is a widely observed feature of many complex networks, such as metabolic networks, airport networks, worldwide maritime transportation networks and public transport networks. Through analyses and comparisons of *APL* and *CC* between the URNs and corresponding random networks, it is shown that these URNs, which consist of roads segments/streets and junctions/intersections, do not show strong evidence of small-worldness. The difference between these URNs and other realistically networked transport networks is that all links are directional and the neighbour nodes of a given junction are less connected with each other.

In order to explore the hierarchical structure of the URNs, detection of communities is attempted. This shows that the larger the URNs are the more communities and hierarchical layers the URNs have. For example, Philadelphia and Berlin have five layers with the number of communities at the lowest layer being 343 and 457 respectively, while Anaheim has just 2 hierarchical layers and 11 communities exist at the lowest layer. In addition, the number of communities at the lowest hierarchy of these URNs is more likely to follow a normal distribution when the size of URNs is larger,

and this finding is compatible with a common phenomenon in natural and social science (Casella and Berger, 2001).

8.1.3 Robustness of the selected URNs suffering from local disruptions

In order to analyse the robustness of URNs suffering from local disruptions, topological indices and more sophisticated operational indices (i.e. those based on User Equilibrium (UE), System Optimal (SO) and price of anarchy (POA)) are systematically presented for the examination of the importance of nodes for selected URNs. The topological approach is comparatively more computationally efficient, while the operational indices takes into account link capacity, travel demand and drivers' behaviour and are calculated through certain iterative algorithms that entail significant computational overheads. These efforts to seek potential relationships between topological and operational indices have brought a huge amount of data valuable for understanding the inherent structural characteristics of the networks.

1. The results for the Sioux Falls network shows that the node (#10) with the largest degree in the network is also the most important as assessed via user equilibrium (RTC_{UE}^{i}) and system optimal (RTC_{SO}^{i}) solutions. Moreover, degree has relatively high correlation with $RPOA^{i}$, RTC_{UE}^{i} and RTC_{SO}^{i} compared to other topological indices.
2. The results for Anaheim show that a certain node (#62), when removed, causes the most deterioration in terms of RTC_{UE}^{i} and RTC_{SO}^{i} while node # 195 has the greatest impact on the price of anarchy. RTC_{UE}^{i} and RTC_{SO}^{i} have poor correlations with topological indices, while the correlation between $RPOA^{i}$ and topological indices is even poorer.
3. The results for the remaining selected URNs show higher correlations between topological and operational indices than Sioux Falls and Anaheim. In addition, weighted betweenness centrality (*WBC*) seems to be relatively highly correlated to the total costs under UE and SO principles when the network experiences local disruptions.

Overall, the Spearman ranking correlations between topological and operational indices are not significant, which is to be expected. Degree and *WBC*, however, stand out as the topological indices with relatively higher correlations with operational indices in some individual cases.

8.1.4 Robustness of the selected URNs suffering from global disruptions

The analyses summarized in **Section 8.1.3** are based on the removal of certain nodes or links in the network, which represent local disruptions. In order to analyse and compare the robustness of URNs with disruptions occurring at larger spatial scales (i.e. global disruption), a new relative area index (RAI) is proposed to conduct comparisons of robustness across different URNs. The results show that MPF and Tiergarten are the most robust networks in terms of RAIs based on UE (RAI-UE) and SO (RAI-SO), and that Anaheim and Sioux Falls are the least robust against global capacity degradation. *WBC* is utilized as the baseline, and the results based on *WBC* show a different ranking from RAI-UE and RAI-SO; the ranking for MPF and Sioux Falls remains in the same place, however. The results also show that the size of URNs has no significant correlation with robustness. These findings regarding robustness can provide valuable insights for the design and management of complex transport systems; they can also be utilized to guide maintenance work and infrastructure management.

8.1.5 Performance of an agent-based day-to-day (ABDTD) dynamic model with information percolation

In a first attempt to incorporate user behaviour and information diffusion into the network dynamics, aiming towards a quantitative description of the network's behaviour when faced with local disruptions, **Chapter 6** developed a novel ABDTD model with information percolation. The goal was to investigate the impact of a communication network on the urban road network by taking into account network demand, drivers' rational/irrational behaviour, supply capacity and travel information dissemination. In a numerical study, the comparisons of network performance associated with different percolation rates show that there is a strong positive correlation between the level of information transparency and the convergence (or the stability) of the network. A

detailed sensitivity analysis was conducted to understand the impact of different modelling parameters on the network performance. A bifurcation phenomenon was observed, along with some negative effects of information dissemination under certain particular circumstances. For example, if too many travel agents have access to the same information pool, the network may experience oscillation that hinders swift convergence.

8.1.6 Robustness and resilience based on the ABDTD model with different control mechanisms

In order to observe the impact of various signal control mechanisms on URNs experiencing different levels of local disruption, travel information provision, Variable Message Sign (VMS) and adaptive signal control were incorporated into the ABDTD model. Through the review in **Section 3.1.4**, rapidity was confirmed to be the KPI of resilience, and RAI was used to quantify the robustness. A numerical example was employed to show the robustness and resilience of the network under different control mechanisms.

Through the analyses and comparisons of results with different information percolation rates (0.0025 and 0), it is shown that rapidity and RAI are both improved when drivers have access to more information. In particular, for moderate (50%) and severe (75%) capacity degradation, the improvement is much more significant. To be more specific, under moderate disruption, the robustness and resilience are improved by approximately 45%, while for severe disruption, they are improved by 69% and 72% approximately.

VMS with different compliance rates (*CR*) are also utilized to improve resilience and robustness, and scenarios in which VMS is combined with information percolation through communication networks are also considered. The results show that such a combination usually facilitates the improvement of robustness and resilience compared to when only VMS is used, although in a few cases, for example, if *CR*=0.2 and capacity reduction is 25%, information percolation actually worsens the resilience and robustness. Overall, however, a larger *CR* does not mean better resilience and robustness since

larger *CRs* tend to cause drivers to overestimate the effects of disruption. This suggests that the use of VMS to combat disruption must be judged carefully and underlying factors such as drivers' socio-economic background and the degree of disruption should be taken into account.

In respect to signal control, P0 and equi-saturation policies are incorporated into the model. The results show that P0 signal control performs better than the equi-saturation policy in terms of improving the robustness and resilience across all levels of disruption, and that it even leads to the robustness of the network being better than before the disruption occurred, which suggests that the P0 policy may lead total travel cost to approach system-oriented optimal. The combination of information percolation and signal control shows that information percolation strengthens the positive effect of signal control during moderate and severe disruptions, but does not improve the robustness and resilience in the case of minor disruptions, compared to just using signal control; probably due to the tendency for information percolation to overestimate the negative impact of disruptions.

8.1.7 Robustness and resilience based on a continuous flow day-to-day (CFDTD) model with signal control

In order to observe the effect of signal control on URNs experiencing different levels of local disruption at the aggregate (i.e. continuous) flow level, P0, equi-saturation and fixed-time signal control were incorporated into a CFDTD model. The small network and Sioux Falls network are used as the numerical examples. The results show that when either of the networks experience severe disruption, the P0 signal policy performs better, in terms of improving robustness and resilience, than the equi-saturation and fixed-time policies, Notwithstanding the above, the fixed-time control policy seems to lead to better robustness and resilience in the small network experiencing moderate and minor disruptions, while the equi-saturation policy leads to better robustness and resilience for the Sioux Falls network when it experiences a capacity degradation of approximately 40%. Compared to the other two signal control policies, however, the P0 policy is highly stable in handling

all levels of disruptions for both networks, and this role is more significant when the network is larger and the disruptions are more severe. In reality, to mitigate significantly the negative effects of disruptions on the robustness and resilience of URNs, the choice of signal policy should take into account many factors such as the magnitude of disruptions and the scale of the URNs.

Moreover, an attempt was made to rank the links in the two networks based on the network rapidity and RAI as individual nodes are removed. The results showed that for the small network, the link ranking based on RAI has a close relationship with whether a given link is frequently passed by routes, and, for the Sioux Falls network, the link ranking based on the P0 policy has high correlations in terms of robustness with that based on fixed-time and equi-saturation signal control. This method may be used to examine the vulnerability of URNs when employing signal control so as to make the networks robust and resilient to all levels of disruptions.

8.2 Contribution of the research

This dissertation makes the following contributions to the literature:

1. Building on existing notions and indicators for the robustness and resilience of transport networks, which are primarily based on their topological features, it proposes a few indicators that take into account the operational characteristics as well as user behaviour in these systems. These include the relative total cost of user equilibrium (RTC_{UE}^{i}), the relative total cost of system optimal ($RPOA^{i}$), the relative price of anarchy ($RPOA^{i}$) and the new relative area index (RAI).
2. Further, the dissertation uses complex network theory to explore Urban Road Networks (URNs) from different countries or regions, and discovers their unique characteristics and quantitative differences from other networks.
3. This work is the first to explore the communities and hierarchical structure of these URNs in order to further uncover the underlying collective characteristics. The results show that the distribution of communities within these URNs tends to follow a normal distribution like

other natural systems in reality. In practice, this finding may provide insightful views on the management and planning of transport networks.

4. This research is the first systematically to investigate the robustness and resilience of URNs using both topological indices (based on complex network theory) and operational indices (based on traffic assignment models), and to analyse the correlations between these different types of indices so as to identify potential connections or gaps.
5. This thesis proposes a new relative area index (RAI) to quantify the robustness of URNs of different sizes when they experience global disruptions, which may provide benchmark measures for the planning and management of URNs.
6. A novel agent-based day-to-day traffic evolution model with information percolation is proposed to explore the impact of travel information sharing on traffic networks, in particular, their stability, robustness and resilience.
7. There have been very few studies that have focused on the impact of active traffic control on network robustness/resilience in the case of local or global degradation. This study attempts this, incorporating different control strategies, including information sharing, VMS and different signal control strategies into traffic assignment models. Both agent-based simulation and analytical assignment models are employed and extensive simulation studies are conducted to assess the network performance under different control. The results provide valuable insights into the design and management of URNs.

8.3 Limitations and future work

This thesis has therefore quantitatively assessed and analysed the robustness and resilience of URNs based on their topological characteristics and traffic assignment models. During the course of the study, the following limitations were identified and future work is proposed accordingly.

8.3.1 Analyses of the relationships between topological characteristics and regional social and economic development

Due to the fact that the data related to URNs are limited, in this thesis, the studied URNs are mainly located in Europe and North America, such as Chicago, Austin, Berlin and Barcelona. In the future, with data sourced from other parts of the world, in particular from less developed countries or regions, it will be possible to expand our comparisons to a wider context. In particular, it is hypothesized that the diversity in social, economic, cultural and geographical characteristics could manifest itself in the formation of URNs, and thus may be reflected in the topological features of these URNs. Future work along these lines may uncover qualitatively different topological or operational features of URNs from a geographically representative set of test networks.

8.3.2 Applications to larger-scale URNs

The studies presented in this thesis are limited by the capabilities of computational architecture and algorithms. In particular, this work relies on extensive computations of user equilibrium and system optimal solutions on large-scale networks, which are time-consuming to conduct with current technology. In the future, the use of high performance computing including parallel/distributed computing and GPU could be considered as means to expedite the computational procedures. More computationally efficient models and algorithms can be considered as well, such as link-based traffic assignment models, as opposed to the path-based models that require path enumeration and that do not scale well when the network size increases. Last, but not least, most of the models and algorithms are implemented in MatLab, and computationally more efficient programming platforms such as C++, Java and Python could be employed as alternatives.

8.3.3 Advanced methods to explore the relationship between network performance indices

This thesis uses traditional methods such as Spearman ranking correlation analysis to explore the relationship between different topological and operational indices, and these do not suggest strong

evidence for the linkages between them. Future studies could consider the use of more advanced statistical/machine learning techniques such as deep learning and artificial neural networks to provide a more profound understanding of the inherent structural connections of different network indices, thereby bridging the gap between complex network theory and traffic network modelling. In particular, it may be possible to incorporate essential network information such as demand distribution and supply constraints into the topological analysis offered here in order to yield efficient indices that reflect network robustness and resilience more effectively.

8.3.4 Dynamic or semi-dynamic modelling of URNs

This research is based on static traffic network models, which means that it does not explicitly incorporate the temporal dimension in network flow propagation. One of the consequences is the lack of accountability for real-time information provision, which plays a critical role in network and congestion management under external stress. One important extension of this work is the dynamic modelling of traffic networks, which takes into account the within-day fluctuation of network conditions such as traffic flow, congestion and control. Dynamic traffic assignment models that incorporate the UE and SO principles could be considered, and dual-timescale models could be proposed to capture both the within-day and day-to-day evolution of traffic dynamics and user behaviour.

8.3.5 Robustness and resilience related to the recover stage

This thesis mainly focus on the network's performance before, during, and after, the disruption without considering the recovery phase of infrastructure or network capacity. In reality, network capacity influenced by certain types of disruptions tends to be restored after a period of time. This causes additional disturbances to the traffic in ways that may not be easily represented due to the presence of potential network paradoxes. Network recovery is therefore another interesting field of inquiry as it encompasses a wide range of topics including network stability, resource allocation, and infrastructure management

REFERENCES

ADERINLEWO, O. & ATTOH-OKINE, N. 2009. Effect of transportation infrastructure network size on its performance during disruptions. *International Journal of Critical Infrastructures,* 5**,** 285-298.

AHUJA, R. K., MEHLHORN, K., ORLIN, J. & TARJAN, R. E. 1990. Faster algorithms for the shortest path problem. *Journal of the ACM (JACM),* 37**,** 213-223.

ALBERT, R., ALBERT, I. & NAKARADO, G. L. 2004. Structural Vulnerability of the North American Power Grid. *Phys. Rev. E,* 69.

ALBERT, R. & BARABASI, A.-L. 2002. Statistic mechanics of complex networks. *Reviews of modern physics,* 74**,** 47-97.

ALBERT, R., JEONG, H. & BARABASI, A.-L. 2000a. Error and attack tolerance of complex networks. *Nature,* 406**,** 378-382

ALBERT, R., JEONG, H. & BARABASI, A. S. 2000b. Error and attack tolerance of complex networks. *Nature,* 406**,** 378-382

ALLSOP, R., E 1974. SOME POSSIBILITIES FOR USING TRAFFIC CONTROL TO INFLUENCE TRIP DISTRIBUTION AND ROUTE CHOICE. *Proceedings of the 6th International Symposium on Transportation and Traffic Theory, Sydney.* **,** 345-374.

AMDAL, J. R. & SWIGART, S. L. 2010. RESILIENT TRANSPORTATION SYSTEMS IN A POST-DISASTER ENVIRONMEN:A Case Study of Opportunities Realized and Missed in the Greater New Orleans Region. *Gulf Coast Research Center for Evacuation and Transportation Resiliency***,** http://www.evaccenter.lsu.edu/1001.pdf Accessed 10/03/2016.

AMERICAN SOCIETY OF CIVIL ENGINEERS 2005 Report Card for America's Infrastructure.

ARIANOS, S., BOMPARD, E., CARBONE, A. & XUE, F. 2009. Power grid vulnerability: a complex network approach. *Chaos,* 19**,** 013119.

ATTOH-OKINE, N. O., COOPER, A. T. & MENSAH, S. A. 2009. Formulation of resilience index of urban infrastructure using belief functions. *IEEE Systems Journal,* 3**,** 147-153.

BAIDUBAIKE**,** http://baike.baidu.com/link?url=PF0Q0jMEY6weHZgKyYUDTxLUC20X0OYzXHJf1Ie6xYX_lKfGpBLnm-z9IG0anos_mO_ngcS1HVQwhyXYf3pAzK Access 01/03/2016.

BALAKRISHNA, R., BEN-AKIVA, M., BOTTOM, J. & GAO, S. 2013. Information Impacts on Traveler Behavior and Network Performance: State of Knowledge and Future Directions. *Advances in Dynamic Network Modeling in Complex Transportation Systems,* 2**,** 193-224.

BARABASI, A.-L. & ALBERT, R. 1999. Emergence of Scaling in Random Networks. *Science,* 286**,** 509-512.

BARABASI, A.-L., ALBERT, R. & JEONG, H. 2000a. Scale-free characteristics of random networks: The topology of the World Wide Web. *Physica A,* 281**,** 69-77.

BARABASI, A.-L., ALBERT, R., JEONG, H. & BIANCONI, G. 2000b. Power-law distribution of theWorldWideWeb. *Science,* 287**,** 2115a.

BARRAT, A., BARTHELEMY, M., PASTOR-SATORRAS, R. & VESPIGNANI, A. 2004. The architecture of complex weighted networks. *Proc Natl Acad Sci USA,* 101**,** 3747-3752.

BECKMANN, M., MCGUIRE, C. & WINSTEN, C. 1956. Studies in The Economics of Transportation. *New Haven: Yale University Press. (see also:http://cowles.yale.edu/sites/default/files/files/pub/misc/specpub-beckmann-mcguire-winsten.pdf)*.

BELL, M. G. 2000. A game theory approach to measuring the performance reliability of transport networks. *Transportation Research Part B: Methodological,* 34**,** 533-545.

BELL, M. G., CASSIR, C., LIDA, Y. & LAM, W. H. K. 1999. A sensitivity based approach to network reliability assessment. *Proceedings of the 14th International Symposium on Transportation and Traffic Theory, Pergamon, Oxford***,** 283-300.

BELLAFIORE, S., BARNECHE, F., PELTIER, G. & ROCHAIX, J. D. 2005. State transitions and light adaptation require chloroplast thylakoid protein kinase STN7. *Nature,* 433**,** 892-5.

BEN-ELIA, E. & SHIFTAN, Y. 2010. Which road do I take? A learning-based model of route-choice behavior with real-time information. *Transportation Research Part A: Policy and Practice,* 44**,** 249-264.

BEN AKIVA, M. & LERMAN, S. R. 1985. Discrete Choice Analysis: Theory and Application in Travel Demand. *MIT Press, Cambridge, MA*.

BENGTSSON, M. & KOCK, S. 2000. "Coopetition" in Business Networks—to Cooperate and Compete Simultaneously. *Industrial Marketing Management,* 29**,** 411-426.

BHAVATHRATHAN, B. & PATIL, G. 2015. Quantifying resilience using a unique critical cost on road networks subject to recurring capacity disruptions. *Transportmetrica A: Transport Science,* 1**,** 836-855.

BIE, J. & LO, H. 2010. Stability and attraction domains of traffic equilibria in a day-to-day dynamicsl system formulation. *Transportation Research Part B: Methodological,* 44**,** 90-107.

BIERLAIRE, M., THEMANS, M. & AXHAUSEN, K. 2006. Analysis of driver's response to real-time information in Switzerland. *European transport\trasporti europei, ISTIEE, Trieste, Italy,* 34**,** 21-41.

BOCCALETTI, S., LATORA, V., MORENO, Y., CHAVES, M. & HWANG., D. U. 2006. Complex Networks: Structure and Dynamics. *Physics Reports,* 424**,** 175-308.

BOMPARD, E., NAPOLI, R. & XUE, F. 2009. Analysis of structural vulnerabilities in power transmission grids. *International Journal of Critical Infrastructure Protection,* 2**,** 5-12.

BOMPARD, E., WU, D. & XUE, F. 2011. Structural vulnerability of power systems: A topological approach. *Electric Power Systems Research,* 81**,** 1334-1340.

BRABHAHARAN, P. 2006. Recent advances in improving the resilience of road networks. *New Zealand Society of Earthquake Engineering Conference 2006*.

BROADBENT, S. R. & HAMMERSLEY, J. M. 1957. Percolation Processes I: Crystals and mazes. *Proc. Camb. Philos. Soc.,* 53**,** 629–641.

BRODERA, A., KUMARB, R. K., MAGHOULA, F., RAGHAVANB, P., RAJAGOPALANB , S., STATAC , R., TOMKINSB, A. & WIENERC, J. 2000. Graph structure in the Web. *Computer Networks,* 33**,** 309-320.

BRUNEAU, M., CHANG, S., EGUCHI, R., LEE, G., O'ROURKE, T., REINHORN, A., SHINOZUKA, M., TIERNEY, K., WALLACE, W. & VON WINTERFELT, D. 2003. A framework to quantitatively assess and enhance the seismic resilience of communities. *Earthquake Spectra,* 19**,** 733-752.

BRUNEAU, M. & REINHORN, A. 2007. Exploring the concept of seismic resilience for acute care facilities. *Earthquake Spectra,* 23**,** 41-62.

BUCKS COUNTY QUICK FACTS FROM THE US CENSUS BUREAU 2014. *U.S. Census Bureau. December 4, 2014. Retrieved March 22, 2016.*

BUREAU OF PUBLIC ROADS 1964. Traffic assignment manual. *U.S. Department of Commerce, Urban Planning Division, Washington, DC.*

CALLAWAY, D. S., NEWMAN, M. E. J., STROGATZ, S. H. & WATTS, D. J. 2000. Network robustness and fragility: Percolation on random graphs. *Phys. Rev. Lett.,* 85**,** 5468-5471.

CAMACHO, J., GUIMERÀ, R. & NUNES AMARAL, L. 2002. Robust Patterns in Food Web Structure. *Physical Review Letters,* 88.

CANTARELLA, G. & CASCETTA, E. 1995. Dynamic Process and Equilibrium in Transportation Networks: Towards a Unifying Theory. *Transportation Science,* 29**,** 305-329.

CANTARELLA, G. E. 2013. Day-to-day dynamic models for Intelligent Transportation Systems design and appraisal. *Transportation Research Part C: Emerging Technologies,* 29**,** 117-130.

CARDILLO, A., SCELLATO, S. & LATORA, V. 2006. A topological analysis of scientific coauthorship networks. *Physica A: Statistical Mechanics and its Applications,* 372**,** 333-339.

CARPENTER, S., WALKER, B., ANDERIES, J. M. & ABEL., N. 2001. From Metaphor to Measurement: Resilience of What to What? *Ecosystems,* 4**,** 765-781.

CASCETTA, E. & CANTARELLA, G. 1993. Modelling dynamics in transportation networks: State of the art and future developments. *Simulation Practice and Theory,* 1**,** 65-91.

CASELLA, G. & BERGER, R. L. 2001. Statistical Inference (2nd ed.). *Duxbury. ISBN 0-534-24312-6.*

CHATTERJEEA, K., HOUNSELLA, N. B., FIRMINB, P. E. & BONSALLB, P. W. 2002. Driver response to variable message sign information in London. *Transportation Research Part C: Emerging Technologies,* 10**,** 149-169.

CHEN, L. & MILLER-HOOKS, E. 2012. Resilience: An Indicator of Recovery Capability in Intermodal Freight Transport. *Transportation Science,* 46**,** 109-123.

CHEN, S., LIU, M., GAO, L., MENG, C., LI, W. & ZHENG, J. 2008. Effects of Variable Message Signs (VMS) for Improving Congestions. *International Workshop on Modelling, Simulation and Optimization***,** 416-419.

CHEUNG, D. P. & GUNES, M. H. 2012. A complex network analysis of the united states air transportation. *Proceedings of the 2012 IEEE/ACM International Conference on Advances in Social Networks Analysis and Mining, ASONAM 2012*, 699-701.

CHI, L. P. & CAI, X. 2004. Structural changes caused by error and attack tolerance in US airport network. *Int. J. Mod. Phys. B,* 18, 2394–2400.

CHOW, A. H. F. 2007a. Trip Assignment – a literature review. Available at https://www.researchgate.net/profile/Andy_Chow2/publication Accessed by 06/06/2016.

CHOW, A. H. F. 2007b. Trip Assignment – a literature review. Available at https://www.researchgate.net/profile/Andy_Chow2/publication Accessed 06/06/2016.

CHU, C. 1989. A paired combinatorial logit model for travel demand analysis. *Proceedings of the Fifth World Conference on Transportation Research, Western Periodicals Co., Ventura, CA*, 295–309.

CLEGG, R. G. 2007. Empirical studies on road traffic response to capacity reduction. *Transportation and Traffic Theory: 17th International Symposium on Transportation and Traffic Theory (ISTTT17)*.

COHEN, R., EREZ, K., BEN-AVRAHAM, D. & HAVLIN, S. 2001. Breakdown of the Internet under intentional attack. *Phys. Rev. Lett.,* 86, 3682.

COMINETTI, R. 2013. Adaptive Dynamics and Equilibrium in Congested Networks. *TRISTAN VIII, Triennial Symposium on Transportation Analysis*.

COMPLEX NETWORKS-NEW MEDIA LAB, http://newmedialab.cuny.edu/project/complex-networks/ Accessed 03/02/2016.

COMPLEX NETWORKS & SYSTEMS, http://www.informatics.indiana.edu/rocha/projects/knowledge-networks/index.php Accessed 01/02/2016.

CROOPE, S. 2010. Managing critical civil infrastructure systems: improving resilience to disasters. *University of Delaware*.

CRUCITTI, P., LATORA, V. & MARCHIORI, M. 2004a. Model for cascading failures in complex networks. *Physical Review E,* 69.

CRUCITTI, P., LATORA, V. & MARCHIORI, M. 2004b. A topological analysis of the Italian electric power grid. *Physica A: Statistical Mechanics and its Applications,* 338, 92-97.

CRUCITTI, P., LATORA, V., MARCHIORI, M. & RAPISARDA, A. 2003. Efficiency of scale-free networks: error and attack tolerance. *Physica A: Statistical Mechanics and its Applications,* 320, 622-642.

CRUCITTI, P., LATORA, V., MARCHIORI, M. & RAPISARDA, A. 2004c. Error and attack tolerance of complex networks. *Physica A: Statistical Mechanics and its Applications,* 340, 388-394.

DAFERMOS, S. C. & SPARROW, F. T. 1968. The Traffic Assignment Problem For A General Network. *Journal of Research of the National Bureau of Standard Journal of Research,* 73B, 91-118.

DAGANZO, C. F. & SHEFFI, Y. 1977. On stochastic models of traffic assignment. *Transportation Science,* 11**,** 253-274.

DAVIS, G. A. & NIHAN, N. L. 1993. Large population approximations of a general stochastic traffic assignment model. *Operations Research* 41**,** 169-178.

DEKKER, A. 2005. Simulating network robustness for critical infrastructure networks. *In 28th australasian computer science conference. Newcastle, Australia*.

DEKKER , A. H. & COLBERT , B. 2004. Scale-Free Networks and Robustness of Critical Infrastructure Networks *In Proceedings of the 7th asia-pacific conference on complex systems. Cairns, Australia*.

DEMETRIUS, L. & MANKE, T. 2005. Robustness and network evolution—an entropic principle. *Physica A: Statistical Mechanics and its Applications,* 346**,** 682-696.

DERRIBLE, S. 2012. Network Centrality of Metro Systems. *PLoS ONE,* 7**,** e40575.

DI PAOLO, E., ZHANG, K., YANG, S., HU, X.-B. & LIU, H. 2011. Application of Complex Network Theory and Genetic Algorithm in Airline Route Networks. *Transportation Research Record: Journal of the Transportation Research Board,* 2214**,** 50-58.

DICKSON, T. J. 1981. A note on traffic assignment and signal timings in a signal-controlled road network. *Transport Research Part B: Methodological,* 15**,** 264-271.

DIMITRIOU, D., KARLAFTIS, M., KEPAPTSOGLOU, K. & STATHOPOULOS, M. 2006. Public Transportation during the Athens 2004 Olympics: From Planning to Performance. *85th Transportation Research Board Annual Meeting, At Washington D.C., U.S.A.*

DONG, G., GAO, J., DU, R., TIAN, L., STANLEY, H. E. & HAVLIN, S. 2013. Robustness of network of networks under targeted attack. *PHYSICAL REVIEW E,* 87**,** 1-11.

DONOVAN, B. & WORK, D. 2015. Using coarse GPS data to quantify city-scale transportation system resilience to extreme events. *94th Transportation Research Board anual meeting in Washington, D.C.,* 5-5465.

DU, Z. P. & NICHOLSON, A. J. 1997. Degradable transportation systems: sensitivity and reliability analysis. *Transportation Research B,* 31**,** 225-237.

DUAN, Y. & LU, F. 2013. Structural robustness of city road networks based on community. *Computers, Environment and Urban Systems,* 41**,** 75-87.

DUBEY, P. 1986. Inefficiency of Nash Equilibria. *Mathematics of Operations Research,* 11**,** 1-8.

DURAND-RAUCHER, Y., YIM, Y. & YGNACE, J. 1993. Traffic information and driver behaviour in Paris region. *Proc., Pacific Rim Transtech Conf.,* 1**,** 1676-169.

EBEL, H., MIELSCH, L.-I. & BORNHOLDT, S. 2002. Scale-free topology of e-mail networks. *Phys. Rev. E,* 66.

ERDŐS, P. & RÉNYI, A. 1960. On the Evolution of Random Graphs *THE MATHEMATICAL INSTITUTE OF THE HUNGARIAN ACADEMY OF SCIENCES***,** 17-61.

FATURECHI, R. & MILLER-HOOKS, E. 2014. Travel time resilience of roadway networks under disaster. *Transportation Research Part B: Methodological,* 70**,** 47-64.

FELL, D. A. & WAGNER, A. 2000. The small world of metabolism. *Nature Biotechnology,* 18**,** 1121-1122.

FERGUSON, E. 1992. Transit ridership, incident effects and public policy. *Transportation Research Part A: Policy and Practice,* 26**,** 393-407.

FORTUNATO, S. 2010. Community detection in graphs. *Physics Reports* 486**,** 75-174

FOSTER, H. D. 1997. The Ozymandias Principles: Thirty one Strategies for Surviving Change. *Victoria, B.C.: UBC Press*.

FRANK, M. & WOLFE, P. 1956. An Algorithm for quadratic programming *Naval Research Logistic Quaterly* 3**,** 95-110.

FRECKLETON, D., HEASLIP, K., LOUISELL, W. & COLLURA, J. 2012. Evaluation of transportation network resiliency with consideration for disaster magnitude. *Proceedings of The 91st Annual Meeting of the Transportation Research Broad, Washington, D.C, USA*.

FRIESZ, T. L. 2010. Dynamic Optimization and Differential Games. *International Series in Operations Research & Management Science, Springer US,* 135.

FRIESZ, T. L., BERNSTEIN, D., MEHTA, N. J. & TOBIN, R. L. 1994. Day-To-Day Dynamic Network Disequilibria and Idealized Traveler Information Systems. *Operations Research,* 42**,** 1120-1136.

GARTNER, N. 1976. Area Traffic Control and Network Equilibrium. *Traffic Equilibrium Methods, Lecture Notes in Economics and Mathematical Systems,* 118**,** 274-297.

GASTNER, M. n.d. Percolation theory. Available at http://wwwf.imperial.ac.uk/~mgastner/percolation/percolation Accessed 01/05/2015.

GASTNER, M. & NEWMAN, M. 2006a. Optimal design of spatial distribution networks. *Physical Review E,* 74.

GASTNER, M. T. & NEWMAN, M. E. J. 2006b. The spatial structure of networks. *The European Physical Journal B,* 49**,** 247-252.

GIULIANO, G. & GOLOB, J. 1998. Impacts of the Northridge Earthquake on Transit and Highway Use. *Journal of Transportation and Statistics,* 1**,** 1-20.

GODSCHALK, D. 2002. Urban hazard mitigation: creating resilient citie. *Urban Hazards Forum, John Jay College, City University of New York, January 2002*.

GREENSHIELDS, B. D. 1934. A study of traffic capacity. *Proceedings of the Highway Research Board,* 14**,** 448-477.

GRIMME, V. & CALABRESE, J. 2011. What is resilience? A short introduction. *VIABILITY AND RESILIENCE OF COMPLEX SYSTEMS. Boston/Dordrecht/London, Kluwer Academic Publishers***,** 3-13.

GRUBINGER, V. 2012. Resilience and sustainability in the food system. *Accessed March 2016***,** http://www.resilientdesign.org/resilience-and-sustainability-in-the-food-system/ Accessed 03/04/2016.

GUIDA, M. & MARIA, F. 2007. Topology of the Italian airport network: A scale-free small-world network with a fractal structure? *Chaos, Solitons & Fractals,* 31**,** 527-536.

GUIMERA, R. & AMARAL, L. A. N. 2004. Modeling the world-wide airport network. *The European Physical Journal B - Condensed Matter,* 38**,** 381-385.

GUIMERA, R., MOSSA, S., TURTSCHI, A. & AMARAL, L. A. 2005. The worldwide air transportation network: Anomalous centrality, community structure, and cities' global roles. *Proc Natl Acad Sci U S A,* 102**,** 7794-9.

GUIMERA, R., SALES-PARDO, M. & AMARAL, L. A. 2007. A network-based method for target selection in metabolic networks. *Bioinformatics,* 23**,** 1616-22.

GUO, L. & CAI, X. 2008. DEGREE AND WEIGHTED PROPERTIES OF THE DIRECTED CHINA RAILWAY NETWORK. *International Journal of Modern Physics C* 19**,** 1909-1918.

GUO, R.-Y., YANG, H., HUANG, H.-J. & TAN, Z. 2015. Link-based day-to-day network traffic dynamics and equilibria. *Transportation Research Part B: Methodological,* 71**,** 248-260.

HAMILL, L. & GILBERT, N. 2009. Social Circles - A Simple Structure for Agent-Based Social Network Models. *Journal of Artificial Societies and Social Simulation,* 12.

HAN, K., MASCIA, M., NORTH, R. J., HU, J. S. & EVE, G. 2015a. Day-to-day Dynamic Traffic Assignment Model with Variable Message Signs and Endogenous User Compliance. *TRB 94th Annual Meeting Compendium of Papers,Washington DC, USA*.

HAN, K., SZETO, W. Y. & FRIESZ, T. L. 2015b. Formulation, existence, and computation of boundedly rational dynamic user equilibrium with fixed or endogenous user tolerance. *Transportation Research Part B: Methodological,* 79.

HAN, L., SUN, H., WU, J. & ZHU, C. 2011. Day-to-day evolution of the traffic network with Advanced Traveler Information System. *Chaos, Solitons and Fractals,* 44**,** 914-919.

HAZELTON, M. & WATLING, D. 2004. Computing of Equilibrium of Markov Traffic-Assignment Model. *Transportation Science,* 38**,** 331-342.

HE, X., GUO, X. & LIU, H. X. 2010. A link-based day-to-day traffic assignment model. *Transportation Research Part B: Methodological,* 44**,** 597-608.

HE, X. & LIU, H. X. 2012. Modeling the day-to-day traffic evolution process after an unexpected network disruption. *Transportation Research Part B: Methodological,* 46**,** 50-71.

HE, X. & PEETA, S. 2015. A Marginal Utility Day-to-Day Traffic Evolution Model. *94th Transportation Research Board Annual Meeting, Wahington, D.C.*

HE, Z., YANG, L. & GUAN, W. 2014. A Day-to-day Route Choice Model based on Travellers' Behavioural Characteristics. *Procedia-Social and Behavioral Science,* 138**,** 738-747.

HEATH, R. A. 2000. Nonlinear dynamics: techniques and applications in psychology. *Lawrence Erlbaum*.

HENSHER, D. A. & BREWER, A. M. 2002. Going for gold at the Sydney Olympics: How did transport perform? *Transport Reviews,* 22**,** 381-399,.

HESSISCHES STATISTISCHES LANDESAMT 2016. Bevölkerung der hessischen Gemeinden (in German). https://statistik.hessen.de/sites/statistik.hessen.de/files/Bevoelkerung_in_Hessen_nach_Gemeinden_am_31_12_2015 Accessed 02/06/2016.

HEYDECKER, B. n.d. Advanced transport modelling. *Lecture material, Imperial College London and University College of London*.

HOFFMAN, E. 2007. Building a Resilient Business. *Raptor Networks Technology Inc*.

HOKAYEM, P. A. & GALLESTEY, E. 2015. Lyapunov Stability Theory. *Nonlinear Systems and Control*, http://people.ee.ethz.ch/~apnoco/Lectures2015/03_Lyapunov.pdf Accessed 22/11/2016.

HOLLING, C. S. 1973. Resilience and stability of ecological systems. *Annual Review of Ecology and Systematics,* 41**,** 1-23.

HOLME, P., KIM, B., YOON, C. & HAN, S. 2002. Attack vulnerability of complex networks. *Physical Review E,* 65.

HOLMGREN, Å. 2007. A Framework for Vulnerability Assessment of Electric Power Systems. *Critical Infrastructure Advances in Spatial Science*.

HOROWITZ, J. 1984. The stability of stochastic equilibrium in a two-link transportation network. *Transportation Research Part B,* 18**,** 13-28.

HOSOYA, H. 1971. Topological index. A newly proposed quantity characterizing he topological nature of structural isomers of saturated hydrocarbons. *Bulletin of the Chemical Society of Japan,* 44**,** 2332–2339.

HU, Y. & ZHU, D. 2009. Empirical analysis of the worldwide maritime transportation network. *Physica A: Statistical Mechanics and its Applications,* 388**,** 2061-2071.

HUANG, H.-J. & LAM, W. H. K. 2002. Modeling and solving the dynamic user equilibrium route and departure time choice problem in network with queues. *Transportation Research Part B,* 36**,** 253–273.

HUBERMAN, B. A. 2001. The Laws of the Web. *MIT Press,Cambridge, MA*

HUGHES, J. & HEALY, K. 2014. Measuring the resilience of transport infrastructure. *NZ Transport Agency research report 546***,** 1-82.

HUNT, J., BROWNLEE, A. & STEFAN, K. 2002. Responses to Centre Street Bridge Closure: Where the "Disappearing" Travelers Went *Transportation research record,* 1807**,** 51-58.

HUO, H. & LEVISION, D. 2003. Effectiveness of Variable Message Signs Using Empirical Loop Detector Data. *University of Minnesota: Nexus Research Group,working paper*.

HUSDAL, J. 2004. Reliability and Vulnerability versus Cost and Benefits. *Molde University College, in: Proceedings of the second International Symposium on Transportation Network Reliability (INSTR), Christchurch and Queenstown, New Zealand***,** 180-186.

IEEE 1990. IEEE standard Computer Dictionary : A Complation of IEEE Standard Computer Glossaries. *Institute of Electrical and Electronical Engineers*.

IMMERS, B., YPERMAN, I., STADA, J. & BLEUKX, A. 2004. Reliability and robustness of transportation networks: problem survey and examples. *Proceedings of the NECTAR cluster meeting on reliability of networks,* Amsterdam, the Netherlands**,** 19-20.

IMMERS, B., YPERMAN, I., STADA, J. & BLEUKX, A. n.d. Reliability and robustness of transportation networks-Problem survey and examples. *www.kuleuven.be/traffic/dwn/P2004F.pdf***,** Accessed 01/02/2016.

INSTITUTO NACIONAL DE ESTADISTICA 2009. Population of Barcelona. http://www.ine.es/jaxi/tabla.do. Accessed 30/03/2016.

IP, W. & WANG, D. 2011. Resilience and Friability of Transportation Networks: Evaluation, Analysis and Optimization. *IEEE System Journal,* 5**,** 189-198.

IVES, A. & CARPENTER, S. 2007. Stability and diversity of ecosystems. *Science,* 317**,** 58–62.

JAMAKOVIC, A., WANG, H. & VAN MIEGHEM, P. 2006. Topological Characteristics of the Dutch Road Infrastructure. *in: Proceedings Seminar Infrastructure Reliability, Delft*.

JANIĆ, M. 2015. Modelling the resilience, friability and costs of an air transport network affected by a large-scale disruptive event. *Transportation Research Part A: Policy and Practice,* 71**,** 1-16.

JEN, E. 2002. STABLE OR ROBUST? WHAT'S THE DIFFERENCE? *Santa Fe Institute***,** http://tuvalu.santafe.edu/~erica/stable.pdf Accessed 01/07/2016.

JEONG, H., TOMBOR, B., OLTVAI, Z. N. & BARABASI, A.-L. 2000. The large-scale organization of metabolic networks. *Nature,* 407**,** 651-654.

JOLI, E., WILLIAM, L. & ZACHARY 2010. *Universiti of Massachusetts*.

JUSTUS, J. 2008. Complexity, diversity, and stability. *In A companion to the philosophy of biology (S. Sarkar and A. Plutynski, eds.)***,** 321-350.Blackwell Publishing.

KALUZA, P., KOLZSCH, A., GASTNER, M. T. & BLASIUS, B. 2010. The complex network of global cargo ship movements. *J R Soc Interface,* 7**,** 1093-103.

KARKUBTHY, F. 1929. Chains, in Everything is Different. *Budapest*.

KAUFFMAN, S. A. 1993. The Origins of Order: Self-Organization and Selection in Evolution. *Oxford University Press: Oxford, UK*.

KERMACK, W. O. & MCKENDRICK, A. G. 1932. The Contribution to the Mathematical Theory of Epidemics. *Proceedings of Royal Society A,* 138**,** 55-83.

KIM, J. & WILHELM, T. 2008. What is a complex graph? *Physica A: Statistical Mechanics and its Applications,* 387**,** 2637-2652.

KING, P., BULDYREV, S., DOKHOLYAN, N., HAVLIN, S., LOPEZ, E., PAUL, G. & STANLEY, H. 2002. Percolation Theory. *Draft on website,* http://www.lps.org.uk/docs/Percolation_Theory.

KONG, Z. & YEH, E. M. 2010. Resilience to Degree-Dependent and Cascading Node Failures in Random Geometric Networks. *IEEE Transactions on Information Theory,* 56**,** 5533-5546.

KOPPELMANA, F. S. & WEN, C.-H. 2000. The paired combinatorial logit model: properties, estimation and application. *Transportation Research Part B: Methodological,* 34**,** 75-89.

KOU, Z. & ZHANG, C. 2007. Reply networks on a bulletin board system. *PHYSICAL REVIEW E,* 67.

KOUTSOUPIAS, E. & PAPADIMITRIOU, C. 1999. Worst-case Equilibria. *Proceedings of the 16th annual conference on Theoretical aspects of computer science***,** 404-413.

KRISHNAMURTHY, B. & WANG, J. 2000. On network-aware clustering of Web clients. *Proceedings of the conference on Applications, Technologies, Architectures, and Protocols for Computer Communication* 30**,** 97-110

LAM, W. H. K. & CHAN, K. S. 1996. A stochastic traffic assignment model for road network with travel time information via variable message signs. *Intelligent Vehicles Symposium,Proceedings of the 1996 IEEE***,** 99-104.

LANCICHINETTI, A., RADICCHI, F., RAMASCO, J. J. & FORTUNATO, S. 2011. Finding Statistically Significant Communities in Networks. *PLoS ONE,* 6**,** 1-18.

LANGTON, C. G. 1989. Artificial Life: Proceedings of an Interdisciplinary Workshop on the Synthesis and Simulation of Living Systems. *(held September 1987, Los Alamos, New Mexico, Vol. VI in Santa Fe Institute Studies in the Sciences of Complexity),Addison-Wesley: Reading, MA*.

LATORA, V. & MARCHIORI, M. 2004. How the science of complex networks can help developing strategies against terrorism. *Chaos, Solitons & Fractals,* 20**,** 69-75.

LATORA, V. & MARCHIORI, M. 2005. Vulnerability and protection of infrastructure networks. *Physical Review E,* 71.

LATORA, V. & MARCHIORI, M. 2007. A measure of centrality based on network efficiency. *New Journal of Physics,* 9**,** 188-188.

LATORA, V. & MARCHIORIB, M. 2002. Is the Boston subway a small-world network. *Physica A,* 314**,** 109-113.

LEE, C.-Y., LEE, J. C. & GUTELL, R. R. 2007. Networks of interactions in the secondary and tertiary structure of ribosomal RNA. *Physica A: Statistical Mechanics and its Applications,* 386**,** 564-572.

LEVINA, E. & TIRPAK, D. 2006. Adaptation to climate change: key terms. *Report for the Organisation for Economic Co-operation and Development and International Energy Agency*.

LEVINSON, D. & KUMAR, A. 1995. A Multi-modal Trip Distribution Model. *Transportation Research Record* 1446.

LEVY, N., MARTENS, K. & BENENSON, I. 2013. Exploring cruising using agent-based and analytical models of parking. *Transportmetrica A: Transport Science,* 9**,** 773-797.

LI, BEI-JIE , DU, W.-B., LIU, C. & CAI, K.-Q. 2014. Topologic and Dynamic Resilience Model of Chinese Airport Network. *11th IEEE International Conference on Control & Automation (ICCA) June 18-20, 2014. Taichung, Taiwan*.

LI, W. & CAI, X. 2004. Statistical analysis of airport network of China. *Physical Review E,* 69.

LI, W. & CAI, X. 2007. Empirical analysis of a scale-free railway network in China. *Physica A: Statistical Mechanics and its Applications,* 382**,** 693-703.

LIU, H., HAN, K., GAYAH, V. V., FRIESZ, T. L. & YAO, T. 2015. Data-driven linear decision rule approach for distributionally robust optimization of on-line signal control. *Transportation Research Part C: Emerging Technologies,* 59**,** 260-277.

LIU, R. & SMITH, M. 2015. Route choice and traffic signal control: A study of the stability and instability of a new dynamical model of route choice and traffic signal control. *Transportation Research Part B: Methodological,* 77**,** 123-145.

LIU, Y. Y., SLOTINE, J. J. & BARABASI, A. L. 2011. Controllability of complex networks. *Nature,* 473**,** 167-73.

LO, S.-C. & HALL, R. W. 2006. Effects of the Los Angeles transit strike on highway congestion. *Transportation Research Part A: Policy and Practice,* 40**,** 903–917.

LORDAN, O., SALLAN, J. M., SIMO, P. & GONZALEZ-PRIETO, D. 2014. Robustness of the air transport network. *Transportation Research Part E,* 68**,** 155-163.

LUCA DALL'ASTA, A. B., MARC BARTHELEMY, ALESSANDRO VESPIGNANI 2006. Vulnerability of weighted networks. *Journal of Statistical Mechanics: Theory and Experiment***,** 4006.

MACAL, C. M. & NORTH, M. J. 2010. Tutorial on agent-based modelling and simulation. *Journal of Simulation,* 4**,** 151-162.

MACTUTOR HISTORY OF MATHEMATICS ARCHIVE n.d. Leonard Euler's Solution to the Konigsberg Bridge Problem. http://www-history.mcs.st-andrews.ac.uk/Extras/Konigsberg.html Accessed 15/11/2016.

MAGUIRE, B. & CARTWRIGHT, S. 2008. Assessing a community's capacity to manage change: a resilience approach to social assessment. *Report for the Australian Government Bureau of Rural Sciences*.

MAHER, M., ZHANG, X. & VAN VLIET, D. 2001. A bi-level programming approach for trip matrix estimation and traffic control problems with stochastic user equilibrium flows. *Transportation Research Part B: Methodological,* 35**,** 23-40.

MAHMASSANI, H. S. 1990. Information Impacts on Traveler Behavior: Experimental Investigation and Application to the Analysis of Planned Traffic Disruptions. *Trans. Res,* 24A.

MAHMASSANI, H. S. & CHANG, G.-L. 1987. On boundedly rational user equilibrium in transportation systems. *Transportation Science,* 21**,** 89-99.

MAIO, M., VITETTA, A. & WATLING, D. 2013. Influence of Experience on Users' Behaviour: A Day-to-Day Model for Route Choice Updating. *Procedia-Social and Behavioural Sciences,* 87**,** 60-74.

MANYENA, S., O'BRIEN, G., O'KEEFE, P. & ROSE, J. 2011. Disaster resilience: a bounce back or bounce forward ability? *Local Environment,* 16**,** 417-424.

MASCIA, M., HU, S. J., HAN, K., NORTH, R., VAN POPPEL, M., THEUNIS, J. & LITZENBERGER, M. 2016. Impact of traffic management on black carbon emissions: A microsimulation study. *Networks and Spatial Economics***,** 1-23.

MASUCCI, A. P. & MOLINERO, C. 2016. Robustness and closeness centrality for self-organized and planned cities. *Eur. Phys. J. B,* 89**,** 53.

MCROBERTS, N. 2010. Sustainability and resilience demystified. www.knowledgescotland.org/briefings.php?id=116 Accessed 11/03/2016

MENEGUZZER, C. 1996. Computational experiments with a combined traffic assignment and control model with asymmetric cost functions. *Proceedings of the th International Conference on Applications of Advanced Technologies in Transportation Engineering. ASCE, New York***,** 609-614.

MENEGUZZER, C. 1998. Stochastic user equilibrium assignment with traffic –responsive signal control. *European Regional Science Association***,** Available from: http://www-sre.wu-wien.ac.at/ersa/ersaconfs/ersa98/papers/337.pdf Accessed 12/05/2016.

MENEGUZZER, C. 2012. Dynamic process models of combined traffic assignment and control with different signal updating strategies. *JOURNAL OF ADVANCED TRANSPORTATION,* 46**,** 351-365.

MERTON, R. K. 1968. The Matthew Effect in Science. *Science,* 159**,** 56-63.

MEYER, M. & MILLER, E. J. 2000. Urban Transportation Planning. *McGraw-Hill, 2nd edition***,** ISBN 0-07-242332-3.

MILGRAM, S. 1967. The small world problem. *Psychology Today,* 2**,** 60-67.

MINNESOTA DEPARTMENT OF TRANSPORTATION 2007. Road-user cost due to unavailability of interstate 35W Mississippi river crossing at Minneapolis, Minnesota, Technical report. *Minneapolis, MN: Office of Investment Management***,** Available from: www.dot.state.mn.us/i35wbridge/rebuild/pdfs/I-35WMississippiRiverCrossingRoad-UserCost.pdf Accessed 23/07/2016.

MIZRUCHI, M. S. 1982. The American Corporate Network. *Sage, Beverly Hills,* 138.

MOBILE CAPITAL 2011. http://www.businesslocationcenter.de/en/business-location/business-location/infrastructure/transport-infrastructure/passenger-and-freight-service Accessed 24/04/ 2016.

MOKHTARIAN, P. L., SALOMON, I. & REDMOND, L. S. 2001. Understanding the demand for travel: it's not perely 'derived'. *Innovation,* 14**,** 1-26.

MORENO, J. L. 1934. Who Shall Survive. *Beacon House,* Beacon.

MOUNCE, R. 2009. Existence of Equilibrium in a Continuous Dynamic Queueing Model for Traffic Networks with Responsive Signal Control. *Proceedings of the Eighteenth International Symposium on Transportation and Traffic Theory, Hong Kong Polytechnic University, Hong Kong (Editors: Lam, W. H. K., Wong, S. C., Lo, H. K.), Springer***,** 327-344.

NAGEL, K. & FLÖTTERÖD, G. 2009. Agent-based traffic assignment: going from trips to behavioral travelers. *Paper presented at the 12th International Conference on Travel Behaviour Research (IATBR), Jaipur, December 2009*.

NAGEL, K. & SCHRECKENBERG, M. 1992. A cellular automaton model for freeway traffic. *Journal de Physique* 2**,** 2221 - 2229.

NAGURNEY, A. 1999. Network economics:A variational Inequality Approach (2nd edn). *Kluwer Academic Publishers,Dordrecht, the Netherlands*.

NAGURNEY, A. 2011a. Building Resilience into Fragile Transportation Networks in an Era of Increasing Disasters. *Transportation Research Board 90th Annual Meeting***,** Available at https://supernet.isenberg.umass.edu/visuals/TRB_Panel_Nagurney_Talk.pdf.

NAGURNEY, A. 2011b. Building Resilience into Fragile Transportation Networks in an Era of Increasing Disasters. *Transportation Research Board 90th Annual Meeting***,** Available at https://supernet.isenberg.umass.edu/visuals/TRB_Panel_Nagurney_Talk.pdf Accessed 07/04/2016.

NAGURNEY, A. & QIANG, Q. 2007. Robustness of transportation networks subject to degradable links. *Europhysics Letters (EPL),* 80**,** 68001.

NAGURNEY, A. & QIANG, Q. 2007a. A network efficiency measure for congested networks. *Europhysics Letters (EPL),* 79**,** 38005.

NAGURNEY, A. & QIANG, Q. 2009. A relative total cost index for the evaluation of transportation network robustness in the presence of degradable links and alternative travel behavior. *International Trabsactions in Operation Research,* 16**,** 49-67.

NAGURNEY, A. & ZHANG, D. 1997. Projected dynamical systems in the formulation, stability analysis, and computation of fixed-demand traffic network equilibria. *Transportation Science,* 31**,** 147-158.

NATIONAL BUREAU OF STATISTICS OF CHINA**,** Available at: http://data.stats.gov.cn Accessed 04/06/2016.

NATIONAL GEOPHYSICAL DATA CENTER n.d. Comments for the Significant Earthquake. Available from http://www.ngdc.noaa.gov/nndc/struts/results?eq_0=5372&t=101650&s=13&d=22,26,13,12&nd=display Accessed 3/07/2016.

NEMYTSKII, V. V. & STEPANOV, V. V. 1960. Quantitative theory of differential equations. *Princeton University Press*.

NEW YORK Deparment of Tansportation. 2001. https://www.dot.ny.gov/news/press-releases/2001 30/03/2016.

NEWMAN, M. E. J. 2003. The Structure and Function of Complex Networks. *SIAM Review,* 45**,** 167-256.

NEWMAN, M. E. J., FORREST, S. & BALTHROP, J. 2002. Email networks and the spread of computer viruses. *PHYSICAL REVIEW E,* 66**,** 035101.

NEWMAN, M. E. J. & PEIXOTO, T. P. 2015. Generalized communities in networks. *Physical Review Letters,* 115**,** 1-5.

NOGAL, M., MARTINEZ-PASTOR, B., O'CONNOR, A. & CAULFIELD, B. 2015. Dynamic Restricted Equilibrium Model to Determine Statistically the Resilience of a Traffic Network to

Extreme Weather Events. *12th International Conference on Application of Statistics and Probability in Civil Engineering*.

O'ROURKE, T. D. 2007. Critical infrastructure, interdependencies, and resilience. *Bridge,Washington-National Academy Of Engineering,* 37**,** 22.

OMER, M., MOSTASHARI, A. & NILCHIANI, R. 2013. Assessing Resilience in a Regional Road-based Transportation Network. *International Journal of Industrial and Systems Engineering,* 13**,** 389-408.

ORTÚZAR, J. & WILLUMSEN, L. 2001. Modelling transport *(3rd Edition). John Wiley & Sons, England.*

OSEI-ASAMOAH, A. & LOWNES, N. E. 2014. Complex network method of evaluating resilience in surface transportation networks. *Transportation Research Record,* 2467**,** 120-128.

PEETA, S. & YANG, T.-H. 2003. Stability issues for dynamic traffic assignment. *Automatica,* 39**,** 21-34.

PETRI , G., EXPERT , P., JENSEN, H. & POLAK, J. 2013. Entangled communities and spatial synchronization lead to criticality in urban traffic. *Scientific Reports,* 3**,** 1-8.

PHYSICS.ORG**,** http://phys.org/news/2015-04-formulas-google-klout-facebook-cybercrime.html Accessed 06/01/2016.

PIEN, K.-C., HAN, K., SHANG, W., MAJUMDAR, A. & OCHIENG, W. 2015. Robustness analysis of the European air traffic network. *Transportmetrica A: Transport Science* 11.

POOL, I. D. S. & KOCHEN, M. 1978. Contacts and influence. *Social Network***,** 1-48.

PRASHKER, J. N. & BEKHOR, S. 2000. Some observations on stochastic user equilibrium and system optimum of traffic assignment. *Transportation Research Part B: Methodological,* 34**,** 277-291.

PRICE, D. J. D. S. 1965. Networks of Scientifi Papers. *Science,* 149**,** 510-515.

RAPOPORT, A. & HORVATH, W. J. 1961. A study of a large sociogram. *Behavioral Sci,* 6**,** 279-291.

REDDY, K. P., KITSUREGAWA, M., SREEKANTH, P. & RAO, S. S. 2002. A graph based approach to extract a neighborhood customer community for collaborative filtering. *Proceedings of the Second International Workshop on Databases in Networked Information Systems (Springer-Verlag, London, UK)***,** 188-200.

REGGIANI, A. & NIJKAMP, P. 2007. Transport Networks and Metropolitan Development: New Analytical Departures. *Networks and Spatial Economics,* 7**,** 297-300.

ROBERTSON 1969. TRANSYT method for area traafic control. *Traffic Engineering and Control,* 11**,** 276-281.

ROBINSON, S. 2004. The Price of Anarchy. *SIAM news,* 37.

SABIDUSSI, G. 1966. The Centrality Index of a Graph *Psychometrika,* 31**,** 581-603.

SAHINI, M. 1994. Applications of percolation theory. *London : Taylor & Francis*.

SAKAKIBARA, H., KAJITANI, Y. & OKADA, N. 2004. Road Network Robustness for Avoiding Functional Isolation in Disasters. *Journal of Transportation Engineering,* 130**,** 560–567.

SANCHEZ, J. & CAIRE, R. 2012. Towards a Complex Networks Modeling of Interdependent Critical Infrastructures.

SANDER, L. M., WARREN, C. P., SOKOLOV, I. M., SIMON, C. & KOOPMAN, J. 2002. Percolation on disordered networks as a model for epidemics. *Math. Biosci.,* 180**,** 293–305.

SCHILLO, M., BÜRCKERT, H., FISCHER, K. & KLUSCH, M. 2011. Towards a definition of robustness for market-style open multi-agent systems. *In: Proceedings of the fifth international conference on Autonomous agents. New York.***,** 75-76.

SCOTT, D. M., NOVAK, D., AULTMAN-HALL, L. & GUO, F. 2005. Network robustness index- a new method for identifying critical links and evaluating the perfomance of transportation networks *Center for spatial analysis working paper*.

SCOTT, J. 2013. Social Network Analysis. 3rd Edition**,** London.

SEVILLE, E. 2009. Resilience: great concept but what does it mean for organisations? *Tephra, Community resilience special issue.***,** 9-15.

SHANG, W., PIEN, K.-C., HAN, K., MAJUMDAR, A. & OCHIENG, W. 2014. Robustness and Topology Analysis of European Air Traffic Network Using Complex Network Theory. *94th Transportation Research Board anual meeting in Washington, D.C.*

SHARGEL, B., SAYAMA, H., EPSTEIN, I. & BAR-YAM, Y. 2003. Optimization of robustness and connectivity in complex networks. *Physical Review Letters,* 90**,** 1-4.

SHEFFI, Y. 1985. Urban Transporation Networks: equilibrium analysis with mathmatical programming methods. *Englewood Cliffs, New Jersey: Prentice Hall*.

SHIFTAN, Y. 2000. The Advantage of Activity-basedModelling for Air-quality Purposes: Theory vs Practice and Future Needs. *Innovation,* 13**,** 1-17.

SIENKIEWICZ, J. & HOŁYST, J. 2005. Statistical analysis of 22 public transport networks in Poland. *Physical Review E,* 72.

SIMON, H. 1957. A behavioral model of rational choice. In Models of Man, Social and Mathematical Essays on Rational Human Behavior in a Social Setting. *New York: Wiley*.

SIMON, H. A. 1955. On a class of skew distribution functions. *Biometrika,* 42**,** 425-440.

SINHA-RAY, P., CARTER, J., FIELD, T., MASHALL, J., POLAK, J., SCHUMACHER, K., SONG, D., WOODS, J. & ZHANG, J. 2003. Container World: Global agent-based modelling of the container transport business. *Proceedings 4th workshop on Agent-Based Simulation, J.-P. Müller, M.-M. Seidel ©SCS Europe BVBA*.

SMITH, M. 1979a. The existence,uniqueness and stability of traffic equilibria. *Transporation Research,* 13B**,** 295-304.

SMITH, M. 2012. Traffic control and route choice: modelling and optimisation. *JCT Signals Symposium (2012)*

SMITH, M., HAZELTON, M. L., LO, H. K., CANTARELLA, G. E. & WATLING, D. P. 2013. The long term behaviour of day-to-day traffic assignment models. *Transportmetrica A: Transport Science,* 10**,** 647-660.

SMITH, M. & MOUNCE, R. 2011. A splitting rate model of traffic re-routeing and traffic control *Proceedings of the 19th International Symposium on Transportation and Traffic Theory, Berkeley, California, USA, July 19, 2011; and Transportation Research Part B (2011)*.

SMITH, M. J. 1979b. A local traffic control policy which automatically maximises the overall travel capacity of an urban road network. *Proceedings of theInternational Symposium on Traffic Control Systems,University of California, Berkeley,* 2A**,** 11-32.

SMITH, M. J. 1979c. Traffic Control and Route-choice: A Simple Example. *Transport Research,* 13B**,** 289-294.

SMITH, M. J. 1984a. The Stability of a Dynamic Model of Traffic Assignment—An Application of a Method of Lyapunov. *Transportation Science,* 18**,** 245-252.

SMITH, M. J. 1984b. The stability of a dynamic model of traffic assignment – an application of a method of Lyapunov. *Transportation Science,* 18**,** 245-252.

SNELDER, M. 2010. Designing Robust Road Networks: A general design method applied to the Netherlands. *PhD thesis. TU Delft University***,** http://repository.tudelft.nl/islandora/object/uuid:82881390-1db0-46ca-8d38-9f89e15c2a92/?collection=research Accessed 12/03/2016.

SOLE, R. V. & MONTOYA, J. M. 2001. Complexity and fragility in ecological networks. *Proc Biol Sci,* 268**,** 2039-45.

SPORNS, O. 2002. Network analysis, complexity and brain function *Complexity,* 8**,** 56-60.

SPORNS, O., TONONI, G. & AL, E. 2000. Theoretical Neroanatomy: relating anatomical and functional connectivity in graphs and cortical connection matrices. *Cerebral Cortex,* 10**,** 127-141.

STATISTICAL INSTITUTE OF CATALONIA 2014. http://www.idescat.cat/emex/?lang=en&id=082798 Accessed 22/03/2016.

STAUFFER, D. & AHARONY, A. 1994. Introduction To Percolation Theory: Revised Second Edition. *Taylor & Francis e-Library*.

STERBENZ, J. P. G. D., HUTCHISON, E. K., ÇETINKAYA, A., JABBAR, J. P., ROHRER, M., SCHÖLLER & SMITH., P. 2010. Resilience and Survivability in Communication Networks: Strategies, Principles, and Survey of Disciplines. *Computer Networks,* 54**,** 1245-1265.

SULLIVAN, J. L., NOVAK, D. C., AULTMAN-HALL, L. & SCOTT, D. M. 2010. Identifying critical road segments and measuring system-wide robustness in transportation networks with isolating links: A link-based capacity-reduction approach. *Transportation Research Part A: Policy and Practice,* 44**,** 323-336.

SUN, X., WANDELT, S. & LINKE, F. 2014. Topological Properties of the Air Navigation Route System using Complex Network Theory. *in the 6th International Conference on Research in Air Transportation (ICRAT2014)***,** 2014:Istanbu Technical University, Turkey.

TAHMASSEBY, S. & VAN NES, R. 2007. Robustness Of Urban Public Transport Networks *Transactions on the Built Environment,* 96**,** 337-346.

TAYLOR, MICHAEL A. P. , SEKHAR, S. V. C. & D'ESTE, G. M. 2006. Application of Accessibility Based Methods for Vulnerability Analysis of Strategic Road Networks. *Networks and Spatial Economics,* 6**,** 267-291.

TRANSPORT BUREAU 1998. Third comprehensive transport study—Consultation document *June 1998, Government Printing, Government of Hong Kong Special Administrative Region of the Peoples' Republic of China, Hong Kong*.

TURNER, M., ROMME, W., GARDNER, R., O'NEILL, R. & KRATZ, T. 1993. A revised concept of landscape equilibrium: disturbance and stability on scaled landscapes. *Landsc Ecol,* 8.

UNITED NATIONS DISASTER RELIEF CO-ORDINATOR (UNDRO) 1980. Natural disasters and vulnerability analysis. *Report of Experts Group, meeting of 9–12 July 1979. Geneva: UNDRO.* .

UNITED NATIONS INTERNATIONAL STRATEGY FOR DISASTER REDUCTION (UNISDR) 2004. Living With risk. A global review of disaster reduction initiatives. *Geneva: UNISDR*.

UNITED STATES CENSUS BUREAU 2010. US Gazetteer files 2010. http://www.census.gov/geo/www/gazetteer/files Accessed 15/11/2016.

UNITED STATES CENSUS BUREAU 2015a. Anaheim (city) QuickFacts. http://www.census.gov/quickfacts/table/PST045215/00 Accessed 02/06/2016.

UNITED STATES CENSUS BUREAU 2015b. Estimates of Resident Population Change and Rankings: July 1, 2014 to July 1, 2015 – United States – Metropolitan Statistical Area; and for Puerto Rico 2015 Population Estimates. *U.S. Census Bureau, Population Division*.

URRUTY, N., TAILLIEZ-LEFEBVRE, D. & HUYGHE, C. 2016. Stability, robustness, vulnerability and resilience of agricultural systems. A review. *Agronomy for sustainable developmen,* 36.

VAN EXEL, N. J. A. & RIETVELDB, P. 2001. Public transport strikes and traveller behaviour. *Transport Policy,* 8**,** 237–246.

VAN VLIET, D. 1987. The Frank-Wolfe algorithm for equilibrium traffic assignment viewed as a variational inequality. *Transportation Research Part B: Methodological,* 21**,** 87-89.

VÁZQUEZ, A., PASTOR-SATORRAS, R. & VESPIGNANI, A. 2002. Large-scale topological and dynamical properties of the Internet. *Physical Review E,* 65.

VON FERBER, C., HOLOVATCH, T., HOLOVATCH, Y. & PALCHYKOV, V. 2007. Network harness: Metropolis public transport. *Physica A: Statistical Mechanics and its Applications,* 380**,** 585-591.

VON FERBER, C., HOLOVATCH, T., HOLOVATCH, Y. & PALCHYKOV, V. 2009. Public transport networks: empirical analysis and modeling. *The European Physical Journal B,* 68**,** 261-275.

WALTING, D. 1999. Stability of the stochastic equilibrium assignment problem- a dynamical systems approach. *Transportation Research Part B,* 33**,** 281-312.

WANG, J., MO, H., WANG, F. & JIN, F. 2011. Exploring the network structure and nodal centrality of China's air transport network: A complex network approach. *Journal of Transport Geography,* 19**,** 712-721.

WANG, Y., LIU, H., HAN, K., FRIESZ, T. L. & YAO, T. 2015. Day-to-day congestion pricing and network resilience. *Transportmetrica A: Transport Science,* 11**,** 873-895.

WARDROP, J. G. 1952. Some theoretical aspects of road traffic research. *Proceedings of the institution of civil engineers,Part 2***,** 325-378.

WATLING, D. 1999. Stability of the stochastic equilibrium assignment problem- a dynamical systems approach. *Transportation Research Part B,* 33**,** 281-312.

WATLING, D. & HAZELTON, M. L. 2003. The Dynamics and Equilibria of Day-to-Day Assignment Models. *Networks and Spatial Economics,* 3**,** 349-370.

WATTS, D. & STROGATS, S. 1998. Collective dynamics of 'small-world' networks. *Nature,* 393**,** 440-442.

WEBSTER, F. V. 1958. Traffic Signal Settings. *Department of Transport, Road Research Technical Paper N0.39, HMSO, London*.

WEI, P., SPIERS, G. & SUN, D. 2014. Algebraic Connectivity Maximization for Air Transportation Networks. *IEEE TRANSACTIONS ON INTELLIGENT TRANSPORTATION SYSTEMS,* 15**,** 685 - 698

WEI, S., WU, J., ZHOU, S., ZHANG, L., TANG, Z., YIN, Y. Y., KUANG, L. & WU, Z. 2009. Variable message sign and dynamic regional traffic guidance *Intelligent Transportation Systems Magazine, IEEE,* 1**,** 15-21.

WEISSMANN, J. 2015. Population growth in U.S. cities: Austin is blowing away the competition. *Slate Magazine*.

WERNER, S. D., TAYLOR, C. E., CHO, S., LAVOIE, J.-P., HUYCK, C. K., EITZEL, C., EGUCHI, R. T. & MOORE II, J. E. 2005. New Developments in Seismic Risk Analysis of Highway Systems. *In Research Progress and Accomplishments 2003-2004***,** 221-238.

WESEMANN, L., HAMILTON, T., TABAIE, S. & BARE, G. 1996. Cost-of -delay studies for freeway closures caused by northbridge earthquake. *Transportation Research Record,* 1559**,** 67-75.

WINNIPEG TANSPORTATION MASTER PLAN 2011. http://transportation.speakupwinnipeg.com/files/2011/11/2011-11-01-TMPConsultationPanels.pdf Accessed 02/01/2016.

WONG, S. C., YANG, C. & LO, H. K. 2001. A path-based traffic assignment algorithm based on the TRANSYT traffic model. *Transportation Research Part B: Methodological,* 35**,** 163-181.

WU, F. & HUBERMAN, B. A. 2004. Finding communities in linear time: a physics approach. *The European Physical Journal B,* 38**,** 331-338.

WU, J., SUN, H., WANG, D. Z. W., ZHONG, M., HAN, L. & GAO, Z. 2013. Bounded-rationality based day-to-day evolution model for travel behavior analysis of urban railway network. *Transportation Research Part C: Emerging Technologies,* 31**,** 73-82.

XIAO, Z., JIANPING, C. & JIALI, S. 2012. Analysis on topological properties of Beijing urban public transit based on complex network theory. *Acta Phys. Sin,* 61**,** 190510.

XIE, F. & LEVINSON, D. 2011. Evaluating the effects of the I-35W bridge collapse on road-users in the twin cities metropolitan region. *Transportation Planning and Technology,* 34**,** 691-703.

XU, X., HU, J., LIU, F. & LIU, L. 2007. Scaling and correlations in three bus-transport networks of China. *Physica A: Statistical Mechanics and its Applications,* 374**,** 441-448.

YANG, F. 2005. An evolutionary game theory approach to the day-to-day traffic dynamics. *Dissertation, University of Wisconsin-Madison*.

YANG Y & YANG HJ 2008. Complex network-based time series analysis. *Physica A: Statistical Mechanics and its Applications,* 387**,** 1381-1386.

YAZDANI, A. & JEFFREY, P. 2011. Complex network analysis of water distribution systems. *Chaos,* 21**,** 016111.

ZHANG, D. & NAGURNEY, A. 1996. On the local and global stability of a travel route choice adjustment process. *Transportation Research Part B,* 30**,** 245–262.

ZHANG, L. & LEVINSON, D. 2004. An agent-based approach to travel demand modeling: An exploratory analysis. *In Transportation Research Record: Journal of the Transportation Research Board No.1898*.

ZHANG, L. & LEVINSON, D. 2008. Investing for Reliability and Security in Transportation Networks. *Transportation Research Board*.

ZHENG, H., SON, Y.-J., CHIU, Y.-C., HEAD, L., FENG, Y., XI, H., KIM, S. & HICKMAN, M. 2013. A Primer for Agent-Based Simulation and Modeling in Transportation Applications *Technical Report,* (No. FHWA-HRT-13-054).

ZHU, S. & LEVINSON, D. 2012. Disruptions to Transportation Networks: A Review. *D.M. Levinson et al. (eds.), Network Reliability in Practice, Transportation Research, Economics and Policy*, http://link.springer.com/chapter/10.1007%2F978-1-4614-0947-2_2 Accessed 01/02/2016.

ZHU, S. & LEVINSON, D. 2015. Do People Use the Shortest Path? An Empirical Test of Wardrop's First Principle. *PLoS ONE,* 10**,** e0134322.

ZHU, S., LEVINSON, D., LIU, H. X. & HARDER, K. 2010. The traffic and behavioral effects of the I-35W Mississippi River bridge collapse. *Transportation Research Part A: Policy and Practice,* 44**,** 771–784.

ZHU, S., LEVINSON, D. M. & ZHANG, L. 2007. An Agent-Based Route Choice Model Available at SSRN: http://ssrn.com/abstract=1743621 Accessed 02/05/2016.

ZOU, X. & LEVINSON, D. 2006. A Multi-Agent Congestion and Pricing Model. *Transportmetrica,* 2**,** 237-249.

APPENDIX A

This section introduces the algorithms frequently used for the solutions of UE and SO.

A.1 Frank-Wolfe Algorithm

Due to the fact that typical urban road networks have hundreds of nodes and links, it is important to develop solution methods for these traffic assignment models, although there are already many methods to resolve constrained optimization problems.

Frank and Wolfe (1956) developed an algorithm to solve quadratic programming problems with linear constraints. The following introduces how this algorithm handles nonlinear programming problems with convex objective functions.

Given the problem:

$$min\, f(x) \qquad \text{(a.1)}$$

$$\text{Subject to} \quad x \in P$$

Where *f* is convex, *P is* a bounded polygon region.

At each stage in the algorithm the search direction d_k needs to be looked for, and this can be obtained by solving a linear programming problem. The objective function f can be replaced by its first order Taylor expansion around x_k, which is a solution at k^{th} step:

$$Z_k(y) \coloneqq f(x_k) + \nabla f(x_k)^T (y - x_k) \qquad \text{(a.2)}$$

Now the problem is transferred to minimize $Z_k(y)$ subject to $y \in P$.

Due to the fact that the first term of function (a.2) is constant, it can be the following minimization problem:

$$\min Z_k(y) = \nabla f(x_k)^T (y - x_k) \quad \text{(a.3)}$$

Subject to $y \in P$

If y_k is a solution of function (a.3), then it should be the extreme point of the polygon region *P, so* the line between y_k and x_k is contained in *P* since *P* is convex, then $y_k - x_k$ is a feasible direction. It is easy to see that the direction $y_k - x_k$ is descent due to the fact that a necessary condition for a local minimum is inequality, which can be shown as follows:

$$\nabla f(x_k)^T (y - \tilde{x}) \geq 0 \quad \forall y \in P \quad \text{(a.4)}$$

The step-size needs to be determined by choosing α_k to satisfy $f(x_k + \alpha_k d_k) < f(x_k)$. Due to the fact that the step-size is restricted to be less than 1, it can be determined by a line search shown as follows

$$\min_{\alpha[0,1]} f(x_k + \alpha d_k) \quad \text{(a.5)}$$

Then according to (a.5), solution can be update:

$$x_{k+1} \leftarrow x_k + \alpha d_k \quad \text{(a.6)}$$

Van Vliet (1987) pointed out that the standard Frank-Wolfe algorithm can be used to solve the Wardrop equilibrium problem. This algorithm can be formulated as iterative steps.

Table A.1 The iterative process of the Frank-Wolfe algorithm solving Wardrop's equilibrium problem

1.	*n=1*, determine the initial feasible link flows $\boldsymbol{x}^{(1)}$ by using all-or-nothing assignment to least-cost routes;
2.	Calculate link costs based on current link flows: $c^n = c(x^{(n)})$; Calculate all-or-nothing assignment $y^{(n)}$ of demand to current least-cost routes;
3.	Determine step size α^n satisfy $\alpha^n = \mathrm{ArgMin}_\alpha Z(x^{(n)} + \alpha(y^{(n)} - x^{(n)}))$;
4.	Update $x^{(n+1)} = x^{(n)} + \alpha(y^{(n)} - x^{(n)})$;

5.	Set *n=n+1*
6.	If converge then stop; if not, go back to step 2.

A.2 Fixed point Algorithm

In the function shown in (2.14), UE can be written as a variational Inequality (VI) problem, which can be solved by using heuristic methods such as a diagonalization algorithm, a gap function method and a fixed-point algorithm, which are effective ways to resolve the UE problem.

The fixed-point problem is introduced as follows:

The purpose of the fixed point problem $FPP(F, \Lambda)$ is to look for a vector y such that

$$\left.\begin{matrix} y\epsilon\ \Lambda \\ y = F(y) \end{matrix}\right\} FPP(F, \Lambda) \tag{a.7}$$

Where $\boldsymbol{\Lambda}$ is a nonempty set and $\Lambda\ \epsilon\ R^n$, and the function is a projection $F\colon \Lambda \to \Lambda$**.**

In fact, the fixed-point algorithm is based on the minimum norm projection. Similarly, $FPP_{min}(F, \Lambda)$ is looking for vector y such that:

$$\left.\begin{matrix} y\epsilon\ \Lambda \\ y = P_{\Lambda}[y - F(y)]) \end{matrix}\right\} FPP_{min}(F, \Lambda) \tag{a.8}$$

Where $P_{\Lambda}[.]$ is the minimum norm operator. Then, the solution of $FPP_{min}(F, \Lambda)$ can be obtained:

$$y = \arg\{\min||v - F(y) - x|| : x\ \epsilon\ \Lambda\} \tag{a.9}$$

As commented in Friesz (2010), any fixed algorithm problem is able to be specified as:

$$y^{k+1} = G\ (y^k) \tag{a.10}$$

Where k denotes the k^{th} iterative steps.

The fix-point problem based on minimum norm projection, $FPP_{min}(F,\Lambda)$, has been proved that it is equivalent to the vibrational inequality problem $VI(F,\Lambda)$ when the condition $\Lambda\ \epsilon\ R^n$ is satisfied (Friesz, 2010). Following this, function (a.10) can be written as:

$$y^{k+1} = P_\Lambda[y - \varphi F(y^k)]) \tag{a.11}$$

Where φ is an exogenous constant that decides the step-size of each iteration and influences the speed and goodness of convergence.

Function (a.11) can be reformulated such that its right side is shown as follows:

$$\min_{y\epsilon\Lambda} Z^k(y) = \frac{1}{2}\left[y^k - \varphi F(y^k) - y\right]^T\left[y^k - \varphi F(y^k) - y\right] \tag{a.12}$$

$$= \tfrac{1}{2}\left[(\mathrm{y^k} - \mathrm{y}) - \varphi \mathrm{F}(\mathrm{y^k})\right]^{\mathrm{T}}\left[\mathrm{y^k} - \mathrm{y}) - \varphi \mathrm{F}(\mathrm{y^k})\right] \tag{a.13}$$

$$= \tfrac{1}{2}\Big\{(\mathrm{y^k} - \mathrm{y})^{\mathrm{T}}(\mathrm{y^k} - \mathrm{y}) - 2\varphi(\mathrm{y^k} - \mathrm{y})^{\mathrm{T}}\mathrm{F}(\mathrm{y^k}) + \varphi^2\left[F(y^k)\right]^T F(y^k)\Big\} \tag{a.14}$$

Due to the fact that the last term is constant so it can be eliminated, after multiplying $\frac{1}{2\varphi}$, above algorithm can be formulated as :

$$\min_{y\epsilon\Omega}(y^k - y)^T F(y^k) + \frac{1}{2\varphi}(y^k - y)^T(y^k - y) \tag{a.15}$$

Function (a.15) can be further reformulated by eliminating constant terms, then it is expressed as:

$$\min_{y\epsilon\Omega} \frac{1}{2\varphi} y^T y + \left[F(y^k) - \frac{1}{\varphi} y^k\right]^T y \tag{a.16}$$

Similarly, UE problem can be expressed as:

$$\min_{h\epsilon\Omega} \frac{1}{2\varphi} h^T h + \left[c_p(h^k) - \frac{1}{\varphi} h^k\right]^T h \tag{a.17}$$

$$s.t.\begin{cases} h_p \geq 0 \quad \forall p\epsilon P \\ Ah = T \end{cases} \tag{a.18}$$

where $A = \left(\delta_{ij}^{p}\right)$ is the incident matrix, $\delta_{ij}^{p} = \begin{cases} 1 & p \epsilon P_{ij} \\ 0 & otherwise \end{cases}$, $T = T_{ij}$ is the demand matrix.

The Lagrange function can be applied here for the optimal solution based on functions (a.17) and (a.18), and can be formulated as:

$$\min_{h \epsilon \gamma} L(h, \alpha, \beta) = \frac{1}{2\varphi} h^T h + \left[c_p\left(h^k\right) - \frac{1}{\varphi} h^k\right]^T h - \alpha^T h - \beta^T (Ah - T) \qquad \textbf{(a.19)}$$

Where α and β are Lagrange multipliers for the constraints shown in (a.18).

The optimum solution $h^* = (h_p^*)$ of function (a.19) can be obtained by the following functions:

$$\frac{\partial L}{\partial h} = \frac{1}{\varphi} h^* + c_p\left(h^k\right) - \frac{1}{\varphi} h^k - \alpha - \beta \delta_{ij}^{p} = 0 \qquad \forall (i,j) \epsilon W, p \epsilon P \qquad \textbf{(a.20)}$$

$$\alpha \frac{\partial L}{\partial h} = \alpha h^* = 0 \qquad \textbf{(a.21)}$$

$$\alpha \geq 0$$

$$\frac{\partial L}{\partial \alpha} = h^* \geq 0 \qquad \forall p \epsilon P$$

$$\frac{\partial L}{\partial \beta} = \sum_{P} \delta_{ij}^{p} h^* - T_{ij} = 0 \qquad \forall (i,j) \epsilon W, p \epsilon P$$

Based on (a.20), we have:

$$h^* = h^k - \varphi c_p\left(h^k\right) + \varphi(\alpha^* + \beta^* A) \qquad \textbf{(a.22)}$$

Then, according to functions (a.21) and (a.22)

$$\sum_{p \epsilon P_{ij}} \left[h^k - \varphi c_p\left(h^k\right) + v_{ij}\right]_+ = T_{ij} \qquad \forall (i,j) \epsilon W \qquad \textbf{(a.23)}$$

Where v_{ij} is equivalent to $\varphi(\alpha^* + \beta^* A)$, which needs to be searched at each iteration step.

Using functions (a.22) and (a.23), the flow at each step can be obtained; the iteration process stops when all route flow converges at a certain level.

A.3 Dijkstra Algorithm

According to Ahuja et al. (1990), Dijkstra's algorithm a very efficient way to resolve shortest path problems, hence this algorithm is used in this thesis to provide the set of shortest paths of a network by producing a shortest path tree.

The algorithm can be conducted in the following six steps.

Table A.2 Iterative steps of Dijkstra algorithm

1.	Set zero to initial node of the network, and assign infinity to other nodes;
2.	Set initial nodes as current, and all other nodes as unvisited, so the set of all these unvisited nodes is named the unvisited set;
3.	All unvisited neighbours of the current node are considered, and their tentative distances are calculated. For a given node, the smaller value is assigned after a comparison between the newly calculated tentative distance and the current assigned value.
4.	When all neighbours of the current node have been considered, the current node is marked as the visited node and removed from the set of unvisited nodes.;
5.	If the smallest tentative distance for nodes in the set of unvisited nodes is infinity, or the destination node is marked as visited, the algorithm has finished.
6.	Select the unvisited node with the smallest tentative cost, mark it as the new 'current node', and then go back step 3.

APPENDIX B

Table B.1 Values of top 30 nodes based on topological indices and operational indices for Anaheim

Indices / Ranking	*Degree*	*WC*	*CC*	*WBC*	*Eff*	*WEff*	RTC_{UE}^{i}	RTC_{SO}^{i}	$RPOA^{i}$
1	0.0145	4.45e-05	0.0613	0.2361	0.1061	4.26e-05	48.1680	48.8343	1.0226
2	0.0145	4.44e-05	0.0613	0.2343	0.1061	4.27e-05	41.3681	41.9423	1.0226
3	0.0145	4.43e-05	0.0613	0.2122	0.1066	4.31e-05	27.5952	27.9769	1.0226
4	0.0120	4.40e-05	0.0613	0.2021	0.1068	4.31e-05	27.0386	27.4126	1.0209
5	0.0120	4.39e-05	0.0613	0.1979	0.1068	4.32e-05	23.4386	23.7628	1.0209
6	0.0120	4.37e-05	0.0613	0.1921	0.1072	4.33e-05	23.2774	23.6004	1.0209
7	0.0120	4.35e-05	0.0613	0.1871	0.1073	4.33e-05	19.5809	19.8518	1.0202
8	0.0120	4.35e-05	0.0613	0.1692	0.1074	4.33e-05	19.2820	19.5487	1.0202
9	0.0120	4.33e-05	0.0575	0.1681	0.1075	4.34e-05	18.3564	18.6089	1.0202
10	0.0120	4.32e-05	0.0558	0.1621	0.1078	4.35e-05	17.4915	17.7322	1.0200
11	0.0120	4.31e-05	0.0558	0.1602	0.1078	4.35e-05	14.9502	15.1613	1.0200
12	0.0120	4.30e-05	0.0558	0.1535	0.1078	4.35e-05	14.9452	15.1520	1.0200
13	0.0120	4.29e-05	0.0558	0.1531	0.1080	4.35e-05	13.1475	13.3293	1.0198
14	0.0120	4.27e-05	0.0540	0.1526	0.1080	4.36e-05	12.8160	12.9930	1.0196
15	0.0120	4.25e-05	0.0540	0.1435	0.1080	4.36e-05	12.7685	12.9429	1.0195
16	0.0120	4.23e-05	0.0526	0.1418	0.1080	4.36e-05	12.6185	12.7930	1.0195
17	0.0120	4.20e-05	0.0526	0.1363	0.1080	4.36e-05	12.1678	12.3361	1.0195
18	0.0120	4.19e-05	0.0526	0.1335	0.1080	4.36e-05	12.1652	12.3335	1.0192
19	0.0120	4.19e-05	0.0526	0.1317	0.1080	4.36e-05	11.7339	11.8962	1.0191
20	0.0120	4.18e-05	0.0526	0.1280	0.1081	4.37e-05	11.7285	11.8907	1.0188
21	0.0120	4.180e-05	0.0526	0.1258	0.1081	4.37e-05	11.4210	11.5821	1.0186
22	0.0120	4.14e-05	0.0489	0.1212	0.1081	4.37e-05	11.4089	11.5668	1.0185
23	0.0120	4.14e-05	0.0489	0.1199	0.1081	4.37e-05	11.1235	11.2774	1.0178
24	0.0120	4.13e-05	0.0466	0.1177	0.1081	4.37e-05	10.6587	10.8068	1.0178
25	0.0120	4.13e-05	0.0466	0.1165	0.1081	4.37e-05	10.6546	10.8020	1.0176
26	0.0120	4.12e-05	0.0466	0.1083	0.1081	4.38e-05	10.6287	10.7757	1.0176
27	0.0096	4.11e-05	0.0466	0.1013	0.1081	4.38e-05	10.5469	10.6930	1.0176

28	0.0096	4.11e-05	0.0466	0.1002	0.1081	4.38e-05	10.5428	10.6886	1.0170
29	0.0096	4.11e-05	0.0466	0.0981	0.1082	4.38e-05	10.2990	10.4415	1.0170
30	0.0096	4.11e-05	0.0466	0.0964	0.1082	4.38e-05	9.5177	9.6493	1.0170

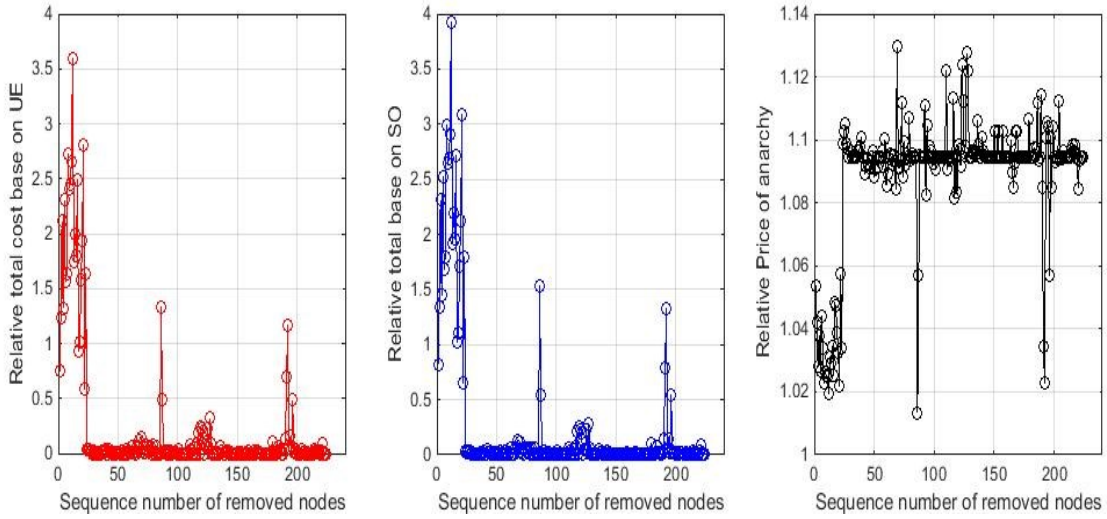

Fig.B.1 Evolution of RTC^i_{UE}, RTC^i_{SO} and $RPOA^i$ of Friedrichshain when nodes are removed

Table B.2 The values of Top 30 nodes based on topological indices and operational indices for Friedrichshain

Indices / Ranking	*Degree*	*WC*	*CC*	*WBC*	*Eff*	*WEff*	RTC^i_{UE}	RTC^i_{SO}	$RPOA^i$
1	190	13	122	20	190	190	3.5914	3.9284	1.1295
2	201	68	221	21	50	20	2.8120	3.0836	1.1276
3	99	72	83	190	66	21	2.7285	2.9892	1.1237
4	127	128	214	3	51	1	2.6547	2.9042	1.1221
5	1	220	135	17	64	17	2.4857	2.7206	1.1221
6	2	69	118	15	184	22	2.4504	2.6841	1.1145

7	3	12	133	13	192	159	2.4133	2.6402	1.1132
8	4	92	129	12	45	8	2.3076	2.5257	1.1125
9	5	94	218	16	151	16	2.1125	2.3127	1.1125
10	6	126	94	1	42	2	2.0006	2.1911	1.1121
11	7	127	121	14	88	7	1.9420	2.11889	1.1120
12	8	7	206	4	127	99	1.8006	1.9627	1.1109
13	9	20	128	5	24	201	1.7441	1.9125	1.1070
14	10	21	58	2	67	3	1.6374	1.7924	1.1063
15	11	22	106	9	201	4	1.6373	1.7921	1.1061
16	12	52	95	8	204	5	1.5779	1.7166	1.1058
17	13	53	210	10	39	6	1.5615	1.6853	1.1049
18	14	60	101	11	125	10	1.3400	1.5270	1.1044
19	15	65	142	6	86	11	1.3220	1.4485	1.1044
20	16	179	220	23	194	12	1.2323	1.3443	1.1044
21	17	190	132	22	176	13	1.1742	1.3263	1.1029
22	18	200	84	159	57	14	1.0160	1.1070	1.1028
23	19	201	197	53	38	15	0.9319	1.0173	1.1028
24	20	202	199	31	53	19	0.7524	0.8200	1.1028
25	21	206	100	19	159	23	0.6954	0.7941	1.1028
26	22	208	107	208	27	9	0.5924	0.6485	1.1028
27	23	59	134	18	20	18	0.4869	0.5393	1.1009
28	31	66	109	62	44	179	0.4869	0.5393	1.1009
29	32	67	192	201	149	200	0.3223	0.2835	1.1009
30	39	64	97	68	69	31	0.2474	0.2603	1.1009

Table B.3 Top 30 nodes based on topological indices and operational indices for Friedrichshain

Indices / Ranking	*Degree*	*WC*	*CC*	*WBC*	*Eff*	*WEff*	RTC_{UE}^{i}	RTC_{SO}^{i}	$RPOA^{i}$
1	190	13	122	20	190	190	12	12	69

2	201	68	221	21	50	20	21	21	127
3	99	72	83	190	66	21	8	8	123
4	127	128	214	3	51	1	11	11	128
5	1	220	135	17	64	17	16	16	110
6	2	69	118	15	184	22	10	10	189
7	3	12	133	13	192	159	9	9	116
8	4	92	129	12	45	8	5	5	124
9	5	94	218	16	151	16	3	3	204
10	6	126	94	1	42	2	14	14	73
11	7	127	121	14	88	7	20	20	186
12	8	7	206	4	127	99	15	15	92
13	9	20	128	5	24	201	13	13	79
14	10	21	58	2	67	3	7	23	179
15	11	22	106	9	201	4	23	7	136
16	12	52	95	8	204	5	19	19	194
17	13	53	210	10	39	6	6	6	26
18	14	60	101	11	125	10	86	86	94
19	15	65	142	6	86	11	4	4	195
20	16	179	220	23	194	12	2	2	199
21	17	190	132	22	176	13	192	192	25
22	18	200	84	159	57	14	18	18	150
23	19	201	197	53	38	15	17	17	153
24	20	202	199	31	53	19	1	1	157
25	21	206	100	19	159	23	191	191	168
26	22	208	107	208	27	9	22	22	169
27	23	59	134	18	20	18	87	87	193
28	31	66	109	62	44	179	196	196	197
29	32	67	192	201	149	200	127	127	39
30	39	64	97	68	69	31	119	119	140

Table B.4 Spearman correlations between any indices pairs for Friedrichshain

	Degree	*WCC*	*CC*	*WBC*	*Eff*	*WEff*	RTC_{UE}^{i}	RTC_{SO}^{i}	$RPOA^{i}$
Degree	1	0.4566	0.0353	0.6479	-0.4199	-0.6641	0.5281	0.5281	-0.2000
WCC	0.4566	1	0.0278	0.3697	-0.3230	-0.4987	0.2947	0.3083	-0.0436
CC	0.0353	0.0278	1	0.0900	-0.0896	0.1740	0.0150	0.0224	0.1835
WBC	0.6479	0.3697	0.0900	1	-0.5075	-0.4770	0.6305	0.6418	-0.1917
Eff	-0.4199	-0.3230	-0.0896	-0.5075	1	0.0718	-0.3765	-0.4024	-0.0689
WEff	-0.6641	-0.4987	0.1740	-0.4770	0.0718	1	-0.4302	-0.4322	0.2612
RTC_{UE}^{i}	0.5281	0.2947	0.0150	0.6305	-0.3765	-0.4302	1	0.9806	-0.0788
RTC_{SO}^{i}	0.5281	0.3083	0.0224	0.6418	-0.4024	-0.4322	0.9806	1	-0.1603
$RPOA^{i}$	-0.2000	-0.0436	0.1835	-0.1917	-0.0689	0.2612	-0.0788	-0.1603	1

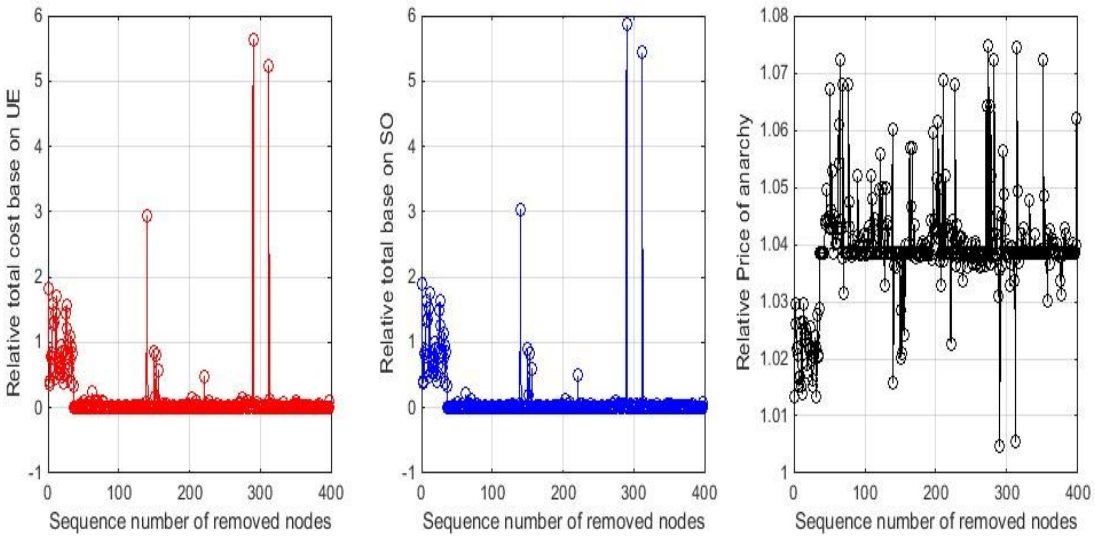

Fig.B.2 Evolution of RTC_{UE}^{i}, RTC_{SO}^{i} and $RPOA^{i}$ of Mitte when nodes are removed

Table B.5 The values of top 30 nodes based on topological indices and operational indices for Mitte

Indices / Ranking	*Degree*	*WC*	*CC*	*WBC*	*Eff*	*WEff*	RTC_{UE}^{i}	RTC_{SO}^{i}	$RPOA^{i}$
1	190	13	122	20	190	190	5.6386	5.8620	1.0747
2	201	68	221	21	50	20	5.2288	5.4328	1.0746
3	99	72	83	190	66	21	2.9447	3.0326	1.0723
4	127	128	214	3	51	1	1.8194	1.8893	1.0723
5	1	220	135	17	64	17	1.7013	1.7667	1.0723
6	2	69	118	15	184	22	1.5886	1.6476	1.0688
7	3	12	133	13	192	159	1.5718	1.6308	1.0681
8	4	92	129	12	45	8	1.4537	1.5071	1.0681
9	5	94	218	16	151	16	1.4514	1.4983	1.0681
10	6	126	94	1	42	2	1.3108	1.3596	1.0673
11	7	127	121	14	88	7	1.2851	1.3345	1.0643
12	8	7	206	4	127	99	1.2005	1.2481	1.0643
13	9	20	128	5	24	201	1.0930	1.1450	1.0620
14	10	21	58	2	67	3	1.0240	1.0598	1.0615
15	11	22	106	9	201	4	0.9612	0.9984	1.0610
16	12	52	95	8	204	5	0.9226	0.9567	1.0602
17	13	53	210	10	39	6	0.8654	0.8961	1.0597
18	14	60	101	11	125	10	0.8611	0.8944	1.0568
19	15	65	142	6	86	11	0.8439	0.8788	1.0568
20	16	179	220	23	194	12	0.8414	0.8758	1.0564
21	17	190	132	22	176	13	0.8304	0.8611	1.0558
22	18	200	84	159	57	14	0.8259	0.8576	1.0542
23	19	201	197	53	38	15	0.7983	0.8292	1.0529
24	20	202	199	31	53	19	0.7955	0.8247	1.0521
25	21	206	100	19	159	23	0.7612	0.7896	1.0521
26	22	208	107	208	27	9	0.7338	0.7546	1.0520
27	23	59	134	18	20	18	0.7268	0.7544	1.0519
28	31	66	109	62	44	179	0.6099	0.6320	1.0514
29	32	67	192	201	149	200	0.6072	0.6308	1.0498

30	39	64	97	68	69	31	0.5982	0.6211	1.0498

Table B.6 Top 30 nodes based on topological indices and operational indices for Mitte

Indices / Ranking	*Degree*	*WC*	*CC*	*WBC*	*Eff*	*WEff*	RTC_{UE}^{i}	RTC_{SO}^{i}	$RPOA^{i}$
1	287	234	313	9	290	32	290	290	274
2	79	141	116	4	312	17	312	312	314
3	129	293	309	7	63	36	140	140	282
4	226	7	289	14	51	270	1	1	351
5	253	50	392	22	85	18	12	12	65
6	315	51	110	15	223	240	7	7	210
7	331	55	297	11	295	70	26	26	69
8	1	59	174	27	140	268	25	10	77
9	2	54	42	25	100	16	10	25	227
10	3	4	321	32	81	317	9	9	51
11	4	23	374	23	158	24	8	8	271
12	5	222	119	231	79	31	27	27	277
13	6	224	172	6	54	33	32	32	398
14	7	226	107	13	300	2	28	28	203
15	8	231	311	2	366	5	18	18	63
16	9	232	97	8	314	19	34	34	139
17	10	263	73	51	150	22	21	21	196
18	11	19	254	1	296	25	150	150	163
19	12	22	118	17	153	26	6	19	167
20	13	228	201	3	301	29	19	6	295
21	14	285	292	24	203	30	29	29	122
22	15	286	115	26	91	287	35	35	64
23	16	287	310	21	358	332	153	153	54
24	17	291	352	19	46	156	4	4	109

25	18	292	136	34	129	255	5	5	278
26	19	357	101	362	170	4	13	31	213
27	20	239	133	20	287	23	31	13	90
28	21	202	117	36	156	75	15	15	201
29	22	288	230	63	122	241	16	16	125
30	23	6	332	16	327	267	30	30	130

Table B.7 Spearman correlations between any indices pairs for Mitte

	Degree	*WCC*	*CC*	*WBC*	*Eff*	*WEff*	RTC_{UE}^{i}	RTC_{SO}^{i}	$RPOA^{i}$
Degree	1	0.4048	0.1286	0.5322	-0.2966	-0.6469	0.4271	0.4307	-0.2311
WCC	0.4048	1	0.0496	0.4661	-0.3374	-0.4785	0.3790	0.3878	0.0170
CC	0.1286	0.0496	1	0.0561	-0.0604	0.0464	-0.0087	-0.0039	0.1086
WBC	0.5322	0.4661	0.0561	1	-0.5271	-0.3607	0.7614	0.7746	-0.1412
Eff	-0.2966	-0.3374	-0.0604	-0.5271	1	-0.0844	-0.4959	-0.5148	-0.2389
WEff	-0.6469	-0.4785	0.0464	-0.3607	-0.0844	1	-0.3609	-0.3622	0.3259
RTC_{UE}^{i}	0.4271	0.3790	-0.0087	0.7614	-0.4959	-0.3609	1	0.9861	-0.0022
RTC_{SO}^{i}	0.4307	0.3878	-0.0039	0.7746	-0.5148	-0.3622	0.9861	1	-0.0727
$RPOA^{i}$	-0.2311	0.0170	0.1086	-0.1412	-0.2389	0.3259	-0.0022	-0.0727	1

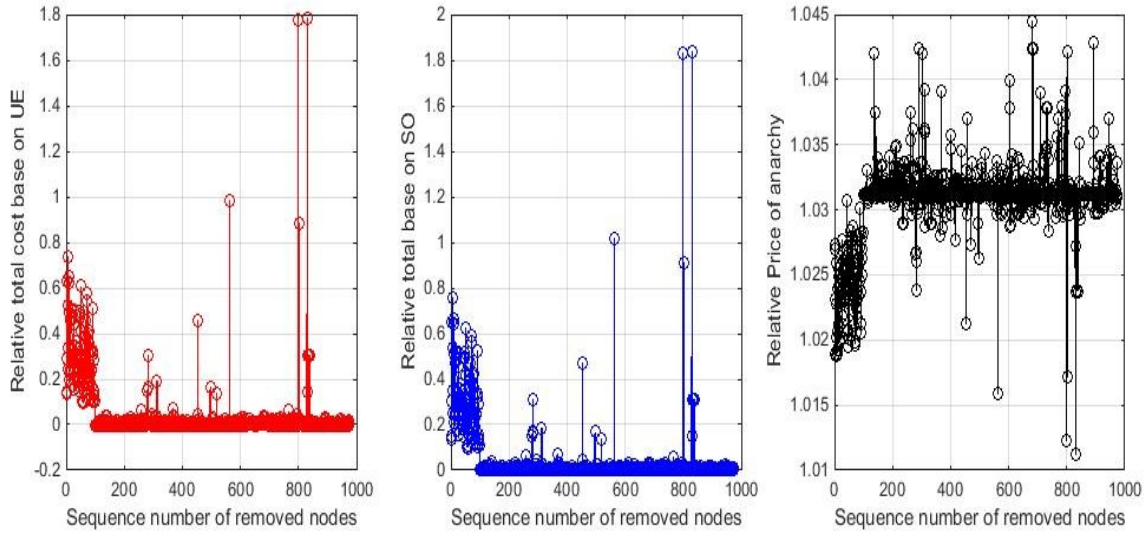

Fig.B.3 Evolution of $RTC_{UE}^{i}, RTC_{SO}^{i}$ and $RPOA^{i}$ of MFT when nodes are removed

Table B.8 The values of top 30 nodes based on topological indices and operational indices for MPF

Indices / Ranking	*Degree*	*WC*	*CC*	*WBC*	*Eff*	*WEff*	RTC_{UE}^{i}	RTC_{SO}^{i}	$RPOA^{i}$
1	611	27	503	272	799	79	1.7821	1.8376	1.0445
2	711	60	624	82	830	38	1.7754	1.8276	1.0428
3	796	63	405	9	802	96	0.9860	1.0161	1.0424
4	269	86	831	63	768	779	0.8848	0.9112	1.0424
5	272	132	965	60	258	39	0.7379	0.7592	1.0424
6	303	200	439	57	139	738	0.6470	0.6666	1.0421
7	370	203	827	50	223	294	0.6323	0.6523	1.0421
8	463	263	798	67	313	777	0.6253	0.6451	1.0420
9	479	265	873	91	707	37	0.6084	0.6261	1.0400
10	508	267	940	26	564	846	0.5742	0.5923	1.0392
11	518	268	961	76	318	45	0.5457	0.5632	1.0391
12	612	272	516	25	945	611	0.5222	0.5387	1.03901
13	719	273	499	27	534	78	0.5085	0.5245	1.0390
14	751	310	514	24	577	80	0.5029	0.5195	1.0380
15	844	323	510	74	288	65	0.5027	0.5192	1.0379

16	860	174	431	48	809	63	0.4992	0.5149	1.0379
17	1	50	811	46	314	91	0.4921	0.5076	1.0378
18	2	67	955	75	496	272	0.4826	0.4980	1.0375
19	3	139	657	92	282	60	0.4719	0.4884	1.0375
20	4	552	104	62	283	92	0.4704	0.4873	1.0374
21	5	583	850	8	677	29	0.4703	0.4852	1.0370
22	6	584	914	14	177	52	0.4655	0.4802	1.0370
23	7	586	442	15	280	27	0.4568	0.4713	1.0370
24	8	587	445	77	231	268	0.4560	0.4704	1.0362
25	9	617	655	61	305	64	0.4555	0.4699	1.0362
26	10	142	383	83	455	66	0.4409	0.4543	1.0360
27	11	177	285	44	774	62	0.4087	0.4216	1.0359
28	12	135	617	6	737	17	0.4083	0.4196	1.0359
29	13	291	829	29	695	88	0.4013	0.4142	1.0357
30	14	288	502	88	366	264	0.3994	0.4137	1.0356

Table B.9 Top 30 nodes based on topological indices and operational indices for MPF

Indices / Ranking	*Degree*	*WC*	*CC*	*WBC*	*Eff*	*WEff*	RTC_{UE}^{i}	RTC_{SO}^{i}	$RPOA^{i}$
1	611	27	503	272	799	79	830	830	681
2	711	60	624	82	830	38	799	799	893
3	796	63	405	9	802	96	564	564	291
4	269	86	831	63	768	779	802	802	682
5	272	132	965	60	258	39	7	7	683
6	303	200	439	57	139	738	9	9	801
7	370	203	827	50	223	294	1	1	303
8	463	263	798	67	313	777	12	12	135
9	479	265	873	91	707	37	52	52	603
10	508	267	940	26	564	846	70	70	311
11	518	268	961	76	318	45	73	73	368

12	612	272	516	25	945	611	8	8	796
13	719	273	499	27	534	78	92	92	708
14	751	310	514	24	577	80	26	20	783
15	844	323	510	74	288	65	20	26	729
16	860	174	431	48	809	63	47	47	733
17	1	50	811	46	314	91	10	10	604
18	2	67	955	75	496	272	46	46	142
19	3	139	657	92	282	60	17	17	263
20	4	552	104	62	283	92	18	48	795
21	5	583	850	8	677	29	48	18	945
22	6	584	914	14	177	52	19	19	456
23	7	586	442	15	280	27	67	67	772
24	8	587	445	77	231	268	454	454	310
25	9	617	655	61	305	64	16	16	269
26	10	142	383	83	455	66	28	28	313
27	11	177	285	44	774	62	50	81	791
28	12	135	617	6	737	17	81	50	891
29	13	291	829	29	695	88	62	75	402
30	14	288	502	88	366	264	75	62	768

Table B.10 Spearman correlations between any indices pairs for MPF

	Degree	*WCC*	*CC*	*WBC*	*Eff*	*WEff*	RTC_{UE}^{i}	RTC_{SO}^{i}	$RPOA^{i}$
Degree	1	0.2743	0.1129	0.5600	-0.2612	-0.6610	0.4646	0.4669	-0.2151
WCC	0.2743	1	-0.0192	0.3533	-0.3647	-0.3111	0.3150	0.3119	0.0934
CC	0.1129	-0.0192	1	0.0268	-0.0777	0.0978	-0.0254	-0.0391	0.0967
WBC	0.5600	0.3533	0.0268	1	-0.4039	-0.3946	0.7382	0.7447	-0.1975
Eff	-0.2612	-0.3647	-0.0777	-0.4039	1	-0.1216	-0.4237	-0.4307	-0.1775
WEff	-0.6610	-0.3111	0.0978	-0.3946	-0.1216	1	-0.3709	-0.3704	0.2571

RTC_{UE}^{i}	0.4646	0.3150	-0.0254	0.7382	-0.4237	-0.3709	1	0.9837	-0.0599
RTC_{SO}^{i}	0.4669	0.3119	-0.0391	0.7447	-0.4307	-0.3704	0.9837	1	-0.1383
$RPOA^{i}$	-0.2151	0.0934	0.0967	-0.1975	-0.1775	0.2571	-0.0599	-0.1383	1

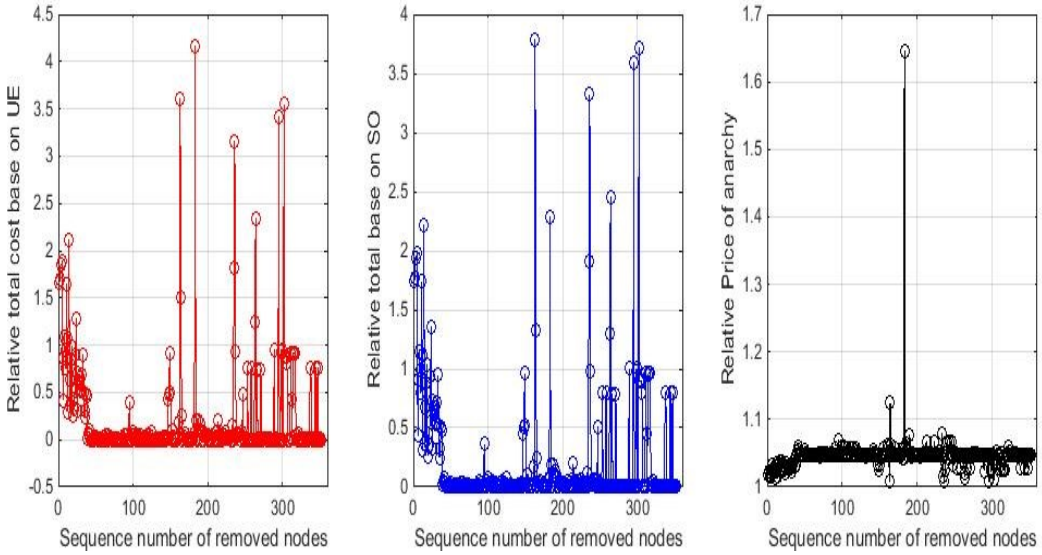

Fig.B.4 Evolution of $RTC_{UE}^{i}, RTC_{SO}^{i}$ and $RPOA^{i}$ of Prenzlauerberg when nodes are removed

Table B.11 The values of top 30 nodes based on topological indices and operational indices for Prenzlauerberg.

Indices / Ranking	*Degree*	*WC*	*CC*	*WBC*	*Eff*	*WEff*	RTC_{UE}^{i}	RTC_{SO}^{i}	$RPOA^{i}$
1	136	21	204	24	264	27	4.1636	3.7886	1.6464
2	139	23	323	28	302	25	3.6049	3.7187	1.1251
3	187	24	152	27	263	139	3.5462	3.5878	1.0787
4	1	97	265	31	295	22	3.4112	3.3203	1.0764
5	2	99	271	26	163	14	3.1542	2.4523	1.0704

6	3	131	200	35	236	12	2.3401	2.2877	1.0670
7	4	133	312	15	42	135	2.1179	2.2197	1.0670
8	5	136	256	2	266	26	1.8886	1.9800	1.0670
9	6	137	202	20	155	28	1.8523	1.9418	1.0669
10	7	238	266	33	183	24	1.8508	1.9370	1.0662
11	8	284	264	19	154	2	1.8237	1.9115	1.0643
12	9	103	172	14	141	131	1.6950	1.7647	1.0641
13	10	94	144	5	95	68	1.6610	1.7413	1.0628
14	11	26	170	16	149	251	1.6466	1.7366	1.0627
15	12	27	173	4	40	187	1.4984	1.3497	1.0606
16	13	28	311	18	119	10	1.2870	1.3280	1.0598
17	14	68	316	21	235	11	1.2416	1.3028	1.0596
18	15	69	183	68	91	16	1.0959	1.1490	1.0594
19	16	70	190	251	147	19	1.0697	1.1212	1.0586
20	17	85	165	23	170	20	0.9859	1.0360	1.0581
21	18	107	235	131	247	32	0.9553	1.0015	1.0577
22	19	249	267	97	253	15	0.9553	1.0015	1.0572
23	20	251	82	107	344	34	0.9521	0.9981	1.0572
24	21	254	83	29	150	100	0.9359	0.9811	1.0571
25	22	255	268	187	190	144	0.9359	0.9811	1.0571
26	23	283	269	13	145	295	0.9164	0.9607	1.0569
27	24	105	270	6	86	21	0.9164	0.9607	1.0566
28	25	98	239	3	196	23	0.9160	0.9603	1.0562
29	26	88	263	10	347	1	0.9151	0.9593	1.0561
30	27	95	164	122	71	3	0.9145	0.9587	1.0554

Table B.12 Top 30 nodes based on topological indices and operational indices for Prenzlauerberg

Indices / Ranking	*Degree*	*WC*	*CC*	*WBC*	*Eff*	*WEff*	RTC_{UE}^{i}	RTC_{SO}^{i}	$RPOA^{i}$
1	136	21	204	24	264	27	183	163	183
2	139	23	323	28	302	25	163	302	164
3	187	24	152	27	263	139	302	295	233
4	1	97	265	31	295	22	295	236	190
5	2	99	271	26	163	14	236	264	95
6	3	131	200	35	236	12	264	183	212
7	4	133	312	15	42	135	14	14	223
8	5	136	256	2	266	26	5	5	246
9	6	137	202	20	155	28	3	3	243
10	7	238	266	33	183	24	4	4	240
11	8	284	264	19	154	2	235	235	185
12	9	103	172	14	141	131	2	2	239
13	10	94	144	5	95	68	1	1	161
14	11	26	170	16	149	251	11	11	165
15	12	27	173	4	40	187	164	24	42
16	13	28	311	18	119	10	24	164	321
17	14	68	316	21	235	11	263	263	162
18	15	69	183	68	91	16	8	8	100
19	16	70	190	251	147	19	13	13	102
20	17	85	165	23	170	20	18	18	91
21	18	107	235	131	247	32	289	289	106
22	19	249	267	97	253	15	299	299	111
23	20	251	82	107	344	34	9	9	114
24	21	254	83	29	150	100	237	298	180
25	22	255	268	187	190	144	298	237	184
26	23	283	269	13	145	295	316	316	170
27	24	105	270	6	86	21	317	317	154
28	25	98	239	3	196	23	315	315	187
29	26	88	263	10	347	1	311	311	119

30	27	95	164	122	71	3	149	149	141

Table B.13 Spearman correlations between any indices pairs for Prenzlauerberg

	Degree	*WCC*	*CC*	*WBC*	*Eff*	*WEff*	RTC_{UE}^{i}	RTC_{SO}^{i}	$RPOA^{i}$
Degree	1	0.4664	0.1405	0.6298	-0.4326	-0.6926	0.4851	0.4879	-0.3043
WCC	0.4664	1	-0.0117	0.3052	-0.2727	-0.4867	0.1402	0.1319	-0.0333
CC	0.1405	-0.0117	1	0.0001	-0.1845	0.0950	0.0744	0.0769	-0.0231
WBC	0.6298	0.3052	0.0001	1	-0.5512	-0.4064	0.6546	0.6670	-0.2839
Eff	-0.4326	-0.2727	-0.1845	-0.5512	1	-0.0148	-0.5813	-0.5893	0.09180
WEff	-0.6926	-0.4867	0.0950	-0.4064	-0.0148	1	-0.2475	-0.2401	0.3234
RTC_{UE}^{i}	0.4851	0.1402	0.0744	0.6546	-0.5813	-0.2475	1	0.9897	-0.4391
RTC_{SO}^{i}	0.4879	0.1319	0.0769	0.6670	-0.5893	-0.2401	0.9897	1	-0.4837
$RPOA^{i}$	-0.3043	-0.0333	-0.0231	-0.2839	0.0918	0.3234	-0.4391	-0.4837	1

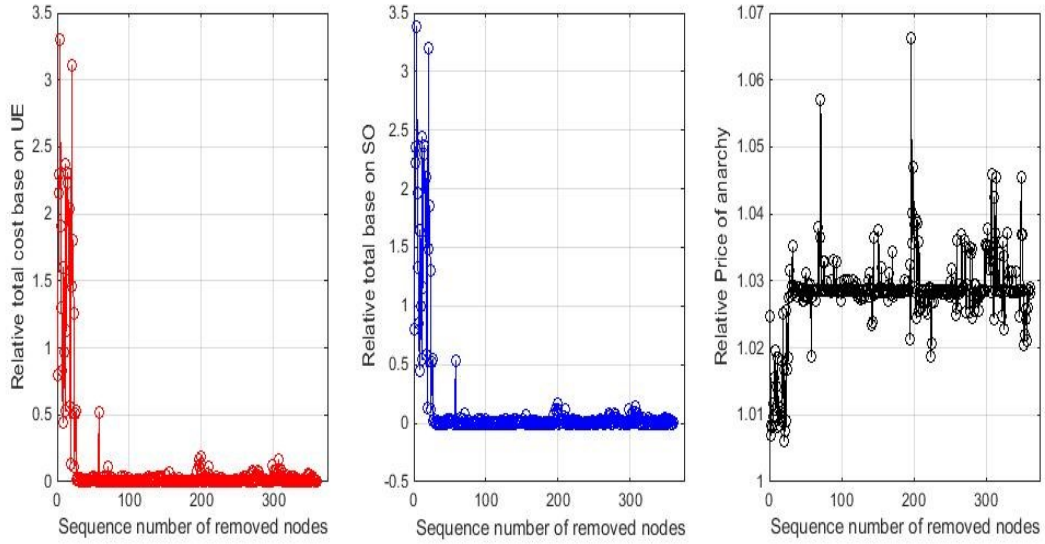

Fig.B.5 Evolution of RTC_{UE}^{i}, RTC_{SO}^{i} and $RPOA^{i}$ of Tiergarten when nodes are removed

Table B.14 Top 30 nodes based on topological indices and operational indices for Tiergarten

Indices / Ranking	*Degree*	*WC*	*CC*	*WBC*	*Eff*	*WEff*	RTC_{UE}^{i}	RTC_{SO}^{i}	$RPOA^{i}$
1	65	5	169	23	127	13	3.3001	3.3851	1.0663
2	89	264	166	17	93	2	3.1100	3.2007	1.0570
3	204	270	265	22	131	3	2.3756	2.4426	1.0471
4	215	272	216	19	147	16	2.3086	2.3736	1.0459
5	1	273	286	8	129	20	2.2913	2.3609	1.0455
6	2	271	112	7	49	22	2.2339	2.2890	1.0455
7	3	280	274	16	48	23	2.1570	2.2188	1.0425
8	4	284	324	3	46	21	2.0392	2.0969	1.0402
9	5	278	64	14	47	206	1.9057	1.9593	1.0391
10	6	53	190	5	115	25	1.7988	1.8563	1.0386
11	7	281	42	352	51	155	1.6019	1.6469	1.0384
12	8	51	264	2	165	209	1.5086	1.5533	1.0379
13	9	263	233	18	50	352	1.4657	1.4935	1.0378
14	10	262	213	11	272	10	1.2968	1.3343	1.0375
15	11	19	167	54	52	24	1.2578	1.3006	1.0371
16	12	46	165	57	53	1	1.1276	1.1603	1.0371
17	13	49	235	50	149	4	0.9692	0.9963	1.0368
18	14	334	236	51	271	5	0.8312	0.8544	1.0368
19	15	337	219	4	76	6	0.7921	0.7984	1.0368
20	16	47	164	127	278	7	0.5611	0.5769	1.0365
21	17	279	170	15	164	8	0.5298	0.5445	1.0365
22	18	17	288	10	167	9	0.5254	0.5400	1.0361
23	19	140	290	20	111	11	0.5225	0.5368	1.0361
24	20	142	206	6	75	12	0.5100	0.5271	1.0359
25	21	149	209	138	122	14	0.4409	0.4533	1.0359
26	22	151	257	129	196	15	0.1879	0.1666	1.0357
27	23	152	258	49	191	17	0.1656	0.1459	1.0355

28	24	144	326	26	330	18	0.1631	0.1359	1.0352
29	26	143	218	140	360	19	0.1323	0.1217	1.0352
30	71	6	56	1	331	26	0.1291	0.1181	1.0352

Table B.15 Top 30 nodes based on topological indices and operational indices for Tiergarten

Indices / Ranking	*Degree*	*WC*	*CC*	*WBC*	*Eff*	*WEff*	RTC_{UE}^{i}	RTC_{SO}^{i}	$RPOA^{i}$
1	65	5	169	23	127	13	4	4	196
2	89	264	166	17	93	2	20	20	71
3	204	270	265	22	131	3	12	12	199
4	215	272	216	19	147	16	14	14	307
5	1	273	286	8	129	20	2	2	314
6	2	271	112	7	49	22	15	15	348
7	3	280	274	16	48	23	3	3	311
8	4	284	324	3	46	21	17	17	197
9	5	278	64	14	47	206	5	5	204
10	6	53	190	5	115	25	22	22	205
11	7	281	42	352	51	155	9	9	200
12	8	51	264	2	165	209	16	16	68
13	9	263	233	18	50	352	21	21	302
14	10	262	213	11	272	10	6	6	151
15	11	19	167	54	52	24	23	23	312
16	12	46	165	57	53	1	13	13	329
17	13	49	235	50	149	4	10	10	266
18	14	334	236	51	271	5	7	7	349
19	15	337	219	4	76	6	1	1	350
20	16	47	164	127	278	7	18	18	70

21	17	279	170	15	164	8	26	26	144
22	18	17	288	10	167	9	11	11	270
23	19	140	290	20	111	11	58	58	259
24	20	142	206	6	75	12	25	25	207
25	21	149	209	138	122	14	8	8	323
26	22	151	257	129	196	15	199	199	198
27	23	152	258	49	191	17	307	307	298
28	24	144	326	26	330	18	196	19	300
29	26	143	218	140	360	19	19	196	301
30	71	6	56	1	331	26	200	200	305

Table B.16 Spearman correlations between any indices pairs for Tiergarten

	Degree	*WCC*	*CC*	*WBC*	*Eff*	*WEff*	RTC_{UE}^{i}	RTC_{SO}^{i}	$RPOA^{i}$
Degree	1	0.3147	0.0975	0.4471	-0.2886	-0.6573	0.4380	0.4390	-0.1653
WCC	0.3147	1	-0.0116	0.4833	-0.3719	-0.2326	0.3660	0.3891	-0.0354
CC	0.0975	-0.0116	1	-0.1002	-0.1007	0.0671	-0.0982	-0.0968	0.0540
WBC	0.4471	0.4833	-0.1002	1	-0.5328	-0.2911	0.6787	0.6836	-0.1870
Eff	-0.2886	-0.3719	-0.1007	-0.5328	1	-0.0640	-0.4405	-0.4402	-0.1568
WEff	-0.6573	-0.2326	0.0671	-0.2911	-0.0640	1	-0.3571	-0.3708	0.2726
RTC_{UE}^{i}	0.4380	0.3660	-0.0982	0.6787	-0.4405	-0.3571	1	0.9888	-0.0388
RTC_{SO}^{i}	0.4390	0.3891	-0.0968	0.6836	-0.4402	-0.3708	0.9888	1	-0.1067
$RPOA^{i}$	-0.1653	-0.0354	0.0540	-0.1870	-0.1568	0.2726	-0.0388	-0.1067	1

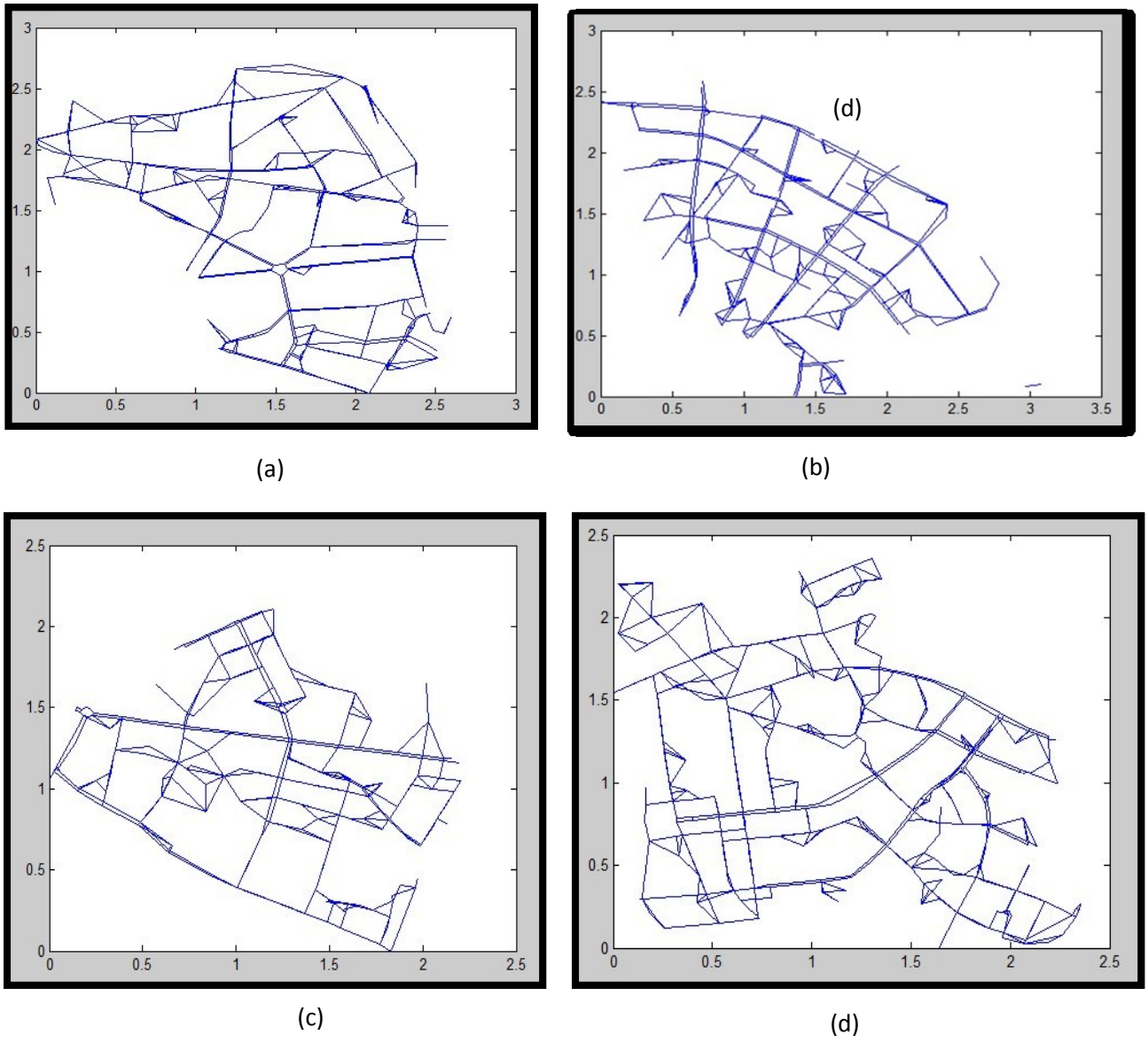

Fig.B.6 Urban road network: (a) Friedrichshain centre; (b) Tiergarten centre; (c) Prenzlauerberg centre; (d) Mitte centre

APPENDIX C

Table C.1 Link parameters of Sioux Falls network

Origin	Destination	Capacity	t_a	b	η
1	2	25900.20064	6	0.15	4
1	3	23403.47319	4	0.15	4
2	1	25900.20064	6	0.15	4
2	6	4958.180928	5	0.15	4
3	1	23403.47319	4	0.15	4
3	4	17110.52372	4	0.15	4
3	12	23403.47319	4	0.15	4
4	3	17110.52372	4	0.15	4
4	5	17782.7941	2	0.15	4
4	11	4908.82673	6	0.15	4
5	4	17782.7941	2	0.15	4
5	6	4947.995469	4	0.15	4
5	9	10000	5	0.15	4
6	2	4958.180928	5	0.15	4
6	5	4947.995469	4	0.15	4
6	8	4898.587646	2	0.15	4
7	8	7841.81131	3	0.15	4
7	18	23403.47319	2	0.15	4
8	6	4898.587646	2	0.15	4
8	7	7841.81131	3	0.15	4
8	9	5050.193156	10	0.15	4
8	16	5045.822583	5	0.15	4
9	5	10000	5	0.15	4

9	8	5050.193156	10	0.15	4
9	10	13915.78842	3	0.15	4
10	9	13915.78842	3	0.15	4
10	11	10000	5	0.15	4
10	15	13512.00155	6	0.15	4
10	16	4854.917717	4	0.15	4
10	17	4993.510694	8	0.15	4
11	4	4908.82673	6	0.15	4
11	10	10000	5	0.15	4
11	12	4908.82673	6	0.15	4
11	14	4876.508287	4	0.15	4
12	3	23403.47319	4	0.15	4
12	11	4908.82673	6	0.15	4
12	13	25900.20064	3	0.15	4
13	12	25900.20064	3	0.15	4
13	24	5091.256152	4	0.15	4
14	11	4876.508287	4	0.15	4
14	15	5127.526119	5	0.15	4
14	23	4924.790605	4	0.15	4
15	10	13512.00155	6	0.15	4
15	14	5127.526119	5	0.15	4
15	19	14564.75315	3	0.15	4
15	22	9599.180565	3	0.15	4
16	8	5045.822583	5	0.15	4
16	10	4854.917717	4	0.15	4
16	17	5229.910063	2	0.15	4

16	18	19679.89671	3	0.15	4
17	10	4993.510694	8	0.15	4
17	16	5229.910063	2	0.15	4
17	19	4823.950831	2	0.15	4
18	7	23403.47319	2	0.15	4
18	16	19679.89671	3	0.15	4
18	20	23403.47319	4	0.15	4
19	15	14564.75315	3	0.15	4
19	17	4823.950831	2	0.15	4
19	20	5002.607563	4	0.15	4
20	18	23403.47319	4	0.15	4
20	19	5002.607563	4	0.15	4
20	21	5059.91234	6	0.15	4
20	22	5075.697193	5	0.15	4
21	20	5059.91234	6	0.15	4
21	22	5229.910063	2	0.15	4
21	24	4885.357564	3	0.15	4
22	15	9599.180565	3	0.15	4
22	20	5075.697193	5	0.15	4
22	21	5229.910063	2	0.15	4
22	23	5000	4	0.15	4
23	14	4924.790605	4	0.15	4
23	22	5000	4	0.15	4
23	24	5078.508436	2	0.15	4
24	13	5091.256152	4	0.15	4
24	21	4885.357564	3	0.15	4

24	23	5078.508436	2	0.15	4

Table C.2 OD demand matrix of the Sioux Falls network

node	1	2	3	4	5	6	7	8	9	10	11	12
1	0	100	100	500	200	300	500	800	500	1300	500	200
2	100	0	100	200	100	400	200	400	200	600	200	100
3	100	100	0	200	100	300	100	200	100	300	300	200
4	500	200	200	0	500	400	400	700	700	1200	1400	600
5	200	100	100	500	0	200	200	500	800	1000	500	200
6	300	400	300	400	200	0	400	800	400	800	400	200
7	500	200	100	400	200	400	0	1000	600	1900	500	700
8	800	400	200	700	500	800	1000	0	800	1600	800	600
9	500	200	100	700	800	400	600	800	0	2800	1400	600
10	1300	600	300	1200	1000	800	1900	1600	2800	0	4000	2000
11	500	200	300	1500	500	400	500	800	1400	3900	0	1400
12	200	100	200	600	200	200	700	600	600	2000	1400	0
13	500	300	100	600	200	200	400	600	600	1900	1000	1300
14	300	100	100	500	100	100	200	400	600	2100	1600	700
15	500	100	100	500	200	200	500	600	1000	4000	1400	700
16	500	400	200	800	500	900	1400	2200	1400	4400	1400	700
17	400	200	100	500	200	500	1000	1400	900	3900	1000	600
18	100	0	0	100	0	100	200	300	200	700	200	200
19	300	100	0	200	100	200	400	700	400	1800	400	300
20	300	100	0	300	100	300	500	900	600	2500	600	500
21	100	0	0	200	100	100	200	400	300	1200	400	300
22	400	100	100	400	200	200	500	500	700	2600	1100	700

23	300	0	100	500	100	100	200	300	500	1800	1300	700
24	100	0	0	200	0	100	100	200	200	800	600	500

node	**13**	**14**	**15**	**16**	**17**	**18**	**19**	**20**	**21**	**22**	**23**
1	500	300	500	500	400	100	300	300	100	400	300
2	300	100	100	400	200	0	100	100	0	100	0
3	100	100	100	200	100	0	0	0	0	100	100
4	600	500	500	800	500	100	200	300	200	400	500
5	200	100	200	500	200	0	100	100	100	200	100
6	200	100	200	900	500	100	200	300	100	200	100
7	400	200	500	1400	1000	200	400	500	200	500	200
8	600	400	600	2200	1400	300	700	900	400	500	300
9	600	600	900	1400	900	200	400	600	300	700	500
10	1900	2100	4000	4400	3900	700	1800	2500	1200	2600	1800
11	1000	1600	1400	1400	1000	100	400	600	400	1100	1300
12	1300	700	700	700	600	200	300	400	300	700	700
13	0	600	700	600	500	100	300	600	600	1300	800
14	600	0	1300	700	700	100	300	500	400	1200	1100
15	700	1300	0	1200	1500	200	800	1100	800	2600	1000
16	600	700	1200	0	2800	500	1300	1600	600	1200	500
17	500	700	1500	2800	0	600	1700	1700	600	1700	600
18	100	100	200	500	600	0	300	400	100	300	100
19	300	300	800	1300	1700	300	0	1200	400	1200	300
20	600	500	1100	1600	1700	400	1200	0	1200	2400	700
21	600	400	800	600	600	100	400	1200	0	1800	700
22	1300	1200	2600	1200	1700	300	1200	2400	1800	0	2100

23	800	1100	1000	500	600	100	300	700	700	2100	0
24	700	400	400	300	300	0	100	400	500	1100	700

Table C.3 Rapidity and RAI as capacity reduction increases for the small network

	Fix-time		P0		Equi-saturation	
Capacity reduction	**Rapidity**	**RAI**	**Rapidity**	**RAI**	**Rapidity**	**RAI**
5%	5	0.0113	9	0.0217	7	0.0122
6%	5	0.0137	9	0.0265	7	0.0149
7%	5	0.0163	9	0.0316	7	0.0177
8%	5	0.0188	9	0.0369	7	0.0205
9%	5	0.0215	10	0.0469	7	0.0235
10%	5	0.0242	10	0.0531	8	0.0302
11%	5	0.0270	10	0.0596	8	0.0338
12%	5	0.0298	10	0.0663	8	0.0375
13%	5	0.0327	10	0.0733	8	0.0413
14%	5	0.0357	10	0.0805	8	0.0453
15%	5	0.0388	10	0.0879	8	0.0494
16%	5	0.0419	10	0.0955	8	0.0536
17%	5	0.0451	10	0.1034	8	0.0580
18%	5	0.0484	11	0.1221	8	0.0626
19%	5	0.0518	11	0.1313	8	0.0673
20%	5	0.0552	11	0.1407	8	0.0721
21%	5	0.0587	11	0.1504	8	0.0772
22%	5	0.0623	11	0.1604	9	0.0923
23%	5	0.0660	11	0.1707	9	0.0983
24%	5	0.0698	11	0.1813	9	0.1046
25%	5	0.0737	11	0.1922	9	0.1111
26%	5	0.0776	11	0.2034	9	0.1178
27%	5	0.0817	11	0.2149	9	0.1248
28%	5	0.0859	11	0.2267	9	0.1321

29%	5	0.0901	11	0.2388	9	0.1396
30%	5	0.0944	11	0.2513	9	0.1474
31%	5	0.0989	11	0.2641	9	0.1555
32%	5	0.1034	11	0.2772	9	0.1639
33%	5	0.1081	12	0.3153	9	0.1726
34%	5	0.1128	12	0.3303	9	0.1817
35%	5	0.1177	12	0.3457	9	0.1911
36%	5	0.1226	12	0.3614	9	0.2009
37%	5	0.1277	12	0.3775	9	0.2110
38%	5	0.1329	12	0.3941	9	0.2215
39%	5	0.1381	12	0.4111	9	0.2325
40%	5	0.1435	12	0.4284	9	0.2438
41%	5	0.1490	12	0.4462	9	0.2556
42%	5	0.1546	12	0.4645	9	0.2679
43%	5	0.1603	12	0.4831	9	0.2807
44%	6	0.1997	12	0.5023	9	0.2939
45%	6	0.2068	12	0.5218	9	0.3077
46%	6	0.2141	12	0.5419	9	0.3220
47%	6	0.2215	12	0.5624	9	0.3368
48%	6	0.2290	12	0.5833	9	0.3523
49%	6	0.2366	12	0.6048	9	0.3684
50%	6	0.2444	12	0.6267	9	0.3851
51%	6	0.2523	12	0.6492	9	0.4026
52%	6	0.2603	12	0.6721	9	0.4207
53%	6	0.2684	12	0.6955	9	0.4397
54%	7	0.3231	12	0.7194	9	0.4595
55%	7	0.3329	12	0.7439	8	0.4333
56%	7	0.3428	12	0.7689	8	0.4532
57%	7	0.3527	12	0.7944	8	0.4742
58%	8	0.4150	12	0.8205	8	0.4963
59%	8	0.4267	12	0.8471	8	0.5198
60%	8	0.4384	12	0.8743	8	0.5449
61%	9	0.5069	12	0.9022	9	0.6299

62%	9	0.5203	12	0.9307	9	0.6608
63%	10	0.5935	12	0.9599	9	0.6940
64%	10	0.6085	12	0.9899	10	0.7946
65%	11	0.6863	12	1.0209	10	0.8360
66%	12	0.7672	12	1.0528	10	0.8812
67%	13	0.8511	12	1.0860	10	0.9307
68%	15	1.0052	12	1.1207	10	0.9853
69%	17	1.1653	12	1.1571	12	1.1968
70%	20	1.4016	12	1.1957	14	1.4245
71%	23	1.6466	12	1.2370	16	1.6703
72%	30	2.1930	12	1.2817	18	1.9362
73%	42	3.1328	12	1.3307	21	2.3093
74%	72	5.4762	11	1.3062	25	2.7985
75%	177	14.8662	11	1.3670	30	3.4126

Table C.4 Rapidity and RAI as capacity reduction increases for the Sioux Falls network

	Fix-time		P0		Equi-saturation	
Capacity reduction	**Rapidity**	**RAI**	**Rapidity**	**RAI**	**Rapidity**	**RAI**
5%	13	0.8242	12	0.4489	13	0.8276
6%	13	1.0102	12	0.5491	13	1.0146
7%	13	1.2040	12	0.6533	13	1.2096
8%	13	1.4061	12	0.7615	13	1.4129
9%	13	1.6167	12	0.8741	13	1.6250
10%	13	1.8363	13	1.0736	13	1.8463
11%	13	2.0653	13	1.2057	13	2.0771
12%	13	2.3041	13	1.3434	13	2.3180
13%	13	2.5532	13	1.4868	13	2.5695
14%	13	2.8132	13	1.6365	13	2.8320
15%	13	3.0843	13	1.7926	13	3.1062
16%	13	3.3673	13	1.9557	14	3.6462
17%	13	3.6626	14	2.2888	14	3.9672

18%	13	3.9709	14	2.4805	14	4.3025
19%	13	4.2926	14	2.6811	14	4.6527
20%	13	4.6285	14	2.8910	14	5.0185
21%	13	4.9791	14	3.1109	14	5.4006
22%	14	5.7416	14	3.3414	14	5.7998
23%	14	6.1516	14	3.5832	14	6.2169
24%	14	6.5796	14	3.8370	14	6.6526
25%	14	7.0264	14	4.1036	14	7.1080
26%	14	7.4928	14	4.3838	14	7.5837
27%	14	7.9797	14	4.6786	14	8.0809
28%	14	8.4880	14	4.9890	14	8.6003
29%	14	9.0187	15	5.6933	14	9.1431
30%	14	9.5725	15	6.0625	14	9.7102
31%	14	10.1507	15	6.4521	14	10.3027
32%	14	10.7541	15	6.8636	14	10.9217
33%	14	11.3838	15	7.2986	14	11.5683
34%	14	12.0410	15	7.7589	14	12.2438
35%	14	12.7268	15	8.2462	14	12.9493
36%	14	13.4424	15	8.7627	14	13.6862
37%	14	14.1889	15	9.3107	14	14.4558
38%	14	14.9678	15	9.8925	14	15.2594
39%	14	15.7804	15	10.5109	14	16.0985
40%	14	16.6280	15	11.1687	14	16.9745
41%	14	17.5123	15	11.8692	14	17.8892
42%	15	19.6650	15	12.6159	15	20.1053
43%	15	20.6883	15	13.4126	15	21.1658
44%	15	21.7557	15	14.2634	15	22.2727
45%	15	22.8691	15	15.1730	15	23.4280
46%	15	24.0307	15	16.1464	15	24.6342
47%	15	25.2432	15	17.1892	15	25.8936
48%	15	26.5091	15	18.3073	15	27.2092
49%	15	27.8316	15	19.5075	15	28.5839
50%	15	29.2143	15	20.7971	15	30.0215

51%	15	30.6612	15	22.1840	15	31.5257
52%	15	32.1769	15	23.6771	15	33.1015
53%	15	33.7671	15	25.2860	15	34.7541
54%	15	35.4382	15	27.0212	15	36.4901
55%	15	37.1980	15	28.8944	15	38.3171
56%	15	39.0556	15	30.9180	15	40.2441
57%	15	41.0218	15	33.1060	15	42.2819
58%	15	43.1095	15	35.4733	15	44.4433
59%	15	45.3339	15	38.0362	15	46.7437
60%	15	47.7128	15	40.8125	15	49.2010
61%	15	50.2668	15	43.8213	15	51.8362
62%	15	53.0202	15	47.0831	15	54.6739
63%	15	56.0012	15	50.6199	15	57.7431
64%	15	59.2436	15	54.4554	15	61.0778
65%	15	62.7881	15	58.6143	15	64.7193
66%	16	70.2449	15	63.1231	16	72.4169
67%	18	82.1377	15	68.0092	17	80.8561
68%	19	91.2950	15	73.3012	19	94.1633
69%	21	105.4305	15	79.0287	21	108.7765
70%	24	125.1977	15	85.2223	23	124.8483
71%	26	142.5069	15	91.9133	25	142.5520
72%	28	161.6175	15	99.1343	28	166.8924
73%	38	221.3415	15	106.9197	39	233.8601
74%	57	332.4289	15	115.3073	58	349.4172
75%	116	665.2010	15	124.3413	103	618.8533

Table C.5 Rapidity and RAI of Sioux Falls network under 50% capacity degradation when links are degraded one by one

	Rapidity			RAI		
Link No.	**Fix-time**	**P0**	**Equi-saturation**	**Fix-time**	**P0**	**Equi-saturation**
1	2	2	2	0.0000	0.0000	0.0000

2	2	4	2	0.0000	0.0001	0.0000
3	2	3	2	0.0000	0.0000	0.0000
4	8	9	8	0.0047	0.0306	0.0081
5	3	3	3	0.0000	0.0000	0.0000
6	6	7	7	0.0007	0.0032	0.0023
7	4	6	7	0.0001	0.0009	0.0019
8	6	6	5	0.0007	0.0008	0.0004
9	8	8	8	0.0029	0.0138	0.0055
10	13	13	13	0.3493	0.4696	0.3579
11	8	8	8	0.0030	0.0080	0.0052
12	13	12	13	0.5169	0.2215	0.4890
13	11	10	11	0.0500	0.0419	0.0465
14	7	7	7	0.0019	0.0029	0.0020
15	13	12	13	0.5207	0.1647	0.4567
16	14	12	14	0.6576	0.3912	0.6343
17	12	11	11	0.0677	0.1308	0.0695
18	7	7	7	0.0016	0.0041	0.0020
19	14	12	14	0.6423	0.2912	0.6003
20	11	11	11	0.0404	0.0642	0.0422
21	12	11	12	0.0756	0.0518	0.0683
22	14	14	14	1.4392	2.1114	1.5286
23	11	10	11	0.0521	0.0435	0.0527
24	12	11	12	0.0610	0.1021	0.0693
25	11	12	11	0.0643	0.3292	0.0972
26	11	10	11	0.0549	0.0458	0.0504
27	14	12	14	0.5574	0.4390	0.5658
28	13	12	13	0.3039	0.4286	0.3256
29	13	15	13	10.9539	6.3532	11.1227
30	14	14	14	0.7866	1.7233	0.8701
31	13	11	13	0.3374	0.0664	0.2770
32	14	13	13	0.5065	0.6591	0.5175
33	13	11	13	0.5852	0.0972	0.4740
34	13	14	13	2.5924	2.4518	2.5926

35	4	5	4	0.0001	0.0003	0.0001
36	13	13	13	0.5851	0.5674	0.5850
37	3	3	3	0.0000	0.0001	0.0000
38	5	6	7	0.0003	0.0019	0.0026
39	14	13	13	0.6523	0.5063	0.6031
40	13	14	13	2.4407	1.1858	2.3587
41	13	14	13	3.0459	1.6346	2.9702
42	13	14	14	1.6443	1.0266	1.7297
43	13	12	13	0.3248	0.4721	0.3704
44	13	14	13	2.7982	2.3803	2.8037
45	13	13	13	0.3784	1.1311	0.4426
46	14	13	14	1.9690	0.9994	1.9479
47	14	13	14	1.7654	0.4843	1.6859
48	13	15	13	10.9941	3.8354	11.0416
49	14	15	14	6.0729	5.9570	6.1441
50	10	8	10	0.0256	0.0117	0.0205
51	14	14	14	0.8581	0.8883	0.9016
52	14	15	14	6.1128	5.0334	6.1991
53	13	15	13	7.4060	6.3296	7.4164
54	5	5	5	0.0004	0.0006	0.0004
55	11	12	11	0.0354	0.4082	0.0664
56	9	11	10	0.0126	0.1094	0.0249
57	13	12	13	0.3771	0.5396	0.3940
58	13	15	13	7.4294	6.9978	7.5103
59	13	14	13	4.0678	1.7202	3.9745
60	9	8	9	0.0125	0.0078	0.0109
61	13	15	13	3.8053	3.8431	3.8500
62	14	13	14	0.5897	0.5107	0.5958
63	14	14	14	1.3649	0.9983	1.3650
64	14	13	14	0.6393	0.6425	0.6519
65	14	14	14	1.0858	1.1327	1.0805
66	14	13	14	1.1155	0.6857	1.0870
67	14	13	14	2.0012	1.1624	1.9501

68	14	14	14	1.3473	0.9709	1.3348
69	14	14	14	1.1036	0.9315	1.0760
70	14	13	14	0.9902	0.7546	0.9848
71	13	14	14	1.6138	1.9970	1.7554
72	14	13	14	1.0977	0.8968	1.0974
73	14	13	14	0.6618	0.6111	0.6498
74	13	13	13	0.4214	0.6404	0.4377
75	14	13	14	1.0988	0.7880	1.0756
76	14	13	14	0.6959	0.7837	0.6954

Table C.6 Ranking of link importance of Sioux Falls network based on rapidity and RAI under 50% capacity degradation

	Rapidity			RAI		
Ranking	**Fix-time**	**P0**	**Equi-saturation**	**Fix-time**	**P0**	**Equi-saturation**
1	16	29	16	48	58	29
2	19	48	19	29	29	48
3	22	49	22	58	53	58
4	27	52	27	53	49	53
5	30	53	30	52	52	52
6	32	58	42	49	61	49
7	39	61	46	59	48	59
8	46	22	47	61	34	61
9	47	30	49	41	44	41
10	49	34	51	44	22	44
11	51	40	52	34	71	34
12	52	41	62	40	30	40
13	62	42	63	67	59	67
14	63	44	64	46	41	46
15	64	51	65	47	40	71
16	65	59	66	42	67	42
17	66	63	67	71	65	47
18	67	65	68	22	45	22

19	68	68	69	63	42	63
20	69	69	70	68	46	68
21	70	71	71	66	63	72
22	72	10	72	69	68	66
23	73	32	73	75	69	65
24	75	36	75	72	72	69
25	76	39	76	65	51	75
26	10	45	10	70	75	70
27	12	46	12	51	76	51
28	15	47	15	30	70	30
29	28	62	28	76	66	76
30	29	64	29	73	32	64
31	31	66	31	16	64	73
32	33	67	32	39	74	16
33	34	70	33	19	73	39
34	36	72	34	64	36	19
35	40	73	36	62	57	62
36	41	74	39	33	62	36
37	42	75	40	36	39	27
38	43	76	41	27	47	32
39	44	12	43	15	43	12
40	45	15	44	12	10	33
41	48	16	45	32	27	15
42	53	19	48	74	28	45
43	57	25	53	45	55	74
44	58	27	57	57	16	57
45	59	28	58	10	25	43
46	61	43	59	31	19	10
47	71	55	61	43	12	28
48	74	57	74	28	15	31
49	17	17	21	21	17	25
50	21	20	24	17	56	17
51	24	21	13	25	24	24

52	13	24	17	24	33	21
53	20	31	20	26	31	55
54	23	33	23	23	20	23
55	25	56	25	13	21	26
56	26	13	26	20	26	13
57	55	23	55	55	23	20
58	50	26	50	50	13	56
59	56	4	56	56	4	50
60	60	9	60	60	9	60
61	4	11	4	4	50	4
62	9	50	9	11	11	9
63	11	60	11	9	60	11
64	14	6	6	14	18	38
65	18	14	7	18	6	6
66	6	18	14	6	14	14
67	8	7	18	8	38	18
68	38	8	38	54	7	7
69	54	38	8	38	8	8
70	7	35	54	7	54	54
71	35	54	35	35	35	35
72	5	2	5	1	2	1
73	37	3	37	2	37	2
74	1	5	1	3	1	3
75	2	37	2	5	3	5
76	3	1	3	37	5	37

PUBLICATIONS

Shang, W., Han, K., Ochieng, W., 2015. An Agent-Based Day-to-Day Traffic Evolution Model using Information Percolation. The 95th Transportation Research Board Annual Meeting, Washington D.C., 11-15 January 2016.

Wang, Y., Han, K., Liu, H., **Shang, W**. 2015. Day-to-Day Congestion Pricing and Network Resilience. The 95th Transportation Research Board Annual Meeting, Washington D.C., 11-15 January 2016.

Shang, W., Han, K., Ochieng, W. Angeloudis, P., 2016. An Agent-Based Day-to-Day Traffic Evolution Model with Information Percolation. Transportmetrica A: Transport Science, DOI: 10.1080/23249935.2016.1209254

Pien, K.C., Han, K., **Shang, W.,** Majumdar, A., Ochieng, W., 2015. Robustness analysis of the European air traffic network. Transportmetrica A: Transport Science, DOI: 10.1080/23249935.2015.1087233.

Shang W., Pien K.C., Han K., Ochieng W., Majumdar A., 2015. Robustness and Topology Analysis of European Air Traffic Network Using Complex Network Theory, The 94th Transportation Research Board Annual Meeting, Washington D.C., 11-15 January 2015.